

# MIKE 11

A Modelling System for Rivers and Channels

Reference Manual





## PLEASE NOTE

### **COPYRIGHT**

This document refers to proprietary computer software which is protected by copyright. All rights are reserved. Copying or other reproduction of this manual or the related programs is prohibited without prior written consent of DHI. For details please refer to your 'DHI Software Licence Agreement'.

### **LIMITED LIABILITY**

The liability of DHI is limited as specified in your DHI Software Licence Agreement:

In no event shall DHI or its representatives (agents and suppliers) be liable for any damages whatsoever including, without limitation, special, indirect, incidental or consequential damages or damages for loss of business profits or savings, business interruption, loss of business information or other pecuniary loss arising in connection with the Agreement, e.g. out of Licensee's use of or the inability to use the Software, even if DHI has been advised of the possibility of such damages.

This limitation shall apply to claims of personal injury to the extent permitted by law. Some jurisdictions do not allow the exclusion or limitation of liability for consequential, special, indirect, incidental damages and, accordingly, some portions of these limitations may not apply.

Notwithstanding the above, DHI's total liability (whether in contract, tort, including negligence, or otherwise) under or in connection with the Agreement shall in aggregate during the term not exceed the lesser of EUR 10.000 or the fees paid by Licensee under the Agreement during the 12 months' period previous to the event giving rise to a claim.

Licensee acknowledge that the liability limitations and exclusions set out in the Agreement reflect the allocation of risk negotiated and agreed by the parties and that DHI would not enter into the Agreement without these limitations and exclusions on its liability. These limitations and exclusions will apply notwithstanding any failure of essential purpose of any limited remedy.





# CONTENTS

<b>Hydrodynamic Reference</b> . . . . .	15
<b>1 HD Reference Manual</b> . . . . .	17
1.1 Manual Format . . . . .	17
1.2 A General Description . . . . .	18
1.3 Bed Resistance . . . . .	18
1.3.1 Chezy and Manning . . . . .	19
1.3.2 Relative Resistance . . . . .	20
1.3.3 Resistance Factor . . . . .	20
1.3.4 Resistance Radius . . . . .	21
1.3.5 Hydraulic Radius . . . . .	21
1.3.6 Resistance Radius vs Hydraulic Radius . . . . .	22
1.3.7 Calculation of resistance using channel bank markers . . . . .	25
1.3.8 Additional resistance due to vegetation . . . . .	26
1.4 Boundary Conditions . . . . .	30
1.4.1 Resolution . . . . .	31
1.4.2 Which Boundary Condition? . . . . .	31
1.5 Bridges . . . . .	31
1.5.1 Arch Bridges (Biery and Delleur) . . . . .	33
1.5.2 Arch Bridges (Hydraulics Research (HR) method) . . . . .	35
1.5.3 Bridge Piers (D'Aubuisson) . . . . .	36
1.5.4 Bridge Piers (Nagler) . . . . .	37
1.5.5 Bridge Piers (Yarnell) . . . . .	39
1.5.6 Energy Equation . . . . .	40
1.5.7 Federal Highway Administration (FHWA) WSPRO method . . . . .	43
1.5.8 US Bureau of Public Roads (USBPR) method . . . . .	54
1.5.9 Multiple Waterway Opening . . . . .	55
1.5.10 Pressure Flow, Federal Highway Administration method . . . . .	56
1.5.11 Road overflow, Federal Highway Administration method . . . . .	58
1.5.12 Fully submerged bridges . . . . .	60
1.5.13 Trouble shooting for bridge structures . . . . .	62
1.6 Broad crested Weir . . . . .	63
1.7 Coefficients, HD default parameters . . . . .	63
1.8 Computational Grid . . . . .	65
1.8.1 General Description . . . . .	65
1.8.2 Selecting the Area to be Modelled . . . . .	65
1.8.3 Selecting Model Branches . . . . .	66
1.8.4 Selecting the Grid Spacing . . . . .	66
1.9 Control Structures . . . . .	67



1.9.1	Hydraulic Aspects - Radial Gates	67
1.9.2	Hydraulic Aspects -Sluice Gates	69
1.9.3	Hydraulic Aspects - Overflow Structures	72
1.9.4	Hydraulic Aspects - Underflow Structures	72
1.9.5	Free Flow	74
1.9.6	Drowned Flow	75
1.10	Cross-Sections	75
1.11	Closed Cross sections, Modelling the Pressurised flow	78
1.12	Culverts, Q-h Relations Calculation	81
1.12.1	Specification	82
1.12.2	Flow Descriptions	82
1.12.3	Construction of Q-h Relationships	85
1.12.4	Closed / Open Section switch	86
1.12.5	Changing Flow Direction	87
1.12.6	Flooded Areas of Adjacent $h$ -points	87
1.12.7	Velocities	87
1.13	Dambreak Structure	87
1.13.1	Energy equation based dam breach modelling	87
1.13.2	Erosion Based Breach Development using the energy equation	89
1.13.3	NWS DAMBRK dam-breach method	94
1.14	Energy Loss	98
1.15	Flooded Areas, (Storage)	99
1.16	Flood control facilities	102
1.16.1	Non control	102
1.16.2	Constant discharging method Type A	102
1.16.3	Constant discharging method Type B	103
1.16.4	Constant ratio discharging method Type A	104
1.16.5	Constant ratio discharging method Type B	105
1.16.6	Bucket-cut (without afterward discharging)	106
1.16.7	Non gate discharging by H/Q curve and H/V curve	106
1.16.8	Non gate discharging by orifice size input	107
1.17	Flood plain Encroachment calculations	109
1.17.1	General	110
1.17.2	Encroachment Methods	111
1.17.3	Additional specifications for encroachment calculations	113
1.17.4	Cross sections after encroachment	114
1.17.5	Encroachments at structures	115
1.17.6	Encroachments at nodes	115
1.18	Flood Plains	115
1.19	Flow Descriptions	118
1.19.1	Dynamic Wave and High Order Dynamic Wave	118
1.19.2	Diffusive Wave	119
1.19.3	Kinematic Wave	119
1.19.4	Which Flow Description?	119
1.20	Initial Conditions	120
1.20.1	User-Specified	120
1.20.2	Auto Start, Quasi-Steady Solution	120



1.20.3	Hot Start	120
1.20.4	Combined Auto Start and user-specified initial conditions	120
1.21	Kinematic Routing Method	120
1.22	Lateral Inflows	125
1.23	Leakage	125
1.24	Low Flow Conditions	126
1.25	Pumps	127
1.25.1	Capacity	127
1.25.2	Start/Stop control	128
1.25.3	Internal outlet	128
1.25.4	External outlet	129
1.26	Quasi-Steady Solution	129
1.27	Quasi-two dimensional steady flow with vegetation	133
1.27.1	Zone classification	136
1.27.2	Solution algorithm	144
1.27.3	Bridges	149
1.27.4	Junctions	152
1.27.5	Variation in water level due to curves	154
1.27.6	Variation in water level due to sand bars	155
1.28	Regulating Structures	156
1.28.1	Function of time	156
1.28.2	Function of $h$ and/or $Q$	156
1.29	Routing	158
1.30	Saint Venant Equations	159
1.31	Solution Scheme	160
1.32	Special Weir	160
1.33	Stability Conditions	161
1.34	Steady State Energy Equation	162
1.35	Structures	167
1.35.1	Zero Flow	168
1.35.2	Drowned Flow	168
1.35.3	Free Overflow	168
1.35.4	Contraction and Expansion Losses	169
1.35.5	Grid spacing at structures	170
1.35.6	Parallel/Composite Structures	170
1.36	Supercritical Flow	171
1.36.1	Suppression of convective acceleration term	171
1.36.2	Effect of convective acceleration suppression on Energy Heads	173
1.37	Supercritical Flow in Structures	173
1.37.1	Flow Directions	174
1.37.2	Testing for Flow Conditions	174
1.37.3	Subcritical Flow through Structure	175
1.37.4	Critical Flow through Structure	175
1.37.5	Supercritical Flow through Structure	176
1.37.6	Contraction and Expansion Losses, Sub- and Supercritical Flow	176
1.38	Tabulated structures	176



1.39	Time Stepping . . . . .	177
1.40	User Defined Structure . . . . .	179
	1.40.1 Tips . . . . .	180
1.41	Weir Formula . . . . .	180
	1.41.1 Weir Formula 1 . . . . .	181
	1.41.2 Weir Formula 2 (Honma) . . . . .	181
	1.41.3 Weir Formula 3 (Extended Honma) . . . . .	181
1.42	Wind . . . . .	182
1.43	References . . . . .	183

## **Advection-Dispersion/**

<b>Cohesive Sediment Transport</b> Reference . . . . .	186
--	-----

<b>2 AD/CST Reference Manual . . . . .</b>	<b>187</b>	
2.1 Who Should Use This Manual . . . . .	187	
2.2 Manual Format . . . . .	187	
2.3 A General Description . . . . .	187	
2.4 Advanced Cohesive Sediment Transport . . . . .	188	
	2.4.1 Cross-Sectional Shear Stress Distribution . . . . .	189
	2.4.2 Settling . . . . .	190
	2.4.3 Deposition . . . . .	191
	2.4.4 Sliding . . . . .	191
	2.4.5 Erosion . . . . .	191
	2.4.6 Consolidation . . . . .	192
2.5 Advection-Dispersion Equation . . . . .	192	
2.6 Boundary Conditions . . . . .	193	
	2.6.1 Open Boundary Outflow . . . . .	193
	2.6.2 Open Boundary Inflow . . . . .	193
	2.6.3 Concentration boundary . . . . .	194
	2.6.4 Transport boundary . . . . .	194
	2.6.5 Closed Boundary . . . . .	194
2.7 Deposition, CST . . . . .	194	
2.8 Dispersion Coefficient . . . . .	196	
2.9 Erosion, CST . . . . .	197	
2.10 Mass transport and mass balance . . . . .	197	
	2.10.1 Mass . . . . .	198
	2.10.2 1st order Decay . . . . .	199
	2.10.3 Transport . . . . .	199
	2.10.4 Advective transport . . . . .	199
	2.10.5 Dispersive transport . . . . .	200
	2.10.6 Mass balance . . . . .	200
2.11 Solution Scheme, AD . . . . .	201	
	2.11.1 Continuity equation: . . . . .	201
	2.11.2 Advective-dispersive transport equation: . . . . .	202
2.12 Stability . . . . .	202	
2.13 Nomenclature . . . . .	203	





2.14	References . . . . .	204
	<b>Non-cohesive Sediment Transport Reference . . . . .</b>	<b>207</b>
<b>3</b>	<b>NST Reference Manual . . . . .</b>	<b>209</b>
3.1	Manual Format . . . . .	209
3.2	A General Description . . . . .	210
3.3	Sediment transport models . . . . .	210
3.4	Bed forms . . . . .	211
3.4.1	Ripples . . . . .	211
3.4.2	Dunes . . . . .	211
3.4.3	Plane bed . . . . .	212
3.4.4	Anti-dunes . . . . .	212
3.5	Morphological model . . . . .	213
3.5.1	Updating of bottom level . . . . .	216
3.5.2	Boundary Conditions . . . . .	220
3.5.3	Low flow correction . . . . .	222
3.5.4	Hints . . . . .	222
3.6	Graded Sediments . . . . .	222
3.6.1	Boundary conditions . . . . .	227
3.6.2	Graded sediments boundary conditions . . . . .	227
3.7	Dune dimensions . . . . .	228
3.7.1	Equilibrium dune height . . . . .	228
3.7.2	Equilibrium dune length . . . . .	230
3.7.3	Non-equilibrium dune height . . . . .	234
3.7.4	Non-equilibrium dune length . . . . .	234
3.8	Flow Resistance . . . . .	235
3.8.1	Flow resistance - dune dimension . . . . .	235
3.8.2	Flow Resistance - $\theta-\theta'$ Relationship . . . . .	237
3.8.3	Flow Resistance - White et al. . . . .	239
3.9	Incipient motion criteria . . . . .	241
3.9.1	Shield's critical parameter . . . . .	241
3.9.2	Iwagaki's critical tractive force . . . . .	242
3.9.3	Modified Egiazaroff equation . . . . .	242
3.10	Ackers and White model . . . . .	243
3.11	Ashida & Michiue model . . . . .	245
3.11.1	Bed load . . . . .	246
3.11.2	Suspended load . . . . .	246
3.12	Ashida, Takahashi and Mizuyama model (ATM) . . . . .	249
3.13	Engelund & Fredsøe model . . . . .	252
3.13.1	Bed Load . . . . .	253
3.13.2	Suspended load . . . . .	254
3.14	Engelund & Hansen model . . . . .	256
3.15	Lane & Kalinske model . . . . .	256
3.16	Meyer-Peter & Müller model . . . . .	258
3.17	Sato, Kikkawa & Ashida model . . . . .	259



3.18	Smart and Jaeggi model . . . . .	260
3.18.1	Revised transport formula . . . . .	260
3.18.2	MIKE 11 version . . . . .	261
3.19	van Rijn model . . . . .	262
3.19.1	Bed load . . . . .	262
3.19.2	Suspended load . . . . .	264
3.20	Nomenclature . . . . .	267
3.21	References . . . . .	271
<b>Rainfall-Runoff Reference . . . . .</b>		<b>275</b>
<b>4</b>	<b>RR Reference Manual . . . . .</b>	<b>277</b>
4.1	NAM - Introduction . . . . .	277
4.2	Data Requirements . . . . .	278
4.2.1	Meteorological data . . . . .	279
4.2.2	Hydrological data . . . . .	280
4.3	Model Structure . . . . .	280
4.4	Basic modelling components . . . . .	282
4.4.1	Surface storage . . . . .	282
4.4.2	Lower zone or root zone storage . . . . .	282
4.4.3	Evapotranspiration . . . . .	282
4.4.4	Overland flow . . . . .	282
4.4.5	Interflow . . . . .	283
4.4.6	Interflow and overland flow routing . . . . .	283
4.4.7	Groundwater recharge . . . . .	284
4.4.8	Soil moisture content . . . . .	284
4.4.9	Baseflow . . . . .	284
4.5	Extended groundwater components . . . . .	284
4.5.1	Drainage to or from neighbouring catchments . . . . .	284
4.5.2	Lower groundwater storage . . . . .	285
4.5.3	Shallow groundwater reservoir description . . . . .	285
4.5.4	Capillary flux . . . . .	285
4.6	Snow module . . . . .	286
4.6.1	Accumulation and melting of snow . . . . .	286
4.6.2	Altitude-distributed snowmelt model . . . . .	287
4.6.3	Extended components . . . . .	290
4.7	Irrigation module . . . . .	291
4.7.1	Introduction . . . . .	291
4.7.2	Structure of the irrigation module . . . . .	292
4.8	Model parameters . . . . .	294
4.8.1	Surface and root zone parameters . . . . .	295
4.8.2	Groundwater parameters . . . . .	298
4.8.3	Snow module parameters . . . . .	300
4.8.4	Irrigation module parameters . . . . .	301
4.9	Initial conditions . . . . .	302
4.10	Model calibration . . . . .	302



4.10.1	Calibration objectives and evaluation measures	303
4.10.2	Manual calibration	304
4.10.3	Automatic calibration routine	305
4.11	NAM - References	309
4.12	UHM	311
4.12.1	Introduction	311
4.12.2	The Loss Model	315
4.12.3	The Unit Hydrograph Routing Model	321
4.12.4	Kinematic wave hydrograph methods	325
4.12.5	Calculation time step	328
4.12.6	UHM - References	329
4.13	SMAP	329
4.13.1	Introduction	329
4.13.2	SMAP model equations	329
4.14	Urban	332
4.14.1	Introduction	332
4.14.2	Urban, model A, Time/area Method	333
4.14.3	Urban, model B, Non-linear Reservoir (kinematic wave) Method	335
4.15	DRiFt	342
4.15.1	Introduction	342
4.15.2	Model structure	342
4.15.3	Data requirements	344
4.15.4	Model calibration	352
4.15.5	DRiFt references	360
<b>Flood Forecasting Reference</b>		363
.....		364
<b>5</b>	<b>FF Reference Manual</b>	365
5.1	Introduction	365
5.2	Updating Procedure	366
5.2.1	Calibration Example	373
5.3	References	377
<b>Data assimilation Reference</b>		379
<b>6</b>	<b>Data Assimilation in MIKE 11</b>	381
6.1	Data assimilation framework	381
6.2	Ensemble Kalman filter	383
6.2.1	Model errors described by auto-regressive processes	386
6.3	Constant weighting function	386
6.3.1	Error forecast modelling	387
6.4	References	389
<b>Appendix A Scientific Background</b>		391



A.1	SCIENTIFIC BACKGROUND . . . . .	393
A.1.1	Manual format . . . . .	393
A.2	AREA PRESERVING SLOT . . . . .	395
A.3	CULVERTS, Q-H RELATIONS CALCULATED . . . . .	397
A.3.1	Loss coefficients . . . . .	397
A.3.2	Momentum equation coefficients . . . . .	398
A.3.3	Critical inflow or outflow . . . . .	399
A.3.4	Critical inflow . . . . .	399
A.3.5	Critical outflow . . . . .	400
A.3.6	Orifice flow at inflow . . . . .	400
A.3.7	Full culvert flow with free outflow . . . . .	401
A.3.8	Downstream controlled flow (submerged flow) . . . . .	401
A.3.9	Partially full inflow and outflow . . . . .	401
A.3.10	Submerged inflow and partially full outflow . . . . .	403
A.3.11	Partially full inflow and submerged outflow . . . . .	403
A.3.12	Fully submerged . . . . .	403
A.3.13	Transition between upstream and downstream control . . . . .	403
A.4	DELTA COEFFICIENT . . . . .	405
A.5	THE DOUBLE SWEEP ALGORITHM . . . . .	407
A.5.1	Branch matrix . . . . .	407
A.5.2	Node matrix . . . . .	409
A.5.3	Bandwidth minimisation . . . . .	411
A.5.4	Boundaries . . . . .	413
A.6	2-D MAPPING, INTERPOLATION ROUTINE . . . . .	417
A.6.1	Mapping . . . . .	417
A.6.2	Generation of a Digital Elevation Model (DEM) . . . . .	420
A.7	MODIFIED DIFFUSIVE WAVE APPROXIMATION . . . . .	423
A.8	SAINT VENANT EQUATIONS . . . . .	425
A.9	SOLUTION SCHEME . . . . .	429
A.9.1	Continuity equation . . . . .	430
A.9.2	Momentum equation . . . . .	432
A.10	STRUCTURES . . . . .	435
A.10.1	Mathematical treatment . . . . .	435
A.10.2	Expansion and Contraction Coefficients . . . . .	438
A.10.3	Determination of structure geometry . . . . .	439
A.10.4	Determination of flow regime . . . . .	439
A.10.5	Determination of flow regime (with Supercritical Flow) . . . . .	440
A.10.6	Zero flow . . . . .	441
A.10.7	Drowned flow . . . . .	441



A.10.8 Free overflow . . . . .	445
A.11 HEAT BALANCE MODULE . . . . .	449
A.11.1 General Description . . . . .	449
A.11.2 Convection . . . . .	450
A.11.3 Vaporisation . . . . .	451
A.11.4 Shortwave Radiation . . . . .	452
A.11.5 Longwave Radiation . . . . .	457
A.11.6 References . . . . .	458
A.12 USER DEFINED STRUCTURE . . . . .	459
A.12.1 General . . . . .	459
A.12.2 Example: Structure with Form Loss Coefficient . . . . .	464
A.12.3 Example: User Defined Output . . . . .	469
A.13 NOMENCLATURE . . . . .	475
<b>Appendix B</b> The MIKE11.ini file . . . . .	481
B.1 MIKE11.INI FILE SETTINGS . . . . .	483
B.1.1 Introduction . . . . .	483
B.1.2 MIKE 11 GIS Linkage . . . . .	483
B.1.3 MIKE 11 HD Settings . . . . .	483
B.1.4 MIKE 11 AD/WQ Settings . . . . .	492
<b>Index</b> . . . . .	495





# HYDRODYNAMIC

## Reference







# 1 HD Reference Manual

This manual should be used when undertaking hydrodynamic (HD) model applications. It provides a description of aspects which are encountered during the development, calibration and application of an HD model. Detailed technical descriptions of the solution scheme, treatment of structures and other aspects are given in Appendix A Appendix (p. 391). The manual should be used in conjunction with the MIKE 11 User Guide.

Some of the features available in the HD module have been developed in cooperation with CTI Engineering, CO., Ltd., Japan. Amongst these are; Tabulated structures, Honma's weir formula, bridges (D'Aubuisson and submerged bridge), Routing along channels, Outflow from Dams/retarding basins and the Steady flow with vegetation.

## 1.1 Manual Format

All descriptions in this Chapter are under headings presented in alphabetical order. A list of headings for this Chapter is given below

- A General Description (p. 18)
- Bed Resistance (p. 18)
- Boundary Conditions (p. 30)
- Bridges (p. 31)
- Broad crested Weir (p. 63)
- Coefficients, HD default parameters (p. 63)
- Computational Grid (p. 65)
- Control Structures (p. 67)
- Cross-Sections (p. 75)
- Closed Cross sections, Modelling the Pressurised flow (p. 78)
- Culverts, Q-h Relations Calculation (p. 81)
- Dambreak Structure (p. 87)
- Energy Loss (p. 98)
- Flood control facilities (p. 102)
- Flood plain Encroachment calculations (p. 109)
- Flood Plains (p. 115)
- Flow Descriptions (p. 118)
- Initial Conditions (p. 120)
- Kinematic Routing Method (p. 120)
- Lateral Inflows (p. 125)



- Leakage (*p. 125*)
- Pumps (*p. 127*)
- Quasi-Steady Solution (*p. 129*)
- Quasi-two dimensional steady flow with vegetation (*p. 133*)
- Regulating Structures (*p. 156*)
- Saint Venant Equations (*p. 159*)
- Solution Scheme (*p. 160*)
- Special Weir (*p. 160*)
- Stability Conditions (*p. 161*)
- Steady State Energy Equation (*p. 162*)
- Supercritical Flow (*p. 171*)
- Supercritical Flow in Structures (*p. 173*)
- Tabulated structures (*p. 176*)
- Time Stepping (*p. 177*)
- User Defined Structure (*p. 179*)
- Weir Formula (*p. 180*)
- Wind (*p. 182*)
- References (*p. 183*)

## 1.2 A General Description

The MIKE 11 hydrodynamic module (HD) uses an implicit, finite difference scheme for the computation of unsteady flows in rivers and estuaries.

The module can describe sub-critical as well as super critical flow conditions through a numerical scheme which adapts according to the local flow conditions (in time and space).

Advanced computational modules are included for description of flow over hydraulic structures, including possibilities to describe structure operation.

The formulations can be applied to looped networks and quasi two-dimensional flow simulation on flood plains.

The computational scheme is applicable for vertically homogeneous flow conditions extending from steep river flows to tidal influenced estuaries. The system has been used in numerous engineering studies around the world.

## 1.3 Bed Resistance

MIKE 11 allows for two different types of bed resistance descriptions:



1. Chezy
2. Manning
3. Darcy-Weisbach

The description is set in the Hydrodynamic Parameters Editor under the Bed Resistance tab.

### 1.3.1 Chezy and Manning

For the Chezy description, the bed resistance term in the momentum equation is described as:

$$\frac{gQ|Q|}{C^2 AR} \quad (1.1)$$

Where,

$Q$  is discharge

$A$  is flow area

$R$  is the resistance or hydraulic radius

For the Manning description, the term is:

$$\frac{gQ|Q|}{M^2 AR^{4/3}} \quad (1.2)$$

The Manning number,  $M$ , is equivalent to the Strickler coefficient. Its inverse is the more conventional Manning's  $n$ . The value of  $n$  is typically in the range 0.01 (smooth channel) to 0.10 (thickly vegetated channel). The corresponding values for  $M$  are from 100 to 10.

The Chezy coefficient is related to Manning's  $n$  by (17):

$$C = \frac{R^{1/6}}{n} = MR^{1/6} \quad (1.3)$$

Values for the resistance numbers,  $C$ ,  $M$  or  $n$ , should be determined through model calibration where possible, or based on other calibrated models with similar topographic characteristics. A rough guide to values of Manning's  $n$  can be found in most publications dealing with open channel hydraulics (e.g. /6/).

The difference between the Chezy and Manning descriptions is the power of  $R$ . The Manning description gives a formulation where the value of  $M$  can, in



general, be considered as independent of the depth of water, while for the Chezy formulation the value of  $C$  varies with depth (as implied by Equation (1.3)). If the user feels it is appropriate the Chezy or Manning coefficient can be defined manually as a function of the depth using the resistance factor (in the Cross Section Editor), see Resistance Factor below.

$R$  is calculated using either a Resistance Radius ( $R^*$ ) or a Hydraulic Radius ( $R_h$ ) formulation as specified by the user in the cross section editor. The default formulation for  $R$  may be set individually for each cross section. The formulations for  $R^*$  and  $R_h$  are discussed further on.



The resistance numbers from a calibrated model which were based on a  $R^*$  formulation **should not** be directly transferred to a model using the  $R_h$  formulation, or vice versa. It is, therefore, not recommended that a combination of  $R^*$  and  $R_h$  be used for different cross-sections in a model setup, as this could lead to different calibrated resistance numbers between similar reaches and other problems.

If necessary the values of  $R$  in the processed cross-section data can be entered manually.

### 1.3.2 Relative Resistance

The variation of resistance across a section can be defined by varying the relative resistance,  $r_p$ , in the cross section editors raw data menu. The effect of the relative resistance values on the hydraulic parameters in the processed data is dependent on whether a  $R^*$  or a  $R_h$  formulation was specified. For details, see Resistance Radius (p. 21) and Hydraulic Radius (p. 21) sections below.

### 1.3.3 Resistance Factor

The variation of resistance with elevation is defined by varying the resistance factor,  $r_f$ , in the processed data editor. At the start of the computation,  $r_f$  is multiplied by the resistance number, thus defining the resistance number as a function of water surface elevation. In most cases  $r_f$  is set to 1.0 (the default) at all elevations.

The effect of  $r_f$  on the bed resistance term,  $\tau_b$  (see above) in the momentum equation is dependent on whether the resistance number is defined as Chezy, Manning  $M$  (Strickler) or Manning's  $n$ . In the case of Chezy and Strickler, an increase in  $r_f$  will cause a decrease in resistance, while for Manning's  $n$  an increase in  $r_f$  will increase the resistance.

The effect on  $\tau_b$  is not directly related to the square of  $r_f$  as may be implied by the above equations because  $A$  and  $R$  will also vary as the bed resistance changes.



### 1.3.4 Resistance Radius

The resistance radius is calculated as (16/):

$$\sqrt{R_*} = \frac{1}{A} \int_0^B y^{\frac{3}{2}} db \quad (1.4)$$

where,  $y$  is the local water depth,  $A$  is the cross sectional area and  $B$  is the water width at the same elevation.

This formulation ensures that the Manning number is almost independent of the water depth in the case of composite cross sections.

The effect of the relative resistance,  $r_r$ , is included in the above formulation by adjusting the physical area to give the effective flow area,  $A_e$  as:

$$A_e = \sum_{i=1}^{n_s} \left( \frac{A_i}{r_r} \right) \quad (1.5)$$

where,  $N_s$  = Number of sub-sections which equals the number of x-z values in the raw data less one.

Equation (1.4) now reads as:

$$\sqrt{R_*} = \frac{1}{A_e} \int_0^B \frac{y^{\frac{3}{2}}}{r_r} db \quad (1.6)$$

### 1.3.5 Hydraulic Radius

The hydraulic radius formulation is based on a parallel channel analysis where the total conveyance,  $K$ , of the section at a given elevation is equal to the sum of the conveyances of the parallel channels. The parallel channels of a cross-section are defined as those parts of the cross-section where the relative resistance,  $r_r$ , remains constant.

Where,  $N$  is the number of parallel channels we have,

$$K = \sum_{i=1}^N K_i \quad (1.7)$$



which may be expressed using Manning's  $n$  as:

$$\frac{AR_h^{\frac{2}{3}}}{n} = \sum_{i=1}^N \frac{A_i R_{h_i}^{\frac{2}{3}}}{nr_{r_i}} \quad (1.8)$$

Setting  $A$  equal to either the effective flow area of the cross-section as given by Equation (1.5) or the total flow area we have the general formula:

$$R_h = \left( \frac{\sum_{i=1}^N \left( \frac{A_i^{5/3}}{r_{r_i} P_i^{2/3}} \right)}{A} \right)^{\frac{3}{2}} \quad (1.9)$$

where,  $P_i$  is the wetted perimeter of the parallel channel.  $P_i$  does not include the interface between adjoining parallel channels, i.e. a zero shear interface has been adopted.

Where the relative resistance is constant across the whole cross-section the well-known form:

$$R_h = \frac{A}{P} \quad (1.10)$$

is used. Both hydraulic radius using effective flow area and hydraulic radius using total flow area are offered as options in the cross section editor.

### 1.3.6 Resistance Radius vs Hydraulic Radius

The choice between  $R^*$  or  $R_h$  should be based on (a) which appears to be the most appropriate from a hydraulic aspect, and (b) which is normally used in local practice so that conventional bed resistance numbers can be used with confidence.

For a technical analysis Lundgren and Jonsson (1964), /12/ present a comparison of five different methods for determining the shear stress distribution over the bed of a shallow channel.

To highlight the differences between  $R^*$  and  $R_h$  the following example is used. Consider the cross-section illustrated in Figure 1.1

In the case of a constant relative resistance of 1.0 over the cross-section, Table 1.1 gives the values of  $R^*$  and  $R_h$  (Case 1), and their corresponding conveyance,  $K$ , (defined here as  $AR^{2/3}$ ) at selected water levels.

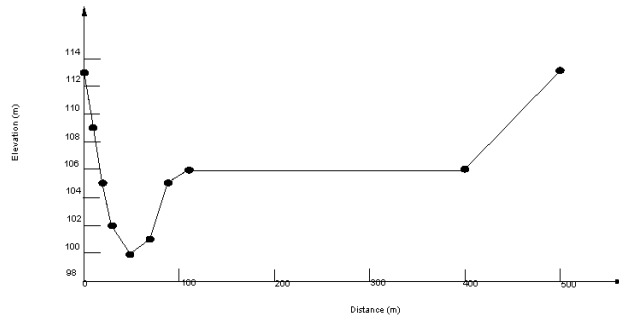


Figure 1.1 Cross-section for comparing  $R^*$  and  $R_h$

Table 1.1 Conveyance calculations for  $R^*$  and  $R_h$

Elev (m)	Area (m <sup>2</sup> )	$R^*$ (m)	$K$	$R_h$ (m) Case 1	$K$	$R_h$ (m) Case 2	$K$
100.0	0.0	0.00	0	0.00	0	0.00	0
103.0	101.7	2.19	171	1.89	155	1.89	155
106.0	306.3	4.41	824	3.27	675	3.27	675
106.1	344.6	3.85	846	0.89	319	2.98	714
107.0	697.1	2.95	1434	1.74	1009	2.62	1325
108.0	1104.8	3.46	2527	2.64	2110	3.18	2389
110.0	1970.5	5.03	5780	4.36	5259	4.66	5498
113.0	3395.0	7.58	13100	6.75	12126	6.93	12340

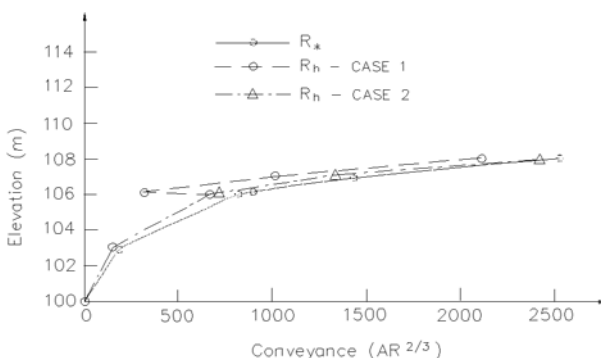


Figure 1.2 Plot of conveyance vs elevation

Comparison of the conveyance values, which are plotted in Figure 1.2, provide a guide to how the hydraulic capacity of the section varies with the water level. The figure shows that:

1.  $R^*$  allows a smooth transition in the conveyance of the channel as the over bank region becomes flooded, while  $R_h$  causes a sharp, incorrect decrease in the conveyance;
2. the conveyance in the deep section is considerably greater for  $R = R^*$ . This is because  $R^*$  can over-estimate the conveyance for very deep and narrow cross-sections as its formulation does not fully take into account the friction from the cross-section sides as does the  $R_h$  formulation.

The conveyance curve for the  $R_h$  case can be improved by separating the cross-section illustrated in Figure 1.1 into two parallel channels (main channel and over bank channel) separated by an apparent third channel of zero width at a distance of 110 m along the  $x$  axis. This can be done by specifying a change in relative resistance where the two parallel channels meet - which in reality is the norm as the over bank channel typically would have a higher resistance than the main channel.  $R_h$  - Case 2 in Table 1.1 is in the case of a  $r_r$  of 1.1 specified for the channel of zero width, and  $r_r$  of 1.0 elsewhere. (This has the effect of splitting the section into three parallel channels with the conveyance of the middle channel being zero.) As can be seen in Figure 1.2 a much improved conveyance -elevation relationship results.

In general,  $R^*$  is suited to sections with significant variations in shape such as over bank flow paths, while  $R_h$ , with no variation of  $r_r$  (i.e. one parallel channel) is more appropriate for very deep and narrow uniform sections. For  $R_h$  where over bank flow paths occur adjustment of  $r_r$  should be made to invoke the parallel channel analysis facility as described above. For wide sections with little variation in depth,  $R^*$  and  $R_h$  will not differ greatly.

In the cross section editors processed Data menu a conveyance column is shown where the conveyance is defined as follows:





For Manning's number

$$K = r_f AR^{2/3} \quad (1.11)$$

where,  $r_f$  is the resistance factor.

This is a useful facility to be able to check that the conveyance is increasing with increasing height. The conveyance can also be plotted to check a smooth representation.

### 1.3.7 Calculation of resistance using channel bank markers

Each cross section in MIKE 11 may be divided into a main channel plus one or two flood plains. The latter may be achieved by the use of the markers indicating the channel banks. The markers are defined by:

- Marker 4: The left low flow bank.
- Marker 5: The right low flow bank.

The markers are used for splitting the cross section into three parallel channels. Thus the reach of the left flood plain is given by markers 1 and 4, the reach of the main channel is defined by markers 4 and 5 and finally the right flood plain is defined through markers 5 and 3. The calculation of the hydraulic parameters is carried out for each of the three channels. From these the compound parameters for the cross section are found through:

#### Hydraulic radius/resistance radius

Using a parallel channel analysis the total conveyance may be expressed through

$$K_{\text{compound}} = K_{\text{left fp}} + K_{\text{channel}} + K_{\text{right fp}}, \quad (1.12)$$

i.e. the compound conveyance is found as the sum of the conveyance of three channels.

The conveyance of each channel is given by

$$K_i = A_i R_{h,i}^{\frac{2}{3}} \quad (1.13)$$

where  $i$  = left fp, channel, right fp.

The compound hydraulic radius /resistance radius is then calculated through

$$R_h = \left( \frac{K_{\text{compound}}}{A_{\text{total}}} \right)^{3/2}, \quad (1.14)$$



where the total area  $A_{\text{total}}$  is determined by

$$A_{\text{total}} = A_{\text{left fp}} + A_{\text{channel}} + A_{\text{right fp}}.$$

### 1.3.8 Additional resistance due to vegetation

The dimensionless Darcy-Weisbach coefficient may be expressed through

$$\lambda = \frac{8g}{C^2} \quad (1.15)$$

Where  $g$  is the acceleration due to gravity and  $C$  is the Chezy coefficient ( $\text{m}^{1/2}/\text{s}$ ).

Alternatively the dimensionless Darcy-Weisbach coefficient  $\lambda$  may be expressed as

$$\frac{1}{\sqrt{\lambda}} = -2 \cdot \log_{10} \left( \frac{k_s}{14,84R} \right) \quad (1.16)$$

This through rearrangement reads

$$\lambda = \frac{1}{\left( 2 \cdot \log_{10} \left( \frac{k_s}{14,84R} \right) \right)^2} \quad (1.17)$$

where  $k_s$  is the resistance number and  $R$  the hydraulic radius for the cross section in question.

The objective of the calculation method is to model the shear caused by the velocity distribution between the main channel and the flood plains. This shear is described through an equivalent Darcy-Weisbach coefficient. A coefficient is determined for each side of the cross section. That is one coefficient for the interaction between the left flood plain and the main channel and one for the interaction between the right flood plain and the main channel. The location of the flood plain/main channel interface is indicated by the markers (4 and 5) in Figure 1.3.

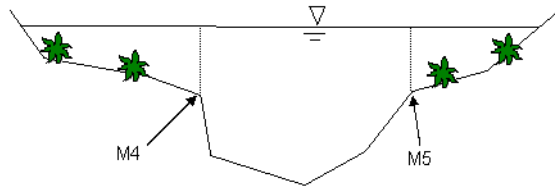


Figure 1.3 Interface between flood plain and main channel

Within each flood plain the vegetation may be taken into account. This is done through a number of user defined parameters:

- $A_x$  - The distance between vegetation elements in the flow direction
- $A_y$  - The distance between vegetation elements in the transversal direction
- $D_p$  - The diameter of a vegetation element

Further the individual vegetation elements give rise to a wake. This wake is described through

- $A_{NL}$  - The length at which the wake is fully developed
- $A_{NB}$  - Half the width of the fully developed wake

The first of these must satisfy the equation

$$0,03 = 0,9 \left( \frac{A_{NL}}{c_{W\infty} D_p} \right) \left( 1 + \frac{g A_{NL} I_E}{V_T^2 / 2} \right) \quad (1.18)$$

where  $c_{W\infty}$  depends on the Reynolds number based on the vegetation element

$$\begin{aligned} c_{W\infty} &= 3,07 Re^{-0,168} && \text{for } Re < 800 \\ c_{W\infty} &= 1 && \text{for } 800 < Re < 8000 \\ c_{W\infty} &= 1,2 && \text{for } Re > 8000 \end{aligned} \quad (1.19)$$

The Reynolds number here is defined by

$$Re = \frac{V_p D_p}{\nu} \quad (1.20)$$

The variation of eq. (1.19) is shown below in Figure 1.4.

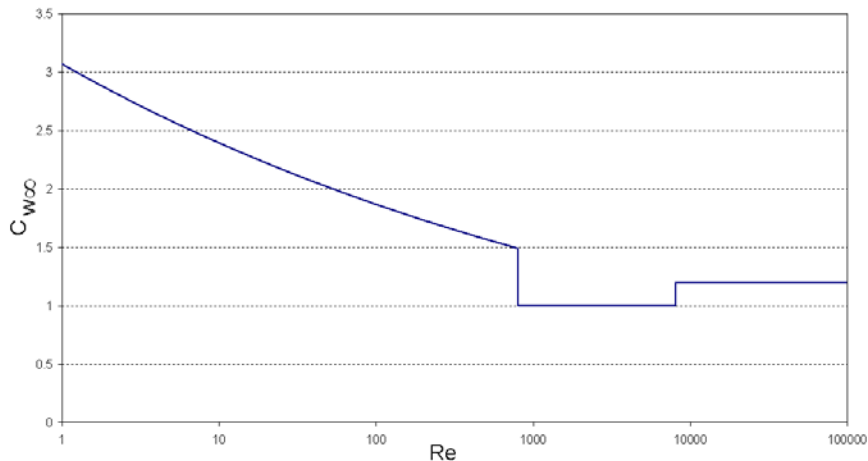


Figure 1.4 Non-dimensional constant as a function of Reynolds number

The velocity  $V_T$  may be expressed using the Chezy formula

$$I_E = \frac{V_T^2}{C^2 R} \quad (1.21)$$

which may be written in terms of the Darcy Weisbach as

$$I_E = \frac{\lambda V_T^2}{8gR} \quad (1.22)$$

Substituting this in the previous equation gives

$$0,03 = 0,9 \left( \frac{A_{NL}}{C_{W\infty} D_p} \right)^{-0,7} \left( 1 + \frac{A_{NL} 2g}{C^2 R} \right)^{-3/2} \quad (1.23)$$

From this equation the length of the wake is to be determined. Unfortunately the wake length depends on the Reynolds number which in turn is dependent on the velocity in the section. This velocity may be estimated from the Chezy formula

$$V_p = C \sqrt{R} \sqrt{I} \quad (1.24)$$



With the gradient being user defined. The value ANB can subsequently be determined from

$$A_{NB} = 0,24A_{NL}^{0,59}(c_{W\infty}D_p)^{0,41} \quad (1.25)$$

The quantity  $\lambda$  is user defined and refers to the flood plain in question, see Figure 1.5.

The next step is to determine the non-dimensional number

$$\Omega = \left(0,07\frac{A_{NL}}{A_x}\right)^{3,3} + \left(\frac{A_{NB}}{A_y}\right)^{0,95} \quad (1.26)$$

This number is determined for both the left and the right flood plain which is to be used to determine the resistance at the interaction plane through

$$\frac{1}{\sqrt{\lambda_T}} = -2 \cdot \log_{10} \left[ 0,07 \left( \frac{b_m}{b_{III}} \right)^{1,07} \Omega \right] = \frac{C}{\sqrt{8g}} \quad (1.27)$$

The quantity  $b_m$  is the contributing width of the flood plain defined through

$$B_m = \frac{ch_T}{\lambda(0,068\exp(0,56c_T) - 0,056)} \quad (1.28)$$

with

$$c_T = -3,27\log_{10}\Omega + 2,85 \quad (1.29)$$

With  $c$  being non-dimensional and user defined:  $c = 1.0$  for subdivided channels and  $c = 1.7$  for trapezoidal profiles with vegetation at the levees.  $h_T$  is the height of the separation plane and thus a function of water level, see Figure 1.5.

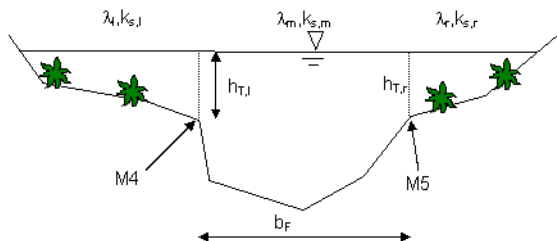


Figure 1.5 Illustration of calculation parameters

$b_{III}$  is the contributive width of the main flow channel of one separation plane. If there are two flood plains then the quantity is determined for the right and the left at the same time through the set of equations

$$b_F = b_{III,r} + b_{III,l} \quad (1.30)$$

$$b_{III,l} \lambda_r = b_{III,r} \lambda_l \quad (1.31)$$

with the main flow channel width  $b_F$  and the contributive widths of the left and right separation planes. If only one flood plain is present then  $b_F = b_{III}$ .

The composite  $\lambda$  is calculated as

$$\lambda = \frac{\sum \lambda_i P_i + h_{T,l} \lambda_{T,l} + h_{T,r} \lambda_{T,r}}{\sum P_{i,r} + h_{T,l} + h_{T,r}} \quad (1.32)$$

In terms of the composite Chezy number this may be written

$$\frac{1}{C^2} = \frac{\sum \frac{P_i}{C_i^2} + \frac{h_{T,l}}{C_{T,l}^2} + \frac{h_{T,r}}{C_{T,r}^2}}{\sum P_{i,r} + h_{T,l} + h_{T,r}} \quad (1.33)$$

## 1.4 Boundary Conditions

External boundary conditions are required at all model boundaries, i.e. all upstream and downstream ends of model branches which are not connected at a junction. The relationships applied at these limits can consist of:



1. constant values of  $h$  or  $Q$
2. time varying values of  $h$  or  $Q$
3. a relationship between  $h$  and  $Q$  (e.g. a rating curve) (Should only be used at downstream boundaries)

The relationships are required to close the system of equations to be solved by the double sweep method, see section A.5 in Appendix A Appendix (p. 391).

### 1.4.1 Resolution

If the resolution of the time varying boundaries is greater than the time step used in the simulation intermediate values in the boundary condition are determined by linear interpolation. Thus, if scanned data are available to describe the boundary such as is often the case with tide levels to describe a tidal cycle, some pre-processing of the data may be necessary to define a smoother transition between known points, e.g. a spline interpolation.

### 1.4.2 Which Boundary Condition?

The choice of boundary condition depends on the physical situation being simulated and the availability of data.

Typical upstream boundaries could be

- constant discharge from a reservoir
- a discharge hydrograph of a specific event

Typical downstream boundaries include:

- constant water level, e.g. in a large receiving water body
- time series of water level, e.g. tidal cycle
- a reliable rating curve, e.g. from a gauging station

## 1.5 Bridges

MIKE 11 offers a number of approaches when modelling flow through bridges. The approach to choose should be based on the assumptions for the different methods and the requirements for the modelling.

The bridge modelling approaches can be divided into pure free flow methods and methods which may be combined with submergence/overflow methods. The pure free flow methods can be further sub-divided into methods for piers and methods for arches.

The methods specially designed for piers are



- Bridge Piers (Nagler) (*p. 37*): An orifice type of flow description with the effect of the piers taken into account through an adjustment factor.
- Bridge Piers (Yarnell) (*p. 39*): An equation derived from experiments for normal flow conditions in the sub critical flow range. Again the effect of piers is handled through the use of adjustment factors.

The free flow arch methods available are

- Arch Bridges (Biery and Delleur) (*p. 33*): An orifice type of equation is used to describe the discharge through the bridge. The equation is derived under the assumption of a rectangular channel and is based on a single span arch opening. Multiple arch openings are handled by a simple multiplication factor.
- Arch Bridges (Hydraulics Research (HR) method) (*p. 35*): The HR method is based on laboratory experiments of both single and multi spanned arch bridges in rectangular channels. The method uses tables describing the relation between the blockage ratio, the downstream Froude number and the upstream water level.

The methods than can be combined with both submergence and overflow methods are the following

- Energy Equation (*p. 40*): A standard step method where a backwater surface profile is determination is used to calculate the discharge through the bridge. The method takes the contraction and expansion loss for bridges of arbitrary shape into account. The method assumes sub-critical flow and may default to critical flow for steep water surface gradients.
- Federal Highway Administration (FHWA) WSPRO method (*p. 43*): The FHWA WSPRO method is based on the solution of the energy equation. Contraction loss is taken into account through the calculation of an effective flow length. Expansion losses are determined through the use of numerous experimentally based tables. The method takes the effect of eccentricity, skewness, wingwalls, embankment slope etc. into account through the use of these tables.
- US Bureau of Public Roads (USBPR) method (*p. 54*): The USBPR method estimates free-surface flow assuming normal depth conditions. the method is based on experiments and takes the effect of eccentricity, skewness and piers into account.

The submergence methods available are

- Pressure Flow, Federal Highway Administration method (*p. 56*): Two orifice equation descriptions are used. One for situations when the orifice is submerged downstream and modified equation for situations when only the upstream part of the orifice is submerged.





- MIKE 11 culvert: A standard MIKE 11 culvert description may be chosen for submergence flow. The culvert to be used is specified by the user. The culvert is only active if submergence occurs.
- Energy equation: The flow under the bridge is determined through a standard backwater step method. The flow is assumed to be in the sub-critical range and thus the method may default to critical flow. Both contraction and expansion loss is taken into account.

Overflow methods available are:

- Energy Equation: The flow over the bridge is determined through a standard backwater step method. The flow is assumed to be in the sub-critical range and thus the method may default to critical flow. Both contraction and expansion loss is taken into account.
- Road overflow, Federal Highway Administration method (p. 58): The overflow is modelled using a weir equation taking tail water submergence into account through the use of a submergence coefficient. The method may be used for both gravel and paved surfaces.
- MIKE 11 weir: A standard MIKE 11 weir description may be chosen for overflow. The weir to be used is specified by the user. The weir is only active if overflow occurs.

Finally there are two additional bridge types which are not pre-processed prior to the simulation. These bridge types form part of a separate module.

- Bridge Piers (D'Aubuisson) (p. 36): The discharge is determined based on a momentum equation assuming no bed slope and that the friction loss is negligible. The method can handle pure rectangular channel descriptions but also gives the option of using cross sections of arbitrary shape.
- Fully submerged bridges (p. 60): The fully submerged takes the drag of the fully submerged bridge into account. Friction is neglected and the bed is assumed horizontal through the bridge.

### 1.5.1 Arch Bridges (Biery and Delleur)

The Biery and Delleur method is specially designed for semi circular arch bridges. It does not consider skewness, eccentricity, entrance rounding or piers (/10/). The method is based on experiments carried out for a rectangular channel.

The discharge, Q, through a semicircular arch in a rectangular channel is calculated from:

$$Q = 0,7083 C_D (2g)^{1/2} Y_{us}^{3/2} b \left[ 1 - 0,1294 \left( \frac{Y_{us-Lim}}{r} \right)^2 - 0,0177 \left( \frac{Y_{us-Lim}}{r} \right)^4 \right] \quad (1.34)$$



where

$C_D$  Coefficient of discharge.

$g$  Acceleration due to gravity.

$Y_{us}$  Average water depth upstream of the bridge (=  $\text{Area}_{us}/\text{Width}_{us}$ ).

$b$  Opening width of the arch.

$r$  Radius of curvature.

Given that the discharge will decrease for high values of  $Y_{us}$  a limit corresponding to the maximum discharge is set for  $Y_{us-Lim}$  :

$$Y_{us-Lim} = \begin{cases} Y_{us} & \text{for } \frac{Y_{us}}{r} < 1,49555 \\ 1,49555r & \text{for } \frac{Y_{us}}{r} \geq 1,49555 \end{cases} \quad (1.35)$$

The upstream depth  $Y_{us}$  is taken as the average depth in the upstream cross section. Upstream direction is based on the water level gradient. The coefficient of discharge  $C_D$  varies with the bridge opening ratio  $M$  and the downstream Froude number  $F_{ds}$ . The default table in MIKE 11 is for a semicircular arch models (1/3).

The downstream Froude number  $F_{ds}$  is given by:

$$F_{ds} = \frac{Q}{A_{ds} \sqrt{g Y_{ds}}} \sqrt{\alpha_{ds}} \quad (1.36)$$

Where

$Q$  Discharge.

$A_{ds}$  Total flow area of downstream cross section.

$\alpha_{ds}$  Velocity coefficient in downstream cross section (see eq. (1.55)).

$g$  Acceleration due to gravity.

$Y_{ds}$  Average depth in downstream cross section (=  $\text{Area}_{ds}/\text{Width}_{ds}$ ).



The bridge opening ratio  $M$  is defined as the ratio between  $b$  and  $B$  :

$$M = \frac{b}{B} \quad (1.37)$$

Where

$b$  Opening width of the arch (user defined).

$B$  Surface width at upstream cross section.

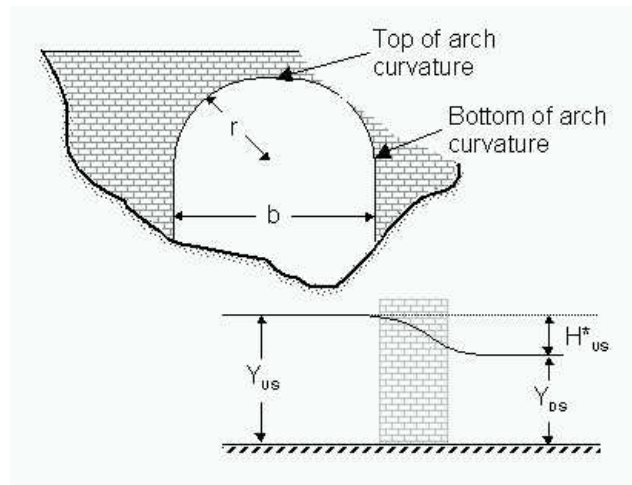


Figure 1.6 Hydraulic variables for Biery and Delleur and HR Arch Bridge.

The Biery and Delleur method assumes that the water surface is free i.e. submergence is not taken into account. If the bridge that is being modelled is submerged or over topped an alternative modelling method should be chosen.

## 1.5.2 Arch Bridges (Hydraulics Research (HR) method)

The Hydraulics Research method estimates the discharge through an arch bridge by the use of a table describing the relation between the upstream afflux, the blockage ratio and the Froude number. The upstream afflux is defined as the increase in water level from normal depth caused by the bridge. The afflux should theoretically be determined one bridge span upstream of the bridge. Thus as a rule of thumb the upstream cross section should be found one bridge span upstream the bridge opening. The default table in MIKE 11 is valid for semicircular arch models (/3/).

$H_{us}^*$  The afflux at the upstream cross section of the bridge.



$Y_{ds}$  Average depth of flow downstream the bridge ( $\text{Area}_{ds}/\text{Width}_{ds}$ ).

$J_{us}$  The upstream blockage ratio defined as  $J_{us} = \frac{b_{arch}}{b_{us}}$ .

$b_{arch}$  The user defined width of the arch.

$b_{us}$  Upstream water surface width.

$F_{ds}$  Froude number downstream of the bridge.

The upstream afflux is defined as:

$$H_{us}^* = h_{us} - h_{ds} - \left(\frac{Q}{K_{ds}}\right)^2 L_{us-ds} \quad (1.38)$$

Where:

$h_{us}$  Water level at upstream cross section.

$h_{ds}$  Water level at downstream cross section.

Q Discharge.

$K_{ds}$  Conveyance in downstream cross section.

$L_{us-ds}$  Distance from upstream to downstream cross section.

MIKE 11 determines the discharge based on the upstream and downstream water level. From the afflux and the upstream blockage ratio a Froude number can be determined through the use of the table expressing the relation between afflux and Froude number. For fixed water levels the Froude number depends solely on the discharge. Since the afflux depends on the discharge an iterative process is needed. If the iterative process does not converge the code defaults to critical discharge at the upstream cross section.

The hydraulic research method assumes that the water surface is free i.e. submergence is not taken into account. If the bridge that is being modelled is submerged or over topped an alternative modelling method should be chosen.

### 1.5.3 Bridge Piers (D'Aubuisson)

Bridge piers may be implemented in MIKE 11 using D'Aubuisson's formula (/10/). The governing equations for bridge piers are derived under the assumption that the bed slope is zero and the effect of the bed friction is negligible. Thus in order to minimise the errors introduced by these assumptions the user should place the cross sections upstream and downstream close to the bridge. Please note that this bridge type can only be implemented with a special module.



The code provides two alternatives for the implementation of this formula:

1. A rectangular channel analysis is used if a positive value is entered for the upstream width of the channel (see section Bridges in the User Guide). D'Aubuisson's formula for a rectangular channel reads

$$H_2 - H_1 = \frac{Q^2}{2g} \left[ \frac{1}{C^2 (b_2 - w_{piers})^2 h_1^2} - \frac{1}{b_2^2 (h_1 + \Delta h)^2} \right] \quad (1.39)$$

where

- Q discharge at the bridge piers.
- $H_1$  water level downstream of piers.
- $H_2$  water level upstream of piers.
- C user defined constant determined by pier geometry.
- $b_2$  user defined channel width upstream of piers.
- $h_1$  local water depth downstream of piers.
- $w_{piers}$  total width of piers.

2. If a non-positive value is entered for the upstream width of the channel (see section Bridges in the User Guide) a momentum equation is solved which takes the effect of an arbitrary shape of the cross section into account:

$$H_2 - H_1 = \frac{Q^2}{2g} \left[ \frac{1}{C^2 (A_1 - h_1 w_{piers})^2} - \frac{1}{A_2^2} \right] \quad (1.40)$$

where

- $A_1$  cross sectional area downstream of bridge piers.
- $A_2$  cross sectional area upstream of bridge piers.



Note that if the Froude number is above the criteria of 0.6, the effect of the bridge piers is neglected. The criteria may be altered by setting the variable BRIDGE\_FROUDE\_CRITERIA in the MIKE11.ini file.

#### 1.5.4 Bridge Piers (Nagler)

The Nagler equation is experimentally based. The equation is applicable to bridge piers with different pier shapes. The pier shape is taken into account through a so-called coefficient of discharge which is found through a table

based on the pier type. The equation is derived from free flow experiments and is not accurate for high velocities (77).

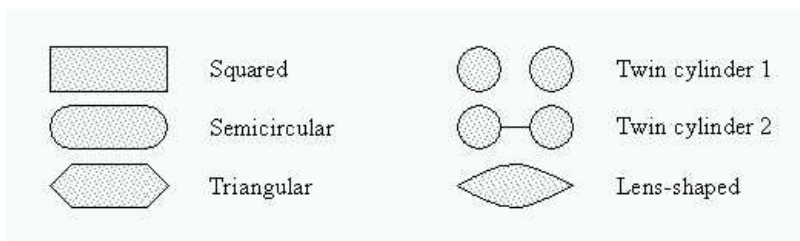


Figure 1.7 Type of pier shapes.

The Nagler equation reads:

$$\alpha = K_N b \sqrt{2g} \left( Y_{ds} - \theta \frac{V_{ds}^2}{2g} \right) \left( h_{us} - h_{ds} + \beta \frac{V_{us}^2}{2g} \right)^{1/2} \quad (1.41)$$

where:

$K_N$  Coefficient of discharge.

$\theta$  Adjustment factor (default 0.3).

$\beta$  Adjustment factor varies with the bridge opening ratio.

$g$  Acceleration due to gravity.

$Y_{ds}$  Depth downstream of the bridge.

$V_{us}$  Velocity upstream the bridge.

$V_{ds}$  Velocity downstream the bridge.

$h_{us}$  Water level in the upstream cross section.

$h_{ds}$  Water level in the downstream cross section.

$b$  The total bridge opening width excluding the piers.

The coefficient of discharge  $K_N$  varies with the bridge opening ratio  $M$  and the pier shape. The adjustment factor  $\beta$  varies with the bridge opening ratio  $M$  and the adjustment factor  $\theta$  can normally be taken as 0.3. The default tables in MIKE 11 are after Yarnell and Nagler.

The bridge opening ratio  $M$  is defined as the ratio between the flow width in the bridge and the flow width upstream of the bridge  $b/B$ .



$b$  Opening width of the arch.

$B$  Opening width at upstream cross section.

Eq. (1.41) can be rewritten as a polynomial of third degree in the discharge squared. In case of multiple roots the smallest positive root is chosen as the solution.

The structure area is defined as the arch width times the minimum water depth upstream or downstream.

### 1.5.5 Bridge Piers (Yarnell)

Like the Nagler equation, the Yarnell equation considers different pier shapes (see Figure 1.7). The pier shape is accounted for through the so-called pier coefficient. The Yarnell equation is a pure experimentally based equation. The equation assumes free flow. Thus if submergence and possible overtopping is to be modelled an alternative method should be used.

The Yarnell equation reads:

$$h_{us} - h_{ds} = KY_{ds} F_{ds}^2 (K + 5F_{ds}^2 - 0,6)(\alpha + 15\alpha^4) \quad (1.42)$$

$$F_{ds}^2 = \frac{Q^2}{A_{ds}^2 2gY_{ds}} \quad (1.43)$$

$$\alpha = 1 - \frac{b}{B_{us}} \quad (1.44)$$

where

$K$  Yarnell's Piers shape Coefficient.

$g$  Acceleration due to gravity.

$Y_{ds}$  Depth downstream the bridge.

$F_{ds}$  Froude number downstream the bridge.

$\alpha$  Channel contraction ratio.

$A_{ds}$  Total flow area of downstream cross section.

$b$  The bridge opening width excluding the piers.

$B_{us}$  The width of the upstream cross section.

$h_{us}$  Water level in the upstream cross section.



$h_{ds}$  Water level in the downstream cross section.

The default tables for pier shape coefficient  $K$  are after Yarnell.

Eq. (1.42) may be re-written as a polynomial of second order in the Froude number squared. If multiple positive roots are present the greatest discharge is chosen.

The structure area is defined as the arch width times the minimum water depth upstream or downstream.

## 1.5.6 Energy Equation

The energy equation may be used to determine the discharge and the back water profile through the bridge. The energy equation takes friction loss and contraction/expansion losses into account. The method requires four cross sections (see Figure 1.8). River cross sections one and four are defined in the cross-section editor. Bridge cross sections two and three are defined through the bridge geometry in the network editor. Ideally the distance between the bridge and the up- and downstream cross-sections should be of the order  $b$ , where  $b$  is the bridge opening width. The latter is to ensure that the streamlines are parallel at section one and section four.

The equation solved from section  $i$  to  $i-1$  reads

$$h_{i-1} + h_{v(i-1)} = h_i + h_{vi} + h_{f(i,i-1)} + h_{e(i,i-1)} \quad (1.45)$$

where:

$h_i$  Water level at cross-section  $i$ .

$h_{vi}$  Velocity head at cross-section  $i$ .

$h_{f(i,i-1)}$  Friction losses between cross-section  $i$  and  $i-1$ .

$h_{e(i,i-1)}$  Expansion losses between cross-section  $i$  and  $i-1$ .

The velocity head is defined as

$$h_v = \frac{\alpha Q^2}{2gA^2} \quad (1.46)$$





with the velocity distribution coefficient defined as

$$\alpha = \frac{\sum_{i=1}^N (k_i^3 / a_i^2)}{K^3 / A^3} \quad (1.47)$$

$$k_i = \frac{a_i r_i^{2/3}}{n_i} \quad (1.48)$$

$$K = \sum_{i=1}^N k_i \quad (1.49)$$

$$A = \sum_{i=1}^N a_i \quad (1.50)$$

Where

$Q$  Discharge at the section.

$\alpha$  Velocity distribution coefficient.

$k$  Subsection conveyance.

$a$  Subsection area.

$K$  Total cross section conveyance.

$A$  Total cross section area.

$r$  Hydraulic radius.

$n$  Manning's roughness coefficient.

$N$  Number of subsections.

Eq. (1.55) is based on a parallel channel analysis. Each parallel channel being defined through subsections. A subsection is understood as segments in series with a constant relative resistance. Further a sub-division may also be achieved through the use of markers 4 and 5. Thus for a cross section with constant relative resistance and no markers 4 or 5 the velocity coefficient is unity.



### Friction loss

The friction loss between cross-sections  $i$  and  $i-1$  is calculated from:

$$h_{f(i,i-1)} = \frac{L_{i,i-1} Q^2}{K_i K_{i-1}} \quad (1.51)$$

Where:

$L_{i,i-1}$  The flow length in the approach reach.

$K_i$  The conveyance for cross-section  $i$ .

### Expansion/Contraction loss

Expansion/contraction losses are only considered from section 4 to section 3 and from section 2 to section 1. The expansion/contraction loss from section  $i$  to section  $i-1$  is expressed as

$$h_{e(i,i-1)} = C \left| \frac{\alpha_i V_i^2}{2g} - \frac{\alpha_{i-1} V_{i-1}^2}{2g} \right| \quad (1.52)$$

where  $C$  is the contraction/expansion coefficient. This coefficient is non-dimensional and is user defined with a value between 0 and 1. The default values are 0.3 for contraction and 0.5 for expansion indicating that the losses due to expansion are typically larger than the losses due to contraction.

### The solution method

The energy equation method assumes that the flow through the bridge is sub-critical. Further the method is an iterative method. The bridges are pre-calculated based on a set of values for the water levels upstream and downstream. Thus for each set of water level values a discharge is to be determined. The algorithm for determining the discharge has the following steps:

1. Initial guess for the discharge.
2. Backwater calculation from section 4 to section 3.
3. Backwater calculation from section 3 to section 2 based on the result from step 2.
4. Backwater calculation from section 2 to section 1 based on the result from step 3.
5. The water level determined through step 4 is compared with the actual water level at section 1.



6. Based on the comparison in step 5 the discharge is either modified and the algorithm returns to step 2 or the algorithm terminates if the deviation is within acceptable limits.

Throughout the calculation the results are compared with critical flow. If the solution found is below critical water level or if one of the steps 2 - 4 do not converge the code defaults to critical flow at that location. Further if the maximum number of iterations (default 50) is reached without obtaining a valid solution the code defaults to critical flow at section one.

### 1.5.7 Federal Highway Administration (FHWA) WSPRO method

The computations of the Federal Highway Administration's WSPRO computer program have been adapted for the calculation of free-surface flow. Some modifications have been necessary in order to fit the MIKE 11 terminology.

The method is based on a standard step method using the energy equation to find the discharge and the backwater water surface profile through the bridge. The method requires four cross sections (see Figure 1.8). River cross sections one and four are defined in the cross-section editor. Bridge cross sections two and three are defined through the bridge geometry in the network editor. Ideally the distance between the bridge and the up- and downstream cross-sections should be of the order  $b$ , where  $b$  is the bridge opening width.

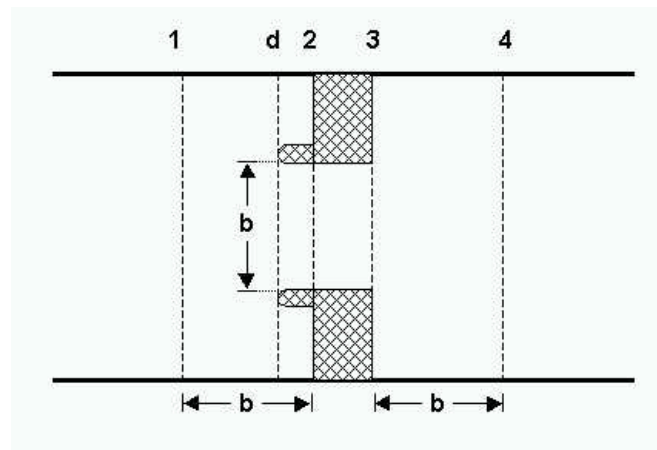


Figure 1.8 Location of cross-sections.

The total energy equation between section one and four can be written:

$$h_1 + h_{v1} = h_4 + h_{v4} + h_f + h_e \quad (1.53)$$



where:

$h_1$  Water level at cross-section 1.

$h_{v1}$  Velocity head at cross-section 1.

$h_4$  Water level at cross-section 4.

$h_{v4}$  Velocity head at cross-section 4.

$h_f$  Friction losses between cross-section 1 and 4.

$h_e$  Expansion losses between cross-section 3 and 4.

The velocity head is defined as

$$h_v = \frac{\alpha Q^2}{2gA^2} \quad (1.54)$$

with the velocity distribution coefficient defined as

$$\alpha = \frac{\sum_{i=1}^N (k_i^3 / a_i^2)}{K^3 / A^3} \quad (1.55)$$

$$k_i = \frac{a_i r_i^{2/3}}{n_i} \quad (1.56)$$

$$K = \sum_{i=1}^N k_i \quad (1.57)$$

$$A = \sum_{i=1}^N a_i \quad (1.58)$$

Where

$Q$  Discharge at the section.

$\alpha$  Velocity distribution coefficient.

$k$  Subsection conveyance.

$a$  Subsection area.

$K$  Total cross section conveyance.



$A$ Total cross section area.

$r$ Hydraulic radius.

$n$ Manning's roughness coefficient.

$N$ Number of subsections.

Eq. (1.55) is based on a parallel channel analysis. Each parallel channel being defined through subsections. A subsection is understood as segments in series with a constant relative resistance. Further a sub-division may also be achieved through the use of markers 4 and 5. Thus for a cross section with constant relative resistance and no markers 4 or 5 the velocity coefficient is unity.

### Friction loss

Without spur dykes the friction loss between cross-sections 1 and 2 is calculated from:

$$h_{f(12)} = \frac{L_{av}Q^2}{K_1K_2} \quad (1.59)$$

With spur dykes the friction loss between cross-sections 1 and 2 is augmented with the friction along the dykes:

$$h_{f(12)} = \frac{L_{av}Q^2}{K_1K_2} + \frac{L_{d2}Q^2}{K_2K_2} \quad (1.60)$$

Where:

$L_{av}$ The effective flow length in the approach reach (see below).

$L_{d2}$ The spur dyke length.

$K_1$ The conveyance for cross-section 1.

$K_2$ The conveyance for cross-section 2.

The friction loss from section 2 to 3 is given by

$$h_{f(23)} = \frac{L_{waterway}Q^2}{K_2K_3} \quad (1.61)$$

Where:

$L_{waterway}$  is the distance from section 2 to section 3.



$K_3$  The conveyance for cross-section 3.

Finally the friction loss from section 3 to section 4 is given by

$$h_{f(34)} = \frac{L_{34} Q^2}{K_3 K_4} \quad (1.62)$$

Where:

$L_{34}$  The flow length from section 3 to 4.

$K_4$  The conveyance for cross-section 4.

### Effective flow length

The effective flow length is determined based on the conveyance distribution. The effective length is determined as the average length of 20 equal conveyance tubes. The conveyance is here taken as

$$K = \int_0^B M(H-z)^{5/3} dx \quad (1.63)$$

Eq. (1.63) is found by taking the limit of  $N$  parallel stream-tubes as  $N$  tends to infinity

$$\lim_{N \rightarrow \infty} \sum_{i=1}^N M_i A_i R_i^{2/3} = \lim_{N \rightarrow \infty} \sum_{i=1}^N M_i (H-z_i) \Delta x_i (H-z_i)^{2/3} \quad (1.64)$$

Using eq. (1.63) for determining the conveyance has the advantage that the locations of the equal conveyance tubes are well defined. Using eq. (1.63) one can express the location of the first tube as

$$\frac{K}{20} = \int_0^{x_1} M(H-z)^{5/3} dx \quad (1.65)$$

which is to be solved for  $x_1$ . For the second tube the equation to be solved is

$$\frac{K}{20} = \int_{x_1}^{x_2} M(H-z)^{5/3} dx \quad (1.66)$$

and so on for the remaining tubes.



The effective flow length is determined under the assumption that the water level in section 1 and 2 are equal. The error made here is minimal since the main contribution to the calculation of the effective flow length is the contraction width which typically does not vary strongly with the water level changes considered here.

Definition sketches of the assumed streamlines are shown in Figure 1.9 and Figure 1.10. The length of a stream tube depends on the location of the upstream cross section. If the upstream distance is greater than the optimal distance  $L_{opt}$  the length is calculated according to Figure 1.9. If the optimal length is greater than the physical distance the stream tubes are assumed to be located as sketched in Figure 1.10.

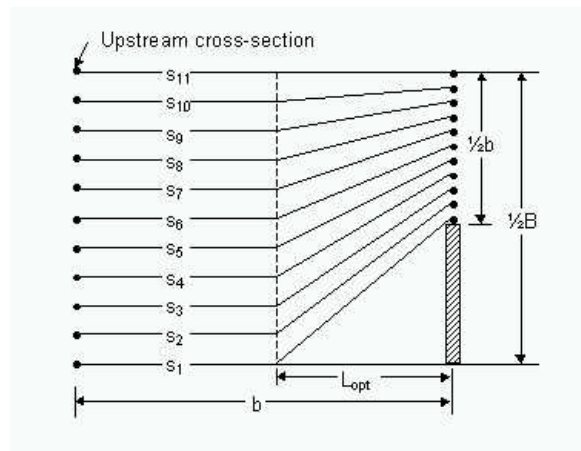


Figure 1.9 Definition sketch of assumed streamlines for low degrees of contraction.

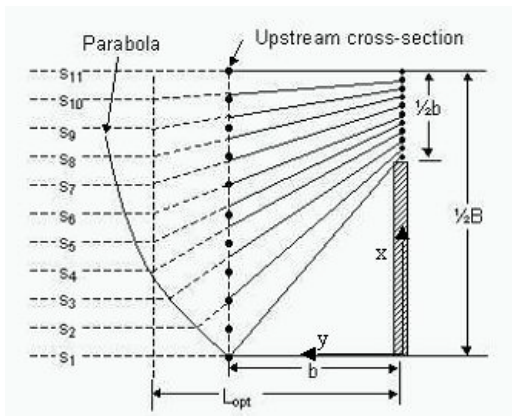


Figure 1.10 Definition sketch of assumed streamlines for high degrees of contraction.

The optimum length is defined as:

$$L_{opt} = \frac{b}{\pi(1-m')} \Phi \quad (1.67)$$

where

$$m' = 1 - b/B \quad (1.68)$$

$$\Phi = \frac{1}{2} \ln \left[ \left( \sqrt{\frac{8}{\varepsilon^2} + 8} - \frac{3}{\varepsilon} - \varepsilon \right) \left( -\sqrt{8 + 8\varepsilon^2} - 3\varepsilon - \frac{1}{\varepsilon} \right) \right] - \ln \left( \varepsilon - \frac{1}{\varepsilon} \right) \quad (1.69a)$$

$$\varepsilon = 1 + \delta + \sqrt{\delta^2 + 2\delta} \quad (1.69b)$$

$$\delta = \frac{2}{\tan^2 \left[ \left( 1 - \frac{b}{2B} \right) \pi \right]} \quad (1.69c)$$

Where:

$b$  The total bridge opening width excluding the piers.

$B$  The total width of the upstream cross section.





Effective flow length:

$$L_{av} = \frac{1}{20} \left[ \sum_{i=2}^{20} S_i + \frac{(S_1 + S_{21})}{2} \right] \quad (1.70)$$

In case the optimal length is greater than the physical distance a parabola is used to describe the stream tubes. Using a coordinate system as indicated in Figure 1.17 and the equation used for the right hand side of the channel is given by:

$$x = \frac{1}{2b}(y^2 - b^2) \quad (1.71)$$

similarly the left hand side uses a parabola described by

$$x = B - \frac{1}{2b}(y^2 - b^2) \quad (1.72)$$

### Expansion loss

The contraction loss from section 1 to 2 is taken into account through the use of an effective flow length as opposed to the physical distance from section 1 to section 2. No contraction or expansion loss is assumed from section 2 to 3. It is further assumed implicitly that from section 3 to section 4 only expansion takes place. If no expansion takes place the loss consists solely of the friction loss from section 3 to 4.

The expansion loss from section 3 to 4 is computed from:

$$h_e = \frac{Q^2}{2gA_4^2} \left[ 2\beta_4 - \alpha_4 - 2\beta_3 \left( \frac{A_4}{A_3} \right) + \alpha_3 \left( \frac{A_4}{A_3} \right)^2 \right] \quad (1.73)$$

$$\beta_3 = \frac{1}{C} \quad (1.74)$$

$$\alpha_3 = \frac{1}{C^2} \quad (1.75)$$

$$\beta_4 = \frac{\sum(k^2/a)}{K^2/A} \quad (1.76)$$

$$\alpha_4 = \frac{\sum(k^3/a^2)}{K^2/A^2} \quad (1.77)$$



Where:

$C$  Coefficient of discharge

$$k \text{ Subsection conveyance } k = Ma r^{2/3}$$

$a$  Subsection area

$$K \text{ Total cross section conveyance } K = \sum k$$

$$A \text{ Total cross section area } A = \sum a$$

Eqs. (1.76) and (1.77) are based on a parallel channel analysis. Each parallel channel being defined through subsections. A subsection is understood as segments in series with a constant relative resistance. Further a sub-division may also be achieved through the use of markers 4 and 5. Thus for a cross section with constant relative resistance and no markers 4 or 5 the velocity coefficient is unity.

### Coefficient of discharge

The coefficient of discharge is a function of the bridge geometry and flow characteristics. Four main types of openings are defined Figure 1.11 to Figure 1.14. For each opening type the coefficient of discharge,  $C$  is obtained by a base coefficient  $C'$  and a number of adjustment factors,  $k$ . The default base coefficients and adjustment factors in MIKE 11 are obtained as described by FHWA /9/.

The coefficient of discharge,  $C$  is given by:

$$C = C' \cdot k_F \cdot k_y \cdot k_x \cdot k_\theta \cdot k_e \cdot k_j \cdot k_a \cdot k_b \cdot k_d \tag{1.78}$$

Table 1.2 Adjustment factors

Adjustment factor		Type	Tabular function of:
$C'$	Base coefficient	All	$m$ , $L/b$ and slope
$k_F$	Froude number	I	$F_3$
$k_r$	Corner rounding	I	$m$ and $r/b$
$k_w$	Wingwall	I	$m$ , $w/b$ and $WW$
$k_y$	Average depth	II	$m$ , $(Y_a + Y_b)/(2b)$ and slope
$k_x$	Unwetted abutment	III	$x/b$ , $L/b$ and slope
$k_\theta$	Wingwall	IV	$m$ , $WW$ and slope
$k_e$	Eccentricity	All	$K_a/K_c$



Table 1.2 Adjustment factors

$k_j$	Piles	All	$m$ and $j$
$k_j$	Piers	All	$m$ , $L/b$ and $j$
$k_a$	Elliptical spur dike angularity	All	$m$ and $L_d/b$
$k_b$	Straight spur dike offset,	All	$m$ and $L_d/b_d$
$k_d$	Spur dike length	All	$m$ and $L_d/b$

Where:

$m$  Channel contraction ratio.

$L$  Bridge waterway flow length (length from section 2 to 3).

$b$  Bridge opening width.

$F_3$  Froude number in downstream bridge section.

$r$  Radius of corner rounding.

$w$  Wingwall width.

$W$  Wingwall angle.

$(Y_a + Y_b)/(2b)$  Average water level in bridge section.

$x$  Unwetted abutment length.

$K_a/K_c \leq 1$  Ratio of conveyance of the approach section on each side of the projected opening.

$j = A_p/A_3$  Portion of waterway blocked by piers/piles.

$L_d$  Spur dike length.

$b_d$  Spur dike offset.

The channel contraction ratio,  $m$  is given by:

$$m = 1 - \frac{K_q}{K_1} \quad (1.79)$$

Where:

$K_q$  The conveyance of that part of section 1 where conveyance discharge can flow through the bridge opening without contraction.

$K_1$  The total conveyance for cross-section 1.

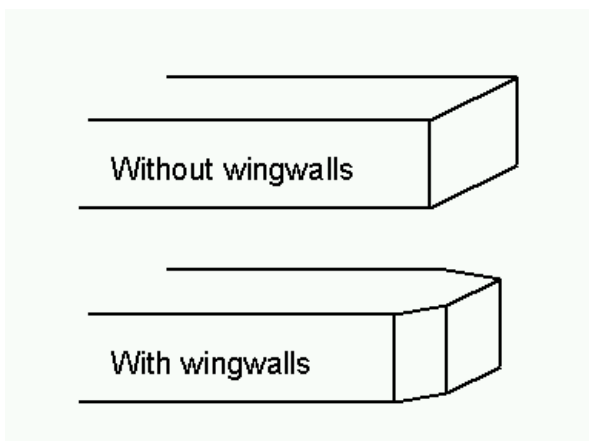


Figure 1.11 Definition sketch of type I opening, vertical embankments and vertical abutments, with or without wingwalls (after Matthai).

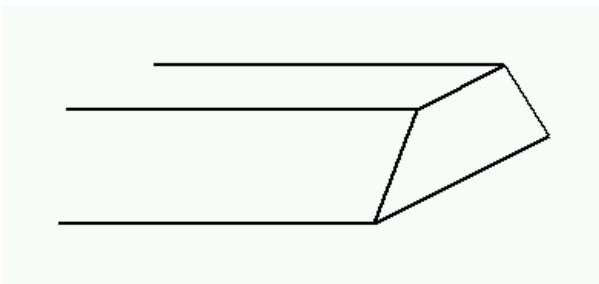


Figure 1.12 Definition sketch of type II opening, sloping embankments without wingwalls (after Matthai).

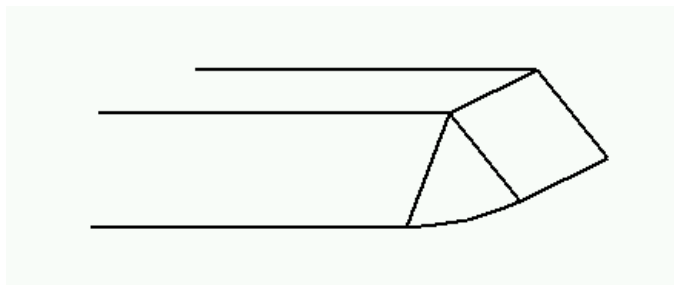


Figure 1.13 Definition sketch of type III opening, sloping embankments and sloping abutments (spillthrough) (after Matthai).

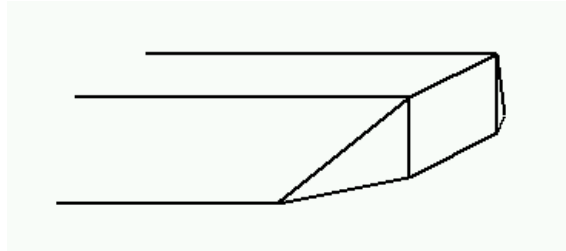


Figure 1.14 Definition sketch of type IV opening, sloping embankments and vertical abutments with wingwalls (after Matthai).

If the abutments are of different types a value of the coefficient of discharge is obtained through a weighted average:

$$C = \frac{C_L K_L + C_R K_R}{K_L + K_R} \quad (1.80)$$

Where:

$C_L$  Coefficient of discharge for left abutment.

$C_R$  Coefficient of discharge for right abutment.

$K_L$  Conveyance for left side.

$K_R$  Conveyance for right side.

#### The solution method

The method assumes that the flow through the bridge is sub-critical. Further the method is an iterative method. The bridges are pre-calculated based on a set of values for the water levels upstream and downstream. Thus for each set of water level values a discharge is to be determined. The algorithm for determining the discharge has the following steps:

1. Initial guess for the discharge.
2. Backwater calculation from section 4 to section 3.
3. Backwater calculation from section 3 to section 2 based on the result from step 2.
4. Backwater calculation from section 2 to section 1 based on the result from step 3.
5. The water level determined through step 4 is compared with the actual water level at section 1.



6. Based on the comparison in step 5 the discharge is either modified and the algorithm returns to step 2 or the algorithm terminates if the deviation is within acceptable limits.

Throughout the calculation the results are compared with critical flow. If the solution found is below critical water level or if one of the steps 2 - 4 do not converge the code defaults to critical flow at that location. Further if the maximum number of iterations (default 50) is reached without obtaining a valid solution the code defaults to critical flow at section one.

### 1.5.8 US Bureau of Public Roads (USBPR) method

The USBPR method estimates free-surface flow assuming normal depth conditions. The maximum afflux  $H_1^*$  at section 1 (see Figure 1.8) is here defined by:

$$H_1^* = k^* \frac{\alpha_2 V_{N2}^2}{2g} + \alpha_1 \left[ \left( \frac{A_{N2}}{A_4} \right)^2 - \left( \frac{A_{N2}}{A_1} \right)^2 \right] \frac{V_{N2}^2}{2g} \quad (1.81)$$

Where:

$k^*$  The backwater coefficient.

$V_{N2}$  Average velocity in bridge section at normal depth.

$A_{N2}$  Cross section area at normal depth.

$A_1$  Cross section area at section 1.

$A_4$  Cross section area at section 4.

$g$  Acceleration due to gravity.

$\alpha_1$  Velocity distribution coefficient - Equation (1.55).

$\alpha_2$  Velocity distribution coefficient for normal depth.

The velocity distribution coefficient,  $\alpha_2$  is a function of  $\alpha_1$  and the opening ratio. The opening ratio defined by

$$M = 1 - b/B \quad (1.82)$$

where  $b$  is the bridge opening width and  $B$  is the width of the upstream river cross-section. In MIKE 11 the coefficient is computed from a user defined table or the pre-computed default table.



The total backwater coefficient is given by:

$$k^* = k_b^* + \Delta k_e^* + \Delta k_\phi^* + \Delta k_p^* \quad (1.83)$$

Where:

$k_b^*$  Base coefficient. Tabular function of the opening ratio.

$\Delta k_e^*$  Eccentricity coefficient. Tabular function of the opening ratio and the eccentricity.

$\Delta k_\phi^*$  Skewness coefficient. Tabular function of the opening ratio and skewness angle  $\phi$ .

$\Delta k_p^*$  Bridge pier coefficient. Tabular function of opening ratio, the portion of waterway blocked by piers and pier type.

The eccentricity  $e$  is given by

$$e = \frac{\min(Q_{\text{left}}, Q_{\text{right}})}{\max(Q_{\text{left}}, Q_{\text{right}})} \quad (1.84)$$

where  $Q_{\text{left}}$ ,  $Q_{\text{right}}$  are the ratio of discharge of the approach section on each side of the projected opening. The portion of the waterway blocked by piers is user defined and should be understood as the ratio of the pier cross sectional area to the cross sectional area of the waterway without the piers.

The coefficients are computed in MIKE 11 from user defined tables or from the pre-computed default tables.

### 1.5.9 Multiple Waterway Opening

When working with multiple openings each opening is evaluated separately. Up- and downstream cross sections are reduced to the part found in between the stagnation points. The stagnation points are the points in the cross section where the flow splits up between the different water way openings. The default stagnation points are evaluated strictly from a geometric point of view. The default stagnation points are set so each sub cross section satisfies:

$$B_{\text{sub}} = \frac{b}{b_{\text{Total}}} B_{\text{total}} \quad (1.85)$$

Where:

$B_{\text{sub}}$  Width of sub cross section.

$b$  Bridge opening width from marker 1 to 3



$b_{Total}$  Total width of all bridge openings.

$B_{Total}$  Total width of cross section from marker 1 to 3.

The user can set the stagnation points if desired.

### 1.5.10 Pressure Flow, Federal Highway Administration method

During significant contact of the water surface with the girders of the bridge structure, free-surface flow cannot exist and pressure flow is established.

#### Fully Submerged Orifice flow

Discharge through the fully submerged bridge opening is computed by:

$$Q_{orifice} = C_D A_2 \sqrt{2g(h_1 - h_{f12} + h_{v1} - h_3)} \quad (1.86)$$

Where:

$A_2$  Flow area in the bridge opening.

$g$  Acceleration due to gravity.

$h_1$  Water level in the upstream cross section.

$h_{v1}$  Velocity head at cross-section 1.

$h_3$  Water level in the downstream bridge section.

$h_{f12}$  The friction loss from the upstream cross section to the upstream bridge section.

$C_D$  Discharge coefficient (default 0.8).

The friction loss is expressed as

$$h_{f12} = \frac{L_{12} Q_t^2}{K_1 K_2} \quad (1.87)$$

where the flow length is either the effective length or the physical length depending on the free bridge modelling method. The discharge  $Q_t$  is the total discharge including possible overflow. The conveyance at sections 1 and 2 are calculated as defined in eqs. (1.56)-(1.58).

The water level in sections 2 is given by

$$h_2 = h_1 - h_{f12} \quad (1.88)$$





and the water level at section 3 is obtained from solving the appropriate version of the energy equation from section 4 to section 4.

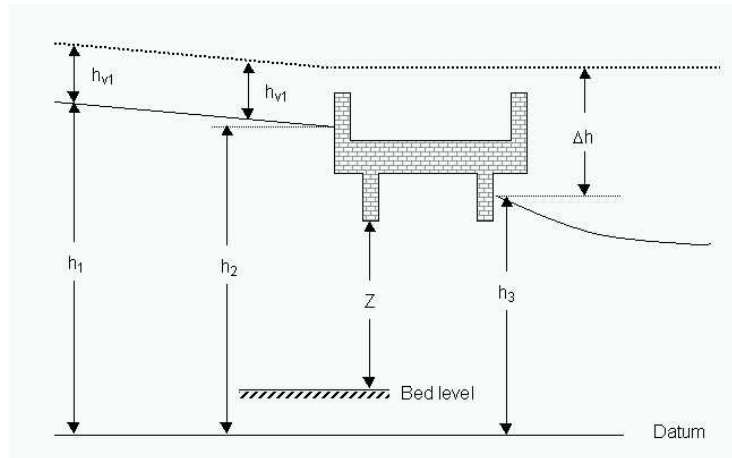


Figure 1.15 Definition sketch for submerged orifice flow.

### Orifice flow

If the water surface is only in contact with the bridge bottom on the upstream side of the bridge the discharge is found through:

$$Q = C_D A_2 \sqrt{2g(Y_2 - Z/2 + h_{v1})} \quad (1.89)$$

Where:

$C_D$  Discharge coefficient. Tabular function of  $Y_2/Z$ .

The quantities are defined in Figure 1.16 note that the bed level is defined as

$$\text{Bed Level} = b_{\text{bottom}} - Z \quad (1.90)$$

where  $b_{\text{bottom}}$  is the bridge bottom level and  $Z = A_2/B_2$ . The quantity  $A_2$  being the area at the opening and  $B_2$  is the width at the bridge bottom level.

Equation (1.89) may be rewritten as

$$Q = C_D A_2 \sqrt{2g\left(h_1 - h_{f12} + h_{v1} - \left(b_{\text{bottom}} - \frac{Z}{2}\right)\right)} \quad (1.91)$$

which is a form equivalent to equation (1.86). Note that the discharge coefficient in the two equations are different. To ensure a smooth transition from free orifice flow to submerged orifice flow a linear transition is made on the

discharge coefficient from free to submergence. That is for water levels below the level  $b_{bottom} - Z/2$  the free submergence coefficient is used whereas as the water level increases downstream and the orifice slowly becomes drowned the coefficient changes continuously into the fully submerged value. Further to avoid an abrupt change in the solution when the downstream water level reaches the bottom of the bridge the orifice equation is modified as

$$Q = C_D A_2 \sqrt{2g(h_1 - h_{f12} + h_{v1} - \hat{h}_3)} \quad (1.92)$$

where the modified downstream water level  $\hat{h}_3$  is given by

$$\hat{h}_3 = \min(h_3, b_{bottom} - Z/2) \quad (1.93)$$

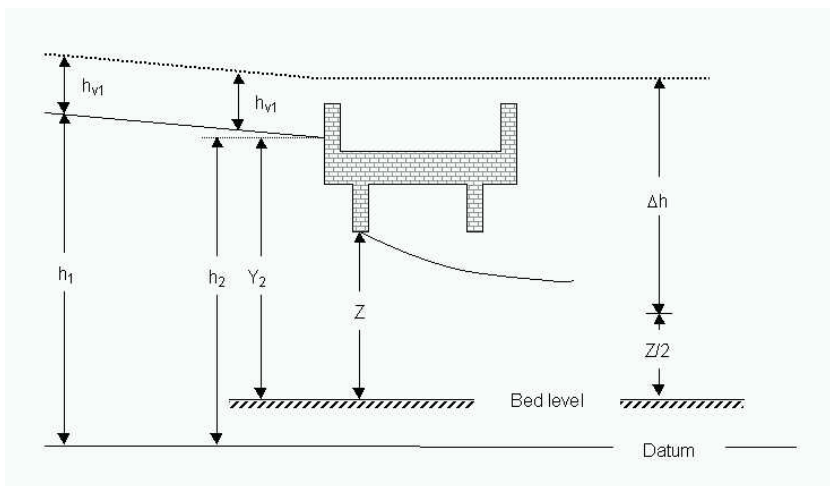


Figure 1.16 Definition sketch for orifice flow.

### 1.5.11 Road overflow, Federal Highway Administration method

When the water surface elevation exceeds the top bridge level the top part of the bridge is assumed to function as a weir. The discharge for the overflow part is computed using a weir formula:

$$Q = k_f C_f B_W H^{3/2} \quad (1.94)$$

Where:

$H$  Total head for weir flow with respect to bridge top level (see Figure 1.17).



$k_t$  Adjustment factor due to possible submergence from downstream water level. Tabular function of tail water level  $h_t$  and total head  $H$ .

$C_f$  Coefficient of free discharge. Tabular function of water depth on the structure  $h_s$ , the crest length in the flow direction  $L_R$  and the total head  $H$ .

$B_w$  Width of overflow part.

The submergence adjustment factor  $k_t$  depends on the ratio of minimum elevation along the top of the embankment  $h_t$  to the total head for weir flow  $H$ .

The total head for weir flow is given by:

$$H = h_1 + h_{v1} - L_{12} \frac{Q_{Tot}^2}{K_1^2} - h_{weir} \quad (1.95)$$

Where:

$h_1$  Water level at cross section 1.

$h_{v1}$  Velocity head at cross-section 1.

$L_{12}$  Distance between section 1 and section 2.

$Q_{Tot}$  Total discharge including under flow through the bridge.

$K_1$  Conveyance for cross-section 1.

$h_{weir}$  Crest level.

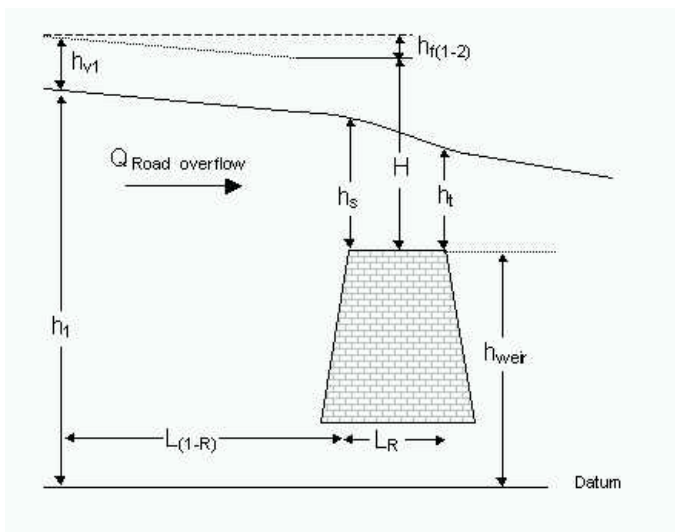


Figure 1.17 Definition sketch for road overflow.

### 1.5.12 Fully submerged bridges

As in the case of bridge piers there are two alternatives for the implementation of submerged bridges. Either the effect of the bridge is determined from a rectangular channel analysis or a momentum equation is solved which takes the effect of an arbitrary shape of the cross section into account.

As for the bridge piers the governing equations for a submerged bridge are derived under the assumption that the bed slope is zero and the effect of the bed friction is negligible. Thus in order to minimise the errors introduced by these assumptions the user should place the cross sections upstream and downstream close to the bridge.

The latter is used if a non-positive value for the channel width is entered (see Fully Submerged Bridge in the User Guide).

1. For a rectangular channel the momentum equation for a submerged bridge reads:

$$\frac{Q^2}{B} \left( \frac{1}{h_1} - \frac{1}{h_2} \right) + \frac{1}{2} g B (h_1^2 - h_2^2) = -\frac{1}{2} \frac{Q^2}{(A_1 - a_{bridge})^2} a_{bridge} C_L \quad (1.96)$$

where

Q discharge.



- $A$  cross sectional area.
- $B$  user defined surface width.
- $h$  local water depth.
- $a_{bridge}$  cross sectional area of submerged bridge.
- $C_D$  drag coefficient.
- $1,2$  indices referring to down-/upstream values respectively.

The terms on the left hand side of eq. (1.96) are the momentum terms and the force exerted by the pressure in the fluid the term on the right is the drag of the submerged bridge.

2. Eq. (1.96) is derived under the assumption of a rectangular channel, though the expression is easily modified to take the effect of non-rectangular channels into account. After this modification the momentum equation reads:

$$Q^2 \left( \frac{1}{A_1} - \frac{1}{A_2} \right) = \frac{1}{2} g \left( \int_0^{B_2} h_2^2 dy - \int_0^{B_1} h_1^2 dy \right) - \frac{1}{2} \frac{Q^2}{(A_1 - a_{bridge})^2} C_D a_{bridge} \quad (1.97)$$

For both eq.(1.96) and (1.97) a modification is applied for situations where the cross sectional area of the bridge is of the same order as the downstream cross sectional area. In such cases the drag will become very large causing among other things numerical problems. This is overcome by applying a suppression of the drag force for small values of  $A_1$ . The suppression is given by

$$\text{supp}_{\text{drag}} = \begin{cases} 0 & \text{for } 0 < \frac{A_1}{a_{bridge}} \leq 1,1 \\ 10 \frac{A_1}{a_{bridge}} - 11 & \text{for } 1,1 < \frac{A_1}{a_{bridge}} \leq 1,2 \\ 1 & \text{for } 1,2 < \frac{A_1}{a_{bridge}} \end{cases} \quad (1.98)$$

This suppression is applied to the drag force so that it is given by

$$-\text{supp}_{\text{drag}} \frac{1}{2} \frac{Q^2}{(A_1 - \text{supp}_{\text{drag}} a_{bridge})^2} C_D a_{bridge} \quad (1.99)$$

The reason for including the suppression factor also in the denominator is to avoid the singularity at  $A_1 = a_{bridge}$ . Please note that this suppression is

included only so that the simulation can continue at low flow conditions where it is very unlikely that the bridge is submerged i.e. the full equation is unphysical.

For both types of bridges the governing equation can be rearranged so that the discharge is a function of the water level up- and downstream respectively i.e.

$$Q = f(H_1, H_2) \quad (1.100)$$

The coefficients  $(\alpha, \beta, \gamma, \delta)$  in the numerical scheme are found by Taylor expanding eq. (1.100).

A bridge may generate steep gradients on the water level which may cause numerical instabilities. Therefore it is recommended to increase the parameter delta from its default setting of 0.5. This will have a dissipating effect on the solution thus smoothing out possible numerical wiggles caused by the bridge. If this shifting of the time centering is not applied a reduction of the time step may be necessary. An increase in the number of iterations at each time step may also be required if a forward centering in time is not applied.

Further even though eq. (1.100) gives a well defined expression for the discharge as a function of the up- and downstream water levels the expression does not secure an unambiguous expression for say the upstream water level as a function of the downstream water level and the discharge. In other words for a given value of the discharge and the downstream water level multiple solutions for the upstream water level may exist (this is an inherent feature of the non-linear equations governing the flow through the bridge). Thus in a dynamic solution one may encounter situations where one of the alternative solutions occur. A possible way of overcoming this is to decrease the time step.



Note that if the Froude number is above the criteria of 0.6, the effect of the submerged bridge is neglected. The criteria may be altered by setting the variable BRIDGE\_FROUDE\_CRITERIA in the MIKE11.ini file.

### 1.5.13 Trouble shooting for bridge structures

During the simulation the discharge through a bridge is determined from a pre-calculated table (except when using Fully submerged bridge and Bridge piers (D'Aubuisson's formula)). Each value in the table is found by an iteration process. Using a pre-calculated table decreases the calculation time.

#### Instability

For bridge structures a number of factors can result in instabilities.

**Time step:** In most cases it is helpful to decrease the MIKE 11 time step.



**Delta:** Delta is a default value in the HD editor. Increasing delta reduces instabilities. The delta value controls the time centering in the scheme.

**Bridge preprocessing:** To speed up simulations the bridges are preprocessed initially at simulation start. The generated H-Q-H tables are saved into files named using the bridge ID. In the present version the files are exported in the dfs2 format which can be readily viewed using standard tools within MIKE Zero. It is recommended to evaluate these files for consistency. Note that non-smooth H-Q-H surfaces may be caused by abrupt changes in bed friction or geometry. Further consult MIKE11.ini for further capabilities with regards to bridge preprocessing.

### Results

'Curtains': 'Curtains' in the result curve may be a result of the pre-calculated table. Increasing the resolution in the pre-calculated table will generally decrease the 'curtain' size. BRIDGE\_TABLE\_GRID\_UPSTREAM and BRIDGE\_TABLE\_GRID\_DOWNSTREAM in MIKE11.ini may be used to specify a different resolution for the water levels used for the pre-calculated tables. The default value is 0.1 meters. The value is given in meters.

## 1.6 Broad crested Weir

The standard formulations for flow over a broad crested weir are established automatically by the program on the basis of the weir geometry and the user specified head loss and calibration coefficients. These formulations assume a hydrostatic pressure distribution on the weir crests. Different algorithms are used for drowned flow and free overflow, with an automatic switching between the two, as described in the section A.10 Structures (p. 435).

## 1.7 Coefficients, HD default parameters

### ALPHA Coefficient

This is the velocity distribution coefficient used in the momentum equation, see section 1.30 Saint Venant Equations (p. 159). The default value is 1.0.

### DELH Coefficient

DELH controls the depth and top elevation of the slot in low flow conditions. The slot is inserted at height DELH above the river bottom and extends to a depth 5 x DELH below this level. See section 1.21 Kinematic Routing Method (p. 120). The default value is 0.1 m.

### DELHS Coefficient

DELHS is used to prevent instabilities arising when the water surface gradient across a structure changes sign, see section A.10.7 Drowned flow (p. 441). It specifies the water level difference across a weir below which the flow description is linearised to obtain a stable solution. The default value is 0.01 m.



### DELTA Coefficient

A forward centring of the  $\partial h/\partial x$ -term in the numerical scheme has a dissipating influence which can be demonstrated using the Taylor-series, see section A.4 DELTA Coefficient (p. 405). The forward centring is automatically introduced into MIKE 11 where the flow has become supercritical.

The dissipative influence of the forward centring can be controlled by the user for sub-critical flows through the coefficient DELTA ( $0.5 \leq \delta \leq 1$ ). A value of 0.5 (the default) has no dissipative effect, while a value of 1.0 has maximum influence.

Changing the value of DELTA from its default value should only be carried out when "short term" fluctuations are unimportant, as in the case of a wave with a period of several days or longer.

### EPS Coefficient

EPS is used in the diffusive wave approximation, see section A.9 Solution Scheme (p. 429) in Appendix A Appendix (p. 391). If the water surface slope becomes greater than EPS then the computational scheme becomes completely upstream centred. The default value is 0.0001.

### FroudeExp

MIKE 11 offers two alternatives to the suppression of the convective terms in the Momentum equation for supercritical flow. If a negative value is entered for FroudeExp or FroudeMax (see below) then the default suppression is applied. FroudeExp is the exponential coefficient in the alternative suppression term.

### FroudeMax

FroudeMax is the value at which the suppression sets in. As above if this is set to a negative value the default suppression is applied.

### Inter1Max

This coefficient gives the maximum number of iterations permitted per time step to obtain a solution at a structure, see section A.10 Structures (p. 435). The default value is 10.

### MaxIterSteady

MaxIterSteady gives the maximum number of iterations permitted at each time step to obtain a steady-state water profile solution for the initial conditions during an auto-start, see 1.20 Initial Conditions (p. 120) and 1.26 Quasi-Steady Solution (p. 129). The default value is 100.

### NODE Compatibility

This is a switch to select whether computations at nodes should be carried out with water level compatibility or with energy level compatibility. At present this switch should be set to the default setting of water level since the energy level compatibility has not yet been implemented.





### NoITER

NoITER specifies the number of iterations used in each time step to obtain a solution. The default value is 1. See section A.9 Solution Scheme (p. 429).

### THETA

THETA is a parameter used in the resistance term when discretising the momentum equation and is introduced because of the possible rapid variation and reversal of discharge, see section A.9.2 Momentum equation (p. 432). The default value is 1.

### Zeta Min

The head loss over structures is calculated according to section A.10 Structures (p. 435). The user has the option of specifying a minimum head loss, Zeta Min which is the lowest acceptable value of the sum of the head loss factors.

## 1.8 Computational Grid

### 1.8.1 General Description

Selection of the computational grid is without doubt the most important task in the modelling process. A carefully selected computational grid will avoid many problems during the calibration and application phase. It is, however, not possible to give detailed guidelines for how to design the computational grid for all cases. The design should be based on a thorough insight into the hydraulics of the area to be modelled and understanding of how the model works. Experience is therefore a key factor in the selection of the computational grid. Some general guidelines for the less experienced user are given below.

### 1.8.2 Selecting the Area to be Modelled

When selecting the extent of the area to be modelled the following should be taken into consideration:

- topographical/bathymetric data should be available for the entire area, see section 1.10 Cross-Sections (p. 75)
- at the model boundaries time series of water level or discharge or a rating curve should be available, see section 1.4 Boundary Conditions (p. 30)
- the boundary should be located at a sufficient distance from the area of interest to ensure that changes in the area of interest being investigated do not affect the boundary. This is of particular importance when the effects of major modifications to the river flow are being investigated, e.g. embankment and channelisation schemes.

### 1.8.3 Selecting Model Branches

Model branches in MIKE 11 represent flow paths, therefore in many cases it is quite clear where branches should be included in the model. The user must note that selection of model branches should be based on a compromise between computational time and level of detail. MIKE 11 is designed in such a way that it is relatively easy to include new model branches to existing set-ups, thus, in general, it is advisable to limit the number of branches in the initial setup and only include more branches, if required.

The following should be considered:

- tributaries can be included in a model setup either as model branches or as lateral inflows. The lateral inflow will cause almost no increase of computational time and will be sufficiently accurate for most minor tributaries. A tributary included as a model branch will give the correct routing (delay and attenuation) of the hydrograph, but will increase data requirements and computational time
- model branches are used in the schematisation of quasi 2-D flow between flood cells, see section 1.18 Flood Plains (*p. 115*).

### 1.8.4 Selecting the Grid Spacing

Given a hydraulic event to be modelled, the user has to determine the distance between grid points in the model. The inexperienced user should base this selection of grid spacing on trial and error. Ideally, the model should be run first with a very small grid spacing followed by runs with larger grid spacing. The coarsest grid spacing adopted should give only insignificant differences in the results compared with the fine grid simulation.

The stability conditions of the model depend mainly on the ratio between the time step and the grid spacing, see section 1.33 Stability Conditions (*p. 161*), i.e. when the space step is reduced it is also necessary to decrease the time step. The implication is that the computational time increases by a factor of 4 every time the space step is reduced by a factor of 2, thus the number of grid points should be kept as low as possible.

From a simplified analysis of the numerical scheme it is possible to find some theoretical guidelines for the selection of the grid spacing (see e.g. /1/). For instance, a certain number of grid points (about 30 to 50) per wave length is required to obtain a reasonable accuracy for the overall solution. In general the wave length(s) of a flow event can be expressed by

$$L = T\sqrt{gy} \quad (1.101)$$

where,

$L$  wave length



$T$  duration of event (wave period)

$y$  water depth

In smaller rivers which experience flash floods a representative "wave period" may be a few hours, thus a relatively small grid spacing will be required in order to resolve the flow events. In tidal flow with a period of more than 12 hours the wave length will mostly be very large implying that a very large (20-30 km) grid spacing may be applied. In practice, however, variability of the cross-sectional shape of the river, junctions with tributaries, etc. will require smaller grid spacing.

A relevant length scale for backwater effects is  $L = y/l_b$ , where  $l_b$  is bottom slope. In models where it is important to resolve backwater effects accurately the grid spacing should be selected in such a way that the grid spacing is at least 4-6 times smaller than this length scale.

## 1.9 Control Structures

Control Structures differ from other structure types in two important respects:

1. the structure may be described as either an underflow structure, an overflow structure or a radial gate or a sluice gate. Thus the structure may be described as either a movable weir or a sluice gate respectively;
2. as for dambreak structures, it is not possible to define beforehand the critical flow characteristic ( $Q-h$ ) relationship of the structure.

### 1.9.1 Hydraulic Aspects - Radial Gates

In MIKE 11 radial gates are automatically divided into an underflow part and an overflow part.

When specifying gate levels for at radial gate the user should specify the level for the underflow part, i.e. the level of the bottom of the gate, and the gate level for the overflow part is then calculated based on geometric considerations.

#### Flow calculated through underflow part of Radial gate.

Calculation of the flow through the underflow part depends on the flow regime at each time step.



For free flow conditions the discharge is calculated as:

$$Q_{free, underflow} = \tau \frac{\delta}{\sqrt{1 + \frac{\delta w}{y_1}}} a \sqrt{2gy_1} \quad (1.102)$$

where:

$\tau$  is a discharge calibration factor

$\delta$  is the contraction coefficient

$g$  acceleration of gravity

$y_1$  upstream water level

$w$  the vertical gate opening

$a$  the flow area through the gate (vertical gate opening multiplied with the width of the gate) and

The contraction coefficient,  $\delta$ , is computed as:

$$\delta = 1 - 0,75(\theta/90^\circ) + 0,36(\theta/90^\circ)^2 \quad (1.103)$$

Where  $\theta$  is the inclination angle of the gate relative to the canal bottom.

For submerged flow conditions the discharge is calculated as:

$$Q_{submerge, underflow} = \tau \frac{\delta}{\sqrt{1 - \left(\frac{\delta w}{y_1}\right)^2}} a \sqrt{2g(y_1 - y_2)} \quad (1.104)$$

where  $y_2$  is the downstream water level.

Determination of actual flow regime is made at each time step of the simulation using the user defined parameters; 'Tran.Bottom' and 'Tran.Depth' (specified in the Graphical Interface for Radial Gate structures).

Free flow occurs if:  $y_2 < y_{Limit} + y_{Tran, Bottom}$

Submerged flow occurs if:  $y_2 > y_{Limit} + y_{Tran, Bottom} + y_{Tran, Depth}$ .

Limiting level,  $y_{Limit}$  is calculated as:

$$y_{Limit} = \frac{\delta w}{2} \left[ \sqrt{1 + 16 \left( \frac{H}{\delta w} - 1 \right)} - 1 \right] \quad (1.105)$$



where  $H$  is the upstream energy head.

In the transition zone between free flow and submerged flow the discharge is calculated by using linear interpolation between (1.102) and (1.104).

### Flow calculated above the Radial gate top level.

If upstream water level is higher than the top of the radial gate then flow above the radial gate will occur. The overtopping flow is calculated as a function of the downstream water level conditions:

When downstream water level is lower than the top of the radial gate, the discharge is calculated using:

$$Q_{\text{Overflow}} = b\alpha y_1^\beta \quad (1.106)$$

where

$b$  is the width of the gate,  
 $\alpha$  and  $\beta$  are user defined coefficients ('Weir Coeff' and 'Weir Exp').

When the downstream water level is above the top of the gate the discharge is calculated using:

$$Q_{\text{Overflow}} = b\alpha y_1^\beta \left[ 1 - \left( \frac{y_2}{y_1} \right)^{\beta-0,385} \right]$$

## 1.9.2 Hydraulic Aspects -Sluice Gates

Sluice gates are physically similar to underflow gates.

The Sluice, Formula type of gate is an underflow gate for which four different flow regimes exist. Each of these four flow regimes are described with its own equation defining the discharge across the spillway. In addition to the flow beneath the gate an 'over-the-top' flow is added to the solution. This happens when the upstream water level exceeds the top of the gate. Which flow regime that applies in a given situation is determined by the values of up- and



downstream water level and the gate position. The different flow regimes and when they apply are listed in below table.

Table 1.3 Flow regimes

Flow Condition	Equation	Restriction	Remarks
Controlled Submerged (CS)	$y_c = aG_0 \left( \frac{H-h}{G_0} \right)^b$ $Q = L \sqrt{gy_c^3}$	$\frac{h}{G_0} \geq 1,0$	Also known as submerged orifice
Controlled Free (CF)	$y_c = aG_0 \left( \frac{H}{G_0} \right)^b$ $Q = L \sqrt{gy_c^3}$	$\frac{h}{G_0} < 1,0 \text{ \& } \frac{H}{G_0} \geq \frac{1}{K}$ $K = \frac{2}{3}$	Also known as free orifice
Un-controlled Submerged (US)	$y_c = aH \left( 1 - \frac{h}{H} \right)^b$ $Q = L \sqrt{gy_c^3}$	$\frac{h}{G_0} < 1,0, \frac{H}{G_0} < \frac{1}{K} \text{ \& } \frac{h}{H} \geq K$ $K = \frac{2}{3}$	Also known as submerged weir



Table 1.3 Flow regimes

Flow Condition	Equation	Restriction	Remarks
Un-controlled Free (UF)	$y_c = aH$ $Q = L\sqrt{gy_c^3}$	$\frac{h}{G_0} < 1, 0, \frac{H}{G_0} < \frac{1}{K} \text{ \& } \frac{h}{H} < K$ $K = \frac{2}{3}$	Also known as free weir
Over-the-top	$Q = L\sqrt{gy_c^3}$ $y_c = a(H - HG - G_0)$	$H > (HG + G_0)$	Computed as a free weir flow

H is the upstream water level measured above the sill level, h downstream water level measured above the sill level, g the acceleration of gravity,  $G_0$  the gate opening, Hg the height of the gate, L the spill way width,  $y_c$  the critical depth and Q the discharge. H, Hg, h and  $G_0$  are shown in below definition sketch.

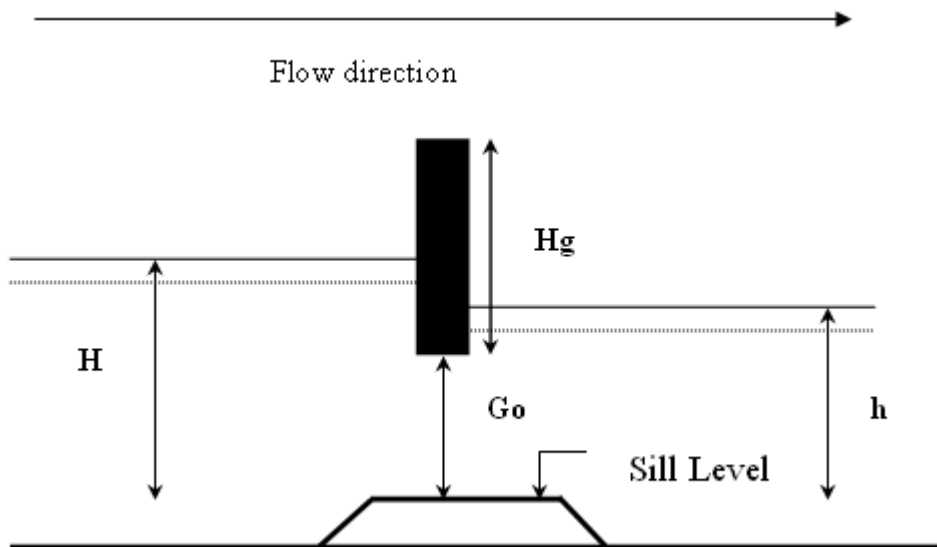


Figure 1.18 Definition sketch

In order to avoid instabilities due to too sharp limits between the different flow regimes it is possible to define an interval across which the solution varies from one flow type to another. This is done using the 'High Limit' and 'Low Limit' option supplied in the user interface.

### 1.9.3 Hydraulic Aspects - Overflow Structures

The calculation of the discharge over a movable weir is identical to that of dambreak structures, i.e. a broad crested weir. The only difference is that the structure width is assumed to remain constant for control and structures.

See section A.10 Structures (p. 435).

### 1.9.4 Hydraulic Aspects - Underflow Structures

The type of underflow structures considered in the control structure operation are rectangular in shape, with a vertical sliding or rotating section. The gate will only have a controlling influence on the flow if the gate level is lower than the upstream water level. If this is not the case, the discharge will be calculated assuming an overflow structure where crest level is taken as sill level, as described above.

If the upstream water level is higher than the gate level, the presence of the gate will force the passing water into a jet, the height of which is less than the gate height due to a severe convergence of streamlines just upstream of the





gate. At the point of maximum contraction, called the vena contracta, the streamlines are once again parallel to the bed, and a hydrostatic pressure distribution may be assumed to occur here, see Figure 1.19

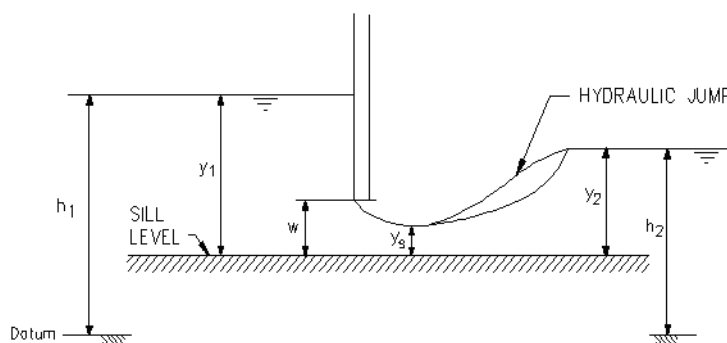


Figure 1.19 Flow under a vertical sluice gate

This contraction of the flow may cause the formation of supercritical flow in the region of the issuing jet. Should this occur in a channel with a high tail water level, a hydraulic jump may occur downstream of the gate. In either case, the discharge through the gate will be a function of the gate geometry and upstream water level only. This is termed free discharge.

As the tail water rises, the hydraulic jump moves upstream, towards the gate. When the jump reaches the gate, it will completely drown the supercritical jet, and the water level at this point will suddenly rise to the tail water depth. This change in the flow at this instant is discontinuous, due to the discontinuous nature of the hydraulic jump itself. At the point of change over, the discharge will suddenly decrease, and may only increase if the water level upstream of the gate also increases.

The minimum downstream water level at which the hydraulic jump is drowned may be calculated from the hydraulic jump equation:

$$y_2 = \frac{1}{2}y_s(\sqrt{1 + 8F^2} - 1) \quad (1.107)$$

where,  $y_s$  and  $y_2$  are the water depths (measured above the sill) at the vena contracta and immediately downstream respectively and  $F$  is the Froude number corresponding to  $y_s$ .



### 1.9.5 Free Flow

For a freely issuing jet (ie. not drowned), the gate discharge is a function of the gate geometry and upstream water level only. The magnitude of the discharge for a given opening will depend on the amount of contraction the jet experiences. The contraction coefficient,  $C_c$ , is a measure of this, and is defined as:

$$C_c = \frac{y_s}{\text{gate opening}(w)} \quad (1.108)$$

The contraction coefficient is dependent on the gate type: for a vertical sluice gate,  $C_c$  is in the region 0.61 - 0.63, whereas for a radial gate, the contraction coefficient is dependent on the gate level. The contraction coefficient is in MIKE 11 an input variable and is by default equal to 0.63.

Head losses across the structure are calculated from the standard MIKE 11 descriptions via the user defined values  $\zeta_{in}$  and  $\zeta_{out}$ , see section A.10 Structures (p. 435).

The inflow head loss is assumed to occur in the region of accelerating flow between the point upstream of the gate and the vena contracta. It would be expected to have a value between 0.0 and 0.50. The outflow head loss occurs in the region of flow expansion, between the vena contracta and the next downstream  $h$  point. Theoretical values of between 0.8 and 1.0 have been calculated for vertical sluice gates, but in practice they can be considerably higher (/14/).

If the flow is determined as free, the energy equation may be applied between the point upstream of the structure and the vena contracta, to yield the free discharge through the gate. Assuming, as in most cases, a zero inflow head loss, it can be shown that this equation is equivalent to the generally accepted form of the vertical sluice equation viz: (/11/)

$$Q = C_d b w \sqrt{2gy_1} \quad (1.109)$$

where,  $b$  is the gate width and  $C_d$  is the effective discharge coefficient, calculated from:

$$C_d = \frac{C_c}{\sqrt{1 + C_c \frac{w}{y_1}}} \quad (1.110)$$



## 1.9.6 Drowned Flow

If drowned discharge is detected, the energy equation is applied between points upstream and downstream of the structure. Note that in calculating the energy losses, the existence of a 'submerged' vena contracta is assumed, overlaid by a body of still water. The energy equation in this form corresponds to the submerged orifice equation of the form:

$$Q = C_d w b \sqrt{2g(h_1 - h_2)} \quad (1.111)$$

where,  $C_d$  is the effective discharge coefficient and  $h_1$  and  $h_2$  are upstream and downstream water elevations respectively.

As mentioned previously, the change between free and submerged flow is discontinuous in nature, the free discharge being greater than the corresponding drowned discharge for the same water levels and gate opening. Such discontinuities will present numerical problems during a computation which may lead to instabilities and eventual termination of the computation. Hence in MIKE 11, a coefficient,  $\psi$ , has been introduced in order to make a smooth transition. By use of this coefficient it is possible to expand the transition zone from free flow to drowned flow. The transition zone is defined as:

$$\frac{1}{2}y_s(\sqrt{1 + 8F^2} - 1)(1 - \psi) \leq y_2 < \frac{1}{2}y_2(\sqrt{1 + 8F^2} - 1)(1 + \psi) \quad (1.112)$$

When downstream water level,  $y_2$ , is within this interval the discharge through the structure will be calculated using an interpolation between the free flow equation and the drowned flow equation. The value of  $\psi$  can be set in the MIKE11.ini file placed in the windows directory. The default value is zero corresponding to a discontinuity when changing from free flow to drowned flow. The user should only change this value if instabilities are encountered during the simulation. A rule is that the value of  $\psi$  should be as low as possible. A first guess at the value of  $\psi$  could be 0.01.

## 1.10 Cross-Sections

The topographical description of the area to be modelled is achieved through the specification of cross-sections of the channel (and flood plain) which lie approximately perpendicular to the direction of flow.

Cross-sections are specified by a number of x-z co-ordinates where x is the transverse distance from a fixed point (often left bank top) and z is the corresponding bed elevation. A resistance value (Relative resistance or actual resistance number) can be specified for each pair of co-ordinates (see section 1.3 Bed Resistance (*p. 18*)). The transverse extent of each cross-section depends on whether the flood plain is to be simulated and by what method (see section 1.18 Flood Plains (*p. 115*)).



The number of cross-sections required is determined from both physical and mathematical requirements. The latter are discussed under section 1.8 Computational Grid (p. 65) and section 1.33 Stability Conditions (p. 161). Physically there should be a sufficient number of cross-sections to define adequately the variation in channel shape along each model branch.

The x-z co-ordinates are entered as raw data in the Cross Section editor. The raw data are then automatically processed into a form used in the hydrodynamic calculations, i.e. the hydraulic parameters; cross-sectional area, hydraulic radius and width are calculated for a number of elevations between a minimum and a maximum which are either determined automatically or defined by the user. The processed data may be edited from the processed data editor where two additional hydraulic parameters appear, additional flooded areas and the resistance factor. These are described respectively under the keywords Bed Resistance (p. 18) and Flooded Areas, (Storage) (p. 99).

If, during a simulation, the water level rises above the maximum elevation in the processed data table, the hydraulic area is calculated by assuming the river banks extend vertically upward, (Figure 1.20). Thus, the width remains constant for increasing water levels above the maximum specified elevation. This facility is intended to prevent a simulation from crashing if any initial instabilities occur and not to accommodate a lack of knowledge concerning the cross-section geometry. An error message will occur if the water level becomes more than N times higher than the maximum elevation and the simulation is terminated. Where N by default is 4 but may be changed in the 'MIKE11.ini' file see Appendix B.

It is strongly recommended that, in defining the cross-section geometry, the maximum elevation is specified in such a way that the cross-section will accommodate the maximum expected water levels.

There are two circumstances where care is required:

1. where the processed width value has been adjusted to accommodate flooded areas (see also section 1.15 Flooded Areas, (Storage) (p. 99)). This will affect the way in which cross-sectional area is calculated for water levels above the maximum elevation mentioned above and described below. Calculation of area above maximum specified.

The cross-sectional area,  $A_{new}$  at  $h_{new}$  is given by:

$$A_{new} = A_{max} + (h_{new} - h_{max}) W_{max}$$

where,

$h_{max}$  is the maximum specified elevation

$W_{max}$  is the width at  $h_{max}$



$A_{max}$  is the cross-sectional area at  $h_{max}$

2. Thus, for example, if  $W_{max}$  has been set to zero in the specification of flooded areas then, for all water levels greater than  $h_{max}$ , the cross-sectional areas will remain constant and equal to  $A_{max}$ .

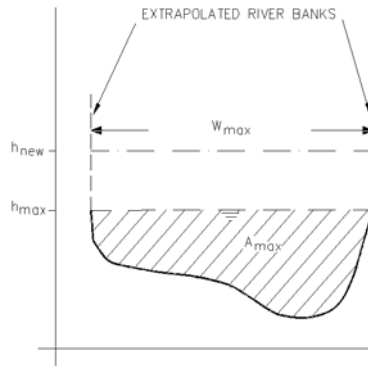


Figure 1.20 Calculation of area above maximum specified height

Where a relative resistance different from 1.0 has been specified in the raw data e.g. in the flood plain, an incorrect area-elevation relationship will result for water levels in excess of the maximum elevation specified. This is illustrated in Figure 1.21a and Figure 1.21b, depicting the same cross-section but where, in Figure 1.21a, the maximum elevation specified,  $h_{max}$ , is below the highest water level occurring. In this instance the calculated effective area does not account for the relative resistance. In Figure 1.21b, the highest occurring water level is below  $h_{max}$  and the effective area is correctly calculated

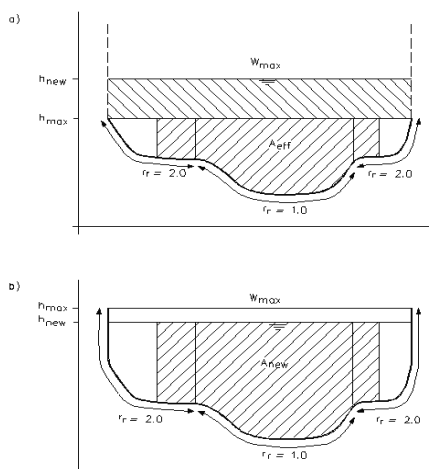


Figure 1.21 Calculation of cross-sectional area for relative resistance values larger than 1.0.  
 a) Highest water level above maximum specified elevation  
 b) Highest water level below maximum specified elevation

## 1.11 Closed Cross sections, Modelling the Pressurised flow

Pressurised flow computations are facilitated through implementation of a narrow 'slot', as a vertical extension of a closed pipe cross section. Free surface and pressurised flows are thus described within the same basic algorithm, which ensures a smooth and stable transition between the two flow types.

The full flow capacity of a closed conduit (pipe) can be defined as a discharge at which the flow depth is equal to the conduit height. Any further increase of discharge fundamentally changes the conditions of flow, i.e. basic assumptions for the derivation of the Saint Venant equations are not valid. Namely, the flow changes from the free surface flow to the pressurised flow.

However, it is possible to generalise the equations for free surface flow, so that the pressurised flow in closed conduits is covered. This is done by introducing a fictitious slot in the top of the conduit, see figure 1.22.

The idea of introducing a fictitious slot was first presented by Preissmann and Cunge, 1961, and has since been used by Cunge and Wagner, 1964 (see ref. /15/).

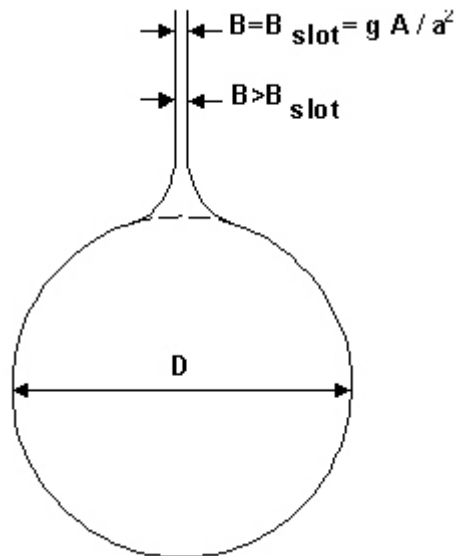


Figure 1.22 Pipe section with fictitious top slot, usually referred to as a 'Preissmann' slot.

The derivation of pressurised flow conditions for free surface flow equations can be obtained from the continuity equation which can be written as:

$$-\frac{\partial(\rho Q)}{\partial x} dx dt = \frac{\partial(\rho A)}{\partial t} dx dt \quad (1.113)$$

assuming the density of water,  $\rho$ , constant over the cross section.

By partial differentiation is found:

$$\frac{\partial Q}{\partial x} + \frac{Q}{\rho} \cdot \frac{\partial \rho}{\partial x} + \frac{\partial A}{\partial t} + \frac{A}{\rho} \cdot \frac{\partial \rho}{\partial t} = 0 \quad (1.114)$$

For a circular pipe, it can be shown that the density of the water can be approximated as:

$$\rho \approx \rho_0 \left( 1 + \frac{g(y-D)}{a_0^2} \right) \quad (1.115)$$

where:

- $\rho$  the density of water for a free surface flow [ $\text{kg/m}^3$ ]
- $a_0$  the speed of sound in water [ $\text{m/s}$ ]
- $y$  the water depth [ $\text{m}$ ]



D the pipe diameter [m].

Furthermore, it can be shown that the cross-sectional area in the case of the excess pressure  $g(y-D)$  approximately equals to:

$$A \approx A_0 \left( 1 + \frac{g(y-D)}{a_r^2} \right) \quad (1.116)$$

where:

$A_0$  = the area without excess pressure and  $a_r$  is given as:

$$a_r = \sqrt{\frac{E_r \cdot e}{\rho_0 \cdot D}} \quad (1.117)$$

with:

$E_r$  = the Young's modulus of elasticity, [N/m<sup>2</sup>]

$e$  = the pipe wall thickness, [m].

The  $a_r$  has the dimension [ms<sup>-1</sup>], and is in the order of 1400 [ms<sup>-1</sup>] for most concrete pipes.

Combining these equations yields:

$$\frac{\partial A}{\partial t} + \frac{A}{\rho} \cdot \frac{\partial \rho}{\partial t} = g \cdot A \frac{\partial y}{\partial t} \left( \frac{1}{a_r^2} + \frac{1}{a_0^2} \right) = \frac{gA_0}{a^2} \cdot \frac{\partial y}{\partial t} \quad (1.118)$$

where:

$$a = \frac{a_0}{\sqrt{1 + (a_0^2/a_r^2)}} \quad (1.119)$$

' $a$ ' represents the speed of sound in water considering the compressibility of water and the deformation of the pipe wall.

Equation (3.10) can now be written as:

$$\frac{\partial Q}{\partial x} + \frac{Q}{\rho} \cdot \frac{\partial \rho}{\partial x} + \frac{gA_0}{a^2} \cdot \frac{\partial y}{\partial t} = 0 \quad (1.120)$$





The analogy with the continuity equation can thus be maintained in case that the fictitious slot width  $b_{slot}$  is specified as:

$$b_{slot} = g \cdot \frac{A_0}{a^2} \quad (1.121)$$

'a' is in the order of 1000 [m/s] for most pipes.

In order to obtain a smooth transition between the free surface flow computations and pressurised flow computations, it is required to apply a "soft" transition between the actual pipe geometry and the fictitious slot. Such a "smooth" transition has been designed based on a series of tests with various slot configurations. The slot configuration thus obtained ensures stable computations without affecting the accuracy significantly. The applied slot width is larger than the theoretical value. The default relation between relative depth and the slot width as implemented in MIKE 11 is given in table 1.4

Table 1.4 Relation between relative Depth and top slot width

$y/D$	$b_{slot}/D$ (D=1 m)
0.98	0.36
1.00	0.19
1.10	0.0166
1.20	0.0151
1.50	0.0105
> 1.50	0.0100

Similar principles apply for generating Preissmann slots for the closed rectangular and closed irregular section types. The width of Preissmann slot for irregular closed sections are defined as 10% of maximum width in closed section.

## 1.12 Culverts, Q-h Relations Calculation

The Culverts Q-h Relations calculation are included in order for a pre-calculation of free-flow relationship for culverts. Following key issues are to be noted on the calculation of Q-h relations:

- the Q-h relationships are calculated by MIKE 11 using the culvert definitions and cross sections up- and downstream. If, for some reason it is required to adjust the calculated values it is possible to change the values in the table and save the network file.
- the culvert can be assigned a length, friction coefficient, slope and bend loss coefficient in addition to the conventional parameters



- the culvert cross-section can be defined by a standard shape (e.g. circle or rectangle) as well as an irregular shape. Surveyed culvert geometry data entered in the cross-section file can also be chosen as the structure geometry definition.

The facility has been designed for modelling culverts of any shape, length or slope. All flow conditions are represented including full submergence, partial submergence, critical inflow and outflow, orifice flow and full culvert flow with a free outflow.

### 1.12.1 Specification

The culvert cross-section shape is specified as either a standard shape (rectangle, circle), an irregular shape defined as a (depth or level)/width relation by the user. Other details required are:

- culvert length (m)
- upstream and downstream invert levels (m)
- number of parallel culverts
- friction coefficient (Manning's  $n$ )
- valve regulation switch which may be set as
  - flow only in negative direction (decreasing chainage)
  - flow in both directions (none)
  - flow only in positive direction (increasing chainage)
- closed/open section switch
- coefficients in both positive and negative flow directions for:
  - inflow losses (typically 0.5)
  - outflow losses (typically 1.0)
  - bend losses (straight culvert would be 0.0)
  - free overflow correction coefficient (typically 1.0)

### 1.12.2 Flow Descriptions

The flow through a culvert can be broadly classified into three areas for computational purposes. The flow conditions mentioned below are illustrated in Figure 1.23

#### Zero Flow

The zero flow condition occurs when one of the following conditions exist:

- the culvert is dry



- the valve regulation switch is set to negative and the flow would be in a positive direction if the valve was open;
- the valve regulation switch is set to positive and the flow would be in the negative direction if the valve was open.

## Upstream Controlled Flow

The upstream controlled flow conditions occur when the downstream water level has no influence on the discharge through the culvert. The discharge,  $Q$ , is therefore solely a function of the river water level at the culvert inflow,  $h_1$ , and can be tabulated ( $Q$ - $h$  relation) prior to the simulation, minimising the computational effort required during the simulation. The flow conditions modelled are:

- critical inflow
- partially full inflow and critical outflow
- submerged inflow and critical outflow
- orifice flow at inflow with free outflow
- full culvert flow with free outflow

Expressions for the loss coefficients, momentum equation coefficients, upstream controlled flow (critical inflow or outflow, orifice flow at inflow and full culvert flow with free outflow) and downstream controlled (submerged) flow are described in detail in Appendix A Appendix (p. 391). The transition between upstream and downstream control is also described in section A.3.

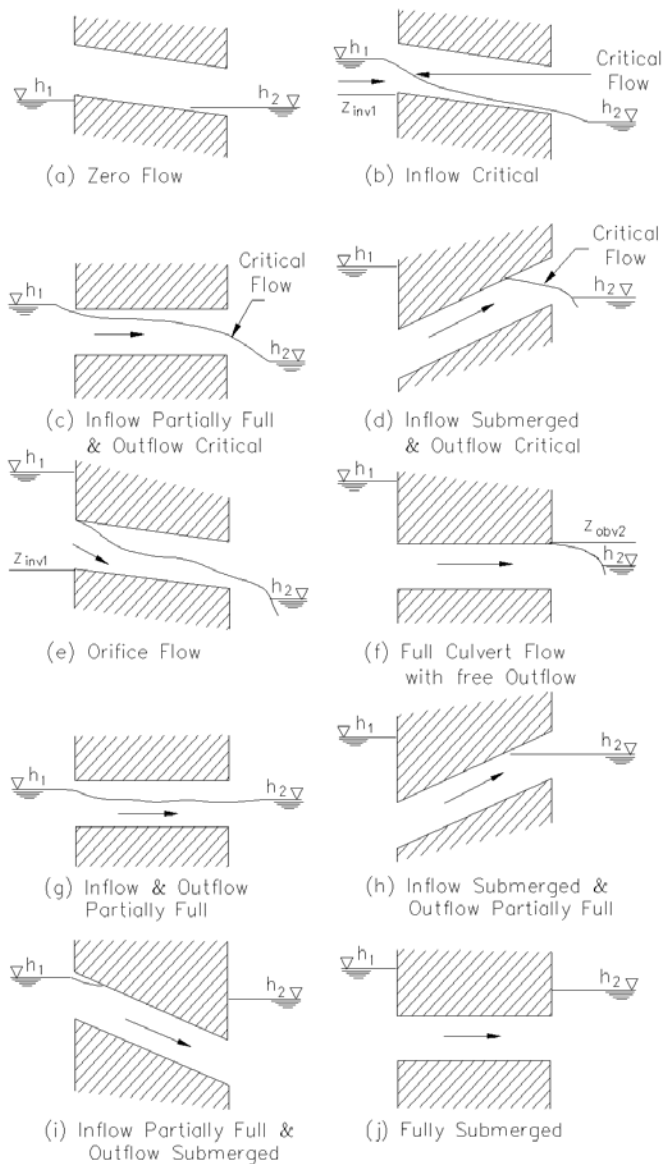


Figure 1.23 Culvert flow conditions

## Downstream Controlled Flow

Downstream controlled flow or submerged flow occurs when the downstream water level imposes a constraint on the flow through the culvert. The calculations take place during a simulation because the discharge is a function of



both upstream and downstream water levels and therefore is not practical to tabulate. The flow conditions modelled are:

- partially full inflow and outflow
- submerged inflow and partially full outflow
- partially full inflow and submerged outflow
- fully submerged

### 1.12.3 Construction of Q-h Relationships

The  $Q$ - $h$  relationships (one for each flow direction) are presented for verification under the  $Q$ - $H$  relations tab. For convenience, the relationships are given as the water depth,  $y_1$ , versus  $Q$ , not  $h_1$  versus  $Q$ . The value of  $h_1$  is equal to the culvert invert level plus  $y_1$ . The construction of the  $Q$ - $h$  relationship is described below.

First, the hydraulic parameters, area, hydraulic radius and critical flow, are tabulated for depths ranging from zero to full culvert depth. A cosine function is used for setting the tabulated depth values in order to give more detail at the bottom and top of the culvert cross-section where the variation of area and hydraulic radius is very non-linear. The values of area and hydraulic radius are shown under the Hydraulic Parameters tab for verification purposes only.

If an irregular section shape is specified, and if the depth or level/width table has more than eight pairs of values, the depths in the depth (or level)/width table are used for calculating the hydraulic parameters, otherwise the cosine function is used. This provides the opportunity for the user to specify the depths at which the hydraulic parameters are to be calculated.

Secondly,  $h_1$  is calculated for critical depths ranging from zero to that at 95% of the full culvert area. Whether the flow is critical at the inflow or outflow is determined according to the description above.

An iteration procedure is used to calculate  $h_1$  because the contraction loss coefficient  $\zeta_1$ , see Appendix A Appendix (p. 391), and the inflow river cross-section area  $A_1$  are functions of  $h_1$ . It is therefore necessary to specify the Topo ID in addition to the river name and chainage of the culvert so that  $A_1$  can be calculated from the cross-section data base.

At the start of a simulation a check is made that the distance between the upstream and downstream cross-sections minus the culvert length is less than DX-MAX. If this is not the case an error message is given. At present there are no checks comparing the cross-section locations and/or Topo ID between that used for calculating the  $Q$ - $h$  relations and that used in the simulation. Ideally the upstream and downstream cross-sections should be located immediately upstream and downstream of the culvert.

When critical flow can no longer occur (submerged inflow and/or outflow), the flow condition will be either orifice flow or full culvert flow. The  $Q$ - $h$  relationship continues to be constructed by calculating the discharge for increasing values of  $h_1$ . The maximum value of  $h_1$  in the tabulation is defined as the greater of (a) the top elevation in the adjacent cross-section, and (b) five times the culvert depth above the invert.

If the inflow river water level exceeds the maximum  $h_1$  value during a model simulation, a linear extrapolation is made based on the last two pairs of values in the  $Q$ - $h$  relation.

Iteration procedures are also necessary for  $Q_o$  (orifice flow) and  $Q_p$  (primed flow). The discharge adopted is taken as the minimum of  $Q_o$  and  $Q_p$ . However, once  $Q_p$  is lower full culvert flow occurs (i.e.  $Q_p < Q_o$ ), and the culvert is assumed to remain flowing full, i.e. the culvert is "primed".

For each iteration procedure mentioned above, convergence usually occurs in two to three iterations except in the case when the culvert inflow cross section area,  $A_{s_1}$  and  $A_1$  are of similar magnitude, i.e. as  $\zeta_1$  approaches zero. A maximum number of one hundred iterations is allowed, and if exceeded a warning message is given. The  $Q$ - $h$  relationships will be successfully calculated, but the user should check the adjacent cross-section description and the culvert specifications.

If  $A_{s_1}$  is greater than  $A_1$  or the  $Q$  values are decreasing with increasing  $h$  the calculation of the  $Q$ - $h$  relationships is suspended and warning messages are given. The point in the  $Q$ - $h$  relationships where the problem occurred can be observed by going to the bottom of the  $Q$ - $y$  tables.



Simulations will not be possible unless the  $Q$ - $h$  relationships have been successfully calculated.

If the Topo ID or the upstream and downstream cross-sections are changed, the  $Q$ - $h$  relationships have to be recalculated.

#### 1.12.4 Closed / Open Section switch

A culvert structure can be modelled as an open section if required by setting the Closed / Open switch. An example where this may be used is a "long" weir where the friction along the length of the weir is of importance and/or the flow areas at the entrance and exit are significantly different.

If set to open the culvert will never run full or partially full, therefore only those flow conditions which represent a free water surface are modelled. When the water level is higher than the soffit the hydraulic parameters are calculated based on a section extended vertically upwards with a width equal to that at the soffit. For example, in the case of a rectangular section the height value is essentially redundant as the cross-section will be modelled as an open section of constant width.



In the case of a circular section, this switch is invalid and will be set to closed.

### 1.12.5 Changing Flow Direction

See the discussion in section 1.34 Steady State Energy Equation (p. 162) for the treatment of when the flow direction changes between positive and negative directions.

### 1.12.6 Flooded Areas of Adjacent $h$ -points

The flooded or storage areas of the two adjacent  $h$ -points are reduced by half of the culvert length multiplied by the cross-section width. In effect the culvert is considered to have a zero contribution to the storage of the system. In the rare case where the storage within the culvert is significant compared to that in the river, the flooded areas at the adjacent  $h$ -points should be adjusted using the additional flooded area parameter, see section 1.10 Cross-Sections (p. 75).

### 1.12.7 Velocities

The velocity through a culvert is calculated as  $Q/A_c$  in the case of critical inflow or outflow where  $A_c$  is the critical flow area, as  $Q/A_{full}$  in the case of orifice flow or full culvert flow and  $A_{full}$  is the full cross-section area of the culvert, and as  $Q/S_{sA}$  when the flow is downstream controlled. In the latter case,  $Q/S_{sA}$  is equal to the mean of  $Q/S_{s_1}$  and  $Q/S_{s_2}$ , the culvert inflow and outflow cross-section areas, respectively.

## 1.13 Dambreak Structure

A dambreak structure is a composite structure composed of a structure representing the flow over the crest (Crest flow structure) and another structure representing the breach of the dam. The breach can be modelled in two different ways i.e. as a failure of the crest (breach-structure) or as piping failure of the dam (pipe failure structure) followed by breach failure. The crest flow at a dam is calculated as separate structures in a composite structure.

A dambreak structure is a dam in which a breach can develop. The flow through a dam breach may be described in MIKE 11 through the use of the energy equation or alternatively the calculation method as implemented in National Weather Services (NWS) DAMBRK program. In the following the two methods are presented separately.

### 1.13.1 Energy equation based dam breach modelling

The flow at the dambreak structure is quite similar to a broad crested weir, but there are two differences:

1. the shape of the dam changes with time, i.e. the breach increases and the dam crest is shortened. As a consequence the critical flow characteristics ( $Q-h$ ) relationship of the crest and of the breach cannot be calculated beforehand
2. the  $Q-h$  relationship for the dam crest and the breach are different therefore the flow over the crest and the flow through the breach are calculated separately, see Figure 1.24.

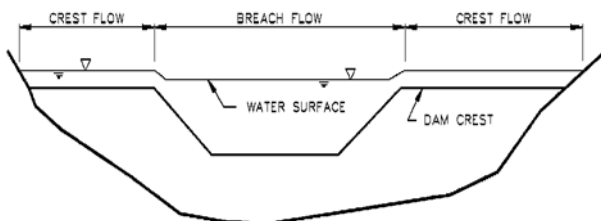


Figure 1.24 Combined flow over breach and crest

#### Initial breach development

The breach may be initiated in a number of ways depending on the method of calculation used. For the NWS method the breach may be initiated either as a trapezoidal breach or as a piping failure. Using the standard dam breach methods the breach is initiated either as a trapezoidal breach or if the erosion based method is used as a circular piping failure.

### Trapezoidal Breach Geometry

During the development of the breach the trapezoid increases in size and changes shape.

The initial breach shape is described by three parameters as shown in Figure 1.25:

- level of the breach bottom (HB)
- width of the breach bottom (WB)
- side slope of the breach (SS) (horizontal: vertical). The left side slope and the right side slope are equal

The development of the breach can either be specified as a known function of time, or it can be simulated from the sediment transport capacity of the breach flow.



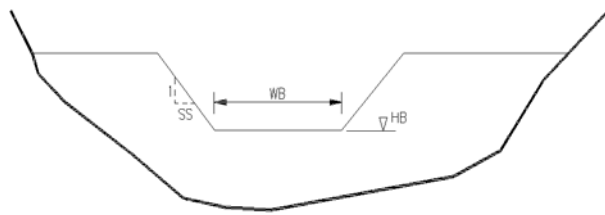


Figure 1.25 The parameters of the breach geometry

### Known Geometry Breach Development

The parameters of the breach are given as a time series in the boundary editor. The time is relative to the start of the breach. Between the specified times the parameters are linearly interpolated as shown in Figure 1.26 for the trapezoidal case. The breach bottom level must not be above the crest level.

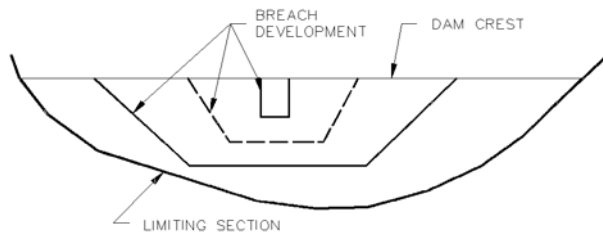


Figure 1.26 The breach is specified for example at times 0h and 1h. The dashed line would be the linear interpolation for time 0.5h

### 1.13.2 Erosion Based Breach Development using the energy equation

If this mode is chosen the initial and the final breach shape must be specified. The increase of the breach during a time step is calculated from the actual prevailing conditions in the breach itself. The Engelund-Hansen sediment transport formula is used (see equations (3.128) and (3.129)) to calculate the sediment transport in the breach.

As a first step, the flow resistance in terms of the total dimensionless shear stress is calculated, based on the Engelund formulation (see section 3.8.2 Flow Resistance -  $\theta-\theta'$  Relationship (p. 237)). This is then compared to the critical shear stress (the Shield's Criterion, defined by the user). If the computed shear stress is greater than the critical one, then the sediment transport is calculated, otherwise it is set to zero.



The sediment transport rate,  $q_t$ , calculated from the Engelund-Hansen formula is in terms of  $m^2/s$  per metre-width of pure sediment only, and this must then be related to a change in bed (i.e. breach) level. It is assumed that the breach remains horizontal. From the given upstream and downstream slopes, the length of the breach in the flow direction,  $L_b$ , may be calculated. By application of the sediment continuity equation in the breach, the change in breach level  $dH_b$  in a time interval  $dt$  is given as:

$$\frac{dH_b}{dt} = \frac{q_t}{L_b(1 - \varepsilon)} \quad (1.122)$$

where,

$H_b$  is the breach level

$q_t$  is the sediment transport rate ( $m^2/s$ )

$\varepsilon$  is the porosity of the sediment

$L_b$  is the breach length in the direction of flow

$t$  is time

Modelling the variation of the width of the breach perpendicular to the flow direction is more difficult to relate to the classical theories of sediment transport. This is because the development of a wall boundary layer along the often very steep side walls of the breach, the theories for bed load and suspended load do not apply. As an approximation, the sediment transport at the sloping walls is assumed to be proportional to that in the central part of the breach. The coefficient of proportionality,  $x$ , (side erosion index) thus relates the increase in breach width,  $W_b$ , to depth as:

$$\frac{dW_b}{dH_b} = 2x \quad (1.123)$$

Generally, the side erosion index is in the order of 0.5-1.0.

## Erosion Based Piping Failure

An erosion based failure of a dam may be initially started by piping failure. In this case a flow forms through the dam wall. Erosion of the soil along the "pipe" causes the pipe to enlarge and the flow to increase. Eventually the dam will collapse into the void created by the piping failure erosion.

This failure scenario is modelled as an option in the erosion based breach development, i.e. there are two options for the initial failure process:



1. initial failure by overtopping
2. initial failure by piping (after collapsing the erosion process returns to that of overtopping as described above).

The assumptions adopted for the piping failure are:

- the shape of the pipe is circular
- the pipe is horizontal
- the pipe must always be running full

The location of the pipe centre in the dam cross-section must be within the final breach shape and, if specified, the limiting section shape. When the circumference of the pipe extends outside these shapes, the hydraulic parameters are based on a reduced cross-section as illustrated in Figure 1.27.

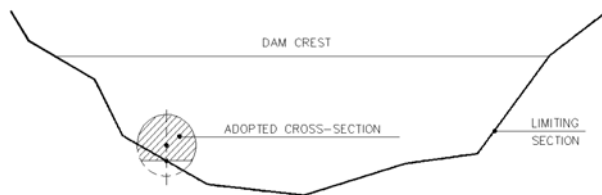


Figure 1.27 Adjustment of a pipe cross-section

The point of collapse is defined by a ratio, which is specified by the user, of the pipe diameter to the distance between the dam crest and the pipe invert as illustrated in Figure 1.28. Once this ratio is exceeded part of the dam is collapsed to form a breach.

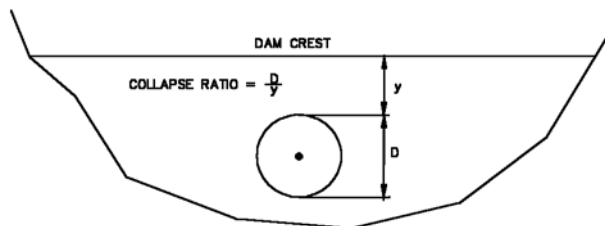


Figure 1.28 Piping failure collapse ratio

The shape of the breach is illustrated in Figure 1.29. The bottom width is first set equal to the pipe diameter and the breach level to the pipe invert. Not all

of the collapsed material will typically be carried out without depositing on the bed of the breach. This is accounted for by a volume loss coefficient,  $f_{lost}$ , which is the fraction of material assumed to be washed out immediately after collapse. The remaining material is evenly distributed on the breach bed as shown in Figure 1.29.

These calculations are made using cross-section areas, not volumes, therefore, the length of the breach and consequently the upstream and downstream slopes of the dam faces are not taken into account.

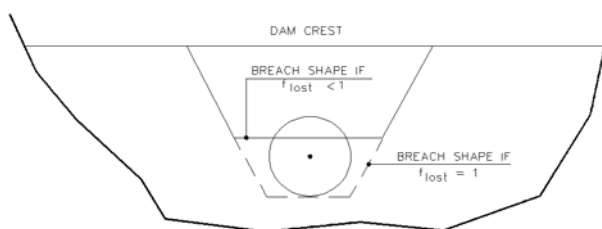


Figure 1.29 Breach shape after collapse

Other parameters required are the initial diameter of the pipe at the start of failure and the pipe roughness,  $k_s$ , which is used to calculate the Darcy friction factor,  $f$ , according to

$$\frac{1}{\sqrt{f}} = 2 \log_{10} \left( \frac{12R}{k_s} \right) \quad (1.124)$$

where,  $R$  is the hydraulic radius.

The discharge,  $Q_p$ , through the pipe is given by

$$Q_p = A \sqrt{\frac{2g\Delta H}{\left(1.5 + \frac{fL}{4R}\right)}} \quad (1.125)$$

where,  $A$  is the flow area,  $L$  is the length of the pipe and  $\Delta H$  is given by

$$\Delta H = h_1 - \max(h_2, z_{obv}) \quad (1.126)$$

where,  $h_1$  is the upstream water level,  $h_2$  is the downstream water level and  $z_{obv}$  is the obvert of the pipe.

In Equation (1.122) an entrance head loss of half the velocity head in the pipe and, when there is a submerged outlet, an exit loss of one velocity head have



been incorporated. Adopting a full velocity head loss in the latter case gives the transition between submerged flow and free outflow to be when the downstream water level,  $h_2$ , equals the pipe obvert,  $z_{obv}$ . (See section 1.12 Culverts, Q-h Relations Calculation (*p. 81*), for a more detailed discussion.)

The enlargement of the pipe is based on the sediment transport relationship described above for breach erosion. The depth of water,  $y_p$ , used in calculating  $q_t$  is given by

$$y_p = \frac{\Delta H}{2} + D \quad (1.127)$$

where,  $D$  is the pipe diameter.

By relating the volume of material eroded to the "effective" transport area (adopted here as the pipe length times half the circumference) the change in the pipe radius,  $\Delta R_p$ , is defined as

$$\Delta R_p = C_{cal} \frac{q_t}{2L_p(1-\varepsilon)} \Delta t \quad (1.128)$$

where,  $C_{cal}$  is a "calibration" coefficient entered as one of the erosion parameters. No sound recommendation can be given for the value of  $C_{cal}$ . It has been provided so the user can adjust the rate of change of  $R_p$  if so desired, or some data becomes available for calibrating the rate of formation of the pipe.

## Limiting Cross-Section

There may be a boundary of an irregular shape beyond which the breach will not develop. This limit may be the surface of hard rock or it may be the natural bottom of the valley. To allow for a boundary of this type a cross section can be specified. In this case only the part of the trapezoid inside the cross-section is used for calculation of the flow. This is illustrated in Figure 1.30.

## Flow Calculations

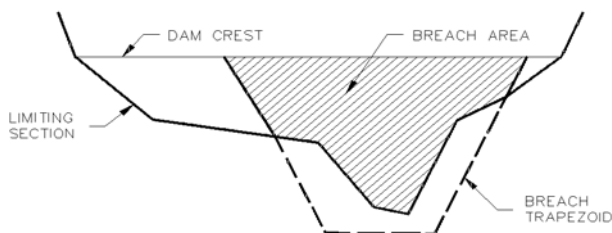


Figure 1.30 The breach (shaded area) is the area of the trapezoid inside the limiting section

Once the breach geometry has been computed the flow can be calculated.

The flow over the dam crest and the flow through the breach are often quite different with respect to water depth, velocity, and flow state. At the breach the water level is lower and the velocity is higher than at the dam crest. When the flow is drowned at the breach the flow at the crest may be either free overflow or drowned. Characteristic discharge and coefficients for the three flow regimes can be computed as shown in section A.10 Structures (p. 435).

The flows through each structure are calculated separately using the upstream water level ( $h_1$ ), the downstream water level ( $h_2$ ) and the total flow ( $Q$ ) from the last iteration. The flow over the crest structure and through the breach structure is calculated as described in section A.10 Structures (p. 435).

### 1.13.3 NWS DAMBRK dam-breach method

The NWS DAMBRK method comes in two flavours

- Breach failure
- Piping failure

The first of these uses a weir type equation to determine the flow through the breach where as the latter is based on an orifice type equation. Both methods rely on the user specifying the full development of the breach geometry as a function of time.

#### Breach failure

The flow through the trapezoidal breach is given by

$$Q = c_v k_s [c_{weir} b \sqrt{g(h-h_b)}(h-h_b) + c_{slope} S \sqrt{g(h-h_b)}(h-h_b)^2] \quad (1.129)$$



where

$b$  The width of the breach bottom

$g$  Acceleration due to gravity

$h$  Upstream water level (reservoir water level)

$h_b$  Level of breach bottom

$S$  Side slope of breach

$c_{weir}$  Weir coefficient for horizontal part (=0.546430)

$c_{slope}$  Weir coefficient for slope part (=0.431856)

$c_v$  Correction coefficient for approach sections. This coefficient compensates for the loss in energy due to the inflow contraction.

$k_s$  Correction coefficient due to submergence.

The weir coefficients have been made non-dimensional e.g.

$$c_{weir}\sqrt{g} = 0,546430\sqrt{9,81(m/s^2)} = 1,7115(m^{1/2}/s) = 3,1(ft^{1/2}/s)$$

The correction coefficient for the approach section is determined through

$$c_v = 1 + \frac{c_B Q^2}{g W_R^2 (h - h_{b,term})^2 (h - h_b)} \quad (1.130)$$

where

$c_B$  Non-dimensional coefficient (= 0.740256) termed the Brater coefficient

$W_R$  Reservoir width given by the un-destroyed crest length.

$h_{b,term}$  The terminal level of the breach bottom. The minimum level in the time series file.

The submergence correction is determined through

$$k_s = \max\left(1 - 27,8 \left(\frac{h_{ds} - h_b}{h - h_b}\right)^3 - 0,67, 0\right) \quad (1.131)$$

where  $h_{ds}$  is the downstream water level.



## Piping failure

The flow through a piping failure is given by

$$Q = c_{orifice} A \sqrt{2g(h - \max(h_p, h_{ds}))} \quad (1.132)$$

where

$c_{orifice}$  Orifice coefficient (= 0.599769)

$A$  Flow area in pipe given by

$$A = b(h_{pt} - h_b) + S(h_{pt} - h_b)^2 \quad (1.133)$$

$h_{pt}$  Top of pipe

$h_b$  Bottom of pipe

$h_p$  Centerline of pipe given by

$$h_p = \frac{(h_{pt} + h_b)}{2} \quad (1.134)$$

The pipe may collapse either due to the top of the pipe reaching the crest level or if the water level upstream isn't high enough to maintain pipe flow. The criteria for the latter is given by

$$h < \frac{3}{2}(h_{pt} - h_b) + h_b \quad (1.135)$$

Once the pipe has collapsed the flow is calculated based on the breach flow equations.

## Crest flow

The flow over the crest of the dam is given by

$$Q = k_s c_{weir} b_c \sqrt{g(h - h_c)}(h - h_c) \quad (1.136)$$

where

$h_c$  the crest level

$b_c$  the remaining crest length (perpendicular to the flow)





and the submergence correction given by

$$k_s = \max\left(1 - 27,8 \left(\frac{h_{ds} - h_c}{h - h_c}\right)^3 - 0,67, 0\right) \quad (1.137)$$

## Failure moment

The user may choose three different definitions of the failure moment namely

- Time in the form of a historic date and time.
- Hours from start of simulation. The user specifies a time span in hours before the dam breaches.
- A reservoir water level. The reservoir water level is defined as the greatest of the water level on either side of the dam.

## Temporal development of breach geometry

Once the failure has initiated the temporal development of the breach will be read from a time series. This time series must contain values for

- The breach bottom
- The breach side slope
- The breach bottom width

Further if piping failure is used the time series must also contain

- The upper level of the pipe

Please refer to Figure 1.31.

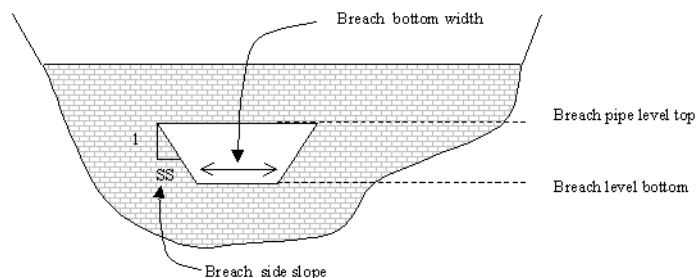


Figure 1.31 Definition sketch for NWS DAMBRK routines.



## 1.14 Energy Loss

### General

The hydrodynamic module includes a facility for modelling the loss of energy at specified river locations. At run-time such points, denoted Energy Loss points, are defined as discharge grid points. At each time level of the computation the discharge at an Energy Loss point is computed by use of the energy equation:

$$\Delta H = \zeta \frac{Q^2}{2gA^2} \quad (1.138)$$

in which  $\Delta H$  is the energy loss encountered in passing the Energy Loss points,  $g$  is the acceleration of gravity,  $Q$  is the discharge and  $A$  is the cross-sectional wetted area at that point. The quantity,  $\zeta$ , denotes the total energy loss coefficient as specified in the network editor. If applied, the energy loss coefficients described below are added up to yield a total energy loss coefficient.

### User-Defined Energy Loss

In order to enable the user to model a known energy loss at a river location Eq. (1.138) is applied in conjunction with a user defined loss coefficient,  $\zeta = \zeta_{\text{user}}$ .

### Energy Loss Caused by Sudden Flow Contraction

The energy loss caused by contraction of the flow is modelled using Eq. (1.138) in conjunction with a contraction loss coefficient,  $\zeta = \zeta_{\text{cont}}$ . The contraction coefficient is given by

$$\zeta_{\text{cont}} = \zeta_{\text{in}} \left(1 - \frac{V_1}{V}\right) \quad (1.139)$$

where  $\zeta_{\text{in}}$  is the inflow coefficient specified by the user,  $V_1$  is the upstream velocity at the previous water level point and  $V$  is the mean (within cross-section) velocity.

### Energy Loss Caused by Expansion of the Flow

Expansion loss is modelled using the following equation:

$$\zeta_{\text{expan}} = \zeta_{\text{out}} \left(1 - \frac{V_2}{V}\right)^2 \quad (1.140)$$

in which  $\zeta_{\text{out}}$  is the outflow coefficient specified in the network editor and  $V_2$  is the downstream velocity at the next water level point. The coefficient,  $\zeta_{\text{expan}}$ , replaces  $\zeta$  in Eq. (1.138).



### Energy Loss Caused by an Abrupt Change in River Alignment

In the case of an abrupt change in river alignment, the energy loss is modelled as

$$\zeta_{abrupt} = 1,1 \left( \frac{\theta}{90} \right)^2 \quad (1.141)$$

in which  $\theta$  denotes the angular change (deg) in river alignment. The coefficient,  $\zeta_{abrupt}$ , replaces  $\zeta$  in Eq. (1.138).

### Energy Loss Caused by a Gradual Change in River Alignment

Using the analogy of pipe flow, the energy loss is modelled as

$$\zeta_{gradual} = \alpha \sin \theta \quad (1.142)$$

where  $\alpha = 0.2$  for rough pipes and  $\alpha = 0.1$  for smooth pipes. The alignment of the gradual bend is assumed to be circular, the radius of the bend being greater than 4 times the pipe diameter for Eq. (1.142) to prove valid. The coefficient,  $\zeta_{gradual}$ , replaces  $\zeta$  in Eq. (1.138). The coefficients,  $\alpha$  and  $\theta$ , are specified in the network editor.

## 1.15 Flooded Areas, (Storage)

The flooded area, or storage area, is defined at each  $h$  point as the summation of the width times the distance between the  $Q$  points either side of the cross-section plus the additional flooded area. The width is automatically calculated when the cross-section raw data are processed (see section 1.10 Cross-Sections (p. 75)) or can be specified manually in the cross section editors processed data menu. Additional flooded area data are specified manually by the user in the same editor.

The flooded area may have to be either increased or decreased manually by the user under certain conditions. An increase is necessary where there is an off-stream storage area (e.g. a harbour) connected to the river. A decrease is necessary where there is a duplication of flooded areas, (discussed below).

To increase the flooded area specify additional flooded areas and/or increase the width values in the processed cross section data editor. To decrease the flooded areas reduce the width values in the cross section editors processed data menu.



**Note** that the width values are not only used for the computation of the flooded area but also in the calculation of the wind friction (see section 1.42 Wind (p. 182)) and in the calculation of cross-sectional area for water levels in excess of the maximum elevation specified (see section 1.10 Cross-Sections (p. 75)). It should be noted that these additional flooded areas are not

included in the total surface area in the computation of wind friction (see section 1.42 Wind (p. 182)).

A zero width value can be specified, noting that a zero flooded area at an  $h$ -point is not acceptable (or realistic) except where the  $h$ -point is connected to other  $h$ -points at a node (the flooded area at a node is the sum of the flooded areas of the connecting  $h$ -points and should also be non-zero).

The modelling of more complex flood plain hydraulics is described section 1.18 Flood Plains (p. 115).

When simulating the exchange of water between the channel and the flood plain care should be exercised when specifying the storage (width and additional flooded area columns) in order to avoid duplication in the calculation of storage volumes at nodes and  $h$ -grid points. This is illustrated by the following simple example (Figure 1.32).

Figure 1.32 is a schematic diagram of flow in a flood plain: flow in the main channel is represented by branch RIVER; flow between the channel and the flood plain is represented by the two branches SPILL1 and SPILL2 in which the W points represent broad crested weirs; flow along the flood plain is represented by the branch PLAIN. The network has 4 nodes as shown in Figure 1.32. Cross-sections are defined at all  $h$ -points as shown in Figure 1.33.

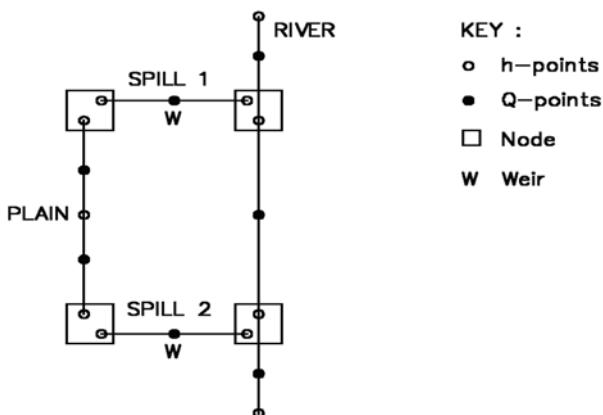


Figure 1.32 Network for flow in channel and adjacent flood plain

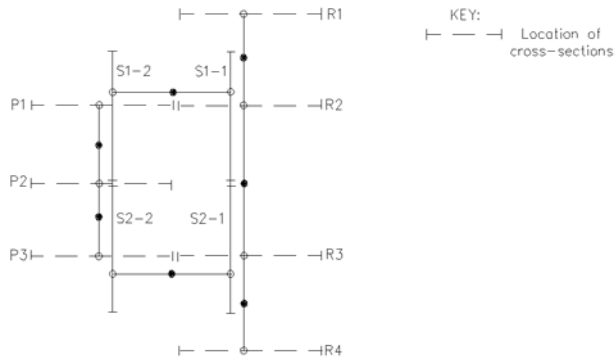


Figure 1.33 Location of cross-sections required for the network shown in Figure 1.32

Without modification to the cross-section descriptions, the storage areas for each  $h$ -point would be as shown in Figure 1.34 considering each branch separately.

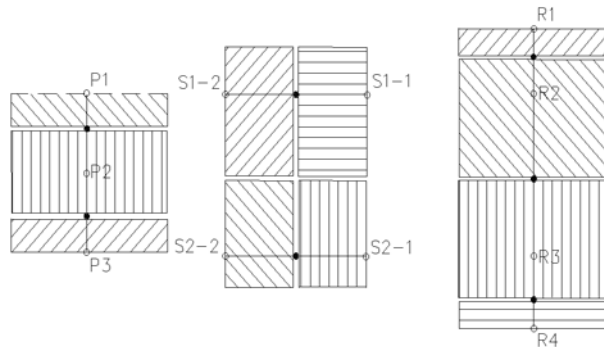


Figure 1.34 Storage areas corresponding to each  $h$ -point for each branch

Figure 1.35 below, shows the branches connected again, with those flooded areas which would be duplicated:

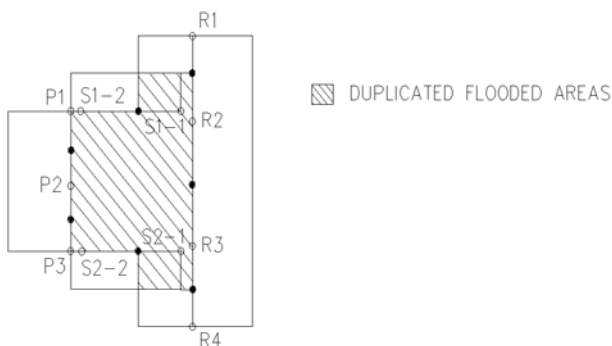


Figure 1.35 Duplication of flooded areas if no adjustment is made

In order to overcome this duplication, the values in the width columns of the processed cross-section data should be set to zero for the cross-sections defining the spill units S1-1 and S2-1 and reduced by the appropriate amount for S1-2 and S2-2. The additional flooded area of all four cross-sections at all levels should be zero.

## 1.16 Flood control facilities

### 1.16.1 Non control

Input:

- NAMET: Dam Name

Output:

- $Q_{out} = Q_{in}$

### 1.16.2 Constant discharging method Type A

Constant discharging method Type A with afterward discharging.

Input

- NAMET: Dam Name.
- QCONST: Inflow rate to start cutting.
- VMAX: Dam Maximum Storage .
- FACA=0

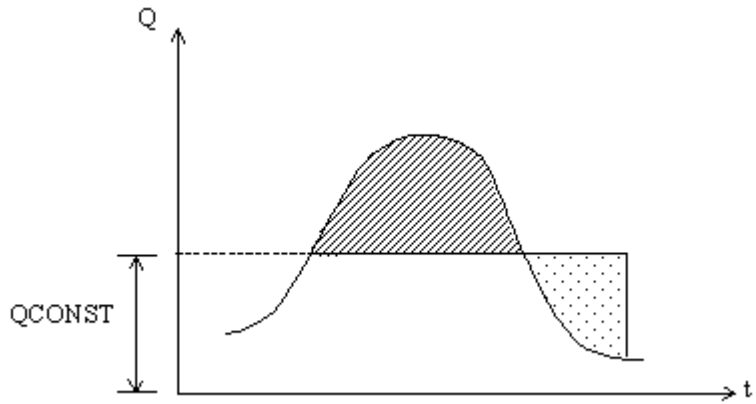


Figure 1.36 Constant discharging method Type A.

Output:

$$Q_{out} = Q_{CONST}$$

Dam burst Case

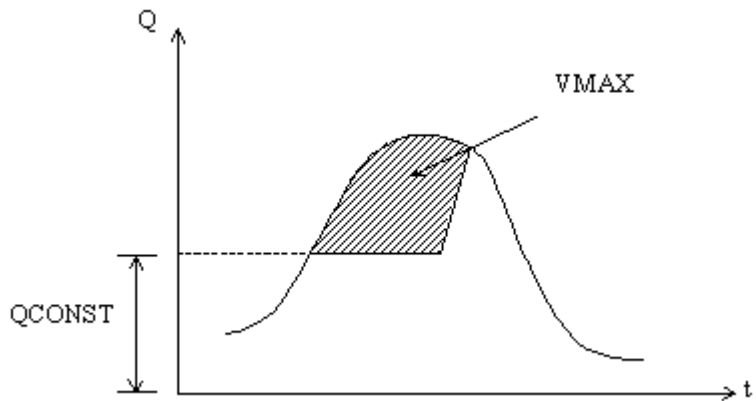


Figure 1.37 Constant discharging method Type A. Dam burst.

### 1.16.3 Constant discharging method Type B

Constant discharging method Type B without afterward discharging.

Input:

- NAMET: Dam Name.



- QCONST: Inflow rate to start cutting.
- VMAX: Dam Maximum Storage .  
FACA = 0

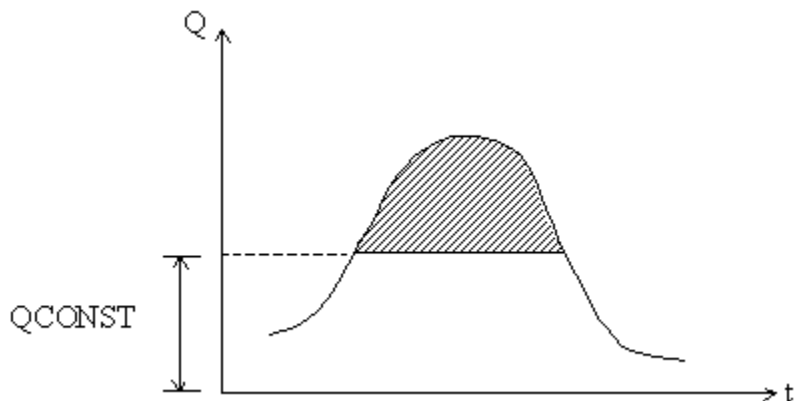


Figure 1.38 Constant discharging method Type B.

Output:

- $Q_{out} = QCONST$ .

#### Dam burst case

$Q_{out}$  is the same as for the constant discharging method Type A.

### 1.16.4 Constant ratio discharging method Type A

Constant ratio discharging method Type A with afterward discharging.

Input:

- NAMET: Dam Name.
- QCONST: Inflow rate to start cutting.
- FACA: Cutting Rate.
- VMAX: Dam Maximum Storage.



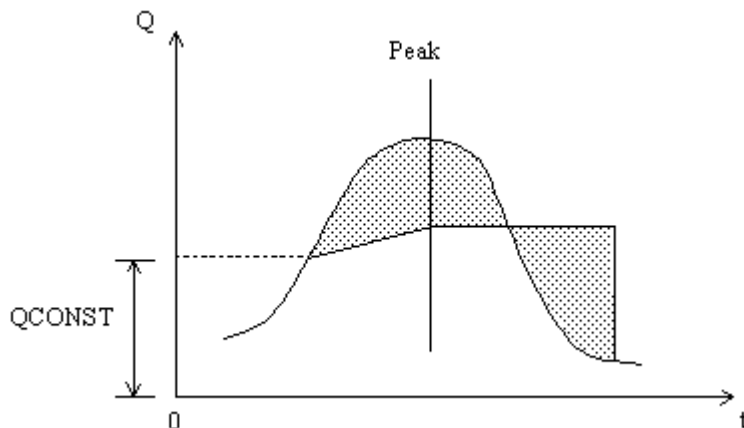


Figure 1.39 Constant ratio discharging method Type A.

Output:

$$Q_{out} = FACA(Q_{in} - QCONST) + QCONST \quad (1.143)$$

#### Inner Implementation

1. When Inflow < QCONST, Discharge = Inflow.
2. When Inflow > QCONST till inflow peak, discharge  $Q_{out}$  is set by Eq. (1.143).
3. After peak,  $Q_{out}$  keeps constant at  $Q_{2p}$  till  $S_2 \geq S_1$ , where  $Q_{2p}$  is the  $Q_{out}$  computed at peak.
4. After  $S_2 \geq S_1$ , set Discharge = Inflow.

### 1.16.5 Constant ratio discharging method Type B

Constant ratio discharging method Type B without afterward discharging.

Input:

- NAMET: Dam Name.
- QCONST: Inflow rate to start cutting.
- FACA: Cutting rate.
- VMAX: Dam Maximum Storage.

Output:

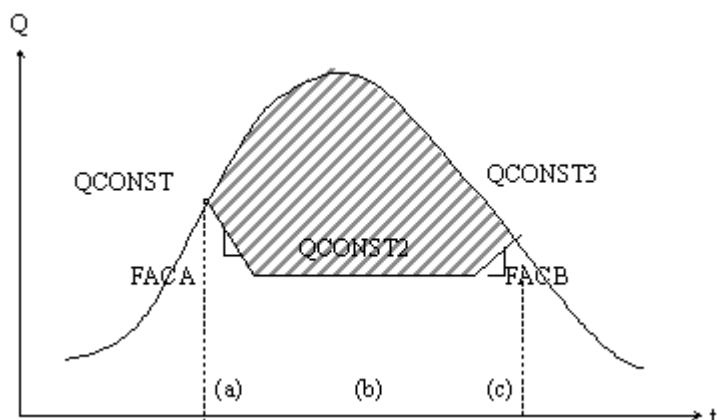
$$Q_{out} = FACA(Q_{in} - QCONST) + QCONST \quad (1.144)$$



### 1.16.6 Bucket-cut (without afterward discharging)

Input:

- NAMET: Dam Name.
- QCONST: Inflow rate to start cutting .
- QCONST2: Constant discharging rate .
- QCONST3: Inflow rate to increase discharging .
- FACA: Decrease of discharging rate per unit time.
- FACB: Increase of discharging rate per unit time.
- VMAX: Dam Maximum Storage .



Output:

1.  $Q_{out} = QCONST - \Delta T FACA$
2.  $Q_{out} = QCONST$
3.  $Q_{out} = QCONST2 + \Delta T FACB$

**Note**  $\Delta T$  is the time increment per step.

### 1.16.7 Non gate discharging by H/Q curve and H/V curve

Input:

- NAMET: Dam Name.
- FASA: Initial Water Level.
- IT1: Number of H/Q relationship.
- IT2: Number of H/V relationship.
- HQ(2,IT1): H/Q relationship.
- HQ(1,IT1): Water level of H/Q relationship.
- HQ(2,IT1): Discharge of H/Q relationship.



- HV(2,IT2): H/V relationship.
- HV(1,IT2): Water level of H/V relationship.
- HV(1,IT2): Volume of H/V relationship.

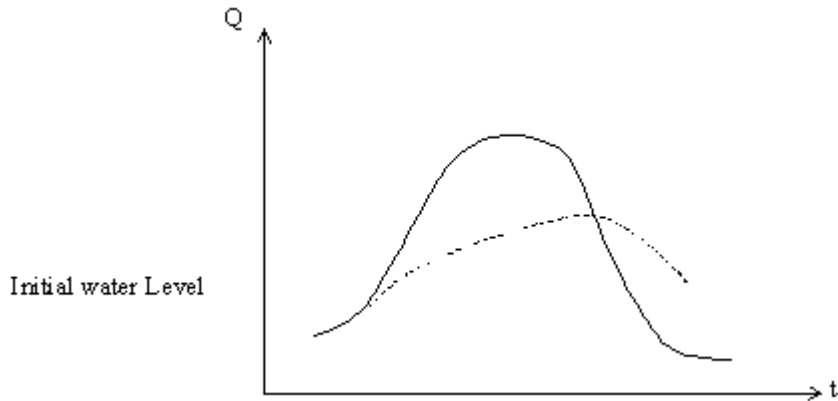


Figure 1.40 Non gate discharging by H/Q-curve and H/V-curve.

Output:

$Q_{out}$  is calculated through the H/Q or the H/V relationship.

### 1.16.8 Non gate discharging by orifice size input

Input:

- NAMET: Dam Name.
- IT1: Number of H/V Relationship.
- NANA: Number of spillways.
- VMAX: Dam Maximum Storage volume.
- HB: Regular foundation height of spillway.
- HT: Emergency foundation height of spillway.
- BL: Regular width of spillway.
- BH: Emergency width of spillway.
- DL: Regular height of spillway.
- DH: Emergency height of spillway.
- C1L: Regular discharging coefficient of spillway (Open channel).
- C1H: Emergency discharging coefficient of spillway (Open channel).
- C2L: Regular discharging coefficient of spillway (Orifice).
- C2H: Emergency discharging coefficient of spillway (Orifice).
- HH: Water level in H/V relationship.
- VV: Volume in H/V relationship.

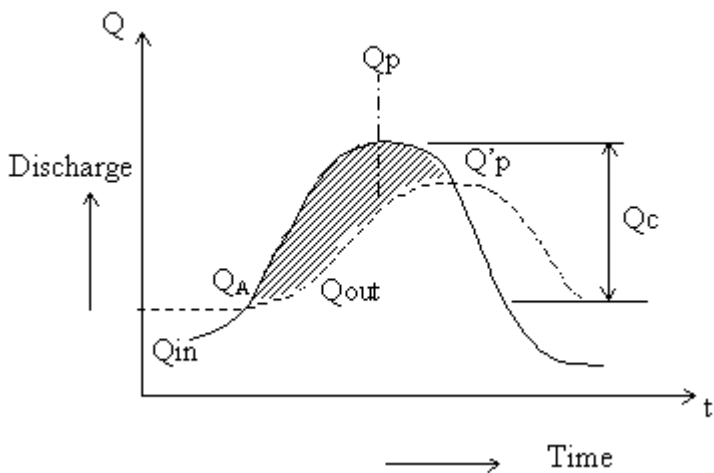


Figure 1.41 Non gate discharging by orifice.

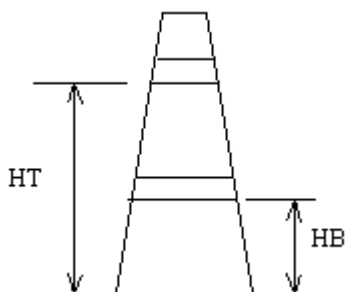


Figure 1.42 Definitions of spillway heights.

Output:

$Q_{out}$  is computed through the following equations ( $Q_{out} = O$ ).

Suppose at time  $t$ , the inflow to the dam is  $I$ , outflow from dam is  $O$ , and the dam storage is  $V$ , the continuity equation can be written as follows.

$$I - O = \frac{dV}{dt} \tag{1.145}$$



The equation below is the discretised form of the continuity equation, which can be solved by the Ekdahl method.

$$\Delta V = (I - O)\Delta t \quad (1.146a)$$

$$I\Delta t = \Delta V + O\Delta t \quad (1.146b)$$

Using subscript 1 to represent elements at time  $t = t_1$  subscript 2 to represent elements at time  $t = t_1 + \Delta t$ , the discretised equation can be expressed as follows

$$\begin{aligned} \frac{1}{2}(I_1 + I_2)\Delta t &= (V_2 - V_1) + \frac{1}{2}(O_1 + O_2)\Delta t \\ &= \left(V_2 + \frac{O_2}{2}\Delta t\right) - \left(V_1 + \frac{O_1}{2}\Delta t\right) \end{aligned} \quad (1.147)$$

Setting,

$$\phi = \frac{V}{\Delta t} + \frac{1}{2}O \quad (1.148a)$$

$$\psi = \frac{V}{\Delta t} - \frac{1}{2}O \quad (1.148b)$$

we have the following equation

$$\phi_2 = \frac{1}{2}(I_1 - I_2) + \psi_1 \quad (1.149)$$

Generally, with the equation

$$\phi_{n+1} = \frac{1}{2}(I_n - I_{n+1}) + \psi_n \quad (1.150)$$

$\phi_{n+1}$  can be thus computed sequentially.

## 1.17 Flood plain Encroachment calculations

The flood plain encroachment module may be used for assessing the impact of a flood plain encroachment on the water level and the energy level. Such assessments are of considerable interest for land developers, engineers etc.

The module works by manipulating the user specified cross sections by inserting encroachment stations thus contracting the cross sectional area with a rise in water level as a result.



**Note:** The encroachment module only works with a Quasi Steady State module installed. Only the default steady state solver may be used with the encroachment module. If a different steady state solver is chosen a warning is issued and the steady state solver is set to the default solver. Further the module may only be used in conjunction with a hydrodynamic simulation. Thus the advection dispersion, rainfall runoff modules etc. are disabled during an encroachment simulation.

### 1.17.1 General

An encroachment analysis consists of minimum two steady state simulations. The first simulation is used to find the water level and discharge throughout the system in the undisturbed situation, i.e. in the situation where no encroachments take place. This is referred to as the reference simulation. The next simulation(s) will be used to find the hydraulic variables throughout the system in the encroached situation. The results from the simulation will then be made available for comparison.

Through the encroachment analysis the cross section will be divided into a main channel and a left and right flood plain. The encroachment can then take place on either of the flood plains or on both flood plains.

#### Limitations on the encroachments

The placing of the encroachment stations are limited to the flood plains.

The flood plains are defined by the markers of the cross sections:

- The left flood plain is defined as the reach from marker 1 to marker 4.
- The right flood plain is defined as the reach from marker 5 to marker 3.

Marker 1 and 3 are the left and right levee bank respectively, and marker 4 and 5 are the left and right low flow bank respectively. Thus markers 4 and 5 defines the reach of the main channel.

The position of the encroachment stations may further be limited by the user defined offsets. The offsets are defined as the distance from marker 4 and 5 respectively (see Figure 1.43). As default these values are set to zero.

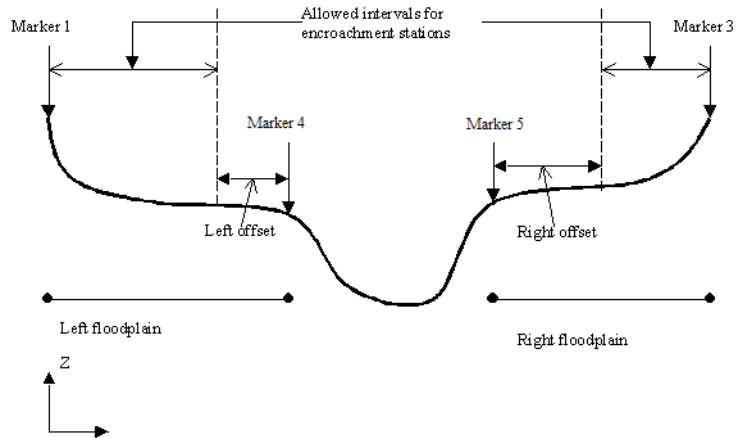


Figure 1.43 Definition sketch of the flood plains.

If the encroachment stations are situated outside the allowed intervals a warning is issued and the encroachment station is set equal to the limiting value (one of the end-points of the interval).

## 1.17.2 Encroachment Methods

Five different encroachment methods are available:

1. Direct specification of fixed encroachment stations.
2. Specification of a fixed encroachment width.
3. Specified conveyance reduction.
4. Target water level.
5. Encroachment through iteration.

The encroachment module of MIKE 11 facilitates local settings for the individual cross sections. Thus different methods may be used along the same river reach if desired.

### Method 1: Direct specification of fixed encroachment stations

Through this method the user specifies the location of the encroachment stations. The location is specified through the variables Left Position and Right position. Each of the fore mentioned are distances from marker 4 and marker 5 respectively. Thus both Left Position and Right Position should be non-negative. If the latter is not the case the simulation uses the absolute values.



## Method 2: Specification of a fixed encroachment width

Method 2 is very similar to method 1. The encroachment stations are determined from a user defined width being the distance between the left and right encroachment stations. The encroachment stations are placed a distance of half the user specified width from the centre line of the channel. The centre line is here defined as the midpoint of marker 4 and marker 5. If a negative value is entered the simulation will use the absolute value.

## Method 3: Conveyance reduction

Based on the reference simulation an encroachment simulation is performed based on conveyance reduction. Using the water level from the reference simulation the total conveyance at the specific station is determined. The cross section is then encroached until the user specified reduction of conveyance at the reference water level has been reached. If this is not possible the optimal encroachment position is returned. The latter may occur if the user specifies a reduction which is greater than the conveyance available on the flood plains.

## Method 4: Target water level

In method 4 the user defines a target water level. This is done through a water level change which is to be added to the reference water level. The encroachment calculation is then carried out so that the conveyance at this higher level is equal to the total conveyance of the reference simulation.

In other words if the user specifies a rise in the water level  $\Delta H$  then the module will try to contract the cross section so that the conveyance of the encroached cross section at water level  $H_{\text{ref}} + \Delta H$  is equal to the reference situation.

## Method 5: Encroachment through iteration

In this method a target value of either water level or energy level is aimed at. The method works by evaluating simulation results and through these modify the cross section until the target value is met. As opposed to method 3 and method 4 this method evaluates the results from simulations instead of just considering conveyance reductions at user specified water levels.

If a non-zero change in water level is specified the method will try to satisfy this request. Further if additionally a non-zero energy level change is also entered the method will check if this level is violated. If the latter is the case the method will modify the cross section until the energy level request is satisfied.

If the user only specifies a change in energy level which is non-zero then the module will aim at satisfying this energy level request.





The maximum number of iterations allowed is user defined but is set to 20 per default. If this limit is reached a warning is issued and the best result from the iteration is used as output.

### 1.17.3 Additional specifications for encroachment calculations

#### Side specification

The user may specify whether the encroachments are to take place on

- both flood plains
- the right flood plain
- the left flood plain

If the fixed width method is used (method 2) then the simulation will carry out the encroachment calculations for both flood plains. In the latter case the side specification is ignored.

#### Conveyance reduction specifications

MIKE 11 allows three different types of conveyance reduction:

- Equal conveyance reduction: The simulation tries to satisfy the request by reducing the conveyance equally on the flood plains. In accordance with the user specified total reduction (in percentage).
- Relative conveyance reduction: The simulation tries to satisfy the request (total reduction) by reducing the conveyance relative to the conveyance on the flood plains in the reference simulation. This is only of importance if method 3 or 4 is used.
- Specified conveyance reduction: The user specifies the left and right reduction. The total reduction equals the sum of the left and right reduction. Note that this setting has only effect for method 3.

#### Target values

For methods 4 and 5 the user must specify one or more target values.

Target values are of two types:

- Water level change.
- Energy level change.

The target water level is then given by the reference water level plus the user specified water level change. Similarly the target energy level is given by the reference level plus the energy level change.

If method 4 is chosen a non-zero value must be entered for the water level change. The target water level is then used to obtain the placing of the encroachment stations. The energy level is ignored using method 4.

If method 5 is chosen then either a non-zero water level change or a non-zero energy level or both should be entered. If both an energy level and a water level is specified the simulations aims at satisfying the water level target without violating the energy target level. If only a water level or an energy level is specified the simulation will only try to satisfy this request.

### 1.17.4 Cross sections after encroachment

The encroachment module manipulates the cross sections by inserting 'vertical' sections at the position of the encroachment stations (see Figure 1.44).

The relative resistance of the left vertical section is set equal to the value at the point just prior to the placement of the vertical section. Similarly the relative resistance of the right vertical section is set equal to the value at the point just post the placement of the vertical section (see Figure 1.45).

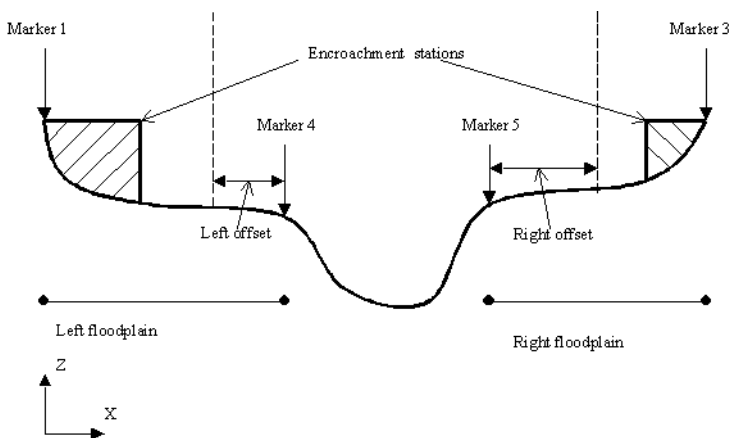


Figure 1.44 The geometry of the cross section after encroachments.

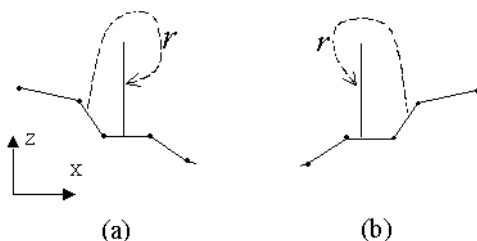


Figure 1.45 The definition of the relative resistance on the vertical sections of the flood plain encroachment stations: (a) left flood plain (b) right flood plain.



### 1.17.5 Encroachments at structures

The encroachment module does not allow encroachments of cross sections just upstream or downstream of structures.

### 1.17.6 Encroachments at nodes

MIKE 11 uses water level compatibility at nodes, thus all cross sections located at the same node will have equal water level. For this reason MIKE 11 does not permit encroachments at cross sections located at nodes.

## 1.18 Flood Plains

Description of flow over flood plains can be achieved with several different types of model schematisations depending on the topography of the flood plain and the nature of the flow.

In spilling areas natural levees are formed along the river by sedimentation due to the abrupt reduction in flow velocity of the entering water. In predominantly drainage areas, these levees are not present. The principal difference between the two situations is shown in Figure 1.46

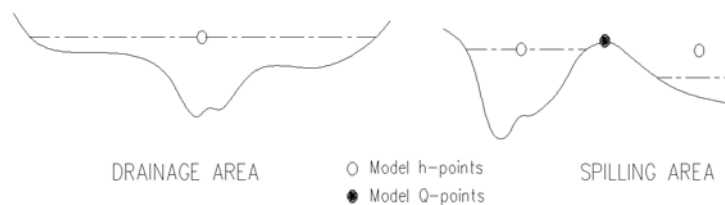


Figure 1.46 Principal difference between drainage and spilling areas

This schematisation of the flood plain may not be adequate if sediment transport is to be calculated especially where the hydraulic resistance in the flood plain is significantly different from that in the channel. This is because the sediment transport is very sensitive to the value of velocity and the cross-sectionally averaged velocity will not be representative of the actual velocity in the flood plain. For this situation, the river and flood plain may be schematised separately using two or more parallel model branches connected by broad crested weirs as for the spilling area defined below.

In a typical drainage area, it is generally reasonable to assume that the water level is the same in the river and on the flood plain. The flood plain storage, thus, can be included directly in the modelled river cross section through the

width parameter, and only one model  $h$ -point is required to determine the water level over the whole area.

In a typical spilling area, the water levels in river and flood plain might differ due to the separation by a levee. One  $h$ -point at each side of the levee is thus required to describe the conditions. Between the two  $h$ -points a  $Q$ -point is placed representing the discharge over the levee. A weir equation is applied to describe the magnitude of the discharge. This discretisation is shown in the right hand part of Figure 1.46. A schematic plan view of such a discretisation is shown in Figure 1.47.

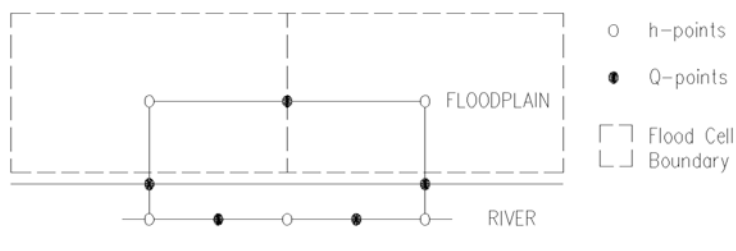


Figure 1.47 Discretisation with flood cells

If water flows along the flood plain then the momentum equation must also be modified. The flood plain is divided into cells with one  $h$ -point describing the water level in each cell. Over the flood plains, flow can take place from one cell to the next. This is described by introducing a model branch between the cells (see Figure 1.47). The boundaries between the cells are normally chosen along natural elevations such as road or railway embankments. Where such features do not exist or are not sufficiently significant to merit explicit representation (but may be implicit in the flood plain roughness), the Saint Venant equations can be applied. The water surface slope will then vary linearly between  $h$ -points.

If no cross-section data exists on the flood plain, the cross-section parameters can be derived from a storage-elevation relationship as described below.

The storage-elevation relationship derived from a contour map is entered as additional flooded areas versus elevation in the cross section editors processed data menu. Care should be taken when defining this relationship for the reasons described under section 1.14 Energy Loss (*p.* 98). The width values should be entered as zero.



From this relationship the storage volume of the cell (denoted by  $V$ ) can be determined as a function of elevation, and the cross-sectional area of the flood cell can be approximated as

$$A(h) = \frac{V(h)}{L} \quad (1.151)$$

where,  $L$  is shown in Figure 1.48.

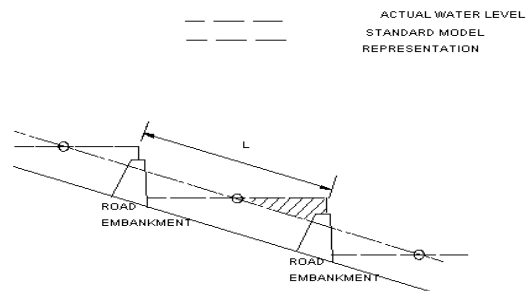


Figure 1.48 Long section of cell discretisation

This will represent a measure for the average cross-section along the flood plain. The average resistance radius can similarly be approximated with:

$$R(h) = \frac{V(h)}{S(h)} \quad (1.152)$$

When spilling starts, huge flows of water may suddenly be generated, possibly causing numerical instabilities. This problem can be overcome by giving the levee along the river a V-formed shape in the mathematical description, see Figure 1.49.

This ensures that spilling starts gradually instead of instantaneously over the whole section. This corresponds, in fact, to the situation in nature, where the irregularities in levee height cause the spilling to start sooner at some places than at others.



Figure 1.49 V-formed levee long section

The computed water level in the cell is not representative for all locations within the cell, but is an average as shown in Figure 1.48. To interpret the model results, the computed water level should be transformed into an average depth of inundation within the cell as given by:

$$\text{average inundation depth} = \frac{V(h)}{S(h)} \quad (1.153)$$

## 1.19 Flow Descriptions

The model provides a choice between 3 different flow descriptions:

1. dynamic wave approach which uses the full momentum equation, including acceleration forces, thus allowing the simulation of fast transients, tidal flows, etc. backwater profiles may also be calculated;
2. diffusive wave approach which only models the bed friction, gravity force, and the hydrostatic gradient terms in the momentum equation. This allows the user to take downstream boundary conditions into account, and thus simulate backwater effects;
3. kinematic wave approach. The flow is calculated on the assumption of a balance between the friction and gravity forces.

Depending on the type of problem, the user can choose the most appropriate description. All three approaches simulate branched as well as looped networks.

### 1.19.1 Dynamic Wave and High Order Dynamic Wave

The dynamic and high order dynamic flow description should be used where the change in inertia of the water body over time and space is of importance. This is the case for all tidal flow, and in river systems where the water surface slope, bed slope and bed resistance forces are small.

The high order flow description includes a high order and upstream centred description of the friction terms in the momentum equation. This formulation allows the simulations to be done with a larger time step, than would be the case for the non-high order description. The non-high order dynamic formulation is only included to allow re-production of simulation results done in previous version of MIKE 11.



See section 1.30 Saint Venant Equations (p. 159) for details of the governing equations.

### 1.19.2 Diffusive Wave

The diffusive wave description ignores the inertia terms and is therefore suitable for backwater analyses, cases where the bed resistance forces dominate, and for slowly propagating flood waves where the change in inertia is negligible. It is not normally suitable for tidal flows.

The modified 'diffusive wave approximation' is derived from the general Saint Venant Equations by neglecting all momentum terms as follows:

This formulation still ensures a backwater description through the  $\partial h/\partial x$  term. For stability reasons the  $\partial h/\partial x$  term is dampened in the solution, which means that only relatively steady backwater phenomena (compared to the time step) are resolved.

### 1.19.3 Kinematic Wave

The assumption of a balance between the friction and gravity means that the kinematic wave approach cannot simulate backwater effects. Thus this description is appropriate for relatively steep rivers without backwater effects.

### 1.19.4 Which Flow Description?

The dynamic wave description is recommended to be used in all cases except where it can be shown that either the diffusive or kinematic descriptions are adequate.

The diffusive and kinematic wave approximations are simplifications of the full dynamic descriptions. They are implemented to offer improved computational efficiency, but should only be used when the omitted terms have insignificant influence. When there is any doubt it is better to use the full dynamic description or trials should be undertaken to establish the difference between alternative methods, and advice sought from experienced persons. It is very important to have a solid understanding of the influence of the different terms.

None of the three wave descriptions includes detailed hydraulic descriptions of hydraulic jumps. However, the chosen formulations ensure a correct description upstream and downstream of the jump.



## 1.20 Initial Conditions

### 1.20.1 User-Specified

The initial conditions can be specified by the user in the Simulation Editor under the Simulation tab.

### 1.20.2 Auto Start, Quasi-Steady Solution

In the automatic calculation, a steady state backwater calculation using the steady state version of the Saint Venant Equations is performed to determine the water levels and discharges in the model using the boundary condition values at the start of the simulation. An iterative procedure is used to obtain a correct discharge distribution between diverging branches. The maximum number of iterations is specified by the `MaxIterSteady` (p. 64) in the Hydrodynamic Parameters Editor under the Default Values tab. See section 1.26 Quasi-Steady Solution (p. 129).

### 1.20.3 Hot Start

User-specified initial conditions for a simulation can be obtained from an existing result file (.res11) as long as it is complete and exactly compatible with the new computation.

### 1.20.4 Combined Auto Start and user-specified initial conditions

In some cases the auto start procedure is not capable of calculating the initial conditions. This is the case for instance if the model includes flood plains described by a separate branch and the initial water level in the main river gives no flow from the main river into the flood plain. The initial  $h$  and  $Q$  in the flood plain is thus not defined. By specifying the initial  $h$  and  $Q$  for the flood branch in the Hydrodynamic Parameters Editor under the Initial tab, it is still possible to use the auto start procedure for calculating initial  $h$  and  $Q$  in the main river. The combined auto start and user specified initial conditions is selected by setting the switch in the initial condition box in the simulation editors simulation tab.

## 1.21 Kinematic Routing Method

### General

Two different routing methods have been incorporated into MIKE 11 HD. At a given time level, the routing methods are used to determine the spatial variation of the discharge at Kinematic Routing branches. The implemented methods are:

- Muskingum method





- Muskingum-Cunge method

Similarly, two methods have been incorporated into the model, which are used to compute the water level at Kinematic Routing branches:

- User-defined discharge-elevation method
- Resistance method

### Definition of a Kinematic Routing Element

Figure 1.50 shows an example of a Kinematic Routing branch, at which two Kinematic Routing points are defined. Each point is located at a discharge point and the temporal transformation of the discharge takes place at this grid point. The quantification of the discharge at a Kinematic Routing point is obtained by considering the inflows to the Kinematic Routing element in question, cf. Figure 1.50. The inflows constitute the discharge at the upstream elevation point (including lateral inflow at that point) and the sum of the lateral inflows at all interior elevation points of the considered Kinematic Routing element.

The extent of each Kinematic Routing element is governed by the number of Kinematic Routing points specified at each Kinematic Routing branch. The upstream boundary of an element is determined as the larger of the following:

- Chainage of upstream node (elevation point)
- Chainage of elevation point located just downstream of closest upstream Kinematic Routing point (elevation point)

The definition of a Kinematic Routing element ensures that the entire branch is described correctly regardless of the number of routing elements specified by the user. Note that a Kinematic Routing element is located from one elevation point to the other, while the Kinematic Routing point is located at a discharge point.

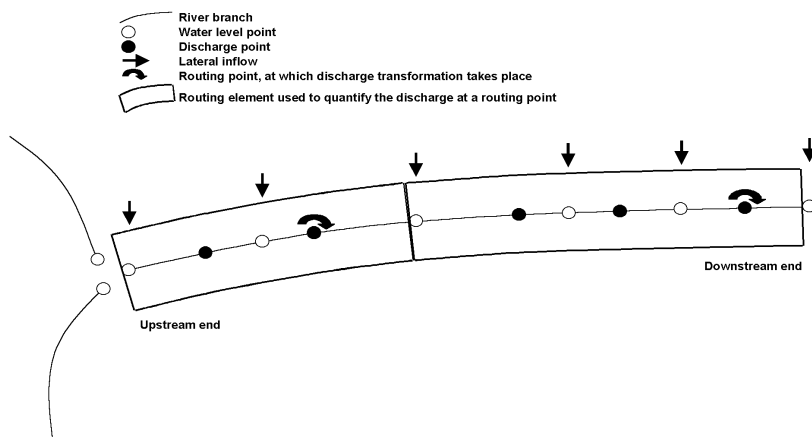


Figure 1.50 Definition sketch of MIKE 11 Routing *branch*, *Kinematic Routing* elements and transformation points.



Figure 1.51 Successive computation of discharge at Kinematic Routing branches. The numbers denote the branch calculation order for a Kinematic Routing branch network.

### Discharge Computation

At Kinematic Routing branches, the discharge is computed in the direction of positive flow. In order to ensure that water is discharged correctly from furthest upstream in the river network the discharge computation starts at the upstream end of those Kinematic Routing branches located furthest upstream in the river network. At a given discharge point this concept ensures that the



discharge values used as input to the Kinematic Routing method at that point have been updated beforehand. In effect, this means that the Kinematic Routing branches are updated in accordance with Figure 1.51.

The Muskingum method is a hydrologic routing method used to handle a variable discharge-storage relationship. The method models the storage volume of flooding in a river by combination of wedge and prism storages. During the advance of a flood wave, inflow exceeds outflow, producing a wedge of storage. During the recession, outflow exceeds inflow, resulting in a negative wedge. The Muskingum method is written:

$$Q_{i+1}^{j+1} = C_1 Q_i^{j+1} + C_2 Q_i^j + C_3 Q_{i+1}^j + C_4 \quad (1.154)$$

where indices  $i$  and  $j$ , respectively, refer to the considered grid point and time level. The variables,  $C_1 - C_4$ , are given by

$$C_1 = \frac{\Delta t - 2Kx}{2K(1-x) + \Delta t} \quad (1.155)$$

$$C_2 = \frac{\Delta t + 2Kx}{2K(1-x) + \Delta t} \quad (1.156)$$

$$C_3 = \frac{2K(1-x) - \Delta t}{2K(1-x) + \Delta t} \quad (1.157)$$

$$C_4 = \frac{Q_{lat} \Delta t}{2K(1-x) + \Delta t} \quad (1.158)$$

In the Muskingum method the computational input parameters,  $K$  and  $x$ , are fixed in time and space. Since in MIKE 11 HD the time step is fixed, too, Eqs. (1.155) - (1.158) need to be evaluated only once.

At a Kinematic Routing points the discharge variable is updated from one time level to the next on the basis of the previous and new discharges at the location of the upstream boundary of the considered Kinematic Routing element as well as the previous discharge at the Kinematic Routing point in question, cf. Figure 1.50. Moreover, the total lateral inflow to the Kinematic Routing element (denoted  $Q_{lat}$ ) is evaluated as the mean of the previous and new total lateral inflows for the considered Kinematic Routing element.

In contrast to the Muskingum method, the Muskingum-Cunge method does not take any input parameters, since these are computed at each Kinematic Routing point and at each time level.

The Muskingum-Cunge method is based on the diffusion wave model, which neglects local and convective acceleration terms but includes the pressure



term. Thus, the Muskingum-Cunge model approximates the diffusion of a natural flood wave.

The Muskingum-Cunge computation uses the same equations as the Muskingum method, but the parameters  $K$  and  $x$  are functions of time and space. They are given by

$$K = \frac{\Delta x}{c_k} \quad (1.159)$$

$$x = \frac{1}{2} \left( 1 - \frac{Q}{B c_k S_0 \Delta x} \right) \quad (1.160)$$

$$c_k = \frac{dQ}{dA} = \frac{\partial Q}{\partial x} \frac{\partial x}{\partial A} + \frac{\partial Q}{\partial t} \frac{\partial t}{\partial A} \quad (1.161)$$

In Eqs. (1.159) - (1.161),  $\Delta x$  is the length of the considered Kinematic Routing element and  $S_0$  is the bed slope. The variables  $B$ ,  $A$  and  $Q$ , respectively, are the width, the cross sectional area and the discharge, all of which represent the Kinematic Routing element in question. The variables  $x$  and  $t$  are space and time variables, respectively.

The variables,  $B$ ,  $A$  and  $Q$  are evaluated at the elevation point just upstream of the considered Kinematic Routing point. Since at this water level point the computation of the water level depends on the new discharge computed at the Kinematic Routing point, the discharge at each Kinematic Routing point is obtained by iteration. Typically, about 10 iterations are required to obtain an accuracy better than  $10^{-4}$ .

### Computation of Water Level

Having computed the discharge at the Kinematic Routing branch under consideration, all the interior elevation points of that branch are computed. Since Kinematic Routing points are defined as  $Q$ -points, computation of the water level may require interpolation between upstream and downstream information. Consequently, both an upstream search and a downstream search for a Kinematic Routing point is done. In the case of both an upstream and a downstream Kinematic Routing point, the water level is computed at both Kinematic Routing points and a linear interpolation is made to obtain the water level at the water level point in question.

Should the search efforts fail to find an upstream and a downstream Kinematic Routing point, the Manning equation is used to compute the water level.

Regardless of the method used to compute the water level, a check is made to ensure that the computed water level is not located below the top of the slot.



At nodes of Kinematic Routing branches, the water level is computed using the same procedures as currently used in MIKE 11 HD. This concept ensures that the water level is continuous from one branch to the other.

If, at a Kinematic Routing point, the user has chosen a QH-relation the discharge computed by use of a Kinematic Routing method is used to interpolate in the QH-table at the elevation point in focus.

If, at a Kinematic Routing point, the user has chosen the Manning resistance method the discharge is computed by employment of the Manning equation. It is written

$$Q = MR^{\frac{2}{3}} S_0^{\frac{1}{2}} A \quad (1.162)$$

in which M is the Manning resistance number, R is the hydraulic radius,  $S_0$  is the bed slope, and A is the cross sectional, wetted area. Since M, R, and A are functions of the water level, the cross sectional area is found by iteration. Once the area has converged to a satisfactory accuracy ( $10^{-3}$ ), the water level is looked up in the cross section table of MIKE 11 HD.

## 1.22 Lateral Inflows

A lateral inflow, for example a side tributary which is specified in the Boundary Editor or NAM input which is specified in the River Network Editor under **Tabular view: Runoff/groundwater links** is described by a Q-t relationship. It represents an addition to the flow in the channel at the point of entry specified in the boundary editor or the network editor respectively, and is thus added into the continuity equation. A lateral momentum contribution is not included. A lateral inflow, therefore, differs from the Q-t relationship which is used in the definition of a regulating structure. For the latter, the Q-t relationship represents the total flow at a control point and replaces the momentum equation at this point, whereas the lateral inflow is an addition to the flow and is not a control point.

## 1.23 Leakage

Ground Water Leakage is calculated as an internal sink, with discharge out of all h-grid points included is a per length contribution proportional to; 1) a constant specified in HD parameter file, 2) the water depth above ground water head, and 3) the wet perimeter of the cross section.

Leakage in MIKE 11 engine is calculated as

$$Q_{Leakage} = C_L \cdot P \cdot D \cdot \Delta x \quad (1.163)$$

where:

- CL : Leakage coefficient (user defined)
- P : Wet perimeter (Area/Hydr.Radius)
- D: Water depth
- $\Delta x$  : grid spacing

## 1.24 Low Flow Conditions

During low flow, the cross-sections along certain model stretches may "dry out" (meaning that the water level falls below the river bottom). Apart from other problems, this gives numerical difficulties which, if no special measures are taken, prohibits a continuation of the computation.

The problem is handled in MIKE 11 by the aid of two numerical features:

1. A narrow slot below the cross-sections is introduced so that the calculations can continue when the water surface falls below the bottom of the bed. If the water level reaches the bottom of the slot, a small amount of water is automatically added to prevent a complete drying out. The applied slot shape starts at a height DELH above the river bottom and extends to 5 x DELH below, Figure 1.52. DELH is specified in the Hydrodynamic Parameters Editor under the Default Values tab. The description above DELH over the river bottom is not affected by the slot. Below this point, the calculation of both  $A$ ,  $R$  and  $b$  is affected as well as the weighting coefficients in the numerical solution. The computed conditions below this point should thus not be given much weight, but should be seen as a "stand-by" condition until flow starts again.

The geometry of the slot may be of two types: 1) the width varies as the square root of the depth in the slot or 2) the geometry is so that the cross sectional area is continuous across the local water level DELH. For the latter case the geometry does not introduce an error in the overall water amount as long as the water level doesn't reach the bottom of the slot. For details on the geometry of the slot please refer to section A.2 Area Preserving Slot (p. 395).



**Note:** The geometry of the second type of slot is different from earlier versions of MIKE 11 (1999b and prior), and may cause instabilities for some setups which are converted into MIKE 11 2000. To overcome this difficulty the old slot description may be chosen by setting the following switch in the MIKE11.ini file (default in v. 2000b and later is OFF):

HD-Variables no 13:

AREA\_PRESERVING\_SLOT=OFF

2. For low flow conditions the use of the Saint Venant equation to describe the momentum balance becomes unphysical. MIKE 11 handles this by



gradually substituting the momentum equation for low flow condition with a zero flow condition. This weighting is a function of the local water depth and is implemented in such a way that the zero flow condition has full weighting if the water level is less or equal to the local bottom level.



**Note:** The suppression of the momentum equation for low flow situations is a new feature for MIKE 11 (v.2000 and later), and may cause instabilities for some set-ups which are converted from an earlier version of MIKE 11 (v.1999b and earlier). To overcome this difficulty the suppression may be overruled by setting the following switch in the MIKE11.ini file (default in v. 2000b and later is ON):

HD-Variables no 12:

QZERO\_METHOD=OFF.

If one of the two above mentioned switches are set to ON the user might be forced to decrease the time step in a set-up. The gain being the increase in accuracy in the mass balance.

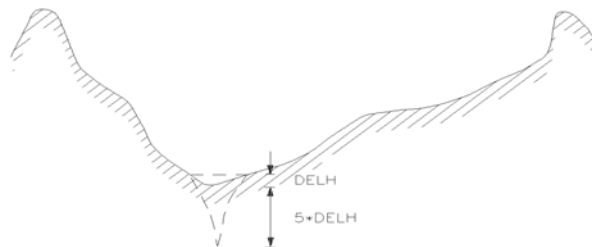


Figure 1.52 Cross-sections with artificial slot

## 1.25 Pumps

Pump structures in MIKE 11 are divided in two distinct groups, pumps with internal outlet and pumps with external outlet. Pumps with internal outlet increases the local water level within a branch whereas pumps with external outlet pumps water out of the branch

Pumps with internal outlet are like most other structures placed in a Q-point, whereas pumps with external outlet are placed in h-points.

### 1.25.1 Capacity

Pumps may be specified either as pumps with fixed capacity or by a pump characteristic. When pumping with fixed capacity the pump pumps with the

given rate whenever it is fully on. The only deviations from the specified capacity appears during start-up, close down and when the pump is of.

Alternatively pumps may be specified by a pump characteristic relating the pump discharge to the lift height. The lift height is calculated as the difference between the larger of the downstream water level and the outlet level and the upstream water level.

$$\Delta h = \max(h_{outlet}, h_{downstream}) - h_{upstream} \quad (1.164)$$

Examples of pump characteristics are included as Figure 1.46.

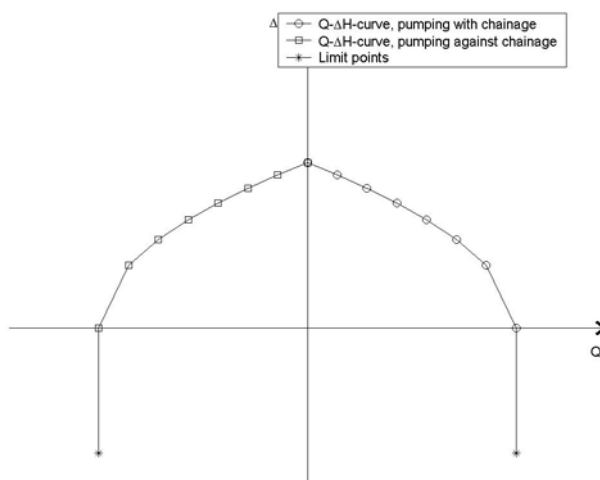


Figure 1.53 Pump characteristic examples.

### 1.25.2 Start/Stop control

The pumps are controlled by simple start-up and close down periods. The periods specifies the time used by the pump for changing its discharge from full to zero and vice versa.

### 1.25.3 Internal outlet

The equation governing the flow through a pump with internal outlet is obtained by Taylor expansion of the discharge at time step  $n+1$ .





### 1.25.4 External outlet

For the external outlet the pumps are modelled as pumping out of the branch to an outlet with the level specified in the input. Mathematically the pumps are modelled by including a source term in the continuity equation. The source describes the pump discharge at time step  $n+\delta$  ( $0 \leq \delta \leq 1$ ). The discharge at time  $n+\delta$  is approximated using linear interpolation between the pump discharge at time  $n+1$  and at time  $n$ . The discharge at time  $n+1$  is approximated using Taylor expansion including both timevarying change due to pump start-up/close down and change due to change in water level.

## 1.26 Quasi-Steady Solution

A solution of the quasi-steady version of the Saint Venant equations is determined iteratively for the automatic calculation of the initial conditions. The boundary condition values used are those at the start of the simulation.

The quasi-steady solution is also used for simulation of long term phenomena such as morphological changes or the effects of pollutants on water quality. As the calculations are based on steady flow conditions there is no upper stability limit to the computational time step. This enables long term simulations to be carried out at a fraction of the computational time that would be required when using the fully dynamic solution.

Generally, the quasi-steady solution requires discharge boundary conditions at all inflow boundaries and water level or  $Q$ - $h$  relationships at outflow boundaries, but the model will often work also for other combinations. However, if only  $Q$ -boundaries are specified the steady solution is undefined mathematically, and the model will not work.

In a system without bifurcations the steady solution is easily obtained with a simple backwater solution procedure starting from outflow boundaries and marching against the flow direction from one  $h$ -point to the next using an iterative method. At bifurcations the discharge should be divided in the bifurcating branches in such a way that the calculated water levels in the bifurcating branches are identical. This discharge distribution is also obtained via an iteration procedure. Thus, the steady state solution is obtained from a nested iteration procedure, viz. an overall iteration procedure to obtain the correct discharge distribution in the system and an iteration procedure to calculate the water level difference between neighbouring  $h$ -points.

A linear relationship is established between the water levels in the upstream ( $h_{\text{upstream}}$ ) and downstream ( $h_{\text{downstream}}$ ) nodal point in a branch and the discharge in the branch, i.e.:

$$Q_{\text{branch}} = e_0 h_{\text{upstream}} + e_1 h_{\text{downstream}} + f \quad (1.165)$$



This equation has the same structure as used in the fully dynamic model at every time step, see section A.5 The Double Sweep Algorithm (p. 407). The boundary conditions are introduced into the solution in the same way as in the fully dynamic solution (in fact the program code is re-used).

The linear relationship is based on three backwater calculations for each branch, assuming that the downstream water level and discharge are known (in the first iteration step a quite primitive first guess is used). The first backwater calculation is carried out with the current iteration values of the discharge and downstream water level. The second one is carried out with a slightly larger discharge (usually a 20% increase), and the third one with the downstream water level increased by 20% of the downstream water depth. From these three backwater calculations the following relationship is calculated:

$$h_{\text{upstream}} = \alpha h_{\text{downstream}} + \beta Q_{\text{branch}} + \gamma \quad (1.166)$$

Comparing Equations (1.165) and (1.166) it is seen that:

$$\begin{aligned} e_0 &= \frac{1}{\beta} \\ e_1 &= -\frac{\alpha}{\beta} \\ f &= -\frac{\gamma}{\beta} \end{aligned} \quad (1.167)$$

After establishing a linear relationship for each branch, and using a water level compatibility and a continuity equation at each node (e.g. the water levels in all connecting branches have to be identical and the sum of inflow and outflow to the node is zero) a linear system of equations for the water levels in all nodes is obtained (similar to that obtained in the double sweep algorithm). These water levels are subsequently used to calculate the discharges in the branches using Equation (1.165). The next iteration starts with the following values

$$h_{\text{new}} = \text{Relax } h_{\text{calculated}} + (1 - \text{Relax})h_{\text{previous iteration}} \quad (1.168)$$

$$Q_{\text{new}} = \text{Relax } Q_{\text{calculated}} + (1 - \text{Relax})Q_{\text{previous iteration}} \quad (1.169)$$

This relaxation of the solution is not required in a single branch system without bifurcations (hence Relax=1). In more complex systems, Relax < 1.0 should be used. The relaxation coefficient (Relax) is an input parameter to the model.

There are some pitfalls using the quasi-steady model. For example, from Equation (1.167) it can be seen that when  $\beta$  is very small or zero the solution



may become unstable. According to Equation (1.166) this occurs when the upstream water level is independent of the discharge (i.e. nearly horizontal branches). This situation occurs in very short branches with cross-sections which have very large conveyance compared to the discharge or in branches with little resistance. In most cases this situation is avoided by increasing the discharge in the backwater simulation with increased  $Q$  until  $\beta$  is greater than a threshold value,  $\beta_{Limit}$ .  $\beta_{Limit}$  is an input parameter to the model (default value  $10^{-8}$ ). However, occasionally the velocity may increase at greater pace than the water level at the upstream end of a branch causing stability problems. Reasonable initial conditions can be obtained by suppressing the convective acceleration term in the momentum equation.

Another problem may occur in nearly horizontal branches. As mentioned above, the backwater calculation is based on an iterative calculation of water levels from one  $h$ -point to the next. If the stop criterion for this iteration is of the same order of magnitude as the total water level difference between upstream and downstream ends of the branch, the coefficients in Equation (1.166) (and hence Equation (1.165)) are inaccurately determined which will generate oscillations in the solution and poor convergence of the solution algorithm. This problem is overcome by using a stop criterion in the backwater algorithm which is related to the total water level difference in the branch, i.e.:

$$h_{conv} = \frac{1}{N}(h_{upstream} - h_{downstream})h_{conv\_factor} \quad (1.170)$$

$N$  = number of  $h$ -points in branch

To avoid underflow problems it has been necessary to limit  $h_{conv}$  by a minimum value  $Min\_Hconv\_In\_Branch$ .  $h_{conv\_Factor}$  and  $Min\_Hconv\_In\_Branch$  are input parameters with default values of  $10^{-2}$  and  $10^{-5}$  respectively. In cases where  $h_{conv}$  is limited by  $min\_h_{conv\_in\_branch}$  oscillations in the discharge may occur, although the water levels will be stable provided  $h_{conv}$  is small. Overall convergence is therefore tested on both  $h$  in nodal points and  $Q$  in branches, where only one of the two has to be satisfied, i.e. the iteration stops when for all branches:

$$(Q_{new} - Q_{old}) < q_{stop}$$

where,

$$q_{stop} = \sum Q_{inflow} q_{conv\_factor} \quad (1.171)$$

and

$$\sum Q_{inflow} = Q_{max} \quad (1.172)$$

or

$$(h_{\text{new}} - h_{\text{old}}) < h_{\text{stop}} \quad (1.173)$$

$q_{\text{conv\_factor}}$  and  $h_{\text{stop}}$  are input parameters with default values  $10^{-3}$  and  $10^{-4}$ , respectively.

In model setup with structures having a zero flow condition the up- and downstream water levels are uncorrelated, hence no linear relationship (Equations (1.165) and (1.166)) between discharge and up- and downstream water levels can be established. The model overcomes this problem by introducing a "slot" in the structure as outlined in Figure 1.54.

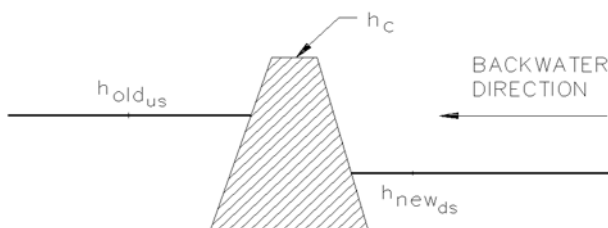


Figure 1.54 Solution at a structure with zero flow

If  $Q < Q_s$  and  $h_c > h_{\text{old}}$  then:

$$h_{\text{new\_upstream}} = h_{\text{new\_downstream}} + \frac{Q}{Q_s} (h_c - h_{\text{new\_downstream}}) \quad (1.174)$$

$Q_s$  is related to the total inflow to the model ( $Q_{\text{max}}$ ) by:

$$Q_s = Q_{\text{max}} q_{\text{struc\_factor}} \quad (1.175)$$

The  $q_{\text{struc\_factor}}$  is an input parameter with default value  $5 \cdot 10^{-3}$ .

In certain model setup a steady solution can not be defined in some areas. This will typically be the case where structures with zero flow are placed in series, see Figure 1.55, and in models with "dry" flood plain cells. If nothing else is specified the model will introduce slots and "leak" a small amount of water through the structures isolating the area of the model without any mathematical solution to the steady flow equation. This may result in undesirable water levels at e.g. flood plains. The user has the option to specify certain areas where the steady-state solution is over ruled by user-specified values of  $Q$  and  $h$ . The user should be careful selecting values which are compatible with the overall hydrodynamic conditions in the model.

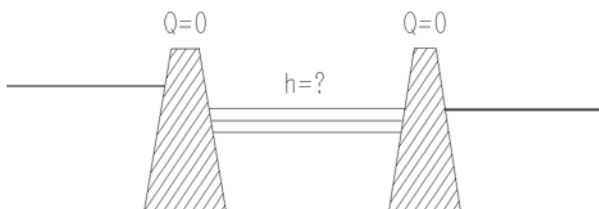


Figure 1.55 Areas with undefined steady solution

The simulation time depends on the complexity of the setup. In systems without bifurcation the iteration converges quickly. The input parameters  $Relax$ ,  $\beta_{limit}$ ,  $h_{conv}$ ,  $min\_h_{conv\_in\_branch}$ ,  $q_{conv\_factor}$  and  $q_{struc\_factor}$  have, naturally, a large effect on the speed of convergence.

In order to optimize the convergence parameters both with respect to accuracy and computational time it is recommended that the parameters be adjusted so that a satisfactory solution is obtained for a low flow condition. If the parameters are adjusted adequately for the low flow conditions then the parameters will also produce accurate results for higher flow conditions.

The optimization is carried out by running the hydrodynamic model for constant low flow conditions until steady conditions are obtained. These results can then be compared with those obtained using the quasi-steady model. It has to be emphasized that the parameters are 'model specific', i.e. each model setup and associated flow conditions require an individual optimization of the parameters.

## 1.27 Quasi-two dimensional steady flow with vegetation

The module takes the effects of vegetation into account for steady flow. Each cross section is divided into subsections. Each subsection being one of four different types:

- Normal zones (p. 136).
- Vegetation zones (p. 139).
- Vegetation zones adjacent to river levee (adjacent vegetation zones) (p. 143).
- Dead water zones (p. 144).

The analysis is based on a parallel channel assumption, where the exchange of momentum between adjacent channels is taken into consideration. The extent of each of the parallel channels/subsections is based on the classification of the individual points in the cross section profile. The extent of a given subsection of a certain type is found as the extent of consecutive points being



of this specific type. The type of the individual segments is determined on the basis of the end point of the segment.

The exchange of momentum between the different subsections is modelled as a shear stress using an expression of the following form

$$\tau = \rho f \Delta V |\Delta V| \quad (1.176)$$

where  $\rho$  is the density of the water  $f$  is a mixing coefficient and  $\Delta V$  is the velocity difference across the given boundary. For a water-water boundary between subsections  $i$  and  $i+1$  the difference in the average velocity is given by  $\Delta V = V_i - V_{i+1}$ . For a water-vegetation boundary the velocity difference is given by  $\Delta V = V_i$ , since it is assumed that there is no flow among the vegetation. The mixing coefficients or diffusion coefficients have (empirically found) default values but can be altered by the user in the Hydrodynamic Parameters Editor if desired (see section 6.18 Mixing Coefficients (p. 359) in the User Guide). Dead water subsections are treated as sections where the velocity is equal to zero.

For each cross section it is assumed that the parallel channels all have the same energy slope  $I$  for a given water level. Based on this assumption a momentum equation is applied to each subsection in the cross section:

$$\begin{aligned} \rho g \frac{n_i^2 V_i^2}{R_i^{1/3}} P_{bed,i} + \tau_{w,l,i} P_{w,l,i} + \tau_{w,r,i} P_{w,r,i} \\ + \tau_{v,l,i} P_{v,l,i} + \tau_{v,r,i} P_{v,r,i} = \rho g A_i I \end{aligned} \quad (1.177a)$$

for  $i = 1, \dots, N$ .

If a resistance radius formulation is used the momentum equation (1.177a) reads

$$\begin{aligned} \rho g \frac{n_i^2 V_i^2}{R_i^{4/3}} A_i + \tau_{w,l,i} P_{w,l,i} + \tau_{w,r,i} P_{w,r,i} \\ + \tau_{v,l,i} P_{v,l,i} + \tau_{v,r,i} P_{v,r,i} = \rho g A_i I \end{aligned} \quad (1.177b)$$

for  $i = 1, \dots, N$ .

where:

$\rho$  density of water.

$g$  acceleration due to gravity.



$R_i$  hydraulic/resistance radius of subsection  $i$ .

$n_i$  Manning's roughness of subsection  $i$ .

$V_i$  average velocity of subsection  $i$ .

$P_{bed,i}$  wetted perimeter of river bed/top of submerged vegetation of subsection  $i$ .

$\tau_{w,l/r,i}$  shear on left/right water-water boundary respectively of subsection  $i$ .

$P_{w,l/r,i}$  'wetted perimeter' of left/right water-water boundary respectively of subsection  $i$  (see Figure 1.56).

$\tau_{v,l/r,i}$  shear on left/right water-vegetation boundary respectively of subsection  $i$

$P_{v,l/r,i}$  'wetted perimeter' of left/right water-vegetation boundary respectively of subsection  $i$  (see Figure 1.56).

$A_i$  water area of subsection  $i$ .

$I$  energy slope at considered cross section.

$N$  Number of subsections at considered cross section.

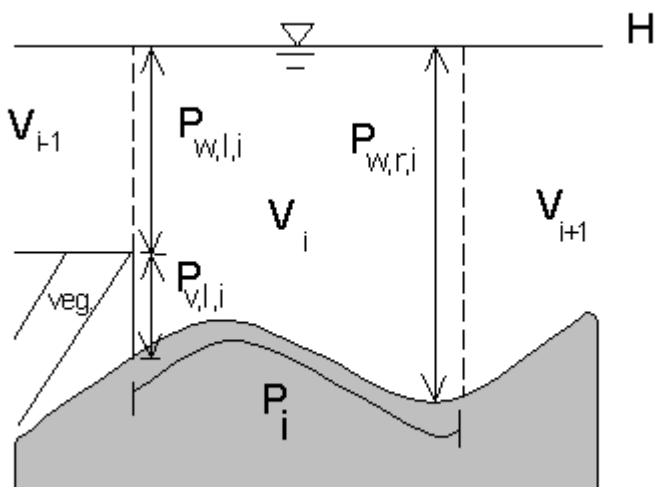


Figure 1.56 Definition of 'wetted perimeters' of a subsection. In the above the right 'wetted perimeter' of the vegetation-water boundary is zero.



Further the subsection average velocities  $V_i$  must satisfy a mass balance equation i.e.

$$\sum_{i=1}^N V_i A_i = Q, \quad (1.178)$$

where  $Q$  is the discharge at the given cross section.

Thus the problem consists of solving  $N+1$  algebraic non-linear equations for the same number of unknowns (subsection velocities and the energy slope  $I$ ). To this end Newton Raphson's method is used.

## 1.27.1 Zone classification

### Normal zones

Zones, which are not dead water zones (zones with velocity equal to zero) and do not have any vegetation, are termed normal zones. The code provides three alternatives for the calculation of the hydraulic radius for a normal subsection:

1. Resistance radius (*p. 136*).
2. Depth integrated hydraulic radius (*p. 137*).
3. Hydraulic radius (*p. 137*).

The radius is set in the "MIKE11.ini" file which is located in the "WINDOWS" directory. The QSSVEG\_RADIUS variable is set to either 1,2 or 3 respectively.

#### Resistance radius

The resistance radius and Manning's  $n$  of a given normal subsection is calculated on the basis of

$$R_h = \left( \frac{1}{A} \int_{y_0}^{y_N} h^{3/2} dy \right)^2, \quad n_c = \frac{\int_{y_0}^{y_N} h^{3/2} dy}{\int_{y_0}^{y_N} \frac{h^{3/2}}{n} dy} \quad (1.179)$$

where  $A$  is the water area of the subsection,  $h$  the local water depth and  $y_0$ ,  $y_N$  are the end points respectively of the subsection.





### Depth integrated hydraulic radius

For a profile without any vertical walls the hydraulic radius and Manning's  $n$  of a given normal subsection may be calculated on the basis of

$$R_h = \left( \frac{1}{A} \int_{y_0}^{y_N} h^{5/3} dy \right)^{3/2}, \quad n_c = \frac{\int_{y_0}^{y_N} h^{5/3} dy}{\int_{y_0}^{y_N} \frac{h^{5/3}}{n} dy} \quad (1.180)$$

where  $A$  is the water area of the subsection,  $h$  the local water depth and  $y_0, y_N$  are the end points respectively of the subsection.

### Hydraulic radius

For a subsection with vertical walls and non-varying Manning's  $n$  the classical expression used for calculating the subsections hydraulic radius is given by

$$R_h = \frac{A}{P} \quad (1.181)$$

For varying Manning's  $n$  the formula used for calculating the hydraulic radius is

$$R_h = \left( \frac{\sum_{i=1}^N A_i R_i^{2/3}}{N} \right)^{3/2} \quad (1.182)$$

where

$$R_i = \frac{A_i}{P_{c,i}} \quad (1.183)$$

and  $A_i, P_{c,i}$  are the area and wetted perimeter of the given segment  $i$  respectively (see Figure 1.57). If the segment does not have vertical walls then  $P_{c,i} = P_i$ .

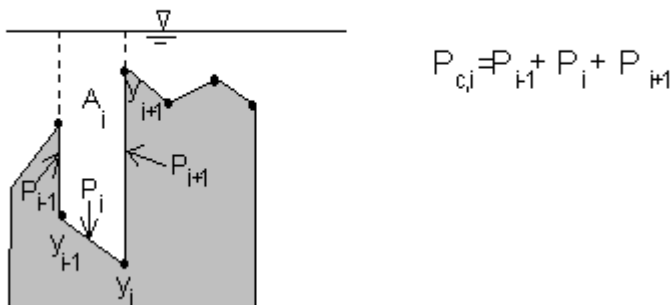


Figure 1.57 The determination of hydraulic radius for a segment with vertical side walls. The compound wetted perimeter of the segment is also illustrated.

Manning's  $n_c$  is determined from

$$n_c = \frac{\sum_{i=1}^N A_i R_i^{\frac{2}{3}}}{\sum_{i=1}^N \frac{A_i R_i^{\frac{2}{3}}}{n_{c,i}}} \quad (1.184)$$

where

$$n_{c,i} = \left( \frac{P_i n_i^{\frac{3}{2}} + \sum_{\text{vertical side walls}} P n^{\frac{3}{2}}}{P_i + \sum_{\text{vertical side walls}} P} \right)^{\frac{2}{3}} \quad (1.185)$$

where  $n$  is Manning's  $n$  for each of the vertical segments.

### Normal zones adjacent to one another

Two normal zones may be adjacent to one another if they lie on either side of a marker indicating a border between the low water channel (LWC) and the high water channel (HWC). The markers which determine these borders may be set in the Cross Section Editor (see Chapter 3 Cross Section Editor



(p. 169) in the User Guide). The markers are numbered 4 and 5 respectively. The mixing coefficients at these boundaries have default values given by

$$f_{wat} = f\left(\frac{b}{B}\right) = \begin{cases} 0,17 & \text{for } \frac{b}{B} < 0,6 \\ 0,07 & \text{for } 0,6 \leq \frac{b}{B} < 0,8 \\ 0,04 & \text{for } 0,8 \leq \frac{b}{B} \end{cases} \quad (1.186)$$

where

$b$  the low flow channel width (distance between marker 4 and 5)

$B$  the width of the channel (water surface width)

The mixing coefficient may be changed under the Mixing Coefficients tab (see 6.18 Mixing Coefficients (p. 359) in the User Guide).

### Vegetation zones

Vegetation zones are implemented so that the top of the vegetation is horizontal. This horizontal level is defined as the average elevation of the vegetation zone plus the average vegetation height in the zone i.e.

$$\text{horizontal level} = \frac{1}{y_2 - y_1} \int_{y_1}^{y_2} z dy + \frac{1}{y_2 - y_1} \int_{y_1}^{y_2} h_v dy \quad (1.187)$$

where  $z$  is the vertical coordinate given with respect to the given datum and  $h_v$  is the local vegetation height (see Figure 1.58).

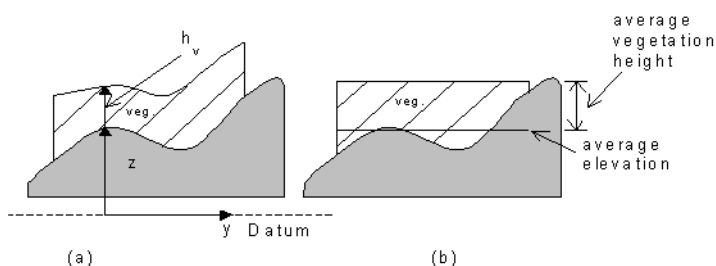


Figure 1.58 The implementation of vegetation subsections in a cross section profile. The profile on the right is the one used for the calculations.

Figure 1.58 illustrates the implementation of a vegetation zone. If the profile has a steep gradient this implementation may give rise to a riverbed having a vertical segment. These vertical segments need special consideration when calculating hydraulic radius and compound roughness of the subsection.

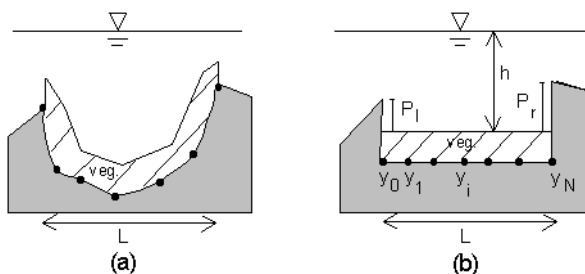


Figure 1.59 A vegetation zone with a steep gradient in the bed topography. (a) Raw data. (b) The profile used for the computations.

The hydraulic radius of a vegetation subsection is calculated using the following formula (see Figure 1.59):

$$R_h = \left( \frac{\sum_{i=1}^N A_i R_i^{2/3}}{A} \right)^{3/2} \quad (1.188)$$

where

$$R_i = \frac{A_i}{\Delta y_i} = \frac{h \Delta y_i}{\Delta y_i} = h \text{ for } i \neq 1, N, \quad (1.189a)$$

$$A = h \sum_{i=1}^N \Delta y_i = hL \quad (1.189b)$$

$$\Delta y_i = y_i - y_{i-1} \quad (1.189c)$$



For the two segments with a partially vertical wetted perimeter the following expressions are used

$$R_1 = \frac{A_1}{\Delta y_1 + P_l} = h \frac{\Delta y_1}{\Delta y_1 + P_l} \quad (1.190a)$$

$$R_N = \frac{A_N}{\Delta y_N + P_r} = h \frac{\Delta y_N}{\Delta y_N + P_r} \quad (1.190b)$$

Manning's  $n$  is calculated on the basis of the following formula:

$$n_c = \frac{\sum_{i=1}^N A_i R_i^{\frac{2}{3}}}{\sum_{i=1}^N \frac{A_i R_i^{\frac{2}{3}}}{n_i}} \quad (1.191)$$

where  $n_i$  is Manning's  $n$  of segment  $i$  with  $n_1, n_N$  given by

$$n_1 = \left( \frac{P_l n_l^{3/2} + \Delta y_1 n_{1,veg}^{3/2}}{P_l + \Delta y_1} \right)^{2/3} \quad (1.192a)$$

$$n_N = \left( \frac{P_r n_r^{3/2} + \Delta y_N n_{N,veg}^{3/2}}{P_r + \Delta y_N} \right)^{2/3} \quad (1.192b)$$

and

$n_l, n_r$  are Manning's  $n$  of the vertical sections to the left and right of the panel respectively

$n_{l,veg}$  is Manning's  $n$  of the vegetation section to the far left of the panel

$n_{r,veg}$  is Manning's  $n$  of the vegetation section to the far right of the panel

As can be seen if  $P_r = P_f = 0$  then the expressions simply become

$$R_c = h \quad \text{and} \quad (1.193)$$

$$n_c = \frac{L}{N \sum_{i=1} \frac{\Delta y_i}{n_i}} \quad (1.194)$$

If further Manning's  $n$  is constant through the subsection then  $n = n_c$

The mixing coefficients at the subsection boundaries have default values, but may be changed by the user under the Mixing Coefficients tab.

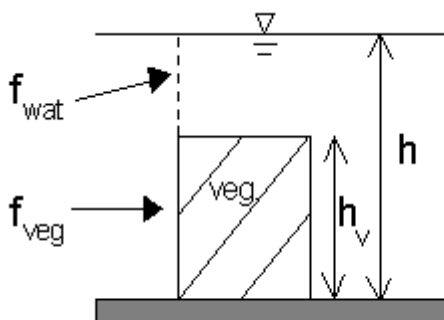


Figure 1.60 Illustration of mixing coefficients at a vegetation zone.

The effect of vegetation is most significant for values of the average vegetation height being of the same order of magnitude as the local water depth. To model this the vegetation height ( $h_v$ ) is taken as being equal to the local water depth ( $h$ ) for  $h_v > 0.9h$  (see Figure 1.60). In other words the water above the vegetation is only considered if it takes up more than 10% of the total panel



area (water and vegetation). The mixing coefficient at a vegetation boundary is a function of the width to height ratio of the vegetation given by

$$f_{veg} = \begin{cases} 0 & \text{for } \frac{W_{veg}}{h_v} < 1 \\ f_{veg,b} \left( \frac{W_v}{h_v} \right)^{0,34} & \text{for } 1 \leq \frac{W_{veg}}{h_v} < 34,5 \\ f_{veg,i} & \text{for } 34,5 \leq \frac{W_{veg}}{h_v} \end{cases} \quad (1.195)$$

where

$h_v$  Average vegetation height of panel.

$W_v$  Total width of vegetation panel.

$f_{veg,b}$  Mixing coefficient used at vegetation zone adjacent to levee (see eq. (1.196)).

$f_{veg,i}$  Mixing coefficient at of independent vegetation zone equal to 0.1 by default but may be changed by the user in the Hydrodynamic Parameters Editor under the Mixing Coefficients tab.

### Vegetation zones adjacent to river levee (adjacent vegetation zones)

Vegetation subsections next to either of the rivers levees are treated more or less as independent vegetation zones. The difference in formulation lies in the values for the mixing coefficients. For an adjacent vegetation the following values are used as default:

$$f_{veg,bank} = 0,03 \quad (1.196)$$

and

$$f_{wat} = f \left( 1 - 2 \frac{W_b}{B} \right) \quad (1.197)$$

where the function  $f$  is the one used for the mixing coefficients at high/low water channel boundaries (e.g. (1.186)),  $W_b$  is the width of the bank vegetation zone and  $B$  is the width of the water surface, dead water zones not included (see Figure 1.61).



**Note** that dead water zones on the lee side of vegetation are treated as a vegetation zone.

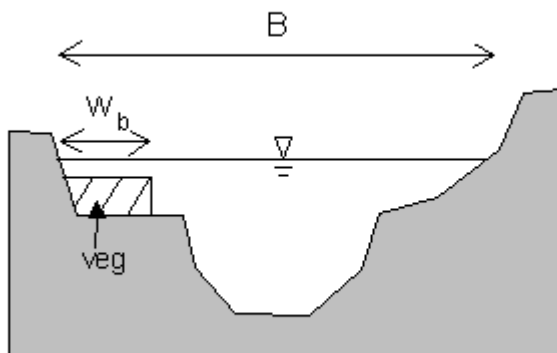


Figure 1.61 Definition of the width  $W_b$  of adjacent vegetation zones.

As for a vegetation zone the water part of the panel is only considered if it is takes up more than 10% of the total panel area (water + vegetation).

## Dead water zones

Dead water zones have zero velocity and appear in two possible situations: as an effect of expansion or contraction of the channel or the zones may be implemented by the user. The mixing coefficient at a water-water boundary at a dead water zone is by default given by  $f_{wat}=0.04$

### 1.27.2 Solution algorithm

The water level profile is found through a backwater analysis. The algorithm consist of two loops:

- An **inner loop** which determines the velocity distribution and energy slope in a specific cross section for a given water level.
- At **outer loop** which determines the water level in the cross section based on the values at the downstream cross section.

#### Inner loop: Determination of subsection velocities and energy gradient for fixed water level.

The inner loop solves the momentum equation and the mass balance equation for a given water level.





The system of equations to be solved can be written on the following form

$$f_i(V_1, \dots, V_N, l) = \rho g \frac{n_i^2 V_i^2}{R_i^{1/3}} P_{bed,i} + \tau_{w,l,i} P_{w,l,i} + \tau_{w,r,i} P_{w,r,i} + \tau_{v,l,i} P_{v,l,i} + \tau_{v,r,i} P_{v,r,i} - \rho g A_i l = 0 \quad (1.198a)$$

$$g(V_1, \dots, V_N) = \sum_{i=1}^N V_i A_i - Q = 0 \quad (1.198b)$$

If a hydraulic resistance formulation is used then equation (1.198a) is formulated as

$$f_i(V_1, \dots, V_N, l) = \rho g \frac{n_i^2 V_i^2}{R_i^{4/3}} A_i + \tau_{w,l,i} P_{w,l,i} + \tau_{w,r,i} P_{w,r,i} + \tau_{v,l,i} P_{v,l,i} + \tau_{v,r,i} P_{v,r,i} - \rho g A_i l = 0 \quad (1.198c)$$

where  $i = 1, \dots, N$ .

Let

$$\mathbf{f}(V_1, \dots, V_N, l) = (f_1, \dots, f_N) \text{ and} \quad (1.199a)$$

$$\mathbf{V} = (V_1, \dots, V_N) \quad (1.199b)$$

be  $N$ -dimensional vectors. Newton-Raphson's method can then be expressed as

$$\mathbf{V}^{m+1} = \mathbf{V}^m + \Delta \mathbf{V}^{m+1}, \quad (1.200a)$$

$$l^{m+1} = l^m + \Delta l^{m+1} \quad (1.200b)$$

where  $m$  is the iteration number and  $\Delta \mathbf{V}^{m+1}$ ,  $\Delta l^{m+1}$  are found as the solution of

$$\begin{bmatrix} \frac{\partial \mathbf{f}(\mathbf{V}^m, l^m)}{\partial \mathbf{V}} & \frac{\partial \mathbf{f}(\mathbf{V}^m, l^m)}{\partial l} \\ \frac{\partial \mathbf{g}(\mathbf{V}^m)}{\partial \mathbf{V}} & 0 \end{bmatrix} \begin{bmatrix} \Delta \mathbf{V}^{m+1} \\ \Delta l^{m+1} \end{bmatrix} = \begin{bmatrix} -\mathbf{f}(\mathbf{V}^m, l^m) \\ -\mathbf{g}(\mathbf{V}^m) \end{bmatrix} \quad (1.201)$$



The above system is not tridiagonal, and the double sweep algorithm thus cannot be applied directly. On the other hand the matrix  $\partial \mathbf{f}(\mathbf{V}^m, I^m) / \partial \mathbf{V}$  is tridiagonal since each subsection only interacts with adjacent subsections. This tridiagonal structure is utilized in the following way. Consider the first  $N$  equations of the above system:

$$\frac{\partial \mathbf{f}(\mathbf{V}^m, I^m)}{\partial \mathbf{V}} \Delta \mathbf{V}^{m+1} = -\mathbf{f}(\mathbf{V}^m, I^m) - \frac{\partial \mathbf{f}(\mathbf{V}^m, I^m)}{\partial I} \Delta I^{m+1} \quad (1.202)$$

This system may be solved with respect to  $\Delta \mathbf{V}^{m+1}$  giving an expression linear in  $\Delta I^{m+1}$ :

$$\begin{aligned} \Delta \mathbf{V}^{m+1} &= -\left(\frac{\partial \mathbf{f}(\mathbf{V}^m, I^m)}{\partial \mathbf{V}}\right)^{-1} \mathbf{f}(\mathbf{V}^m, I^m) \\ -\left(\frac{\partial \mathbf{f}(\mathbf{V}^m, I^m)}{\partial \mathbf{V}}\right)^{-1} \frac{\partial \mathbf{f}(\mathbf{V}^m, I^m)}{\partial I} \Delta I^{m+1} &= \mathbf{x}_1 + \mathbf{x}_2 \Delta I^{m+1} \end{aligned} \quad (1.203)$$

By taking the scalar product with  $\frac{\partial \mathbf{g}(\mathbf{V}^m)}{\partial \mathbf{V}}$  and inserting the last equation of the linear system one finds

$$\frac{\partial \mathbf{g}(\mathbf{V}^m)}{\partial \mathbf{V}} \Delta \mathbf{V}^{m+1} = -\mathbf{g}(\mathbf{V}^m) = \frac{\partial \mathbf{g}(\mathbf{V}^m)}{\partial \mathbf{V}} \mathbf{x}_1 + \frac{\partial \mathbf{g}(\mathbf{V}^m)}{\partial \mathbf{V}} \mathbf{x}_2 \Delta I^{m+1}, \quad (1.204)$$

which can be solved with respect to  $\Delta I^{m+1}$  giving:

$$\Delta I^{m+1} = \frac{-\mathbf{g}(\mathbf{V}^m) - \frac{\partial \mathbf{g}(\mathbf{V}^m)}{\partial \mathbf{V}} \mathbf{x}_1}{\frac{\partial \mathbf{g}(\mathbf{V}^m)}{\partial \mathbf{V}} \mathbf{x}_2} \quad (1.205)$$

The expression for  $\Delta \mathbf{V}^{m+1}$  is now easily computed. Notice that  $\mathbf{x}_1$  and  $\mathbf{x}_2$  are obtained by solving a tridiagonal system with two right hand sides.

### Outer loop: The determination of the water level

The inner loop is used for determining the velocity distribution in a cross section for a given value of the water level. The outer loop is the determination of



the water level in each cross section. For the latter a momentum equation is solved for neighbouring cross sections:

$$\begin{aligned}
 & \alpha \left( \frac{1}{A} \sum_{i=1}^N \frac{V_i^2 A_i \beta_i}{2g} \right)_2 - \alpha \left( \frac{1}{A} \sum_{i=1}^N \frac{V_i^2 A_i \beta_i}{2g} \right)_1 = H_1 - H_2 \\
 & + \frac{1}{2} \left[ \left( \frac{1}{A} \sum_{i=1}^N \frac{n_i^2 V_i^2}{R_i^{1/3}} P_{bed,i} \right)_1 + \left( \frac{1}{A} \sum_{i=1}^N \frac{n_i^2 V_i^2}{R_i^{1/3}} P_{bed,i} \right)_2 \right] \Delta X \\
 & + \frac{1}{2} \left[ \frac{1}{\rho g A} \sum_{i=1}^N (\tau_{w,l,i} P_{w,l,i} + \tau_{w,r,i} P_{w,r,i} + \tau_{v,l,i} P_{v,l,i} + \tau_{v,r,i} P_{v,r,i}) \right]_1 \Delta X \\
 & + \frac{1}{2} \left[ \frac{1}{\rho g A} \sum_{i=1}^N (\tau_{w,l,i} P_{w,l,i} + \tau_{w,r,i} P_{w,r,i} + \tau_{v,l,i} P_{v,l,i} + \tau_{v,r,i} P_{v,r,i}) \right]_2 \Delta X
 \end{aligned} \tag{1.206}$$

Where

$\alpha$  velocity distribution coefficient.

$A$  water area of cross section.

$H$  water level.

$\beta_i$  suppression factor for the panel  $i$  (see Suppression of the convective terms (p. 148)).

$\Delta X$  distance between cross sections.

Further terms with subscript 1 are values at the downstream cross section and terms with subscript 2 are evaluated at the upstream cross section. The goal is the determination of  $H_2$  being the upstream value of the water level. Terms with subscript 2 in the above equation implicitly depend on the water level  $H_2$  one therefore needs to run the inner loop to determine the subsection velocities and energy gradient for each new value of  $H_2$ . Since all other values can be determined on the basis of  $H_2$ , the above equation constitutes essentially an equation in one unknown ( $H_2$ ). The solution to this equation is found by iteration. To ensure convergence a bisection method is used.

As an alternative to the above equation for obtaining the water level the law of energy conservation is available for cases with no vegetation/dead water zones:

$$\left[ H_2 + \frac{\alpha \beta_2}{2g} \left( \frac{Q_2}{A_2} \right)^2 \right] - \left[ H_1 + \frac{\alpha \beta_1}{2g} \left( \frac{Q_1}{A_1} \right)^2 \right] = \frac{1}{2} \left( \frac{n_1^2 Q_1^2}{A_1^2 R_1^{4/3}} + \frac{n_2^2 Q_2^2}{A_2^2 R_2^{4/3}} \right) \Delta X \tag{1.207}$$



To use the energy equation for the determination of the water level the "QSSVEG\_ENERGY" variable should be set to "ON" in the "MIKE11.ini" file located in the "WINDOWS" directory.



**Note** that when utilizing the energy equation the cross section is considered as one panel thus the inner loop for determining the velocity distribution is not needed.

### Suppression of the convective terms

There are three alternatives for the suppression of the convective terms in either of the equations (1.206) and (1.207):

1. The Froude number is calculated for each of the panels upstream and downstream and the maximum of these Froude numbers is used for determining the suppression factor according to section 1.36.1 *Suppression of convective acceleration term (p. 171)*.
2. A suppression factor is calculated and used for each panel upstream and downstream. Thus the suppression factor is specific to each panel in the cross sections. The suppression factors are found according to 1.36.1 *Suppression of convective acceleration term (p. 171)*.
3. No suppression is applied to the convective terms. **Caution is recommended when using this possibility since it may cause severe numerical instability.**



The suppression strategy is set using the variable "QSSVEG\_SUPPRESSION\_STRATEGY" in the "MIKE11.ini" file located in the "WINDOWS" directory.

### Upstream centering of bed friction term

To increase the numerical stability of the algorithm an upstream centering of the friction terms may be applied.

The centering is given by:

$$\text{friction} = \begin{cases} \left( \frac{b_1}{\text{fric}_{\text{down}}} + \frac{1-b_1}{\text{fric}_{\text{up}}} \right)^{-1} & , \text{ for } \text{fric}_{\text{up}} < \text{fric}_{\text{down}} \\ b_1 \text{fric}_{\text{down}} + (1-b_1) \text{fric}_{\text{up}} & , \text{ for } \text{fric}_{\text{up}} \geq \text{fric}_{\text{down}} \end{cases} \quad (1.208)$$

Subscripts up and down refer to upstream and downstream values respectively.

The terms fric are given by

$$\text{fric} = \frac{1}{2A} \sum_{i=1}^N \frac{n_i^2 V_i^2}{R_i^{4/3}} A_i \quad (1.209a)$$



if a resistance radius or depth integrated hydraulic radius formulation is chosen and by

$$\text{fric} = \frac{1}{2A} \sum_{i=1}^N \frac{n_i^2 V_i^2}{R_i^{1/3}} P_i \quad (1.209b)$$

if a hydraulic radius formulation is chosen.

The weighting term  $b_1$  is calculated from

$$b_1 = \begin{cases} 0,1 + 0,4(1 - Fr_{\max}^2) & , \text{ for } Fr_{\max} < 1 \\ 0,1 & , \text{ for } Fr_{\max} \geq 1 \end{cases} \quad (1.210)$$

where  $Fr_{\max}$  is the maximum Froude number of the upstream and downstream cross sections. The Froude number is expressed as

$$Fr = \frac{Q}{A\sqrt{gR}} \quad (1.211)$$

The centering can be switched on by setting the variable "QSSVEG\_CENTERING\_FRICTION" to "ON" in the "MIKE11.ini" file located in the "WINDOWS" directory.

### 1.27.3 Bridges

When utilising the steady flow with vegetation module it is possible to include the effect of bridges on the water level. The water level increment is calculated under the assumption that the bed slope is zero and the effect of the bed friction is negligible. Thus in order to minimise the errors introduced by these assumptions the user should place the cross sections upstream and downstream of the bridge close to the bridge.

Bridges may be of two types:

- Bridge Piers (p. 150).
- Submerged bridges (p. 151).



**Note** that the increment due to bridges is only considered if the Froude number of the flow is less than 0.6. If this is not the case a warning is issued.



## Bridge Piers

The increment in water level due to bridge piers is found on the basis of D'Aubuisson's formula (/10/). The code provides two alternatives for the implementation of this formula:

1. A rectangular channel analysis is used if a positive value is entered for the upstream width of the channel (see section Bridges in the User Guide) thus the increment is obtained through

$$\Delta h = \frac{1}{2g} \left[ \frac{Q_1^2}{C^2 (b_2 - w_{piers})^2 h_1^2} - \frac{Q_2^2}{b_2^2 (h_1 + \Delta h)^2} \right] \quad (1.212)$$

where

$\Delta h$  increment in water level due to the presence of bridge piers.

$Q_1$  discharge downstream of piers.

$Q_2$  discharge upstream of piers.

$C$  user defined constant determined by pier geometry.

$b_2$  channel width upstream of piers.

$h_1$  local water depth downstream of piers.

$w_{piers}$  total width of piers.

By rearranging eq. (1.212) a third degree polynomial in  $\Delta h$  is obtained. The code determines all real roots of this polynomial and the smallest positive root is used in case of more than one root.

2. If a non-positive value is entered for the upstream width of the channel (see section Bridges in the User Guide) a momentum equation is solved which takes the effect of an arbitrary shape of the cross section into account:

$$H_2 - H_1 = \frac{1}{2g} \left[ \frac{Q_1^2}{C^2 (A_1 - h_1 w_{piers})^2} - \frac{Q_2^2}{A_2^2} \right] \quad (1.213)$$

where

$H_1$  water level downstream of bridge piers.

$H_2$  water level upstream of bridge piers.

$Q_1$  discharge downstream of bridge piers.



- $Q_2$  discharge upstream of bridge piers.
- $h_1$  water depth downstream of bridge piers.
- $A_1$  cross sectional area downstream of bridge piers.
- $A_2$  cross sectional area upstream of bridge piers.
- $C$  user defined constant determined by pier geometry.
- $w_{piers}$  total width of piers.

Eq. (1.213) is solved with respect to  $H_2$  using a bisection method. Note that iteration is needed since  $A_2$  depends on the water level upstream of the piers.



**Note** that if the Froude number is above the criteria of 0.6, the effect of the bridge piers is neglected. The criteria may be altered by setting the variable BRIDGE\_FROUDE\_CRITERIA in the MIKE11.ini file.

### Submerged bridges

As for the case of bridge piers there are two alternatives for the implementation of submerged bridges. Either the effect of the bridge is determined from a rectangular channel analysis or a momentum equation is solved which takes the effect of an arbitrary shape of the cross section into account.

The latter is used if a non-positive value for the channel width is entered (see Fully Submerged Bridge in the User Guide).

1. For a rectangular channel the momentum equation for a submerged bridge reads

$$\frac{1}{B} \left( \frac{Q_1^2}{h_1} - \frac{Q_2^2}{h_2} \right) + \frac{1}{2} g B (h_1^2 - h_2^2) = -\frac{1}{2} \frac{Q_2^2}{(A_1 - a_{bridge})^2} a_{bridge} C_D \quad (1.214)$$

where

- $Q$  discharge.
- $A$  cross sectional area.
- $B$  surface width.
- $h$  local water depth.
- $a_{bridge}$  cross sectional area of submerged bridge.
- $C_D$  drag coefficient.

$1,2$  indices referring to down-/upstream values respectively.

The terms on the left hand side of eq. (1.214) are the momentum terms and the force exerted by the pressure in the fluid the term on the right is the drag of the submerged bridge.

2. Eq. (1.214) is derived under the assumption of a rectangular channel, though the expression is easily modified to take the effect of non-rectangular channels into account. After this modification the momentum equation reads:

$$\frac{Q_1^2}{A_1} - \frac{Q_2^2}{A_2} = \frac{1}{2}g\left(\int_0^{B_2} h_2^2 dy - \int_0^{B_1} h_1^2 dy\right) - \frac{1}{2} \frac{Q_2^2}{(A_1 - a_{bridge})^2} C_D a_{bridge} \quad (1.215)$$

Eq. (1.215) is solved using bisection. Notice that  $A_2, B_2$  and  $h_2$  depend on the upstream water level  $H_2$ .

This is to decrease the time step.



**Note** that if the Froude number is above the criteria of 0.6, the effect of the submerged bridge is neglected. The criteria may be altered by setting the variable BRIDGE\_FROUDE\_CRITERIA in the MIKE11.ini file.

#### 1.27.4 Junctions

The effect of river junctions on the water level can be incorporated into the calculations. Figure 1.62 gives a definition sketch of the terms used for the determination of the increment in the water level due to the presence of a junction.



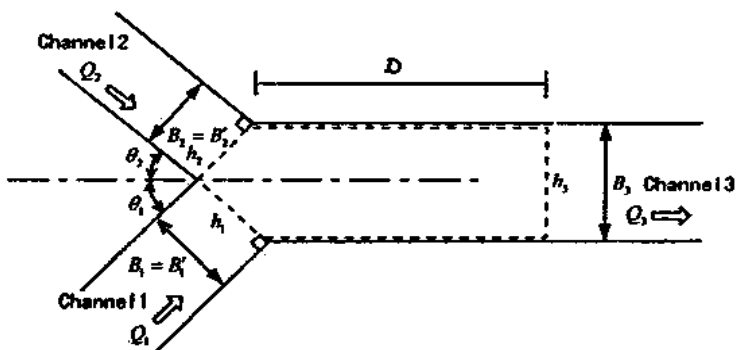


Figure 1.62 Definition sketch for a river junction. Note  $h_1=h_2=h$  where  $h$  is the local water depth in channel 1 and 2.

The increment in the water level is found using the following equation

$$\left(\frac{h}{h_3}\right)^3 - (1 + 2\alpha F_3^2) \frac{h}{h_3} + 2\alpha \left\{ \left(\frac{Q_2}{Q_3}\right)^2 \frac{B_3}{B_2} \cos\theta_2 + \left(\frac{Q_1}{Q_3}\right)^2 \frac{B_3}{B_1} \cos\theta_1 \right\} F_3^2 = 0 \quad (1.216)$$

where

$\alpha$  momentum correction coefficient.

$h_3$  local water depth of channel 3 at distance  $D$  from the node. Calculated as cross sectional area divided by channel width.

$Q$  discharge.

$\theta$  direction angle of river with respect to channel 3.

$B$  width of channel.

$F_3$  Froude number of channel 3 defined by

$$F_3^2 = \frac{Q_3^2}{gB_3^2h_3^3} \quad (1.217)$$

Further indices refer to the river number in Figure 1.62.

Concerning the derivation of eq. (1.216) please refer to /13/ for details. The equation is derived using a rectangular channel analysis under the assumption of no bed slope. Thus the user should for safety ensure that the bottom level of the three channels meeting in the junction are the same.



The average water depth at distance  $D$  along channel 3 is found using linear interpolation if  $D$  is not at a cross section. The channel widths are user defined and are entered under the tab named Junctions in the River Network Editor (see Junctions in the User Guide). Eq. (1.217) constitutes a third degree polynomial in the ratio  $h/h_3$ . The code determines all real roots of this equation and in the case of more than one real root chooses the smallest one which is greater than unity.

Since eq. (1.216) is derived under the assumption of a horizontal bed level the average water level in channel 1 and 2 may be expressed as

$$H = H_3 + \Delta h \quad (1.218)$$

where  $\Delta h$  is the increment due to the junction given by

$$\Delta h = h_3 \left( \frac{h}{h_3} - 1 \right) \quad (1.219)$$

and  $H_3$  is the water level in channel 3 at the distance  $D$  from the node. The water level given by eq. (1.218) is applied at the first cross section after the junction in channel 1 and 2 respectively.

### 1.27.5 Variation in water level due to curves

The effect of river curvature on the water level may be included in the computations. This is done through the W. L. Incr.- Curve dialog tab (section 6.19 W. L. Incr.- Curve (p. 360) in the User Guide).

The increment is calculated from

$$\Delta H = \frac{1}{2} \frac{BV^2}{gr_c} \quad (1.220)$$

where

$\Delta H$  increment in water level.

$B$  channel width.

$r_c$  curvature radius of river.

$g$  acceleration of gravity.

$V$  mean velocity of cross section.

In each branch the curvature radius in the individual digitization point is calculated as the radius of the circle through the digitization point itself, the previ-



ous and the next digitization point. The radius in the first and the last digitization point in each branch is respectively set equal to the radius in the second and the last but one digitization point in the branch. Once the curvature radius in the digitization points is calculated, the curvature radius in each grid point is calculated by linear interpolation of the curvature radius in the digitization points. This interpolation is based on chainage.



**NOTE!** The increment due to curvature is added after the backwater analysis has been done. In other words the increment is added to the steady flow computations. The increments is only added if

$$\frac{r_c}{B} < 10 \quad (1.221)$$

is satisfied.

Further if also the variation due to sand bars is considered only the greatest of the two increments is added to the calculated water level.

### 1.27.6 Variation in water level due to sand bars

The effect of sand bars on the water level may be included in the computations. This is done through the W. L. Incr.- Sand Bars dialog tab (section 6.20 W. L. Incr.- Sand Bars (p. 363) in the User Guide).

The increment is calculated from

$$\frac{\Delta H}{h_m} = f\left(\frac{B}{h_m}, \frac{1}{I_b}\right) \quad (1.222)$$

where

$\Delta H$  increment in water level.

$h_m$  mean water depth of low water channel.

$B$  low water channel width.

$A$  curvature radius of river.

$I_b$  slope of the channel bed.

The function  $f$  expresses the water level increments dependence on the width/depth-ratio and the bed slope. The function is based on empirical results which are tabulated in MIKE 11, any intermediate value is obtained through linear interpolation.



**NOTE!** The increment due to sand bars is added after the backwater analysis has been done. In other words the increment is added to the steady flow computations. Further if also the variation due to curvature (see section 1.27.5) is considered only the greatest of the two increments is added to the calculated water level.

## 1.28 Regulating Structures

Regulating Structures are structures for which the operation is user-defined. They fall into two main categories:

### 1.28.1 Function of time

A structure may be specified in the River Network Editor → Tabular view: Structures → Regulating with a pre-determined operation as defined by a  $Q-t$  relationship specified in the boundary editor. Examples include pumps and some types of reservoir outflows. The  $Q-t$  relationship replaces the momentum equation at a  $Q$ -point and physically separates the model into upstream and downstream branches. The discharge is interpolated linearly at each time step from the specified  $Q-t$  table. The location of the  $Q-t$  relationship is specified in the boundary editor.

### 1.28.2 Function of $h$ and/or $Q$

A structure may also be specified with an operation which is a user-specified function of the water level or discharge at other locations in the model. This function is specified in the River Network Editor → Tabular view: Structures → Regulating → Regulation factor box and is given by:

$$Q = A Q_a \quad (1.223)$$

where,

$Q_a$  is the discharge at location  $a$

$A$  is a coefficient given by:

$$A = f(Z_b) \quad (1.224)$$

where,

$Z_b$  is either water level  $h$ , or discharge  $Q$ , at location  $b$ .

This feature allows the flow at the control point to be related dynamically to any two variables in the system giving flexibility in the description of operating policies. For example, the outflow from a reservoir could be related to the res-



ervoir inflow (location a) and the reservoir stage or a stage downstream (location b). Such an example is illustrated in Figure 1.63 for which the user-defined relationship is indicated in Table 1.5.

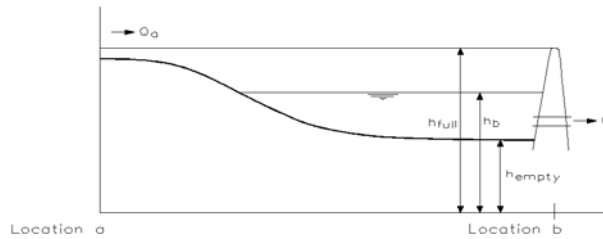


Figure 1.63 Reservoir outflow as a user-defined regulating structure

From Table 1.5 and Equations (1.223) and (1.224) it can be seen that when the reservoir is full the outflow at location b ( $Q$ ) is set equal to the inflow at a ( $Q_a$ ) and that when the reservoir is empty the outflow is set to zero as shown by the expressions in Equation (1.225).

$$Q = \begin{cases} Q_a & \text{for } h_b = h_{full} \\ 0 & \text{for } h_b = h_{empty} \end{cases} \quad (1.225)$$

Table 1.5 User-defined relationship for example in Figure 1.63

Reservoir level $h(z)$	$A$
Full	1
.	.
Empty	0

$Q$  is evaluated explicitly on the basis of the values of  $Q_a$  and  $Z_b$  from the previous iteration. If grid point  $a$  or  $b$  is situated close to the structure and there is little physical damping (like that of a full reservoir), the formulation may give rise to numerical instabilities. However, in most practical situations this structure type is used in connection with the operation of a reservoir operating during flood periods where the physical damping from the reservoir will be sufficient to ensure numerical stability.



In some specialized circumstances, a more complex Regulating Structure may be required to adequately describe a particular operation. In this case the MIKE 11 add-on module Control Str. should be used.

## 1.29 Routing

### Non-linear storage function

#### Governing equations

Momentum equation:

$$S = KQ_o^P - T_1 Q_o \quad (1.226a)$$

Continuity equation:

$$\frac{dS}{dt} = Q_i - Q_o \quad (1.226b)$$

where:

$S$  apparent basin storage.

$Q_i$  inflow at water way.

$Q_o$  runoff at water way.

$T_1$  time of delay.

$K, P$  constants.

And,  $T_1$  is the time of delay:

$$Q(t) = Q(t + T_1) \quad (1.227)$$

#### Solution

The continuity equation is discretized

$$\frac{S_{t+\Delta t} - S_t}{\Delta t} = Q_i - \frac{Q_{o,t+\Delta t} + Q_{o,t}}{2}, \quad (1.228)$$

and the momentum equation is substituted giving

$$\frac{KQ_{o,t+\Delta t}^P - T_1 Q_{o,t+\Delta t} - (KQ_{o,t}^P - T_1 Q_{o,t})}{\Delta t} = Q_i - \frac{Q_{o,t+\Delta t} + Q_{o,t}}{2} \quad (1.229)$$



## 1.30 Saint Venant Equations

MIKE 11 HD applied with the dynamic wave description solves the vertically integrated equations of conservation of continuity and momentum (the ‘Saint Venant’ equations), based on the following assumptions:

- the water is incompressible and homogeneous, i.e. negligible variation in density
- the bottom-slope is small, thus the cosine of the angle it makes with the horizontal may be taken as 1
- the wave lengths are large compared to the water depth. This ensures that the flow everywhere can be regarded as having a direction parallel to the bottom, i.e. vertical accelerations can be neglected and a hydrostatic pressure variation along the vertical can be assumed
- the flow is subcritical (Supercritical flow is modelled in MIKE 11, using more restrictive conditions, however (see section 1.36)).

The derivation of the equations of continuity and momentum, as used by MIKE 11, is given in section A.8 Saint Venant Equations (*p. 425*). The resulting equations are:

$$\frac{\partial Q}{\partial x} + \frac{\partial A}{\partial t} = q \quad (1.230a)$$

$$\frac{\partial Q}{\partial t} + \frac{\partial \left( \alpha \frac{Q^2}{A} \right)}{\partial x} + gA \frac{\partial h}{\partial x} + \frac{gQ|Q|}{C^2 AR} = 0 \quad (1.230b)$$

where,

$Q$  discharge

$A$  flow area

$q$  lateral inflow

$h$  stage above datum

$C$  Chezy resistance coefficient

$R$  hydraulic or resistance radius

$\alpha$  momentum distribution coefficient

## 1.31 Solution Scheme

The solution of the equations of continuity and momentum is based on an implicit finite difference scheme developed by Abbott and Ionescu (1967). Details of the scheme are given in section A.9 Solution Scheme (p. 429).

The scheme is structured in order to be independent of the wave description specified (i.e., kinematic, diffusive or dynamic).

A computational grid of alternating  $Q$  (discharge) and  $h$  (water level) points is used as illustrated in Figure 1.64. The computational grid is automatically generated on the basis of the user requirements.  $Q$ -points are placed midway between neighbouring  $h$ -points and at structures, while  $h$ -points are located at cross-sections, or at equidistant intervals in between if the distance between cross-sections is greater than maximum  $dx$  (River Network Editor → Tabular view: Network → Branches). The discharge is defined by convention as positive in the positive  $x$ -direction (increasing chainage).

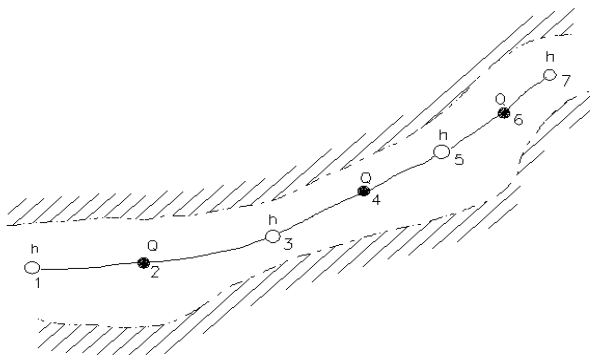


Figure 1.64 Channel section with computational grid

## 1.32 Special Weir

Special weirs are used to model a structure whenever the standard formulation for a broad crested weir or a culvert is not sufficiently flexible.

The special weir enables a user-defined relationship to be specified for critical flow and free overflow conditions.

Two relationships are required, one for flow in positive direction and one for flow in negative direction. The  $h$ -values correspond to water levels at the  $h$ -point upstream of the structure. From these user-defined relationships and from the energy loss relationship, a table relating the critical depth and the critical flow at the structure is derived. The derived relationship is also used during the computation to determine whether the flow is submerged or free





overflow. The descriptions for zero flow and submerged flow are given under section 1.34 Steady State Energy Equation (p. 162).

### 1.33 Stability Conditions

It is not possible to give a single general rule for the selection of  $\Delta t$  and  $\Delta x$  covering all possible situations. The user should note that MIKE 11 assumes a linear variation of all the variables between each time step and grid point. Hence one criterion for  $\Delta t$  and  $\Delta x$  is that they should be small enough to resolve non-linear variations in the time and space, respectively. For example, simulation of tidal variations require time steps in the order of 10-30 minutes in order to fully describe the tidal cycle in time. Similarly, rapidly changing river geometry requires space steps small enough to describe the topography accurately.

In order to obtain a stable and accurate solution to the finite difference scheme the following conditions have to be fulfilled:

- the topographic resolution must be sufficiently fine that non-linearities in water levels and discharges are adequately resolved. The maximum allowable value for  $\Delta x$  (dx-max) should be selected on this basis
- the time step,  $\Delta t$ , should be fine enough to provide an accurate representation of a wave. For example, the maximum time step for a tidal simulation is generally around 30 minutes
- if structures are being used a smaller time step may be required
- the Courant condition (given below) can be used as a guide for selecting the time step providing the above conditions are also satisfied. Typically a value of  $C_r$  is of the order of 10 to 15, but much higher values have been used (up to 100)

$$C_r = \frac{\Delta t(V + \sqrt{gy})}{\Delta x} \quad (1.231)$$

where,  $V$  is velocity;

- the velocity condition as given below can sometimes impose a limitation on the time step,  $\Delta t$ , in the case of rapidly varying cross-sections

$$\frac{V\Delta t}{\Delta x} \leq 1 \text{ to } 2 \quad (1.232)$$

#### The Courant criterion

The term  $\sqrt{gy}$  is the celerity of a small disturbance (wave) in shallow water. This assumption is hardly ever satisfied in rivers and channels, where the wave celerity may be significantly smaller.

The Courant criterion is often applied in connection with rivers and channels. The Courant number expresses the number of grid points a wave, generated from a minor disturbance, will move during one time step.

The finite difference scheme used in MIKE 11 (6-point Abbott scheme), allows Courant numbers up to 10-20 if the flow is clearly sub-critical (Froude number less than 1). Computations with a Courant number of 250 have produced results with an error of less than 2% in some very special cases.

## The velocity criterion

The velocity criterion requires that  $\Delta t$  and  $\Delta x$  are selected in the order that a water body will not be transported more than one grid point per time step. When applying the kinematic wave equation, and at weirs, it is acceptable that the velocity times  $\Delta t/\Delta x$  is considerably larger than 1.

An estimation of the qualities of a differential scheme is often based on the following two types of errors:

- error in amplitude
- error in phase

Figure 1.65 shows the phase error for several Courant numbers as a function of the number of h-points per wave length. It shows, for example, that with 24 h-points per wave length and  $Cr=2$ , the computed wave celerity is about 3% too small.

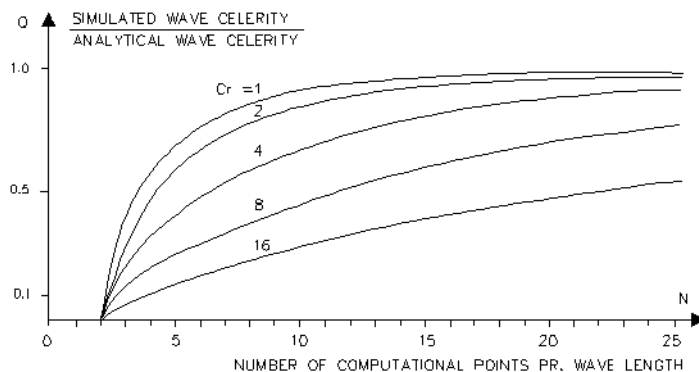


Figure 1.65 The phase error as a function of the number of h-points per wave length for a 6-point Abbott scheme.

## 1.34 Steady State Energy Equation

The steady state is calculated using the energy equation when selecting the switch "Use energy equation" in the page "Quasi Steady" HD parameter editor.



The layout of the energy equation set-up is shown in Figure 1.66.

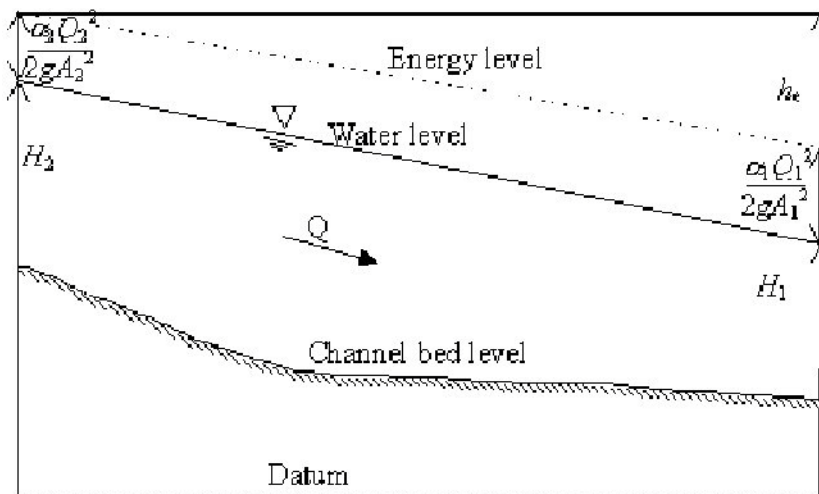


Figure 1.66 The control volume used for determining the water level profile by the use of the energy equation.

The integrated steady state energy equation reads

$$H_1 + \alpha_{m11} \beta_{sup} \frac{\alpha_1 Q^2}{2gA_1^2} = H_2 + \alpha_{M11} \beta_{sup} \frac{\alpha_2 Q^2}{2gA_2^2} + h_e \quad (1.233)$$

where

$H_1, H_2$	Water levels in cross sections
$Q$	Discharge
$\alpha_1, \alpha_2$	Velocity distribution coefficients
$g$	Acceleration due to gravity
$A_1, A_2$	Flow areas
$h_e$	Energy head loss
$\alpha_{M11}$	User defined velocity distribution coefficient (default = 1)
$\beta_{sup}$	Suppression factor



The velocity distribution coefficients  $\alpha_1$  and  $\alpha_2$  are calculated from

$$\alpha = \frac{A_t^2 \left( \frac{K_{LF}^3}{A_{LF}^2} + \frac{K_{CH}^3}{A_{CH}^2} + \frac{K_{RF}^3}{A_{RF}^2} \right)}{K_{TOT}^3} \quad (1.234)$$

where

$K_{LF}$ ,  $K_{CH}$  and  $K_{RF}$

Conveyance for left floodplain, channel and right floodplain respectively.

$A_{LF}$ ,  $A_{CH}$  and  $A_{RF}$

Flow area for left floodplain, channel and right floodplain respectively.

The conveyance for each subsection is determined as

$$K_i = \frac{A_i R_i^{2/3}}{n} \quad (1.235)$$

Where  $n$  is the Manning's number for the cross section. The transversal variation is taken into account through the relative resistance, thus  $n$  factors out.

The suppression factor depends on the Froude number and is given by

$$\beta_{sup} = \begin{cases} 1 - Fr^2 & \text{for } Fr \leq 1 \\ 0 & \text{for } Fr > 1 \end{cases} \quad (1.236)$$

where the Froude number  $Fr$  used is given by

$$Fr = \max \left( \frac{Q^2}{A_1^2 g R_1}, \frac{Q^2}{A_2^2 g R_2} \right) \quad (1.237)$$

The suppression can be omitted if desired.

The energy head loss consists of a friction loss and a contraction or expansion loss

$$h_e = \bar{L} l_{fric} + C \alpha_{M11} \left| \frac{a_1 Q^2}{2g A_1^2} - \frac{a_2 Q^2}{2g A_2^2} \right| \quad (1.238)$$



where

$\bar{L}$  the mean reach length

$I_{fric}$  friction slope

$C$  user defined contraction/expansion coefficient (default 0.1/0.3)

The friction slope is determined through

$$I_{fric} = \begin{cases} \frac{Q|Q|}{\bar{M}^2 \bar{A}} \left( \frac{1}{\phi A_2 R_2^{4/3} + (1-\phi) A_1 R_1^{4/3}} \right) & \text{for } A_1 R_1^{4/3} < A_2 R_2^{4/3} \\ \frac{Q|Q|}{\bar{M}^2 \bar{A}} \left( \phi \frac{1}{A_2 R_2^{4/3}} + (1-\phi) \frac{1}{A_1 R_1^{4/3}} \right) & \text{for } A_1 R_1^{4/3} \geq A_2 R_2^{4/3} \end{cases} \quad (1.239)$$

with the weighting term defined by

$$\phi = \left( \frac{9}{10} - \frac{4}{10} \beta_{sup} \right) \quad (1.240)$$

and the average flow area  $\bar{A}$  determined by

$$\bar{A} = \left( \frac{1}{10} + \frac{4}{10} \beta_{sup} \right) A_1 + \left( \frac{9}{10} - \frac{4}{10} \beta_{sup} \right) A_2 \quad (1.241)$$

and the mean Manning's number

$$\bar{M} = \frac{1}{2} (M_1 + M_2) \quad (1.242)$$

The factor  $f$  increases stability for high Froude numbers through a upstream centering of the friction term as the Froude number increases. If desired the suppression term  $\beta_{sup}$  can be fixed at one thus no suppression is applied and the friction term is thus centered at the midpoint between sections 1 and 2.

The above is the default way of handling the friction slope. MIKE 11 has 4 alternative evaluations of the friction slope. These may be changed by the user. The chosen evaluation method is a global setting thus it is used for all reaches in a given set-up.

The four friction slope alternatives are:



Average conveyance:

$$I_{fric} = \frac{(Q_1 + Q_2)^2}{(K_1 + K_2)^2} \quad (1.243)$$

Average friction:

$$I_{fric} = \frac{1}{2} \left( \frac{Q_1^2}{K_1^2} + \frac{Q_2^2}{K_2^2} \right) \quad (1.244)$$

Geometric mean:

$$I_{fric} = \sqrt{\frac{Q_1^2 Q_2^2}{K_1^2 K_2^2}} \quad (1.245)$$

Harmonic mean:

$$I_{fric} = 2 \frac{\frac{Q_1^2 Q_2^2}{K_1^2 K_2^2}}{\frac{Q_1^2}{K_1^2} + \frac{Q_2^2}{K_2^2}} \quad (1.246)$$

Finally the cross section reach length is determined from

$$L_i = \frac{L_{LF}K_{LF,i} + L_{CH}K_{CH,i} + L_{RF}K_{RF,i}}{K_{TOT,i}} \quad (1.247)$$

where the index is either 1 or 2.

The mean reach length is found through

$$\bar{L} = \frac{1}{2}(L_1 + L_2) \quad (1.248)$$

If no reach lengths are specified for the overflow banks the reach length is set equal to the main channel reach length (standard MIKE 11 method).



## 1.35 Structures

MIKE 11 includes descriptions for a wide range of structures which act as control points. The formulation of these features permits great flexibility since they range both in their degree of user-intervention and in their level of complexity.

Structures which operation is calculated automatically within the program under sub-critical flow conditions while user-defined  $Q$ - $h$  relationships are applied for critical flow conditions are described under the keywords:

- Broad crested Weir (*p. 63*)
- Special Weir (*p. 160*)
- Weir Formula (*p. 180*)
- Culverts,  $Q$ - $h$  Relations Calculation (*p. 81*)

The structures which operation is user-defined under all flow conditions are described under section 1.28 Regulating Structures (*p. 156*). These include both structures with a pre-determined operation such as a pump, ( $Q = f(t)$ ) and structures for which the operation is a function of water level or discharge at other locations in the model ( $Q = f(h, Q)$ ).

More complex regulating structures are modelled using the add-on module described under 1.9 Control Structures (*p. 67*).

Control structures and dambreak structures, are structures which operation is calculated automatically within the program during all flow conditions.

For the structure types; broad crested weir, special weir culvert, overflow control structure, dam break (crest flow) dam break /breach flow), the hydraulic description is similar and is described below.

The structures are modelled in MIKE 11 as control points at  $Q$ -points in the computational grid. Depending on the structure category, a relationship between the discharge and the upstream and downstream water levels is determined based on the flow condition, entrance and exit losses, and a critical flow correction factor.

Given the upstream and downstream water level and the river discharge the flow regime can be determined.

Zero flow in the structure occurs if it is closed by a valve, or if both the upstream and the downstream water levels are below the structure invert (crest level).

To differentiate between free overflow (critical flow) and drowned flow (submerged flow) it is as an initial guess assumed that the flow is critical and the associated discharge is computed. The flow is critical if the energy head at



the weir crest is larger than downstream water level. If the flow is not critical a submerged iteration is applied to determine the discharge.

Comparing the critical discharge with the submerged determines the flow regime finally as the smaller discharge is taken.

The different flow conditions defined for a structure are:

- Zero Flow
- Drowned Flow
- Free Overflow

### 1.35.1 Zero Flow

The flow is set to zero when the water level at both sides of the structure lies below its invert or when the upstream and downstream water levels are equal.

### 1.35.2 Drowned Flow

The flow on either side of the structure is in the same state as over the structure itself, i.e. both subcritical or both supercritical.

The discharge  $Q$  over a broad crested weir, for example, with constant width  $b$  in the case of drowned flow is generally given in the following form:

$$Q = \mu b (h_1 - Z_c) (h_1 - h_2)^{1/2} \quad (1.249)$$

where,  $\mu$  is the weir discharge coefficient,  $h_1$  and  $h_2$  the upstream and downstream water levels respective, and  $Z_c$  the weir crest elevation. This equation is easily converted to a general description for the head loss across a structure.

For further details refer to Appendix A.

### 1.35.3 Free Overflow

In the case of free overflow, the water levels at both sides are such that the system seeks to deliver the maximum discharge for a given energy head at the upstream side of the structure. This leads to critical flow at (or very near to) the most narrow section (control section).

In the case of free overflow the discharge is independent of the downstream water level, i.e. upstream controlled. In principle the discharge can be computed from the condition that the flow is critical at the control section for the given upstream energy head.





For example, for broad crested weirs with a rectangular cross-section the critical flow discharge is calculated by:

$$Q_c = 1,705bH_s^{3/2} \quad (1.250)$$

where,  $H_s$  is the available energy head above the weir crest.

Using Equation (1.250), a relationship between the upstream head and critical flow is tabulated for use by the structures algorithm (see A.10 Structures (p. 435) in Appendix A). The accuracy depends on the refinement in the tabulation.

Several factors influence the actual free overflow discharge through a structure:

- the section where critical flow occurs is often located downstream of the most narrow section, especially for well designed spillways
- the velocity is not distributed uniformly over the cross-section, thus the critical discharge is reduced
- the water level is not constant over the cross-section, especially in the case of an irregular section

The critical discharge is therefore corrected with the free overflow factor,  $\alpha_c$ , (in the Head Loss Factors box) giving the real discharge as:

$$Q = \alpha_c Q_c \quad (1.251)$$

Free overflow is modelled on the basis of a relationship between the discharge and the upstream water level. The relationship is generated automatically by MIKE 11 for the structure types: broad crested weirs and culverts  $Q/h$  relations calculated. In the case of user-defined structures (i.e. special weirs and culverts) the specified  $Q/h$  relation is applied. For the remaining structure types (control structure and dam break (crest flow, breach flow)), the critical discharge is computed during the simulation.

### 1.35.4 Contraction and Expansion Losses

Expressions for the head losses at structures are given in Appendix A. The head losses upstream and downstream of the structures are functions of the coefficients  $\zeta_{in}$  and  $\zeta_{out}$  (specified in the Head Loss Factors box) and the ratios of the structure area and the cross-section areas in the immediately adjacent river, see below.



**IMPORTANT!** During pre-processing of  $Q/h$ -relation in broad crested weirs, the ratio of structure area and river cross-section area is used to compute the  $Q/h$ -relation. The expressions require that the cross-sectional area of the river section is always greater than that at the structure. An error message



will appear in case the weir area is larger than the up- or downstream cross-sectional area, as it is not possible to establish the  $Q/h$ -relation for free overflow. To correct this, check cross-sections and weir geometry. The values of  $\zeta_{in}$  and  $\zeta_{out}$  are typically 0.5 and 1.0, respectively.

### 1.35.5 Grid spacing at structures

It is necessary to describe a river cross-section immediately upstream and downstream of any structure since the loss formulations are based on the relationships between the available cross-sectional area at the structure and that of the immediately adjacent river. A check in the code requires that these river cross-sections be within maximum  $dx$  (River Network Editor → Branches) of the structure. An error message is given if this is not the case.

These relationships are described under section A.10 Structures (*p.* 435) in Appendix A.

### 1.35.6 Parallel/Composite Structures

It is possible to model several structures at the same control point (Q-point) thus modelling a structure composed of several individual structures.

A parallel structure could describe e.g. the structures in connection with a hydro power station, i.e. to model the combination of turbines, ship locks, and spillway structures. Another application could be to model fish friendly structures in irrigation channels, etc.

A parallel/composite structure is defined simply by specifying the location (same river name and chainage) for each individual structure.

The discharge for the composite structure is computed by treating each structure separately and adding the coefficients for each structure and applying the final coefficients in the final solution for the Q-point, i.e.:

$$\alpha_{c,s} = \sum_{i=1}^n \alpha_{s,i} \quad (1.252a)$$

$$\beta_{c,s} = 1 \quad (1.252b)$$

$$\gamma_{c,s} = \sum_{i=1}^n \gamma_{s,i} \quad (1.252c)$$

$$\delta_{c,s} = \sum_{i=1}^n \delta_{s,i} \quad (1.252d)$$



where,

$c,s$  represents the coefficient for the composite structure

$s,i$  represents coefficient for the  $i$  structure

$n$  represent number of structures in the composite/parallel structure.

## 1.36 Supercritical Flow

The solution scheme in MIKE 11 will not truly simulate supercritical flow. The solution scheme is designed for subcritical flow, and compensations are made to enable supercritical flow to occur. As discussed below (Suppression of convective acceleration term (p. 171)), the  $\beta$  factor reduces the convective momentum term at a rate according to the Froude number. This means that model results will be less accurate with increasing Froude number.

For supercritical flow a reduced momentum equation (Saint Venant Equation) is applied which neglects the convective momentum term:

$$\frac{\partial Q}{\partial t} + gA \frac{\partial h}{\partial x} + \frac{gQ|Q|}{C^2 AR} = 0 \quad (1.253)$$

As long as the flow situation is not changing rapidly compared to the velocity, the description will still remain accurate. The advantage is that a stable solution can still be obtained within the same algorithmic structure as that used for sub-critical flow. For the transition from sub-critical to supercritical flow, a gradual reduction of the momentum terms is made resulting in a smooth description. Similarly, the differential equation is gradually centred upstream as the influence of the upstream conditions increases.

### 1.36.1 Suppression of convective acceleration term

The characteristics of the St. Venant equations are given by

$$C_{1,2} = \frac{Q}{A} \pm \sqrt{gA/w} = \frac{Q}{A} \left( 1 \pm \frac{1}{F} \right) \quad (1.254)$$

where

$Q$  the discharge

$A$  cross-sectional area

$w$  surface width of cross-section

$g$  acceleration due to gravity



$F$  Froude number

For  $F > 1$  the characteristics are both positive, implying that the St. Venant Equations take two upstream boundary conditions, and for  $F = 1$  the solution becomes singular. The numerical algorithm adopted in MIKE 11 is based on a staggered computational grid and cannot accommodate two boundary conditions at the same boundary or a singular solution. To avoid these situations a modified momentum equation is implemented in MIKE 11, viz.

$$\frac{\partial Q}{\partial t} + \beta \frac{\partial \left( \alpha \frac{Q^2}{A} \right)}{\partial x} + gA \frac{\partial h}{\partial x} + \text{friction} = 0 \quad (1.255)$$

where

$H$  water surface elevation

$\alpha$  momentum distribution coefficient

$\beta$  factor for suppression of convective momentum term

The default formulation in MIKE 11 is

$$\beta = \begin{cases} 1 - F^2 & \text{for } F \leq 1 \\ 0 & \text{for } F > 1 \end{cases} \quad (1.256)$$

This ensures excellent stability properties of the numerical solution and is sufficiently accurate for most flood routing studies where generally the Froude number is relatively small and the resolution used is coarse (the space step  $\gg$  water depth).

For water surface profiling with high Froude number and small space steps (space step =  $O$  (water depth)) an alternative formulation has been implemented, viz.

$$\beta = \begin{cases} 1 & \text{for } F \leq a \\ 1/(F+1-a)^b & \text{for } F > a \end{cases} \quad (1.257)$$

For the default value of  $a$  and  $b$  ( $a=1$  and  $b=2$ ) the two characteristics never have the same sign; they are either of different sign ( $F < 1$ ) or one is zero ( $F \geq 1$ ). The variation of  $\beta$  is shown in Figure 1.67. The alternative formulation is somewhat less stable than the default (Equation (1.256)) and therefore requires the application of a smaller time step for high Froude numbers. The solution is, however, considerably more accurate for high Froude numbers. Various tests have shown that the new formulation performs well for transition from sub- to supercritical flow, whereas hydraulic jumps are less accurate.



Note that  $a$  and  $b$  can be adjusted and do not necessarily have to be set at  $a=1$  and  $b=2$ . However the solution scheme is unstable if the suppression factor  $\beta$  lies outside the curve shown in Figure 1.67. Thus  $a=0.5$  and  $b=2$  can be applied, but  $a=2$  and  $b=2$  cannot.

The alternative formulation can be selected by setting the values FroudeMax (a) and FroudeExp (b) to positive values in the Hydrodynamic Parameters Editor under the Default Values tab.

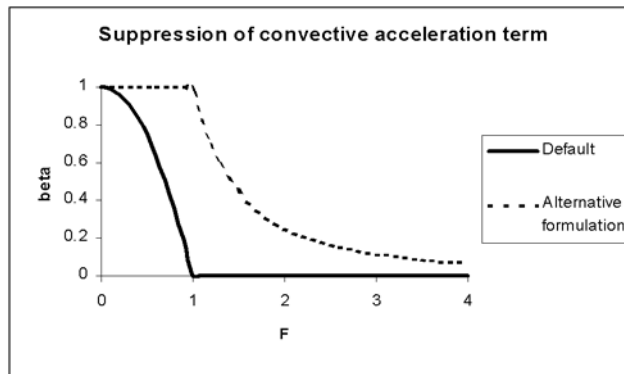


Figure 1.67 Factor for suppression of convective momentum term versus Froude number.

### 1.36.2 Effect of convective acceleration suppression on Energy Heads

As discussed, when the solution scheme approaches critical conditions the convective momentum term is gradually reduced. The suppression factor  $\beta$  varies from 1 (full convective term) to 0 (no convective term) according to the Froude number.

The  $\beta$  factor also modifies the energy calculation, thus energy head at any location in a model is affected. This means that when velocities are high (when the convective term is significant), energy head is significantly affected by the value of beta. This can be seen in a profile plot of energy levels along a river reach, which shows that energy is not conserved and varies according to velocity.

## 1.37 Supercritical Flow in Structures

Structures are used in MIKE 11 to represent real structures (weirs, etc.) and locations where critical flow or changes in flow conditions occur. Being a time dependent model, the MIKE 11 structures can be subject to a wide range of flow conditions, often more than is usually covered by textbooks. As an illustration, a supercritical flow condition at a structure is likely to occur in MIKE 11



when the structure is actually representing something more like a natural cross-section rather than a "typical" structure. This means that the MIKE 11 structures need to be capable of simulating flow conditions unlike those that a "typical" structure would encounter.

The solution scheme in MIKE 11 will not truly simulate supercritical flow. The solution scheme is designed for subcritical flow, and compensations are made to enable supercritical flow to occur (see Suppression of convective acceleration term (*p. 171*)). Head losses through a structure are proportional to the square of the velocity. This means that when supercritical flow occurs (which usually involves high velocities) head losses become more sensitive to changes in velocity. Further, small changes to the head loss coefficients can have a more pronounced effect upon head losses through a structure when velocities are high.

Accurately simulating flow through structures in MIKE 11 during fully supercritical flow is difficult, and results should be considered with caution. Having said this, MIKE 11 will provide a reasonable representation if supercritical flow occurs during a simulation.

### 1.37.1 Flow Directions

If supercritical flow is occurring either upstream or downstream of a structure it is impossible for the flow direction to change. A change in flow direction can only occur during subcritical flow. Thus, if subcritical flow is occurring, flow direction is calculated by comparison of water level upstream and downstream of the structure. If any other flow condition occurs, flow direction is equal to the previous flow direction.

A zero (or no) flow condition exists when there is subcritical flow and the water levels upstream and downstream of the structure are lower than the invert of the structure. If flow is supercritical then zero flow is impossible.

### 1.37.2 Testing for Flow Conditions

Energy levels in MIKE 11 are influenced by the convective suppression factor  $\beta$  (see Suppression of convective acceleration term (*p. 171*)). Also, there are distinctly different formulations for different flow conditions within a structure. This means that the state of flow (sub or super) must be known both upstream and downstream of the structure to decide the appropriate flow regime (either definitively or with other factors). The state of flow upstream and downstream of a structure is found using the Froude Number ( $F_R$ ):

$$F_R = \frac{v}{\sqrt{gy}} = \frac{Q}{A\sqrt{gy}} \quad (1.258)$$



If  $F_R < 1$  then subcritical flow, if  $F_R = 1$  then critical flow and if  $F_R > 1$  then supercritical flow. Using the Froude Number upstream ( $F_{R1}$ ) and downstream ( $F_{R2}$ ) of the structure, the following tests are made to decide the flow condition inside the structure:

- If  $F_{R1} < 1$  and  $F_{R2} > 1$  and  $F_{R1+} < 1$  then flow through structure = critical
- If  $F_{R1} > 1$  and  $F_{R2} < 1$  then flow through structure = critical
- If  $F_{R1} < 1$  and  $F_{R2} < 1$  and  $E_2 < h_1$  then flow through structure = critical
- If  $F_{R1} > 1$  and  $F_{R2} > 1$  then flow through structure = supercritical
- If  $F_{R1} < 1$  and  $F_{R2} > 1$  and  $F_{R1+} > 1$  then flow through structure = supercritical
- If  $F_{R1} < 1$  and  $F_{R2} < 1$  and  $E_2 > h_1$  then flow through structure = subcritical

Note the conditions:

- $F_{R1+}$  is the Froude number at the q point immediately upstream of the structure. This is included to enable a transition from critical to supercritical flow, depending upon conditions further upstream. If the q point upstream of the structure does not lie on the same branch or does not exist at all, this test is removed.
- $E_2$  is downstream energy level,  $h_1$  is upstream water level – this indicates a free overflow condition with upstream subcritical flow.  $E_2$  includes the  $\beta$  factor and (for the flow condition test only) is calculated as:

$$E_2 = \left( h + \beta \frac{Q^2}{2gA^2} \right)_2 \quad (1.259)$$

### 1.37.3 Subcritical Flow through Structure

See Drowned Flow (*p. 168*) and Drowned flow (*p. 441*).

### 1.37.4 Critical Flow through Structure

If flow through the structure is critical, qh relationships are used (see Free overflow (*p. 445*)). The flow condition can be either subcritical upstream to supercritical downstream (free overflow), or supercritical upstream to subcritical downstream (hydraulic jump). They can be considered as the same problem - critical flow is occurring in the structure.

Free overflow is modelled on the basis of a relationship between the discharge and the upstream water level, which is calculated initially assuming that upstream flow is subcritical. When upstream flow is supercritical, critical conditions (depth and area) are recalculated and the qh relationship is updated.



### 1.37.5 Supercritical Flow through Structure

When drowned flow occurs during subcritical flow conditions, the energy equation is used to calculate head loss. When supercritical flow occurs the energy equation becomes very sensitive to small changes in head drop and structure area, to such an extent that it cannot be applied to the MIKE 11 structure routines. Instead, the momentum equation is used when a structure is in supercritical flow conditions. This is applied in the same way as for a normal  $q$  point in MIKE 11, except that structure geometry is used and that friction losses are substituted by the structure losses.

### 1.37.6 Contraction and Expansion Losses, Sub- and Supercritical Flow

Consider the following:

- Expansion and contraction losses across a structure are less during supercritical flow compared to subcritical flow.
- Losses are a function of velocity head and velocities are much higher during supercritical flow, so model predictions can become extremely sensitive to the value of loss coefficient.
- During subcritical flow through a structure, there is an upstream contraction loss and a downstream expansion loss.
- During supercritical flow through a structure, there is an upstream expansion loss and a downstream contraction loss.

MIKE 11 modifies the loss coefficients to account for changes in velocity and area through a structure. As discussed in Appendix A.10.1, this accommodates the changes in expansion and contraction that occur during subcritical and supercritical flows.

Care must be taken when selecting loss coefficients, particularly in situations where both subcritical and supercritical flow conditions occur. When flow conditions change from subcritical to supercritical (or the Froude number  $F_R$  becomes greater than 1), the loss coefficients  $\zeta_{in}$  and  $\zeta_{out}$  (specified in the Head Loss Factors box) are modified:

- If  $F_R > 1$  in upstream h-point then  $\zeta_{in} = \zeta_{in} / 2$
- If  $F_R > 1$  in downstream h-point then  $\zeta_{out} = \zeta_{out} / 2$

Note that this adjustment is not made for bridge structures.

## 1.38 Tabulated structures

A tabulated structure can be defined as:

- A discharge as a function of up- and downstream water levels.





- An upstream water level as a function of the discharge and the downstream water level.
- A downstream water level as a function of the discharge and the upstream water level.

During calculation the discharge is found by area weighting of four values in the table. When three out of the four surrounding points have the same value and minimum one point outside also is found equal then the area weighting is overruled by a constant solution.

## 1.39 Time Stepping

Mike 11 includes three time stepping models: Fixed, tabulated and adaptive. Fixed time stepping is the traditionally used time stepping where a time step is specified as input and used throughout the simulation period.

The tabulated time step covers time steps given as a time series. Tabulated time stepping is especially useful when studying events that occur at a certain time that is known in advance of the simulation. For instance a dambreak known to occur at a certain date and time or a massive inflow occurring in a certain month every year due to a rainy season, etc.

The adaptive time stepping is used for modelling scenarios where the preferred time step is not known in advance. The adaptive time step may be used for obtaining a more detailed modelling of certain critical parts of a simulation, typically parts where large changes appear or it may be used for preventing calculations to blow up due to numerical instabilities.

The adaptive time stepping facility has two types of modelling constraints. The first type is a constraint on the boundaries and helps avoiding input details to be neglected due to application of too large time step. The boundary constraint limits the acceptable residual between the boundary value obtained by linear interpolation between two solution times ( $t$  and  $t+\Delta t$ ) and the actual boundary value given in the boundary time series. Figure 1.68 and equation 1.260 quantify the criteria.

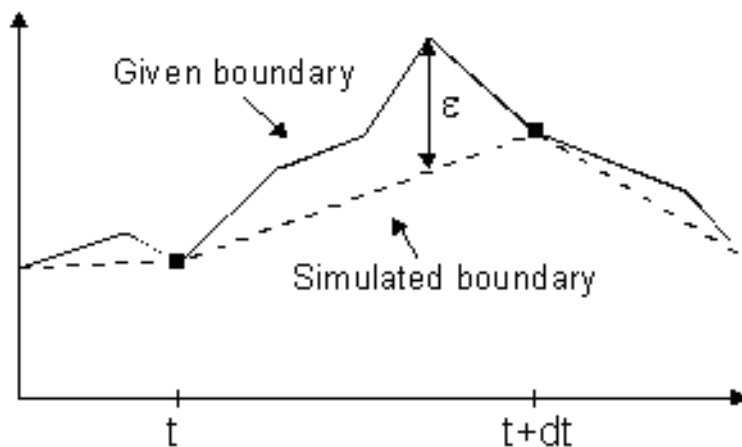


Figure 1.68 Boundary deficit limitation. Full line: given boundary time series. Dotted line: Boundary values applied in the simulation.

$$\left| \frac{\varepsilon}{BC} \right| < val_1 \quad \text{For} \quad |BC| > val_2 \quad (1.260)$$

In equation 1.260,  $BC$  is the actual value found in the time series,  $\varepsilon$  is the difference between the actual time series value and the value interpolated between the value at  $t$  and the value at  $t+\Delta t$ .  $val_1$  and  $val_2$  refers to the values given as input. The criteria is important when applying time steps larger than the resolution of the boundary time series. Further the criteria is cheap in regard of computational time since it, in contrast to the remainder of the criteria, may be evaluated in advance of calculating the time step.



The second type of criteria are limitations to the actual solution calculated. Hence this time step adaption is based on trial and acceptance and is therefore more expensive in regard of computational time. The criteria are:

$$|\Delta Q| < val_3 \quad (1.261)$$

$$\left| \frac{\Delta Q}{Q} \right| < val_4 \quad \text{for} \quad |Q| < val_5 \quad (1.262)$$

$$|\Delta h| < val_6 \quad (1.263)$$

$$\left| \frac{\Delta h}{h} \right| < val_7 \quad \text{for} \quad |h| > val_8 \quad (1.264)$$

$$|Cr_{HD}| = \frac{|v + \sqrt{gD}| \Delta t}{\Delta x} < val_9 \quad (1.265)$$

$$|Cr_{AD}| = \frac{|v| \Delta t}{\Delta x} < val_{10} \quad (1.266)$$

In equations 1.261 through 1.266,  $val_1$  to  $val_{10}$  are user specified values.

All constraints are optional. In case the constraints are not met the time step is reduced with a factor specified as change ratio in the input. The time step is allowed to vary between a user specified minimum and maximum value.

## 1.40 User Defined Structure

The user defined structure is available to create customised structures in MIKE 11. However, the potential application goes beyond this, allowing for the customisation of almost any specialist application or modification to MIKE 11.

When activated, the user defined structure will access a DLL (Dynamic Link Library) written by the user. The Network Editor interface contains a number of variables that can be used in the DLL. In addition, the DLL can access any variable in MIKE 11 through several records.

### 1.40.1 Tips

- MIKE 11 is written in PASCAL using Borland DELPHI. Any code written must be compatible with the compiled unit files (DCU) provided. The easiest way to ensure this is to have Delphi and write your programs in PASCAL.
- There are several options specified in the Project Options in Delphi. These options have been set to be compatible with the latest build of MIKE 11.
- The user defined structure routine is called within the MIKE 11 structure procedure. The aim of the structure procedure is to take the most recent flow calculations and produce the coefficients of the momentum equation. These coefficients are then used in the solver.
- Therefore, the user defined structure routine (if actually simulating a structure) should use the available flow information to create suitable coefficients for the momentum equation. Any programming performed must consider this. The values of  $co1$ ,  $co2$ ,  $co3$  and  $co4$  are set to zero at the commencement of the structure procedure.
- The user defined structure routine is called prior to the final sweep in the solution scheme. This means that any output or model parameters for the current time step have not yet been calculated. Results from the previous time step are valid.

For more information, see Appendix A.12.

## 1.41 Weir Formula

With the Weir Formula the discharge through a structure can be modelled by using standard weir formulas.

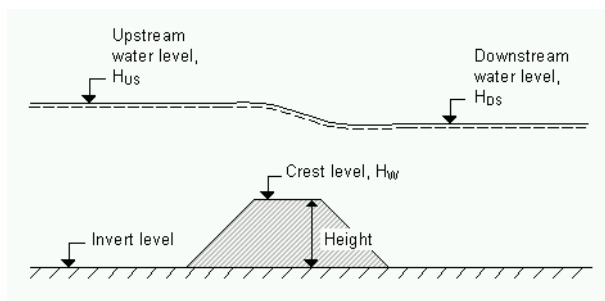


Figure 1.69 Definition sketch for Weir Flow



### 1.41.1 Weir Formula 1

Weir formula 1 is based on a standard weir expression, reduced according to the Villemonte formula:

$$Q = W \cdot C \cdot (H_{us} - H_w)^k \cdot \left[ 1 - \left( \frac{H_{ds} - H_w}{H_{us} - H_w} \right)^{k-0.385} \right] \quad (1.267)$$

Where  $Q$  is discharge through the structure,  $W$  is width,  $C$  is weir coefficient,  $k$  is the weir exponential coefficient,  $H_{us}$  is upstream water level,  $H_{ds}$  is downstream water level and  $H_w$  is weir crest level. (See Figure 1.69).

### 1.41.2 Weir Formula 2 (Honma)

Weir formula 2 is the Honma formula:

$$Q = \begin{cases} C_1 W (H_{us} - H_w) \sqrt{(H_{us} - H_w)} & \text{for } (H_{ds} - H_w)/H_{us} < 2/3 \\ C_2 W (H_{ds} - H_w) \sqrt{(H_{us} - H_{ds})} & \text{for } (H_{ds} - H_w)/H_{us} \geq 2/3 \end{cases} \quad (1.268)$$

Where  $Q$  is the discharge through structure,  $W$  is the width,  $C_1$  is the first weir coefficient,  $C_2 = (3/2)\sqrt{3}C_1$  is the second weir coefficient,  $g$  is the acceleration due to gravity  $H_{us}$  is the upstream water level,  $H_{ds}$  is the downstream water level and  $H_w$  is weir level. (See Figure 1.69).

### 1.41.3 Weir Formula 3 (Extended Honma)

Weir formula 3 is the extended Honma formula

The flow is calculated in three flow regimes called perfect, imperfect and submerged overflow. The choice of regime is defined by the ratio between downstream and upstream water depth above the crest.

$$Q = \begin{cases} \left[ \begin{array}{ll} C_0 W h_u^{3/2} & \text{for } h_d/h_u \leq (h_d/h_u)_i \\ C_0(\alpha \cdot (h_d/h_u)^q + \beta) W h_u^{3/2} & \text{for other cases} \\ C_0(\gamma \cdot (h_d/h_u)^r + \delta) W h_d (h_u - h_d)^{1/2} & \text{for } h_d/h_u \geq (h_d/h_u)_s \end{array} \right] \\ C_0 = a \cdot (h_u/H)^p + b & \text{for all} \end{cases} \quad (1.269)$$

$W$  is weir width

$H$  is weir height above cross section invert



$h_d$  is the upstream water level above the crest

$h_u$  is the down stream water level above the crest

$(h_d/h_u)_i$  is a user specified depth ratio limit between perfect and imperfect flow regime.

$(h_d/h_u)_s$  is a user specified depth ratio limit between imperfect and submerged flow regime.

$a$ ,  $b$ ,  $p$ ,  $\alpha$ ,  $\beta$ ,  $r$ ,  $\gamma$ ,  $\delta$  and  $\rho$  are user specified parameters.

MIKE 11 simulation engine or user interface does not check if there is a continuous transition from one flow regime to the next. This has to be ensured by the user through proper selection of the parameters.

## 1.42 Wind

Wind friction on the water surface can be accounted for in MIKE 11 by inclusion of the wind shear stress in the momentum equation. If wind shear is to be included and a wind field has been specified as a boundary condition in the Boundary Editor then the switch in the Hydrodynamic Parameters Editor under the Wind tab has to be set.

The wind shear stress is expressed as:

$$\tau_w = t_{fac} C_w \rho_a V_{10}^2 \quad (1.270)$$

where,

$C_w$  Wind friction coefficient (approx. 0.0025)

$t_{fac}$  Factor depending on the surrounding topography (1.0 for open water and reduced at locations which are sheltered from the wind)

$V_{10}$  Velocity 10 m above the water surface

$\rho_a$  Density of air (approx. 1.2 kg/m<sup>3</sup>)

The wind force projection in the length direction of the channel is included in the local momentum equation in each Q-point. The wind direction and velocity specified as a time series is implemented in the boundary editor. The branch orientations are calculated from the network grid which is always oriented north/south. The topographical factor ( $t_{fac}$ ) can be defined globally or locally for each location (in the Hydrodynamic Parameters Editor under the Wind tab). The surface area to which the wind stress applies excludes any



additional flooded areas and is equal to the width multiplied by the distance between  $h$ -points either side of the  $Q$ -point.

## 1.43 References

- /1/ Abbott, M.B., 1979: Computational Hydraulics. Elements of the Theory of Free Surface Flows. Pitman.
- /2/ Abbott, M.B. and Ionescu, F., 1967: On the numerical computation of nearly-horizontal flows. J.Hyd.Res., 5, pp. 97-117.
- /3/ Bier, P.E. and Delleur, J.W. (1962) Hydraulics of single span bridge constructions. Proceedings of the American Society of Civil Engineers, Journal of the Hydraulics Division, 88(HY2), March, 75-108.
- /4/ Bradley, J.N., 1978: Hydraulics of Bridge Waterways, Hydraulic Design Series No. 1, Federal Highway Administration, U.S. Department of Transportation, Second Edition, revised March 1978, Washington D.C.
- /5/ Carter, R.W.: Computation of Peak Discharge at Culverts, U.S. Geological Survey Circular 376, 1957.
- /6/ Chow, V.T., 1959: Open-Channel Hydraulics. McGraw Hill.
- /7/ Cunge J.A., Holly F.M., Jr. and Verwey A. (1980): Practical Aspects of Computational River Hydraulics. Pitman.
- /8/ Engelund, F., 1966: Hydraulic resistance of alluvial streams. ASCE, Vol. 92, No. Hy. 2.
- /9/ Federal Highway Administration, 1986: Bridge Waterways Analysis Model: Research Report, Report No. FHWA/RD-86/108, July 1986, Washington D.C.
- /10/ Hamil, L., 1999: Bridge Hydraulics. E & FN Spon.
- /11/ Henderson, F.M. (1966): Open Channel Flow. MacMillan.
- /12/ Lundgren, H. and Jonsson, I.G., 1962: Shear and velocity distribution in shallow channels. ASCE, Vol. 90, No. HY1, pp. 1-21.
- /13/ Murota, A. and Tada, H. (1989): Modelling of one-dimensional analysis on the open-channel with a tributary.
- /14/ Toch, A.J. (1953): Discharge Characteristics of Tainter Gates, Transactions ASCE Paper No. 2739, pp. 290-300.
- /15/ Cunge J.A. and Wegner M. (1964): Integration numerique des equations d'ecoulement de Barre de Saint-Venant par un schema



implicite de differences finies: Application au cas d'une galerie tantot en charge, tantot a surface libre. La Houille Blanche, No 1.

/16/ Engelund, F (1964): Flow resistance and Hydraulic Radius, Acta Polytechnica Scandinavia, Copenhagen





# ADVECTION-DISPERSION/ COHESIVE SEDIMENT TRANSPORT



## Reference



## 2 AD/CST Reference Manual

### 2.1 Who Should Use This Manual

This manual should be used when undertaking advection-dispersion (AD) or cohesive sediment transport (CST) modelling applications. It provides a description of aspects which are encountered during the development, calibration and application of AD/CST models including detailed technical descriptions of the numerical methods used. The manual should be used in conjunction with the MIKE 11 User Guide.

### 2.2 Manual Format

All descriptions in this Chapter are under headings presented in alphabetical order. A list of the headings for this Chapter is given below.

- A General Description (*p. 187*)
- Advanced Cohesive Sediment Transport (*p. 188*)
- Advection-Dispersion Equation (*p. 192*)
- Boundary Conditions (*p. 193*)
- Deposition, CST (*p. 194*)
- Dispersion Coefficient (*p. 196*)
- Erosion, CST (*p. 197*)
- Solution Scheme, AD (*p. 201*)
- Stability (*p. 202*)
- Nomenclature (*p. 203*)
- References (*p. 204*)

### 2.3 A General Description

The advection-dispersion (AD) module is based on the one-dimensional equation of conservation of mass of dissolved or suspended material, i.e. the advection-dispersion equation. The module requires output from the hydrodynamic module, in time and space, in terms of discharge and water level, cross-sectional area and hydraulic radius.

The advection-dispersion equation is solved numerically using an implicit finite difference scheme which, in principle, is unconditionally stable and has negligible numerical dispersion. A correction term has been introduced in order to reduce the third order truncation error. This correction term makes it possible to simulate advection-dispersion of concentration profiles with very steep fronts.



The cohesive sediment transport (CST) module also forms part of the AD module. In contrast to the non-cohesive sediment transport (NST) module, the sediment transport cannot be described by local parameters only because the settling velocity of the mostly very fine sediment is very low. The cohesive module uses the AD module to describe the transport of the suspended sediment. Erosion/deposition is modelled as a source/sink term in the advection-dispersion equation. The erosion rate depends on the local hydraulic conditions whereas the deposition rate depends on the concentration of the suspended sediment and on the hydraulic conditions.

The CST module is not provided with a roughness predictor. It does, however, calculate the erosion/deposition rate directly without applying a continuity equation for the sediment as performed in the morphological NST module. In a similar way to the explicit NST module, the accumulated sediment erosion/deposition during the simulation period is determined.

## 2.4 Advanced Cohesive Sediment Transport

This add-on module provides an alternative, more complex, analysis for cohesive sediment transport than that in the standard formulation described under Deposition, CST (*p. 194*) and Erosion, CST (*p. 197*) (sections 2.7 and 2.9 respectively). This module is especially useful in situations where a mass balance of cohesive sediment is required in order to simulate the accumulation of sediment. Then, knowing the exact location of sediment pools, it is possible to estimate e.g. the siltation in navigation channels, waterways, harbours etc. The module could also be used when resuspension of sediment affects water quality. This is because the resuspension of cohesive sediment often gives rise to oxygen depletion because of the high organic content and associated oxygen demand (COD) in the cohesive sediment. Likewise resuspension of cohesive sediment can give rise to heavy metal pollution since heavy metals adhere to the sediment.

The advanced cohesive sediment transport module is part of the advection-dispersion (AD) module. As for the standard formulation, the cohesive sediment transport is described in the AD-model through the transport of suspended solids. Erosion and deposition of cohesive sediment is represented in the AD-model as a source/sink term. Whereas the erosion rate depends only on local hydraulic conditions (bed shear stress), the deposition rate depends also on the suspended sediment concentration.

In the advanced cohesive model the transport of sediment is described in a pseudo two-dimensional manner through the description of the velocity and shear stress distribution across each section.

In each h-point of the solution domain the cohesive bed layer is modelled as three separate sediment sub-layers. The top layer is named sub-layer 1 and the bottom layer sub-layer 3. The thickness of the three sub-layers is calculated for each increment of elevation describing the cross-section as given in the processed data (see section 1.10 Cross-Sections (*p. 75*)).



Erosion and deposition rates are then integrated over the cross-section and added to the coefficients in the AD-equation.

The results of the cohesive sediment transport model during a simulation are:

- accumulated erosion/deposition.
- mass balance of the sub-layers.
- mass balance of the total bed layer.
- The results are given at  $h$ -points only.

The following descriptions are applied in the advanced cohesive model: cross-sectional velocity and shear stress distribution, settling, deposition, sliding, erosion and consolidation.

### 2.4.1 Cross-Sectional Shear Stress Distribution

Assuming the local velocity is proportional with the local water depth, i.e.:

$$\begin{aligned} u &\propto y^{1/2} \\ u &= C(y)^{1/2} \end{aligned} \quad (2.1)$$

where,  $y$  is the local water depth,  $u$  the local velocity and  $c$  the Chezy constant and using the Manning formula

$$\frac{Q}{A} = U = MR^{2/3}I^{1/2} \quad (2.2)$$

where  $Q$  is the discharge,  $A$  the cross-section area,  $U$  the mean velocity,  $M$  the Manning number and  $R$  the hydraulic or resistance radius (see section 1.3 Bed Resistance (p. 18)) the local velocity can be expressed as:

$$u = \frac{Q}{A} \left( \frac{y}{R_*} \right)^{1/2} \quad (2.3)$$

Using Equation (2.3), the local bed shear stress can be given by:

$$\tau_b = \left( \frac{u}{C} \right)^2 \rho g \quad (2.4)$$

where  $\tau_b$  is the local shear stress,  $C$  the Chezy resistance number,  $\rho$  the density of water and  $g$  the acceleration of gravity. Thus, it can be seen from Equation (2.4) that the local bed shear stress increases with the water depth.



## 2.4.2 Settling

An important parameter in the description of the sedimentation of cohesive materials is the settling velocity of flocs.

Through extensive field and laboratory studies it is evident that the settling velocity is dependent on the suspended sediment concentration. In the present model two settling regimes are described.

The first regime describes the effect of flocculation on settling velocity. Below a user specified suspended sediment concentration the settling velocity is given by:

$$W_s = kVC^m \quad (2.5)$$

where  $W_s$  is the settling velocity of flocs,  $VC$  the volume concentration,  $m$  a coefficient and  $k$  is a constant.

Below the user specified value of suspended sediment concentration, the settling velocity usually increases with concentration due to the enlargement of sediment flocs.

An increase in sediment concentration above the specified concentration causes a decrease in settling velocity due to the hindered settling effect. Settling velocity is then given by:

$$W_s = W_0(1 - VC)^\gamma \quad (2.6)$$

where  $W_0$  is the free settling velocity and  $\gamma$  a coefficient.

In Equation (2.5), the constant  $k$  is given by:

$$k = \frac{W_0(1 - VC)^\gamma}{VC^m} \quad (2.7)$$

In this one-dimensional model ideal mixing is assumed, thus the settling velocity remains constant in the vertical direction.



### 2.4.3 Deposition

Deposition dominates when the bed shear stress,  $\tau_b$  from Equation (2.4), is smaller than a critical shear stress for deposition ( $\tau_{c,d}$ ). In the advanced cohesive model the rate of deposition ( $S_d$ ) is given by

$$S_d = W_s \left( 1 - \frac{\tau_b}{\tau_{c,d}} \right) c \text{ for } \tau_b < \tau_{c,d} \quad (2.8)$$

where  $S_d$  is the rate of deposition,  $\tau_{c,d}$  the critical shear stress for deposition and  $c$  the suspended sediment concentration.

All deposited material is added to sub-layer 1. In the model the concentration  $c$  is weighted in time by the factor  $\theta$ , viz:

$$c = (1 - \theta)c_j^n + \theta c_j^{n+1} \quad (2.9)$$

where  $j$  is the spatial index and  $n$  is the time index.

### 2.4.4 Sliding

As deposition occurs a portion of the deposited material will slide down to the lower parts of the cross-section immediately after deposition due to the sloping river banks. The remaining material will, when liquified by excess pressure at low water levels, also slide down the sloping banks. These individual processes are modelled as one continuous process with a friction type formula, viz:

$$F = c_F \sqrt{I} D^{3/2} \quad (2.10)$$

where  $F$  is the lateral sediment flux,  $c_F$  the friction coefficient,  $I$  the lateral surface slope of the bed layer and  $D$  the total thickness of bed layer.

### 2.4.5 Erosion

The river bed will erode when the applied bed shear stress,  $\tau_b$  from Equation (2.4), exceeds a critical shear stress for erosion, ( $\tau_{c,e}$ ) which depends on bed material characteristics.

In the present advanced cohesive model two types of erosion are applied, viz:



### Instantaneous Erosion

Instantaneous erosion occurs when the above mentioned bed shear stress exceeds the critical shear stress for erosion of the sediment. This implies that all sediment is resuspended instantaneously.

### Gradual Erosion

The erosion rate is assumed to be a non-linear function of the excess stress, viz:

$$S_E = E_0 \left( \frac{\tau_b}{\tau_{c,e}} - 1 \right)^n \quad \text{for } \tau_b > \tau_{c,e} \quad (2.11)$$

where  $S_E$  is the rate of erosion,  $E_0$  the erosion coefficient,  $\tau_{c,e}$  the critical shear stress for erosion and  $n$  is the erosion exponent.

For sub-layer 1 it is possible to choose which erosion formulation should be used (Instantaneous or Gradual), while gradual erosion is automatically applied for sub-layers 2 and 3. Thus, it is possible to describe each sub-layer separately through the parameters  $E_0$ ,  $\tau_{c,e}$  and  $n$ .

## 2.4.6 Consolidation

The transition from sub-layer 1 to sub-layer 2 and from sub-layer 2 to sub-layer 3 is a process that includes both hindered settling and consolidation. The speed of the process is described by transition rates which are specified in the model by the user.

## 2.5 Advection-Dispersion Equation

The one-dimensional (vertically and laterally integrated) equation for the conservation of mass of a substance in solution, i.e. the one-dimensional advection-dispersion equation reads:

$$\frac{\partial AC}{\partial t} + \frac{\partial QC}{\partial x} - \frac{\partial}{\partial x} \left( AD \frac{\partial C}{\partial x} \right) = -AKC + C_2 q \quad (2.12)$$

where  $C$  is the concentration,  $D$  the dispersion coefficient,  $A$  the cross-sectional area,  $K$  the linear decay coefficient,  $C_2$  the source/sink concentration,  $q$  the lateral inflow,  $x$  the space coordinate and  $t$  the time coordinate.

The equation reflects two transport mechanisms:

1. advective (or convective) transport with the mean flow;
2. dispersive transport due to concentrations gradients.

The main assumptions underlying the advection-dispersion equation are:





- the considered substance is completely mixed over the cross-sections, implying that a source/sink term is considered to mix instantaneously over the cross-section
- the substance is conservative or subject to a first order reaction (linear decay)
- Fick's diffusion law applies, i.e. the dispersive transport is proportional to the concentration gradient

## 2.6 Boundary Conditions

At external boundaries, a series of conditions can be applied:

- open boundary outflow
- open boundary inflow - User defined values of the concentration (time varying or constant)
- closed boundary

### 2.6.1 Open Boundary Outflow

The open boundary outflow condition is

$$\frac{\partial^2 C}{\partial x^2} = 0 \quad (2.13)$$

### 2.6.2 Open Boundary Inflow

Time varying or constant values of the concentration at an inflow boundary are treated similarly to corresponding values of discharges or water levels as discussed in Chapter 1 of this manual.

When an outflow boundary becomes an inflow boundary, the boundary condition changes the user defined value according to:

$$C = C_{bf} + (C_{out} - C_{bf}) e^{-t_{mix} K_{mix}} \quad (2.14)$$

where  $C_{bf}$  is the boundary concentrations (specified in the input),  $C_{out}$  the concentration at the boundary immediately before the flow direction changed,  $K_{mix}$  a time scale specified in the input and  $t_{mix}$  the time since the flow direction changed.

The boundary concentration calculated according to the above is applied differently at open concentration boundaries and at open transport boundaries.



### 2.6.3 Concentration boundary

The concentration at the boundary is set equal to the calculated.

### 2.6.4 Transport boundary

The discharge at the boundary is multiplied with the calculated boundary concentration and added to the AD equation in the first grid point.

Concentration and transport only differ if there is a significant storage of water taken place in the first grid point, i.e. if the discharge at the boundary is different from the discharge at the boundary is different from the discharge in the second grid point.

### 2.6.5 Closed Boundary

This boundary condition is characterized by  $Q=0$  and

$$\frac{\partial C}{\partial x} = 0 \quad (2.15)$$

i.e., no transport through the boundary.

## 2.7 Deposition, CST

Deposition of suspended material occurs when the mean flow velocity is sufficiently low for particles and sediment flocs to fall to the bed and remain there without becoming resuspended immediately. Particles and flocs remain on the bed if the bed shear stress is less than the critical shear stress for deposition.

The rate of deposition can be expressed by:

$$S = \frac{wC}{h_*} \left( 1 - \frac{\tau}{\tau_{c,d}} \right) \quad \text{for } (\tau \leq \tau_{c,d}) \quad (2.16)$$

where  $S$  is the source term in the advection dispersion equation,  $C$  is the concentration of the suspended sediment,  $w$  is the mean settling velocity of suspended particles,  $h_*$  is the average depth through which the particles settle,  $\tau_{c,d}$  is the critical shear stress for deposition and  $\tau$  is the bed shear stress.

A detailed description on the mean settling velocity is found in the NST-reference manual, section of Suspended Load for the Engelund-Fredsoe sediment transport model.



The bed shear stress can be given by, for instance, the Manning formula:

$$\tau = \rho g \frac{V^2}{M^2 h^{1/3}} \quad (2.17)$$

where  $\rho$  is the fluid density,  $g$  the acceleration of gravity,  $M$  the Manning number,  $h$  the flow depth and  $V$  the flow velocity.

By substituting the expression for the bed shear stress, equation (2.17) into equation (2.16) the deposition rate can be expressed by equation (2.18):

$$S = \frac{wC}{h_*} \left( 1 - \left( \frac{V}{V_{cd}} \right)^2 \right) \text{ for } V \leq V_{cd} \quad (2.18)$$

where  $V_{cd}$  is the critical deposition velocity.

According to Engelund and Fredsøe (1982), /19/, deposition occurs whenever:

$$\sqrt{\frac{\tau}{\rho}} \leq 1,25w \quad (2.19)$$

Hence, by substituting Equation (2.16) and (2.19) into Equation (2.18),  $V_{cd}$  is expressed as:

$$V_{c,d} = 1,25w \frac{Mh^{1/6}}{\sqrt{g}} \quad (2.20)$$

The vertical variation of concentration of suspended sediment is defined as:

$$\int_0^1 \left( \frac{1}{s} - 1 \right)^z ds \quad (2.21)$$

in which  $z$  is the Rouse Number:

$$z = \frac{w}{0,4} \sqrt{\frac{\tau}{\rho}} \quad (2.22)$$

and  $s$  is a normalized vertical co-ordinate.



Hence, the average depth,  $h_*$ , through which the particles settle during deposition can be obtained from equation (2.23):

$$\frac{h_*}{h} = \frac{\int_0^1 s \left(\frac{1}{s} - 1\right)^z ds}{\int_0^1 \left(\frac{1}{s} - 1\right)^z ds} \tag{2.23}$$

The resulting relation between  $h_*/h$  and  $z$  is shown in Figure 2.1

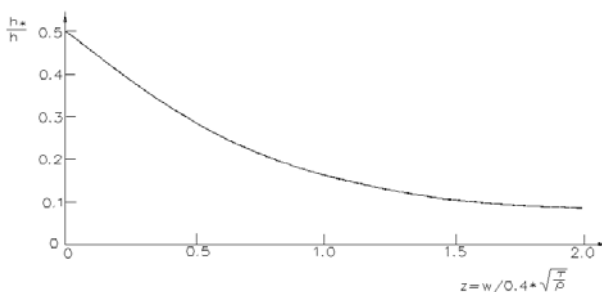


Figure 2.1 Relative depth through which settling particles must fall

## 2.8 Dispersion Coefficient

Longitudinal dispersion is caused by the combined action of a non-uniform velocity distribution and diffusion. The longitudinal spreading under the influence of a non-uniform velocity distribution is much greater than would be achieved by molecular and turbulent diffusion alone. The dispersive transport follows Fick's diffusion law (see section 2.5 Advection-Dispersion Equation (p. 192)).

The dispersion coefficient is determined as a function of the mean flow velocity, viz:

$$D_j^{n+1} = a \left| \frac{Q^{n+1/2}}{A^{n+1/2}} \right|_j^b \tag{2.24}$$

where,  $a$  and  $b$  are constants to be specified by the user. A constant dispersion coefficient is obtained by selecting  $b=0$ .

In rivers the dispersion coefficient is in the order of 5 to 10 m<sup>2</sup>/s increasing to between 30 and 100 m<sup>2</sup>/s as two-dimensional processes (secondary currents, wind induced turbulence) become more dominant, e.g. in estuaries.



## 2.9 Erosion, CST

The resistance against erosion of cohesive sediments is determined by the submerged weight of the individual particles and by the interparticle electro-chemical bonds which must be overcome by the shear forces before the erosion starts.

The rate of erosion has been described by the expression (177):

$$S = \frac{M_*}{h} \left( 1 - \frac{\tau}{\tau_{ce}} \right) \text{ for } \tau \geq \tau_{ce} \quad (2.25)$$

where  $S$  is source term in the advection dispersion equation,  $\tau$  the bed shear stress,  $\tau_{ce}$  the critical shear stress for erosion,  $M_*$  the erodibility of the bed and  $h$  the flow depth.

The bed shear stress can be given by, using the Manning formula:

$$\tau = \rho g \frac{V^2}{M^2 h^{1/3}} \quad (2.26)$$

where  $\rho$  is the fluid density,  $g$  the acceleration of gravity,  $M$  the Manning number,  $h$  the flow depth, and  $V$  the flow velocity.

By substituting Equation (2.25) into Equation (2.26) above, the erosion rate is expressed by:

$$S = \frac{M_*}{h} \left( 1 - \left( \frac{V}{V_{ce}} \right)^2 \right) \text{ for } V \geq V_{ce} \quad (2.27)$$

where  $V_{ce}$  is the critical erosion velocity.

## 2.10 Mass transport and mass balance

The advection/dispersion model computes the concentration of matter in each computational grid point. However, often the transport of matter at a specific location is of more interest. Based on simulated concentrations the total transport (convective and dispersive) is computed at each grid point and the results are stored in a MIKE 11 '.res11' file.

Relating the transport to the change of mass within a control volume at each point a complete mass balance can be established at each time step. The mass balance will automatically reveal any mass error problems.

The AD-mass error is always zero when the conditions below are satisfied:

- The mass error in the hydrodynamic simulation is zero.
- Cross sectional data are available in all computational grid points (i.e. there are no interpolated data).
- The advection/dispersion calculations are fully consistent with the hydrodynamic simulation.

In order to ensure fully consistency between the HD and the AD simulation, the time step in the simulations should be identical. During “dry out” (the water level falls below the river bottom level) consistency can not be sustained in the two simulations.

Referring to Figure 2.2 the equations for transport and mass balance are established.

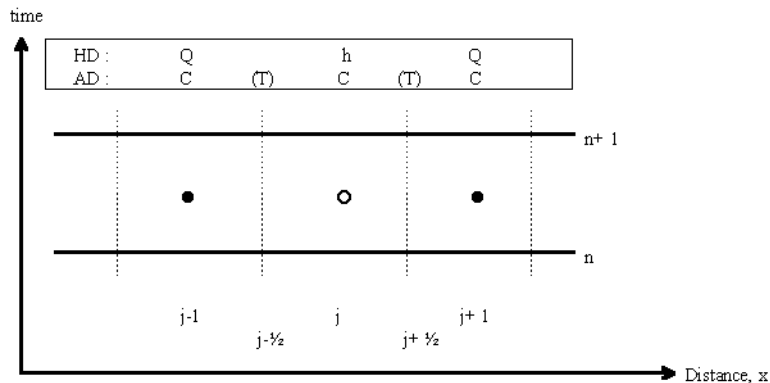


Figure 2.2 Calculation scheme and subscript notation in MIKE 11.

### 2.10.1 Mass

The mass in grid point  $j$ ,  $M$ , is given as:

$$M_j^{n+1} = stv_j^{n+1} C_j^{n+1} \quad (2.28)$$

where:

$stv$  volume of water

$C$  Concentration



## 2.10.2 1st order Decay

The 1st order decay,  $D$ , is calculated as:

$$D_j^{n+1} = K_j(\Phi C_j^{n+1} + (1 - \Phi)C_j^n)stv_j^{n+1} \quad (2.29)$$

where:

$K$  Decay constant ( $h^{-1}$ )

$F$  time centring coefficient

The time centering coefficient is given as:

$$\Phi = \begin{cases} 0,5 + 0,083 K_j \Delta t & , \text{ for } K_j \Delta t \leq 0,1 \\ -\frac{1}{K_j \Delta t} + \frac{1}{1 - e^{-K_j \Delta t}} & , \text{ for } K_j \Delta t > 0,1 \end{cases} \quad (2.30)$$

## 2.10.3 Transport

The total transport is given as the sum of advective and dispersive transport into or out of a control volume.

The transport,  $T$ , of a component is not calculated in a grid point, but as a transport from one grid point/calculation box to a neighbouring grid point/calculation box, i.e.  $T_{j-1/2}$  and  $T_{j+1/2}$ , see Figure 2.2. However, for presentation of the calculated transport in a longitudinal profile, MIKE 11 presents  $T_{j+1/2}$ , at grid point  $j$ .

## 2.10.4 Advective transport

The advective transport,  $AT$ , is calculated from the mean value of the discharge in two neighbouring control volumes and the concentrations in both boxes. Additionally, the advective transport is corrected with an explicit third order correction term.

$$AT_{j+1/2}^{n+1/2} = \frac{1}{2}(q_j^{n+1/2} + q_{j+1}^{n+1/2})\left(\frac{1}{4}(C_j^{n+1} + C_{j+1}^{n+1} + C_j^n + C_{j+1}^n) + \text{Corr}\right) \quad (2.31)$$

Correction term:

$$\text{Corr} = (C_{j-1}^{n+1/2} - C_j^{n+1/2} + C_{j+1}^{n+1/2})\text{Corfac} \quad (2.32)$$

where:



$q$  discharge

and

$$\text{corfac} = \begin{cases} \frac{1}{6} \left( 1 + \frac{1}{2} \sigma^2 \right), & \text{for } \sigma \leq 1 \\ \frac{1}{4\sigma}, & \text{for } \sigma > 1 \end{cases} \quad (2.33)$$

where  $\sigma$  is the Courant number:

$$\sigma = \frac{u \Delta t}{\Delta x} \quad (2.34)$$

### 2.10.5 Dispersive transport

The dispersive transport,  $DT$ , between two neighbouring control volumes is calculated as follows:

$$DT_{j+1/2}^{n+1/2} = \frac{1}{4} (A_j^{n+1} + A_{j+1}^{n+1}) (Diff_j + Diff_{j+1}) - \frac{1}{2} ((C_j^n + C_{j+1}^{n+1}) - (C_j^n + C_j^{n+1})) \quad (2.35)$$

where:

$AArea$

$Diff$  Dispersion coefficient

### 2.10.6 Mass balance

The mass balance,  $MB$ , is given as the difference between mass on time  $n$  plus all mass transported into the box and mass on time  $n+1$  plus all mass transported out of the control volume:

$$MB_j^{n+1} = M_j^n - M_j^{n+1} + (DT_{j+1/2}^{n+1/2} + AT_{j-1/2}^{n+1/2} - DT_{j-1/2}^{n+1/2} - AT_{j+1/2}^{n+1/2} + LAT_j^{n+1/2} - D_j^{n+1/2}) \Delta t \quad (2.36)$$

The total mass balance is given as the sum of all mass balances in the river setup.





## 2.11 Solution Scheme, AD

The advection-dispersion equation is solved with a fully time and space centred implicit finite difference scheme in order to minimize any artificial (numerical) dispersion. Moreover, it has been ensured that the discretization is mass conservative. The finite difference scheme is derived by considering the mass flux into a control volume situated around the grid point  $j$ . The boundaries of this control volume are the river bed, the water surface and the two cross-sections situated at  $j-1/2$  and  $j+1/2$ , respectively, see Figure 2.3.

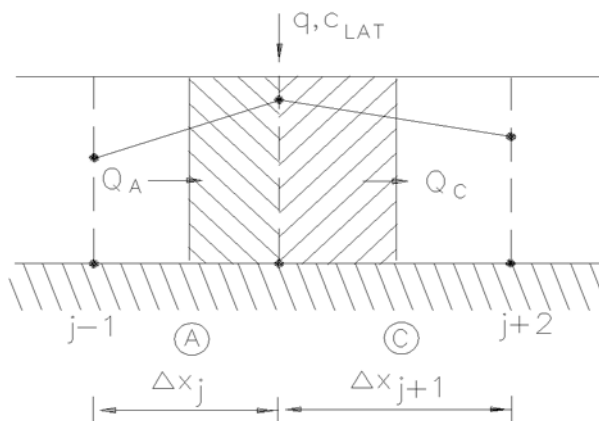


Figure 2.3 Definition sketch for the control volume.

The two equations considered are the continuity equation and the advective-dispersive transport equation.

### 2.11.1 Continuity equation:

$$\begin{aligned} \frac{V_j^{n+1/2} C_j^{n+1}}{\Delta t} - \frac{V_j^{n+1/2} C_j^n}{\Delta t} + T_{j+1/2}^{n+1/2} - T_{j+1/2}^{n+1/2} \\ = q^{n+1/2} C_q^{n+1/2} - V_j^{n+1/2} K C_j^n \end{aligned} \quad (2.37)$$

where  $C$  is the concentration,  $V$  the storage volume,  $T$  the transport through box walls,  $q$  the lateral inflow,  $\Delta t$  the time step,  $C_q$  the concentration of lateral inflow source,  $K$  the linear decay coefficient,  $j$  the grid point and  $n$  the time level.



### 2.11.2 Advective-dispersive transport equation:

$$T_{j+\frac{1}{2}}^{n+\frac{1}{2}} = Q_{j+\frac{1}{2}}^{n+\frac{1}{2}} C_{j+\frac{1}{2}}^* - A_{j+\frac{1}{2}}^{n+\frac{1}{2}} D \frac{C_{j+1}^{n+\frac{1}{2}} - C_j^{n+\frac{1}{2}}}{\Delta x} \quad (2.38)$$

where,

$Q_{j+\frac{1}{2}}^{n+\frac{1}{2}}$  is the discharge at the right wall of the box

$A_{j+\frac{1}{2}}^{n+\frac{1}{2}}$  is the cross sectional area of the right wall

$D$  is the dispersion coefficient

$C_{j+\frac{1}{2}}^*$  is an upstream interpolated concentration given by:

$$C_{j+\frac{1}{2}}^* = \frac{1}{4}(C_{j+1}^{n+1} + C_j^{n+1} + C_{j+1}^n + C_j^n) \quad (2.39)$$

$$- \min\left(\frac{1}{6}\left(1 + \frac{\sigma^2}{2}\right), \frac{1}{4\sigma}\right)(C_{j+1}^n - 2C_j^n + C_{j-1}^n)$$

in which  $\sigma$  is the Courant number ( $u\Delta t/\Delta x$ ). The last term of Equation (2.39) is an explicit third order corrective term.

Substitution and rearrangement of the above equations give a general implicit finite difference equation which relates the concentration in three neighbouring grid points to each other at any time level as:

$$\alpha_j C_{j-1}^{n+1} + \beta_j C_j^{n+1} + \gamma_j C_{j+1}^{n+1} = \delta_j \quad (2.40)$$

Unlike the general formulation for water levels and discharges (see Appendix A Appendix (p. 391)), the concentrations are defined in each grid point, i.e. non-staggered.

The system of linear equations are solved by the "double sweep" algorithm as presented in section 1.31 Solution Scheme (p. 160) and in section A.9 Solution Scheme (p. 429).

## 2.12 Stability

The applied computation scheme in the advection-dispersion model is stable even for large Peclet numbers, ie for:

$$Pe = v \frac{\Delta x}{D} > 2 \quad (2.41)$$

where,



$v$  is the velocity

$\Delta x$  is the distance between the computational points

$D$  is the dispersion coefficient.

The space and time step should be selected in such a way that the convective Courant number  $Cr$  is less than 1.

$$Cr = v \frac{\Delta t}{\Delta x} < 2 \quad (2.42)$$

Notice that  $\Delta x$  is the distance between two computational points in the AD computation. MIKE 11 places computational points in the AD scheme in both  $h$ - and  $Q$ -points, ie  $\Delta x$  in an AD computation is  $0.5 \Delta x$  in the corresponding HD computation. Hence if, the time step used in the HD computation criteria has been limited by the velocity criteria, this should be reduced by a factor of two in the succeeding AD computation.

If convective Courant numbers greater than unity appear in the computation, a warning will be displayed. If this warning is ignored more than 5 times, the computation will continue without further warnings. The computational results should, in this case, be treated with care, and preferably the computation should be repeated with altered time steps.

## 2.13 Nomenclature

$A$  Across-sectional area.

$C$  concentration.

$C_b$  concentration at a model boundary.

$C_{out}$  concentration at a model boundary prior to change in the flow direction.

$C_q$  concentration of lateral inflow source.

$D$  dispersion coefficient.

$h$  flow depth.

$h$ -average depth through which particles settle.

$I$  energy slope.

$j$  grid point.

$K$  linear decay coefficient.



$K_{mix}$  time scale specified in input.

$M$  Manning number.

$M$  erodibility of the bed.

$n$  time level.

$q$  lateral inflow.

$s$  relative density of sediment.

$S$  source term in advection-dispersion equation.

$T$  transport through control volume walls.

$T$  temperature.

$t$  actual time.

$t_{mix}$  time since flow direction changed.

$t_{up,down}$  time of sunrise and sunset.

$u$  flow velocity.

$V$  storage volume.

$V_{c,d}$  critical deposition velocity.

$W_0$  free settling velocity.

$W_S$  settling velocity of flocs.

$w$  mean settling velocity of suspended particles.

$\rho$  fluid density.

$\tau_b$  bed shear stress.

$\tau_{c,d}$  critical shear stress for deposition.

$\tau_{c,e}$  critical shear stress for erosion.

$\sigma$  Courant number.

## 2.14 References

- /17/ Ariathurai, R., MacArthur, R.C. & Krone, R.B. (1971): Mathematical Model of Estuarial Sediment Transport. Department of Civil Engi-



- neering, University of California at Davis.
- /18/ DHI/VKI: River Usk Barrage, Sediment Transport Modelling. June 1990, Volume 2.
- /19/ Engelund, F. and Fredsøe, J., 1982. "Hydraulic theory of alluvial rivers", *Advances in Hydro Science*, Vol. 13, pp. 187-215.





# NON-COHESIVE SEDIMENT TRANSPORT

Reference







## 3 NST Reference Manual

This manual should be used when undertaking sediment transport and/or morphological model applications. It provides a description of aspects which are encountered during the development, calibration and application of these models. Derivation of resistance and sediment transport relationships are described under the relevant headings. The manual should be used in conjunction with the MIKE 11 User Guide.

Some of the sediment transport formulas and other features of the Non Cohesive Sediment Transport module have been developed in cooperation with CTI Engineering, CO., Ltd., Japan.

### 3.1 Manual Format

All descriptions in this Chapter are under headings presented in alphabetical order. A list of the headings for this Chapter is given below.

- A General Description (*p. 210*)
- Sediment transport models (*p. 210*)
- Bed forms (*p. 211*)
- Morphological model (*p. 213*)
- Graded Sediments (*p. 222*)
- Dune dimensions (*p. 228*)
- Flow Resistance (*p. 235*)
- Incipient motion criteria (*p. 241*)
- Ackers and White model (*p. 243*)
- Ashida & Michiue model (*p. 245*)
- Ashida, Takahashi and Mizuyama model (ATM) (*p. 249*)
- Engelund & Fredsøe model (*p. 252*)
- Engelund & Hansen model (*p. 256*)
- Meyer-Peter & Müller model (*p. 258*)
- Sato, Kikkawa & Ashida model (*p. 259*)
- Smart and Jaeggi model (*p. 260*)
- van Rijn model (*p. 262*)
- Nomenclature (*p. 267*)
- References (*p. 271*)

## 3.2 A General Description

The non-cohesive sediment transport module (NST) can be run in two modes; explicit and morphological. In the explicit mode output is required from the hydrodynamic module (HD) in terms of discharge water levels, (cross-sectional area and hydraulic radius) both in time and space. There is no feedback from the sediment transport calculations to the HD module. Results are in the form of volume transport rates and accumulated volumes of deposition or erosion. The explicit mode is useful where significant morphological changes are unlikely to occur. An estimate of the sediment budget can then be obtained economically with this mode (in terms of computer time).

In the morphological mode sediment transport is calculated in tandem with the HD module. The feedback from the sediment transport calculations to the HD is achieved through solution of the sediment continuity equation and through the updating of the bed resistance and the following sediment transport. Results are in the form of sediment transport rates, bed level changes, resistance number and dune dimensions (depending on the transport relationship adopted). This model requires considerably more computation time than the explicit model but is more representative of the dynamic alluvial processes.

The NST module is equipped with five different models for the calculation of sediment transport rate and alluvial roughness. These are the Engelund and Hansen model, the Ackers and White model, and the Smart and Jaeggi model for the calculation of the total load, and the Engelund and Fredsøe and van Rijn models for the calculation of bed load and suspended load separately. Branches in the model where no sediment transport takes place can be specified as passive branches. All these models can be run using a single representative grain size or using a number of grain sizes representing grain size fractions in graded material as an add-on module. Provision is also made for specifying the geometric standard deviation of the grain size distribution to enable the mean diameter of the suspended bed material to be computed. All the options mentioned above are available in both modes; explicit and morphological.

## 3.3 Sediment transport models

Multiple sediment transport models are available in MIKE 11. These are listed hereunder and described individually in sections below:

- Ackers and White model (*p.* 243)
- Ashida & Michiue model (*p.* 245)
- Ashida, Takahashi and Mizuyama model (ATM) (*p.* 249)
- Engelund & Fredsøe model (*p.* 252)
- Engelund & Hansen model (*p.* 256)



- Lane & Kalinske model (*p.* 256)
- Meyer-Peter & Müller model (*p.* 258)
- Sato, Kikkawa & Ashida model (*p.* 259)
- Smart and Jaeggi model (*p.* 260)
- van Rijn model (*p.* 262)

The selection of transport model for a particular application depends on the nature of the water course under study and on local experience in sediment transport modelling. In the absence of any such knowledge, trial simulations should be carried out with each model to see which gives better agreement with measurements.

Once the most appropriate transport model has been selected, further adjustments can be made to the predicted transport rates during the calibration procedure by the use of the two factors Factor 1 and Factor 2. These are specified in ST parameter editor → Calibration Factors and are used to apply a linear correction factor to the predicted suspended and bed load transport rates, respectively (or to the total load, Factor 1 only).

## 3.4 Bed forms

The bed of a stream where sediment transport occurs will not generally be flat but will be covered by bed forms belonging to one of the following categories, illustrated in Figure 3.1.

- Ripples
- Dunes
- Plane bed
- Anti-dunes (standing waves - chute and pool)

### 3.4.1 Ripples

Ripples are triangular waves with a small wave length (compared to the water depth). Ripples are usually formed in fine sediments at rather low transport rates, while coarse sediments normally form dunes. Ripples are therefore associated with hydraulically smooth beds.

### 3.4.2 Dunes

Dunes are the most important bed form encountered in river hydraulics and most work on the hydraulic resistance of alluvial rivers has been concerned with dune covered beds.

Dunes are large, triangular waves and are long compared to the depth of flow. Dunes are generally irregular and three dimensional.

Both ripples and dunes have a gently curved upstream side and a steep downstream side with a slope close to the angle of repose. At the crest of the bed forms the flow separates and a bottom roller is formed. The formation of ripples and dunes on an originally plane bed has been explained through stability analyses (127). Small sinusoidal perturbations of the bed are found to increase with time and the wave length with the highest amplification corresponds to the wave length of the emerging bed waves.

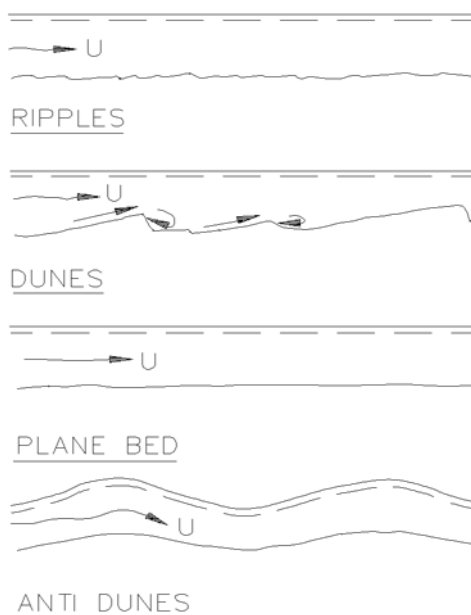


Figure 3.1 Development of bed forms for increasing flow velocity

### 3.4.3 Plane bed

The stability analyses have shown that, in the case of a high suspended load, a plane bed will remain stable. This is due to the lag between the local hydraulic conditions and the suspended load.

### 3.4.4 Anti-dunes

Anti-dunes appear when the perturbation of the water surface is in phase with the bed perturbations. This occurs when the Froude number,  $F$ , exceeds the limit for critical flow:

$$F > \sqrt{\frac{\tanh(kD)}{kD}} \quad (3.1)$$



where,

$k$  is the wave number of the bed forms

$D$  is the water depth.

Anti-dunes are nearly sinusoidal bed waves which generally move upstream. The water surface is also sinusoidal, in phase with the bed waves and with a larger amplitude.

The anti-dunes may vary in a cyclic manner, growing until breaking of the surface wave occurs, after which they are washed out and new, small ones form again.

### 3.5 Morphological model

The morphological model updates the bed level due to erosion or deposition using the continuity equation for sediment transport. The model updates the level of the entire cross-section or only a part of it (normally representing the river channel) and leaving the bottom level of the remaining part of the cross-section (normally representing the flood plains) unchanged. The model distinguishes between the river channel and flood plain using a divide level specified in the cross-section editor, i.e. levels in the cross-section below this divide level are assumed to belong to the river channel. It is possible to specify a specific flood plain resistance (in the HD editor under the flood plain resistance tab) to be used on the flood plain above the level of divide. Note that this facility is only implemented when running the hydrodynamic module and the sediment transport modules coupled i.e. in the morphological mode.

Various possibilities for morphological changing of the cross-section shape is available. If a divide level has been specified only the river channel is updated, which implies that sediment transport only takes place in the river channel.

The sediment transport is calculated on the basis of flow velocity ( $u$ ), depth ( $D$ ) and transporting width ( $W_t$ ) and is obtained in the following way:

$$u = \frac{Q_c}{A_c} \quad (3.2)$$

$$D = R_c \quad (3.3)$$

$$W_t = \frac{A_c}{R_c} \quad (3.4)$$

where,



- $Q$  is discharge  
 $A$  is cross-sectional area  
 $R$  is resistance radius

and subscript  $c$  refers to the river channel values. If the cross-sections are not divided into river channel and flood plain components the corresponding values for the entire cross-section are used.

Assuming that the friction slope is constant across the free water surface width the discharge in the river channel can be expressed as:

$$Q_c = Q_t \begin{cases} \frac{M_c R_c^{2/3} A_c}{M_t R_t^{2/3} A_t} & \text{Manning No.} \\ \frac{C_c R_c^{1/2} A_c}{C_t R_t^{1/2} A_t} & \text{Chezy No.} \end{cases} \quad (3.5)$$

where,

$M$  is Manning roughness coefficient

$C$  is Chezy roughness coefficient

$R_t$  composite resistance radius

$M_t$  composite Manning roughness coefficient

$C_t$  composite Chezy roughness coefficient

The three latter are given by

$$R_t = \left( \frac{\sqrt{R_c} A_c + \sqrt{R_f} A_f}{A_t} \right)^2 \quad (3.6a)$$

$$M_t = \frac{M_c \sqrt{R_c} A_c + M_f \sqrt{R_f} A_f}{\sqrt{R_t} A_t} \quad (3.6b)$$

$$C_t = \frac{C_c \sqrt{R_c} A_c + C_f \sqrt{R_f} A_f}{\sqrt{R_t} A_t} \quad (3.6c)$$

Where subscript  $t$  refers to the entire cross-section,  $c$  to the river channel part and  $f$  to the flood plain part.



The sediment continuity equation is solved at  $h$ -points using a Preissmann Scheme.

$$(1 - \varepsilon) \left[ (1 - \psi) \frac{W \Delta z_j^{n+1}}{\Delta t} + \psi \frac{W \Delta z_{j+1}^{n+1}}{\Delta t} \right] + \theta \frac{Qt_{j+1}^{n+1} - Qt_j^{n+1}}{\Delta x} + (1 - \theta) \frac{Qt_{j+1}^n - Qt_j^n}{\Delta x} = 0 \quad (3.7)$$

where,

$W$  width of the river channel or entire cross-section, defined as the width of the cross-section at the calculated water surface

$\Delta z^{n+1}$  change of bottom level.

$$Qt_j^n = W_t qt_j^n .$$

$qt_j^n$  sediment transport rate per unit width.

$\varepsilon$  porosity of sediment.

$\psi$  space centring coefficient ( $0,5 \leq \psi \leq 1$ ) (PSI: ST parameter editor → Transport Model).

$\theta$  time centring coefficient ( $0,5 \leq \theta \leq 1$ ) (FI: ST parameter editor → Transport Model).

The transport at  $t = (n+1)\Delta t$  is approximated by:

$$Qt_j^{n+1} = Qt_j^n + \left( \frac{\partial Qt}{\partial u} \frac{\partial u}{\partial z} + \frac{\partial Qt}{\partial D} \frac{\partial D}{\partial z} \right)_j \Delta z_j^{n+1} \quad (3.8)$$

or introducing the term  $\alpha$

$$Qt_j^{n+1} = Qt_j^n + \alpha \Delta z_j^{n+1} \quad (3.9)$$

where,

$u$  is flow velocity

$D$  is flow depth

$\partial u / \partial z$  and  $\partial D / \partial z$  are, by default, calculated assuming locally steady flow (back water curve).



Further, it is possible to select:

$$\frac{\partial D}{\partial z} = -1 \quad \text{and} \quad \frac{\partial u D}{\partial z u} = +1 \quad (3.10)$$

(ST parameter editor → Transport Model → dH/dz switch), which is an acceptable approximation in strongly unsteady (tidal) flow.

$\partial Qt / \partial zu$  and  $\partial Qt / \partial D$  are obtained by numerical differentiation, e.g.:

$$\frac{\partial Qt}{\partial u} \approx \frac{Qt(u + \Delta u, D) - Qt(u, D)}{\Delta u} \quad (3.11)$$

or

$$\frac{\partial Qt}{\partial u} \approx \frac{Qt(u \text{ fac } D) - Qt(u, D)}{u \text{ fac} - u} \quad (3.12)$$

where,

$$\text{fac} = \frac{u + \Delta u}{u} \quad (3.13)$$

and may be set in ST parameter editor → Transport Model → Fac.

### 3.5.1 Updating of bottom level

Various assumptions regarding the change in bathymetry of a cross-section during erosion and deposition can be made. In some cases sediment will accumulate in the deepest parts of the cross-section before deposition occurs closer to the bank (e.g. in a reservoir behind a dam). For tidal estuaries another deposition pattern with pronounced deposition along the banks can occur. Such considerations are necessary when the results from the MIKE 11 morphological model are interpreted, as the model is only one-dimensional. However, the MIKE 11 provides different options, see below, for how to update the bottom level. The appropriate model should be chosen based on engineering judgement.

Instead of solving equation (3.7) with respect to  $\Delta z^{n+1}$ , the change in cross-sectional area  $\Delta A$  is calculated,  $\Delta A^{n+1} = W \Delta z^{n+1}$ . The cross-section is subsequently updated (i.e. the processed cross-sectional data tables used in the computation are changed) in one of the following ways, see below and Figure 3.2.

In the following model descriptions subscript  $i$  refers to the levels in the processed data table. Subscript  $k$  in model 1 refers to the level in the processed data table where the area is larger than the change in cross-section area  $\Delta A$ .





## Model 1

*Deposition in horizontal layers.*

Erosion as model 5:

Levels:

$$z_i^{n+1} = z_k^{n+1} + \frac{\Delta A - A_k^n}{W_{k+1} - W_k} \text{ for } z_i^n \leq z_k^n$$

$$A_k^n < \Delta A < A_{k+1}^n \quad (3.14)$$

$$z_i^{n+1} = z_i^n \text{ for } z_i^n > z_k^n$$

Widths: unchanged

Areas:

$$A_i^{n+1} = 0 \quad \text{for } z_i^n \leq z_k^n$$

$$A_i^{n+1} = A_i^n - \Delta A \text{ for } z_i^n > z_k^n \quad (3.15)$$

Hydraulic radii:

$$R_i^{n+1} = 0 \quad \text{for } z_i^n \leq z_k^n$$

$$R_i^{n+1} = \left[ \frac{\sum_{j=1}^i (z_i^{n+1} - z_j^{n+1})^{3/2} \Delta W_j}{A_i^{n+1}} \right]^2 \text{ for } z_i^n > z_k^n \quad (3.16)$$

## Model 2

*Deposition and erosion uniformly distributed below the water surface. No deposition and erosion above:*

Levels:

$$z_i^{n+1} = z_i^n + \frac{\Delta A}{W_{surface}} \text{ for } z_i^n \leq h$$

$$W_{surface} = \text{width of cross section at water surface level } h \quad (3.17)$$

$$z_i^{n+1} = z_i^n \text{ for } z_i^n > h$$



Widths: unchanged

Areas:

$$\begin{aligned}
 A_i^{n+1} &= A_i^n && \text{for } z_i^n \leq h \\
 A_i^{n+1} &= A_i^n - \Delta A && \text{for } z_i^n > h
 \end{aligned}
 \tag{3.18}$$

Hydraulic radii:

$$\begin{aligned}
 R_i^{n+1} &= R_i^n && \text{for } z_i^n \leq h \\
 R_i^{n+1} &= \left[ \frac{\sum_{j=1}^i (z_i^{n+1} - z_j^{n+1})^{3/2} \Delta W_j}{A_i^{n+1}} \right]^2 && \text{for } z_i^n > h
 \end{aligned}
 \tag{3.19}$$

### Model 3

*Deposition and erosion proportional with depth below water surface. No deposition and erosion above:*

Levels:

$$\begin{aligned}
 \alpha &= \frac{\Delta A}{A_{surface}^n} \\
 z_i^{n+1} &= z_i^n + \alpha(h - z_i^n) && \text{for } z_i^n \leq h \\
 A_{surface} &= \text{area of cross-section at water surface level } h \\
 z_i^{n+1} &= z_i^n && \text{for } z_i^n > h
 \end{aligned}
 \tag{3.20}$$

Widths: unchanged

Areas:

$$\begin{aligned}
 A_i^{n+1} &= (1 - \alpha)A_i^n && \text{for } z_i^n \leq h \\
 A_i^{n+1} &= A_i^n - \Delta A && \text{for } z_i^n > h
 \end{aligned}
 \tag{3.21}$$



Hydraulic radii:

$$\begin{aligned}
 R_i^{n+1} &= (1 - \alpha)R_i^n && \text{for } z_i^n \leq h \\
 R_i^{n+1} &= \left[ \frac{\sum_{j=1}^i (z_i^{n+1} - z_j^{n+1})^{3/2} \Delta W_j}{A_i^{n+1}} \right]^2 && \text{for } z_i^n > h
 \end{aligned} \tag{3.22}$$

#### Model 4

*Deposition and erosion uniformly distributed over the whole cross-section (i.e. below the bank level):*

Levels:

$$z_i^{n+1} = z_i^n + \frac{\Delta A}{W_{top}} \tag{3.23}$$

$W_{top}$  = width of cross-section at the top level  $z_{max}$

Widths: unchanged

Areas:

$$A_i^{n+1} = A_i^n \tag{3.24}$$

Hydraulic radii:

$$R_i^{n+1} = R_i^n \tag{3.25}$$

#### Model 5

*Deposition and erosion proportional with depth below bank level (top level):*

Levels:

$$\begin{aligned}
 \alpha &= \frac{\Delta A}{A_{top}^n} \\
 z_i^{n+1} &= z_i^n + \alpha(h - z_i^n)
 \end{aligned} \tag{3.26}$$

$A_{top}$  = area of cross-section at top level  $z_{max}$

Widths: unchanged

Areas:

$$A_i^{n+1} = (1 - \alpha)A_i^n \quad (3.27)$$

Hydraulic radii:

$$R_i^{n+1} = (1 - \alpha)R_i^n \quad (3.28)$$

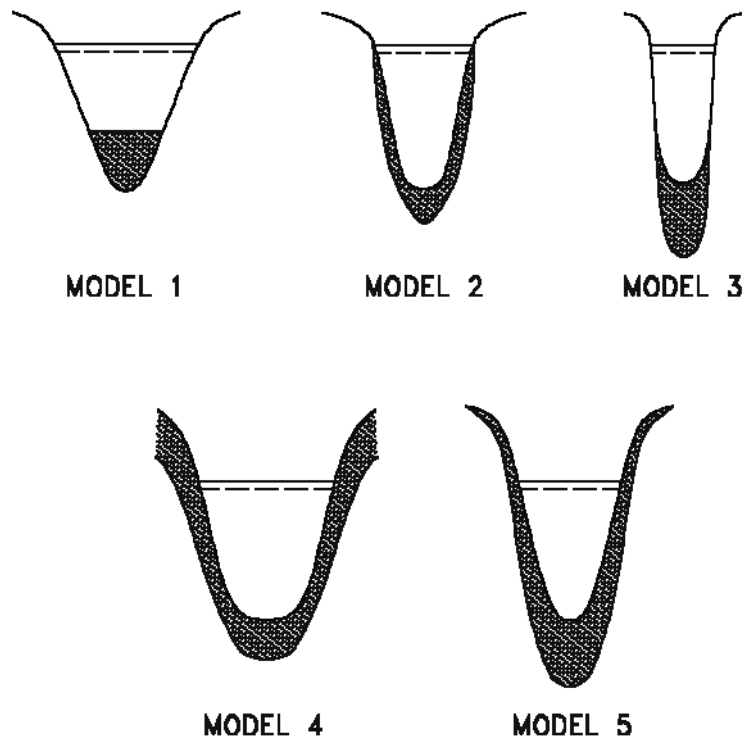


Figure 3.2 Update of bed level in MIKE 11 morphological model

### 3.5.2 Boundary Conditions

The unknown variable in the finite difference scheme is  $Z$ . This becomes evident by substituting Equation (3.15) into Equation (3.14). Boundary conditions should therefore be given in terms of bed level variation, although a sediment transport boundary condition can also be given. In this case Equation (3.20) is normally used to determine  $\Delta Z$  with  $Q_t^{n+1}$  replaced by the boundary sediment transport. However, when there is a serious imbalance at the boundary point, i.e. when  $\alpha$  is small and  $Qt_{bnd} \gg Qt^n$  this formulation



may give rise to numerical stability problems. In this case the difference between the transport specified at the boundary and the calculated transport at the in-flow point (first or last grid point depending on the flow direction) is assumed to erode/deposit at the inflow point, (one point continuity), i.e.:

$$Qt_{bnd}/W - (Qt_j^n + \alpha \Delta z_j^{n+1}) = \frac{\Delta x}{\Delta t} (1 - \varepsilon) \Delta z_j^{n+1} \quad (3.29)$$

which is solved for  $\Delta z_j^{n+1}$ .

Boundary conditions should be given at all inflow boundaries. In tidal models, boundary conditions should also be given at the tidal boundary (alternating in- and outflow).

At nodal points the sediment is distributed according to the flow discharge,  $Q$ , (i.e. with coefficients  $K_1$  to  $K_4$  and exponents  $n_1$  to  $n_4$  equal to 1) or according to a user specified distribution (i.e. with  $K_1$  to  $K_4$  and/or  $n_1$  to  $n_4$  different from 1). For example, in Figure 3.3 the transport rate in branch 3 is expressed as:

$$Q_{t_3}^{n+1} = \frac{K_3 Q_3^{n_3}}{K_3 Q_3^{n_3} + K_4 Q_4^{n_4}} (Qt_1^{n+1} + Qt_2^{n+1}) \quad (3.30)$$

and similarly for branch 4. The first grid points in branches 3 and 4 are treated in the same way as external boundaries with  $Qt_{bnd}$  replaced by  $Qt_3^{n+1}$  and  $Qt_4^{n+1}$ , respectively.

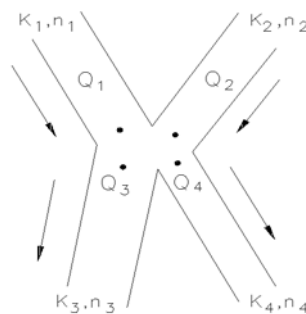


Figure 3.3 Distribution of sediment according to discharge

In nodal points sediment can be transported into a branch which has been specified as passive, but no sediment can be transported out of a passive branch.



### 3.5.3 Low flow correction

When the water level becomes less than a certain threshold value ( $delh$ , given in HD parameter editor → Default Values) the hydrodynamic model introduces an artificial slot, see Chapter 1 HD Reference Manual (p. 17). In this case the calculated velocity may have a rather arbitrary value, which may give rise to unrealistically large sediment transport rates. This problem has been solved by multiplying the calculated transport rate with a reduction factor  $f$  given by:

$$f = \begin{cases} 0 & D \leq delh \\ \frac{(D - delh)}{D} & delh < D \leq 2delh \\ 1 & 2delh < D \end{cases} \quad (3.31)$$

### 3.5.4 Hints

The Preissmann scheme is well suited to the solution of hyperbolic problems with only one characteristic. However, it has a drawback. At small Courant numbers it may generate short wave oscillations (wave length  $2\Delta x$ ). The oscillations can be damped by space forward centring the scheme (i.e. by using a large value of  $y$ ). This, however, will give rise to numerical dispersion at high Courant numbers. At a later stage an option for automatic selection of the optimum value of  $y$  will be incorporated, i.e. the value which just prevents the short wave oscillations.

The factor  $fac$  used in the numerical differentiation of the sediment transport formula should not be made too small because this will give rise to 'overshoot' phenomena in the numerical solution. A value of about 1.5 will be on the safe side in most cases unless very strong gradients occur.

The sediment transport Courant number can be approximated by

$$C_r = 5 \frac{\Delta t q_t}{\Delta x D} \frac{1}{1 - \varepsilon} \quad (3.32)$$

This implies that the morphological model can run with a much larger time step than the dynamic flow model and that a quasi-steady flow simulation will be sufficiently accurate, (see also de Vries, 1981, /41/). Often the time step will be limited only by the ability to resolve the boundary conditions.

## 3.6 Graded Sediments

An add-on module is available for model applications in non-uniform sediments in which the sediment transport can be calculated by fraction and the



variation in time and space of the particle size distribution determined. As a general guideline the graded sediment module should be used where the bed shear stress is close to the critical value for erosion. Where the bed shear is much greater than the critical value then using a single representative grain size is acceptable.

The simulation of graded sediment transport is an option available in the morphological mode (see section 3.5 Morphological model (p. 213)) and for each of the 5 sediment transport formulae (see section 3.5.1 Updating of bottom level (p. 216)).

For the simulation of graded sediments and sediment sorting the bed material is considered to comprise two layers; an active layer overlying a passive layer. This is illustrated in Figure 3.4. The active layer is the layer within which the bed load transport takes place and its depth ( $Z_a$ ) is defined as one half of the dune height.

The dune height is predicted according to the selected transport model type, viz.:

- Engelund-Hansen
- Ackers and White
- Engelund-Fredsøe
- Smart and Jaeggi
- Meyer, Peter and Muller
- Sato, Kikkawa and Ashida
- Ashida and Michiue
- Ashida, Takahashi and Mizuyama (ATM)

$$\frac{H}{R} = \frac{2I}{2+I} \text{ where } I = \frac{1}{3} \left( 1 - \frac{\theta_c}{\theta'} \right) \quad (3.33)$$

- van Rijn

$$\frac{H}{R} = 0,11 \left( \frac{d_{med}}{R} \right)^{0,3} \left\{ 1 - \exp \left[ \left( \frac{u'_f}{u_f} \right)^2 - 1 \right] \right\} \left[ 26 - \left( \frac{u'_f}{u_f} \right)^2 \right] \quad (3.34)$$

where,

$H$  is the dune height and  $\theta'$  and  $u'_f$  are calculated as described under the appropriate transport-model section.

$$Z_a^{n+1} = 0,5 H$$

For decreasing dune height (i.e. decreasing bed shear stress) the minimum dune height is specified by the user.

If erosion of the bed material occurs, the composition of the material in the passive layer ( $Z-Z_a$ ) stays the same. However, if deposition occurs active bed material is (instantaneously) mixed with the material in the passive layer and the composition is modified accordingly.

The additional input data required to simulate the transport of graded sediment are the initial percentage size distributions of both the active ( $P_a$ ) and passive ( $P_{bed}$ ) layer (they may have the same distribution initially). The data are specified as a number of fractions,  $N$  (referred to by subscript  $i$  for class-number), which remain fixed, and the corresponding percentage and mean grain size for the fraction. This percentage varies as sediment is transported selectively and mixed between the layers.

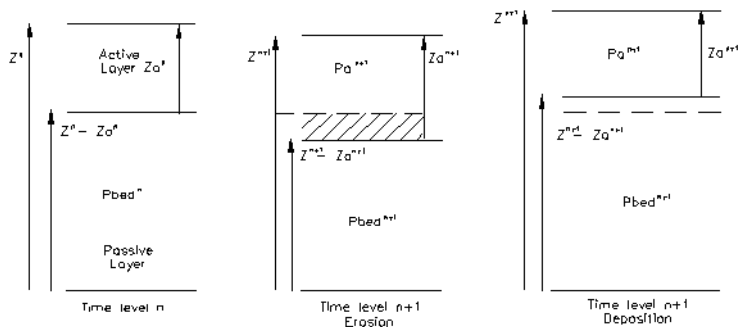


Figure 3.4 Active and passive sediment layers for the simulation of graded sediments

The transport and mixing of graded sediments is simulated in the following manner. The sediment transport is calculated for each specified class size separately. The calculation is modified in two ways from the calculation of a uniform material. Firstly, the criterion for the threshold of movement ( $\theta_c$  or  $A$  in the Ackers and White Model) is modified to allow for the hiding of finer particles and the greater exposure of larger particles as well as the mutual interference between particles of different size.  $\theta_c$  is modified by applying Egiazaroff's (1965),/24/, correction factor as follows:

$$\theta_{c_i} = \theta_c \left[ \frac{\ln(19)}{\ln\left(\frac{19 d_i}{d_{med}}\right)} \right]^2 \quad (3.35)$$

where,





$\theta_{c_i}$  is the dimensionless critical bed shear stress for class  $i$

$\theta_c$  is the dimensionless critical bed shear stress for a uniform sediment

$d_{med}$  is the mean grain size of the total sediment population

For the Ackers and White Model, the modified value of  $A$  is expressed as follows:

$$A_i = A \left( \frac{d_i}{d_{med}} \right)^{-0.2} \quad (3.36)$$

where,

$A_i$  is the critical flow mobility number for class  $i$

$A$  is the critical flow mobility number for a uniform sediment

The second modification is to multiply each class sediment transport,  $qt_i$ , by its percentage contribution,  $p_i$ . After the transport rate in each class has been calculated, the total transport,  $qt$ , is determined by summation over all classes,  $N$ :

$$qt = \sum_{i=1}^N qt_i p_i \quad (3.37)$$

The sediment continuity equation is then solved in the same way as for a uniform sediment using the total transport to obtain the change in bed level,  $\Delta z$ . Once  $\Delta z$  is known the sediment continuity equation is solved for each class size using the class transport rate,  $qt_i$ , and the total bed level change,  $\Delta z$ , to obtain the new percentage contribution of the active layer,  $p_i$ . The following relationships are applied:

The sediment continuity equation for each fraction may be expressed as:

$$(1 - \varepsilon) \frac{\partial W \overline{p_i Z}}{\partial t} + \frac{\partial qt_i}{\partial x} = 0 \quad (3.38)$$

where,

$\varepsilon$  is sediment porosity

$W$  is channel width

$\overline{p_i Z}$  is the average proportion of class  $i$  in both passive and active layer (i.e. over depth  $Z$ )

Expanding the first term of Equation (3.38) gives:

$$(1 - \varepsilon) \frac{\partial W \bar{\rho}_i Z}{\partial t} = (1 - \varepsilon) \left[ \left( \frac{\partial W \rho_i Z}{\partial t} \right)_j \Psi + \left( \frac{\partial W \rho_i Z}{\partial t} \right)_{j-1} (1 - \Psi) \right] \quad (3.39)$$

in which the time derivatives are expressed by:

$$\bar{\rho} Z^{n+1} = \rho_a^{n+1} Z_a^{n+1} + \rho_{bed}^{n+1} (Z^{n+1} - Z_a^{n+1}) \quad (3.40)$$

and similarly for time level  $n$  (subscript  $i$  has been removed for convenience).

The composition of the material in the passive layer at time level  $n+1$  depends on whether the interface between the active and passive layer moves up or down and is expressed by:

$$(Z^{n+1} - Z_a^{n+1}) \leq (Z^n - Z_a^n) \text{ (Erosion):}$$

$$\rho_{bed}^{n+1} = \rho_{bed}^n \quad (3.41)$$

implying that the passive layer is assumed to be totally mixed.

$$(Z^{n+1} - Z_a^{n+1}) > (Z^n - Z_a^n) \text{ (Deposition):}$$

$$\begin{aligned} \rho_{bed}^{n+1} (Z^{n+1} - Z_a^{n+1}) &= \rho_{bed}^{n+1} Z^n - Z_a^n \\ &+ \frac{1}{2} (\rho_a^{n+1} + \rho_a^n) [(Z^{n+1} - Z_a^{n+1}) - (Z^n - Z_a^n)] \end{aligned} \quad (3.42)$$

The symbols used in the above expressions are as shown in Figure 3.4.

Similarly, a weighted time average is used to expand the space derivative in the transport term in Equation (3.38).

where,  $qt_i^{n+1}$  is approximated by:

$$\frac{\partial qt_i}{\partial x} = \frac{qt_{i,j} - qt_{i,j-1}}{\Delta x} = \frac{(1-\theta)(qt_{i,j}^n - qt_{i,j-1}^n)}{\Delta x} + \frac{\theta(qt_{i,j}^n - qt_{i,j-1}^n)}{\Delta x} \quad (3.43)$$

$$qt_i^{n+1} = \rho_{a_i}^{n+1} qt^{n+1} - \rho_{a_i}^n qt^{n+1} + qt_i^n + \Delta Z^{n+1} \alpha_i \quad (3.44)$$



and

$$\alpha_i = \frac{\partial q t_i \partial u}{\partial u \partial z} + \frac{\partial q t_i \partial D}{\partial D \partial z} \quad (3.45)$$

and is calculated for each fraction.

The above expressions, ((3.39) to (3.45)), are solved for the unknowns  $p_a$  and  $p_{bed}$  at time level  $n+1$ .

### 3.6.1 Boundary conditions

The unknown variable in the finite difference scheme is  $p_i$ . Boundary conditions should therefore be given in terms of fraction values for each fraction and bed levels. Boundary conditions can also be specified as fraction sediment transport rates (either defined by a time series file or by defining the sediment supply boundary type). In the case of a fraction sediment transport boundary, Equation (3.44) is normally used to determine  $p_{a_i}^{n+1}$  with  $q t_i^{n+1}$  replaced by the boundary sediment transport  $Q_{ibnd}/W$ . If there is a serious imbalance at the boundary point, i.e. when alpha is small and  $Q_{ibnd} \gg Q t_i^n$ , numerical instabilities may occur. In this case a one point continuity equation is solved, i.e.:

$$\frac{Q_{ibnd}}{W} - q_i^{n+1} = \frac{\Delta X}{\Delta t} (1 - \varepsilon) \Delta(\overline{P_i Z}) \quad (3.46)$$

The boundary condition is given by the summation of all the fraction sediment boundaries:

$$Q_{tbnd} = \sum_{i=1}^N Q_{ibnd} \quad (3.47)$$

### 3.6.2 Graded sediments boundary conditions

In the case where  $Q_{tbnd}=0$ , i.e. there is no transport of any fraction across the boundary, all the fraction proportions are automatically set to zero except for the most coarse fraction which is set to 1.

The distribution of sediment at nodal points is determined as described below in section 3.5 Morphological model (p. 213).

## 3.7 Dune dimensions

### 3.7.1 Equilibrium dune height

With the model presented by Fredsøe (1979) /31/, /32/ the equilibrium dune height can easily be found as a function of  $\theta_{top}$  (the dimensionless shear stress taken at the top of the dune).

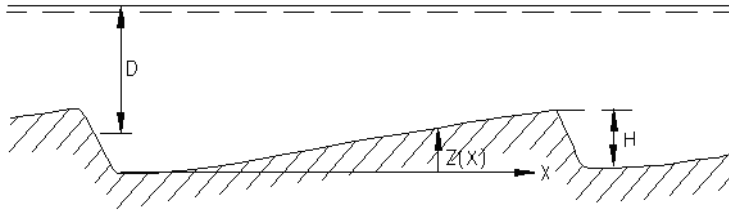


Figure 3.5 Definition sketch

The friction factor is assumed to be constant near the dune top. This means that the local dimensionless shear stress,  $\theta$ , is proportional to the velocity squared:

$$\theta = \theta_{top} \frac{q^2}{(D-z)^2} \frac{(D-H)^2}{q^2} = \theta_{top} \frac{(1-H/D)^2}{(1-z/H)^2} \quad (3.48)$$

where,

$D$  is water depth

$z$  is local dune height

$H$  is total dune height

$q$  is flow discharge per unit width

In the case of small transport rates, i.e. bed load only, the local sediment transport can be expressed as a function of  $\theta$ :

$$\Phi_b = \Phi_b(\theta) \quad (3.49)$$

The spatial variation of  $\Phi_b$  near the top of the dune is expressed by:

$$\left. \frac{\partial \Phi_b}{\partial x} \right|_{top} = \left. \frac{\partial \Phi_b}{\partial \theta} \right|_{\theta = \theta_{top}} \frac{\partial \theta}{\partial x} = \left. \frac{\partial \Phi_b}{\partial \theta} \right|_{\theta = \theta_{top}} \theta_{top} \frac{2}{1-H/D} \left. \frac{\partial (z/D)}{\partial x} \right|_{top} \quad (3.50)$$



where,

$z$  is the local height of the dune.

The migration velocity of the dune,  $c$ , is calculated under the assumption that all of the bed load transport is deposited on the lee side of the dune:

$$c = \frac{q_b}{(1-\varepsilon)H} \quad (3.51)$$

where,

$$q_b = \Phi_b \sqrt{(s-1)gd^3}$$

$\varepsilon$  = the porosity of the bed material

The change in the bed level near the dune top (on the upstream side) can be expressed as:

$$\frac{\partial z}{\partial t} = -c \frac{\partial z}{\partial x} = -\frac{q_b}{(1-\varepsilon)H} \frac{\partial z}{\partial x} \quad (3.52)$$

using the continuity equation for sediment:

$$\frac{\partial z}{\partial t} = -\frac{1}{1-\varepsilon} \frac{\partial q_b}{\partial x} \quad (3.53)$$

Equations (3.50) and (3.52) can be related to each other as follows:

$$\left. \frac{\partial \Phi_b}{\partial \theta} \right|_{\theta = \theta_{top}} \frac{2\theta_{top}}{1-H/D} \left. \frac{\partial(z/D)}{\partial x} \right|_{top} = \left. \frac{\Phi_b}{H/D} \frac{\partial(z/D)}{\partial x} \right|_{top} \quad (3.54)$$

or as:

$$\frac{H/D}{1-\frac{1}{2}H/D} = \left. \frac{\Phi_b}{2\theta \frac{\partial \Phi_b}{\partial \theta}} \right|_{top} \quad (3.55)$$

Equation (3.55) expresses the equilibrium height of the dunes in the case of pure bed load. At the dune top  $\partial z / \partial x = 0$  in which case Equation (3.55) does not apply. However, the equation must still hold a short distance upstream of the top where the local dune height is almost equal to  $H$ .

## The influence from the suspended load

If the sediment transport consists of both bed load and suspended load the equations are modified as follows:

- The total sediment transport ( $\Phi_t = \Phi_b + \Phi_s$ ) is still assumed to be a function of the local bed shear stress:  $\Phi_t = \Phi_t(\theta')$
- $\Phi_b$  is replaced by  $\Phi_t$  in Eq. (3.50)
- $\theta_b$  is retained in Equations (3.50) and (3.52) as it is assumed that only the bed load is deposited at the lee side of the dune

The general equation describing the equilibrium dune height thus reads:

$$\frac{H/D}{1 - \frac{1}{2}H/D} = \frac{\Phi_b}{2\theta \frac{\partial(\Phi_b + \Phi_s)}{\partial\theta}} \Bigg|_{top} \quad (3.56)$$

The variation of  $H/D$  as a function of  $\theta'$  is shown in Figure 3.6 for sand with a mean diameter of 0.3 mm using the Engelund and Fredsøe transport model.

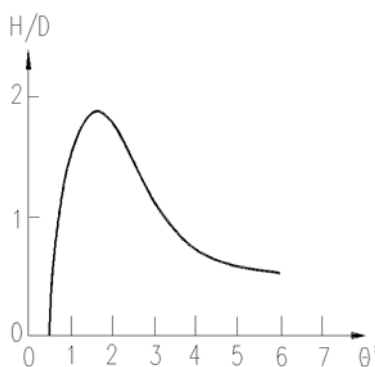


Figure 3.6  $H/D$  as a function of  $\theta'$ .  $d_{50} = 0.3$  mm

### 3.7.2 Equilibrium dune length

An expression for the equilibrium dune length has been obtained by Fredsøe (1982) /33/ through a consideration of the dune shape. The end of the dune is defined as the point where  $\partial z/\partial x$  is equal to zero, where  $z$  is the local dune height. Negative values of  $\partial z/\partial x$  will result in diverging flow and, consequently, in very small transport rates. The transported sediment avalanches down the lee slope due to gravity so that the lee slope is very steep.



The dune shape is calculated by use of the continuity equation for sediment in the following way:

1. it is shown (/30/) that for bed forms which are travelling downstream with a constant form and celerity,  $c$ , the height is proportional to the total bed material sediment transport,  $\theta_t$ :

$$q_t = (1 - \varepsilon)cH + \text{const.} \quad (3.57)$$

where,

$H$  is the dune height

$\varepsilon$  is porosity

If only bed load,  $\theta_b$ , is considered, the transport is zero in the troughs and the constant is, therefore also zero. Thus:

$$q_t = (1 - \varepsilon)cH \quad (3.58)$$

2. Fredsøe (1982) /33/ calculated the bed load along the dune through a description of the local dimensionless bed shear stress,  $\theta_t$ , taken to be proportional to the local mean velocity squared, and a function,  $f$ , of the distance from the downstream dune front:

$$\theta = \theta_t \frac{(1 - H/D)^2 f(x/H)}{(1 - z/D)^2 f(L/H)} \quad (3.59)$$

where,

$L$  is the dune length

$D$  is the flow depth.

The function,  $f$ , is assumed to be general, regardless of the shape and size of the dune. The bed load transport along the dune is calculated by use of a bed load formula. The effect of gravity on the bed load,  $\theta_b$ , is taken into account by adding to  $\theta$  the correction:

$$-0,1 \frac{\partial z}{\partial x} \text{ giving } q = \sqrt{(s-1)gd^3} \Phi_b \left( \theta - 0,1 \frac{\partial z}{\partial x} \right) \quad (3.60)$$

where,  $\Phi_b$  is the dimensionless bed load transport.



By combining Equations (3.58) and (3.59) a differential equation describing  $\partial z/\partial x$  is found. The dune shape and length is found from the boundary conditions:

$$\left. \begin{array}{l} \frac{\partial z}{\partial x} = 0 \\ z = H \end{array} \right\} \text{for } x = L \quad (3.61)$$

The function,  $f$ , has a maximum at  $x = 17 H$  so this is the length of the dune if the effect of gravity and suspended load is neglected. For small  $\theta_t$  values, however, the effect of gravity is important and causes the dune length to be larger than  $17 H$ .

As indicated above, the calculations are rather laborious and, therefore, the following approximation is suggested for the ratio between the dune height and length for bed load transport only:

$$\frac{H}{L} = \begin{cases} 0,06 - 146(0,15 + \theta_c - \theta)^{4,26} & \text{for } \theta < 0,15 + \theta_c \\ 0,06 & \text{for } 0,15 + \theta_c \leq \theta \end{cases} \quad (3.62)$$

where,

$\theta$  is the dimensionless bed shear stress

$\theta_c$  is the critical value

## Influence of Suspended Load

The sediment transport has its maximum at the dune crest, see Equation (3.58). The bed load is a function of the local bed shear stress so that the dune crest is the position with maximum bed shear stress in the case of bed load only.

The suspended load is not a function of the local bed shear stress. A spatial lag,  $\delta$ , exists between the hydraulic parameters and the suspended load because it takes some time for the suspended particles to settle or to be picked up from the bed. The lag is given by:

$$\delta = \frac{\varepsilon U_b}{w^2} \quad (3.63)$$

where,





$\varepsilon$  is the average eddy viscosity:

$$\varepsilon = 0,077u_f h \quad (3.64)$$

and  $u_b$  is the 'slip velocity':

$$u_b = u_f(2 + 2,5 \ln(h/k)) \cong 15u_f \quad (3.65)$$

where,  $u$ ,  $u_b$  and  $u_f$ , respectively, are current velocity, near bed and friction velocities,  $h$  is water depth and  $k$  is the equivalent sand roughness.

Consequently, the point of maximum transport is moved downstream from the point of maximum bed shear stress. The lag distance is determined from the ratio between the bed load and the suspended load transport so that the dune length is given by:

$$L = L_o + \delta \frac{\Phi_s}{\Phi_s + \Phi_b} \quad (3.66)$$

where,  $L_o$  is the dune length in the case of bed load transport only determined by Equation (3.62).

The dune length as a function of  $\theta'$  is depicted in Figure 3.7 for 0.3 mm sand.

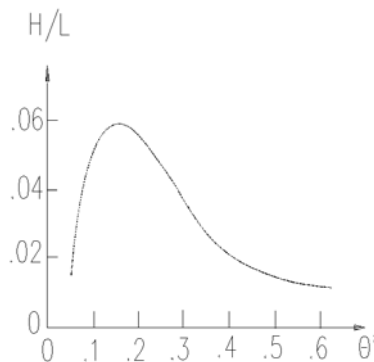


Figure 3.7 The ratio of the dune height and the dune length as a function of  $\theta'$ .  $d_{50} = 0.3 \text{ mm}$

### 3.7.3 Non-equilibrium dune height

The rate of change of the dune height has been analysed by Fredsøe (1979), /31/, /32/. It can be described by the equations used to calculate the equilibrium dune height.

The rate of change of the bed level  $z$  near the dune top is expressed as:

$$\frac{\partial c}{\partial t} = -c \frac{\partial z}{\partial x} + \frac{dz}{dt} \quad (3.67)$$

where the celerity of the dune front is

$$c = \frac{q_{bt}}{(1-\varepsilon)H} \quad (3.68)$$

where,  $q_{bt}$  is the transport rate at the dune top,  $\varepsilon$  is the sediment porosity and  $\partial z / \partial t$  is found from the equation of continuity:

$$\frac{\partial z}{\partial t} = \frac{-1}{1-\varepsilon} \frac{\partial(q_b - q_s)}{\partial x} \Big|_{top} = \frac{-1}{1-\varepsilon} \frac{\partial(q_b - q_s)}{\partial \theta} \Big|_{top} \frac{2\theta_{top}}{1-H/D} \frac{\partial z}{\partial x} \quad (3.69)$$

Equations (3.67), (3.68) and (3.69) yield:

$$\frac{dH}{dt} = \frac{1}{1-\varepsilon} \frac{\partial z \phi_b}{\partial x H} - \frac{\partial(\phi_b - \phi_s)}{\partial \theta} \Big|_{top} \frac{2\theta_{top}}{D-H} \sqrt{(s-1)gd^3} \quad (3.70)$$

In order to obtain a value of the change of the dune height which is representative for most of the dunes, the 'integrated' value for  $\partial z / \partial x : H/L$  is used in Equation (3.70) leading to:

$$\frac{dH}{dt} = \frac{\sqrt{(s-1)gd^3}}{1-\varepsilon} \frac{1}{L} \Big|_{\phi_b} - \frac{2\theta_{top}}{D/H-1} \frac{\partial(\phi_b - \phi_s)}{\partial \theta} \Big|_{top} \quad (3.71)$$

### 3.7.4 Non-equilibrium dune length

At present no satisfactory theory for the change of dune length exists. The dune length is of less importance for the hydraulic resistance than the dune height, so an approximate description will suffice.

A possible definition of the dune length is the total length of a river reach divided by the number of dunes in that reach. By that definition, the dune length can (under uniform conditions) only be changed, if dunes disappear or new ones are created. Consequently, it seems reasonable to include the



average life time of a dune in the expression for  $dL/dt$ . A plausible assumption is that the average lifetime  $T_1$  of the dunes can also be used as the time scale for the change in dune length:

$$\frac{dL}{dt} = \frac{L - L_e}{T_1} \quad (3.72)$$

where,  $L_e$  is the equilibrium dune length. A stability analysis shows that, if the position of the dune front of a single dune in a row of regular dunes in equilibrium is perturbed, the celerity of the dune  $c$  will be reduced regardless of whether the dune front has been advanced or retarded. This implies that the dunes are unstable. If the dune front is retarded, the dune will be overtaken by the following dune.

The time required for this process has been estimated from the calculated celerity of the dune when the length has been reduced to  $L_e/2$ . This celerity is about 85-90% of the celerity of the equilibrium dunes. It has, therefore, been estimated that the dune will move a distance of the order of magnitude  $10 L_e$  before it is overtaken.  $T_1$  is thus approximately  $10 L_e/c$ , yielding:

$$\frac{dL}{dt} = \left( \frac{L - L_e}{T_1} \right) c = \left( \frac{L}{L_e} - 1 \right) q_b \frac{1}{10(1 - \varepsilon)H} \quad (3.73)$$

where,  $\varepsilon$  is the sediment porosity.

## 3.8 Flow Resistance

The calculation of the flow resistance is far more complex in the case of an alluvial river than in the case of a channel with a fixed bed. This is because a large part of the hydraulic resistance in the alluvial case may be caused by a form drag on the bed forms whose configuration is determined by the sediment transport and the flow. The most important bed forms in natural streams are dunes and the flow resistance in the case of a plane bed or a dune covered bed is treated in 3.8.1 Flow resistance - dune dimension (*p. 235*) and Flow Resistance -  $\theta$ - $\theta'$  Relationship (*p. 237*). For flow resistance according to White et al., see section 3.8.3 Flow Resistance - White et al. (*p. 239*).

### 3.8.1 Flow resistance - dune dimension

If the dimensions (height and length) of the dunes are known, the hydraulic resistance (bed shear stress) can be calculated from the water depth and the specific discharge. Furthermore, the portion of the dimensionless bed shear stress,  $\theta'$ , which is acting as skin friction on the gently curved upstream side of the dunes can be determined.



The total bed shear stress,  $\tau$ , is split up into the skin friction,  $\tau'$ , and a portion which is caused by the form drag on the dunes  $\tau''$ :

$$\tau = \tau' + \tau'' \quad (3.74)$$

$\tau''$  is mainly caused by the expansion loss behind each dune and can therefore be described as Carnot losses (/30/):

$$\frac{\tau''}{\rho} \approx \frac{\alpha q^2 D}{2L} \left( \frac{1}{D} - \frac{1}{D+H} \right)^2 \approx \frac{\alpha u^2 H^2}{2DL} \quad (3.75)$$

where,

$H$  is the total dune height

$D$  is the flow depth

$L$  is dune length

$\alpha$  is the velocity distribution coefficient which is close to one

$u$  is current velocity

$\theta$  the discharge per unit width

Thus, the dimensionless shear stress,  $\theta$ , can be written as:

$$\frac{\tau}{(s-1)\rho g d} = \theta = \theta' + \frac{\alpha u^2 H^2}{2(s-1)gdDL} \quad (3.76)$$

$\theta'$  is by definition:

$$\theta' = \frac{u m p_f'^2}{(s-1)gd} \quad (3.77)$$

and  $u_f'$  can be found from the boundary layer equation:

$$\frac{u}{u_f'} = 2,5 \left[ \ln \left( \frac{30D'}{k} \right) - 1 \right] \quad (3.78)$$

where,

$D'$  is the boundary layer thickness (/30/)



$k$  is the equivalent sand size

$$D' = D \frac{\theta'}{\theta} \quad (3.79)$$

The four equations can be solved in a few iterations, starting with (3.78), then (3.11.4), (3.76), and (3.79). See also section 3.8.2 Flow Resistance -  $\theta$ - $\theta'$  Relationship (p. 237).

### 3.8.2 Flow Resistance - $\theta$ - $\theta'$ Relationship

When the bed is covered by bed forms, the total bed shear stress,  $\tau$ , can be divided into two parts,  $\tau'$  and  $\tau''$ .

$\tau'$  is the shear stress acting on the gently curved upstream surface of the dunes, and  $\tau''$  is caused by the form drag on the dunes.

Engelund (1966) found, by applying a principle of similarity, that a relationship exists between the dimensionless total bed shear stress,  $\theta$ , and the dimensionless skin friction,  $\theta'$ , Figure 3.8. The relationship for a dune covered bed can be approximated by:

$$\theta' = 0,4\theta^2 + 0,06 \quad (3.80)$$

where,

$$\theta = \frac{\tau/\rho}{(s-1)gd} \quad \text{and} \quad \theta' = \frac{\tau'/\rho}{(s-1)gd}$$

$\rho$  is the density of water,  $s$  is the specific gravity of the bed material,  $d$  is the mean grain size of the bed material and  $g$  is the acceleration of gravity.

In the case of a plane bed, the form drag becomes zero and the relationship reads:

$$\theta' = \theta \quad (3.81)$$

The relationship given in Equation (3.80) has been determined from flume observations. However, due to discontinuities in natural rating curves where two water levels may exist for a single discharge, there are two possible solutions to Equation (3.80) rendering it unsuitable for computer modelling. To overcome this problem, Challet and Cunge (1980),/22/ proposed a modified  $\theta$ - $\theta'$  relationship as shown below. This is the formulation used in MIKE 11.

$$\theta \leq 0,06 \quad \text{for} \quad \theta' = \theta$$

$$0,06 < \theta \leq 0,30 \text{ for } \theta' = 0,136\theta^{0,292}$$

$$0,30 < \theta \leq 0,90 \text{ for } \theta' = 0,06 + 0,4\theta^2$$

$$0,90 < \theta \leq 1,10 \text{ for } \theta' = 0,667\theta^{5,24}$$

$$1,10 < \theta \quad \text{for } \theta' = \theta$$

The flow over the 'smooth' upstream side of the dune can be described by the boundary layer equation:

$$\frac{u}{u'_f} = 2,5 \left[ \ln \left( \frac{30D'}{k} \right) - 1 \right] \quad (3.82)$$

$u$  is the mean flow velocity,  $u'_f = \sqrt{\tau'/\rho}$ ,  $D'$  is the boundary layer thickness,  $D' = D\theta'/\theta$ ,  $D$  is the mean flow depth, and  $k$  is the equivalent sand roughness of the dune surface,  $k \sim 2.5 d$ .

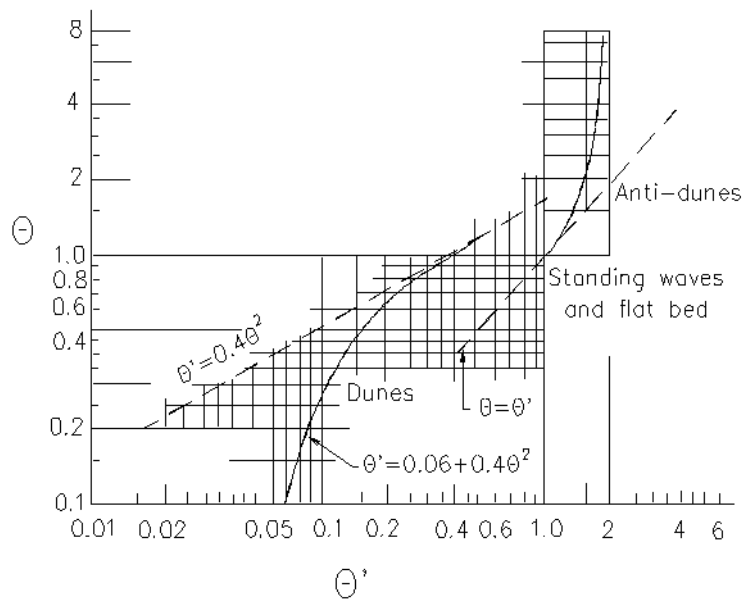


Figure 3.8 Plot of  $\theta$  versus  $\theta'$  (experimental data)



Under weak non-uniform flow conditions, the steady state flow conditions can thus be found as a function of the specific discharge and the depth through the following four equations:

$$u'_f = \frac{u}{2,5 \left[ \ln \left( \frac{30D'}{2,5d} \right) - 1 \right]} \quad (3.83)$$

$$\theta' = \frac{u'^2_f}{(s-1)gd} \quad (3.84)$$

$$\theta = \sqrt{\frac{(\theta' - 0,062)}{0,4}}, \text{ (if } \theta' \leq 0.062 \text{ then } \theta = \theta') \quad (3.85)$$

$$D' = D \frac{\theta'}{\theta} \quad (3.86)$$

Equations (3.83) to (3.86) can be solved by iteration.

The Manning or Chezy coefficient can, if required, be calculated from the mean flow velocity, the depth and the total dimensionless bed shear stress, viz:

$$\frac{\rho g}{C^2} = \frac{\theta(s-1)gd\rho}{u^2} \quad (3.87)$$

See also section 3.8.1 Flow resistance - dune dimension (p. 235).

### 3.8.3 Flow Resistance - White et al.

The flow resistance model developed by White et al. (1979) /42/ is an extension to the Ackers and White model (p. 243). The model is semi-empirical; the governing parameters are found by dimensional analysis and, from the analysis of a large amount of data, a functional relationship has been determined.

White et al. suggests that the alluvial roughness is a function of three dimensionless variables defined below, (see also Ackers and White (1973), /20/ and section 3.10 Ackers and White model (p. 243)).

1. A dimensionless grain size, defined as the cube root of the ratio of immersed weight to viscous forces

$$D_{gr} = d \left[ \frac{g(s-1)}{\nu^2} \right]^{1/3} \quad (3.88)$$



where,

$n$  is the viscosity of water ( $\sim 10^{-6}$  m<sup>2</sup>/s)

$d$  is the grain size

2. A general sediment mobility number given by

$$F_{gr} = \frac{u_f^n}{\sqrt{gd(s-1)}} \left( \frac{u}{\sqrt{32} \log\left(\frac{10D}{d}\right)} \right)^{1-n} \quad (3.89)$$

where,

$n$  is a function of  $D_{gr}$  ranging from 0 (coarse sediment) to 1 (fine sediment)

$n$  is defined in section 3.10 Ackers and White model (p. 243).

3. A fine grain sediment mobility number given by substituting  $n=1$  in Equation (3.89), i.e.:

$$F_{fg} = \frac{u_f}{\sqrt{gd(s-1)}} \quad (3.90)$$

- note that  $F_{fg} = \sqrt{\theta}$  (see also section 3.8.2 Flow Resistance -  $\theta$ - $\theta'$  Relationship (p. 237)).

Based on a large number of experimental data White et al. found a functional relationship of the form:

$$\frac{F_{gr}-A}{F_{fg}-A} = f(D_{gr}) \quad (3.91)$$

where,  $A$  is the critical mobility number for initiation of motion and is given as a function of  $D_{gr}$  (see section 3.10 Ackers and White model (p. 243)). The range of applicability for Equation (3.91) is  $F < 0.8$  and  $1 < D_{gr} < 60$ .

Curve fitting suggested two different expressions for the right hand side of Equation (3.91), viz:

$$f(D_{gr}) = 1 - 0,76 \left[ 1 - \frac{1}{\exp [(\log D_{gr})^{1,7}]} \right] \quad (3.92)$$





when  $D_{gr}$ ,  $F_{gr}$  and  $F_{fg}$  are based on  $d_{35}$ , and

$$f(D_{gr}) = 1 - 0,70 \left[ 1 - \frac{1}{\exp [(1,4 \log D_{gr})^{2,65}]} \right] \quad (3.93)$$

when the parameters are based on  $d_{65}$ .

Testing the model on a set of independent data (both experimental and prototype data) White et al. found that Equation (3.92) gave slightly better results than Equation (3.93).

An iterative procedure is used to determine the alluvial roughness coefficient. The general sediment mobility number can be expressed in terms of the fine grain mobility as follows:

$$F_{gr} = F_{fg}^n t \quad (3.94)$$

where,  $t$  depends on  $u$ ,  $D$  etc., but is known:

$$t = \left[ \frac{u}{\sqrt{32 g d (s-1)}} \log \left( \frac{10 D}{d} \right) \right]^{1-n} \quad (3.95)$$

Inserting Equation (3.94) into Equation (3.91) yields:

$$F_{fg} = \frac{t}{f(D_{gr})} F_{fg}^n + \left( 1 - \frac{1}{f(D_{gr})} \right) A \quad (3.96)$$

This formula can be used iteratively to calculate  $F_{fg}$  because both  $t/f(D_{gr})$  and  $n$  are greater than 0 but smaller than 1. Subsequently,  $F_{fg}$  can be substituted into Equation (3.89) to obtain  $u_f$ . It is now possible, using Equations (3.90) and (3.93) in section 3.10, Ackers and White model, to solve the sediment transport rate.

## 3.9 Incipient motion criteria

### 3.9.1 Shield's critical parameter

Many sediment transport theories imply that a certain threshold of the bed shear is exceeded in order to initiate motion. One of the important contributions in this respect is the classical work by Shields. The theory will not be described here. Only will be mentioned that Shield established a relation between the particle Reynolds number and a dimensionless parameter for motion,  $\theta$ , which describes the ratio between driving and stabilising forces. If  $\theta$  exceeds a certain value  $\theta_c$  (Shields critical parameter) then sediment motion will initiate.



$\theta_c$  is defined by

$$\theta_c = \frac{u_{f,c}^2}{(s-1)gd} \quad (3.97)$$

When the right-hand side exceeds a value of approximately 0.056, then motion will initiate.

### 3.9.2 Iwagaki's critical tractive force

Whenever any of the sediment transport formulas Meyer-Peter & Müller, Ashida, Takahashi & Mizuyama, Ashida & Michiue or Sato, Kikkawa & Ashida is chosen and uniform sediments is simulated, then the critical shear stress (or critical tractive force) is estimated by the model of Iwagaki. If any other sediment transport formula is used then the critical shear stress is calculated according to the principles of Shields. However, if the following line is set into the file MIKE11.ini in the section [ST\_SIMULATION]

CRITICAL\_TRACTIVE\_FORCE = on

then the critical shear stress is calculated according to Iwagaki's model for these formulas as well. By default the above parameter is set to 'off'.

#### Iwagaki's Model:

The model relates the critical shear velocity  $u'_{f,c}$  to the grain diameter  $d$ .

$$u'^2_{f,c} = \begin{cases} 226d & \text{for } d < 0,0065 \\ 8,41d^{11/32} & \text{for } 0,0065 \leq d < 0,0565 \\ 55,0d & \text{for } 0,0565 \leq d < 0,118 \\ 134,6d^{31/22} & \text{for } 0,118 \leq d < 0,303 \\ 80,9d & \text{for } 0,303 \leq d \end{cases} \quad (3.98)$$

where,

$d$  the average grain diameter

$u'_{f,c}$  the critical friction velocity corresponding to  $d$

### 3.9.3 Modified Egiazaroff equation

If any of the sediment transport formulas Ashida & Michiue or Sato, Kikkawa & Ashida is chosen and graded sediments simulated, then the critical shear stress (or critical tractive force) is estimated by the modified Egiazaroff model.



### Modified Egiazaroff Model:

The model modifies the critical shear stress for average grain size by a factor representing the influence of the actual grain size.

$$\begin{aligned} \frac{d_i}{d} \geq 0,4; \theta_{ci} &= \theta_c \left( \frac{\log_{10} 19,0}{\log_{10} 19,0 (d_i/d)} \right)^2 \\ \frac{d_i}{d} \leq 0,4; \theta_{ci} &= \theta_c \cdot \frac{0,85}{d_i/d} \end{aligned} \quad (3.99)$$

where,

$d_i$  the representative grain diameter for fraction  $i$  (cm)

$\theta_{ci}$  the dimensionless critical tractive force corresponding to grain size  $d_i$ .

$\theta_c$  the dimensionless critical tractive force corresponding to the average grain size.

$\theta_c$  is calculated from the relation

$$\theta_c = \frac{u_{f,c}'^2}{(s-1)gd} \quad (3.100)$$

where the critical friction velocity  $u_{f,c}'$  is determined from Iwagaki's equation.

## 3.10 Ackers and White model

Ackers and White (1973) /20/ presented a semi-empirical sediment transport model. The model is partly based on dimensional analysis but physical arguments have been used to derive the form of the function that was tested. See also under section 3.8.3 Flow Resistance - White et al. (p. 239).

The Ackers-White transport model reads:

$$G_{gr} = C \left( \frac{F_{gr}}{A} - 1 \right)^m \quad (3.101)$$

where,



$G_{gr}$  is the general transport parameter, and  $C$ ,  $m$  and  $A$  are model parameters determined from the dimensionless grain diameter,  $D_{gr}$ , defined as:

$$D_{gr} = d \left[ \frac{g(s-1)}{\nu^2} \right]^{1/3} \quad (3.102)$$

where,

$d$  is grain size

$\nu$  is kinematic viscosity

$s$  is the relative density of the sediment.

$F_{gr}$  in Equation (3.101) is a general sediment mobility number defined as:

$$F_{gr} = \frac{u_f^n}{\sqrt{gd(s-1)}} \left( \frac{u}{\sqrt{32} \log\left(\frac{10D}{d}\right)} \right)^{1-n} \quad (3.103)$$

where,

$u_f$  is the friction velocity

$D$  is water depth

$n$  is a model constant determined from  $D_{gr}$  and ranges from 0 (coarse material) to 1 (fine material).

Inserting these values of  $n$  into Equation (3.103) gives the sediment mobility numbers for coarse ( $F_{cg}$ ) and fine ( $F_{fg}$ ) material, respectively:

$$F_{cg} = \frac{u}{\sqrt{32} gd(s-1) \log\left(\frac{10D}{d}\right)} \quad (3.104)$$

$$F_{fg} = \frac{u_f}{\sqrt{gd(s-1)}} \quad (3.105)$$

$G_{gr}$  is the general transport parameter defined as:

$$G_{gr} = \frac{XD \left(\frac{u_f}{u}\right)^n}{sd} \quad (3.106)$$



where,

$X$  is the sediment transport as a mass flux per unit mass flow rate.

In determining the model parameters, Ackers & White distinguished between three cases, viz. fine grains, coarse grains and a transitional grain size. The classification is based on  $D_{gr}$ .

$D_{gr} < 1$  (fine grains):

$$n = 1$$

$$A = 0.37$$

$$C = 2.95 \cdot 10^{-4}$$

$$m = 11$$

$1 < D_{gr} < 60$  (transitional grain size):

$$n = 1.0 - 0.56 \log D_{gr}$$

$$A = \frac{0.23}{\sqrt{D_{gr}}} + 0.14$$

$$\log C = 2.86 \log D_{gr} - (\log D_{gr})^2 - 3.53$$

$$m = \frac{9.66}{D_{gr}} + 1.34$$

$D_{gr} > 60$  (coarse grains):

$$n = 0$$

$$A = 0.17$$

$$C = 0.025$$

$$m = 1.50$$



**NOTE!** When  $D_{gr} > 60$  the formulation assumes that all material moves as bed load. This might be wrong under extreme conditions.

### 3.11 Ashida & Michiue model

The Ashida & Michiue model consists of two parts: one which describes bed load, and one describing suspended load transport.



### 3.11.1 Bed load

The bed load model of Ashida & Michiue relates the transport to the friction velocity, critical shear velocity and a effective friction velocity. The bed load equation reads

$$q_b = 17 \cdot \frac{u'_{f,eff}{}^3}{(s-1)g} \cdot \left(1 - \frac{u'_{f,c}{}^2}{u'_{f,c}{}^2}\right) \cdot \left(1 - \frac{u'_{f,c}}{u'_{f,c}}\right) \quad (3.107)$$

where  $u'_f$  is the friction velocity,  $u'_{f,c}$  is the critical friction velocity obtained from Shield's relation, and  $u'_{f,eff}$  is the effective friction velocity determined from the relation

$$\frac{V}{u'_{f,eff}} = 6,0 + 5,75 \cdot \log\left(\frac{R}{d(1+2\theta')}\right) \quad (3.108)$$

where  $V$  is the cross sectional averaged flow velocity,  $R$  is hydraulic radius,  $d$  is grain diameter and  $\theta'$  is the dimensionless shear stress related to the grains.

Automatic updating of the bed resistance according to the formulation by Engelund (see page 3.8.2) is optional.

In case of uniform sediments the critical shear stress is computed by the principles of Iwagaki, see section 3.9.2. If graded sediments are modelled then the critical shear stress derived from Iwagaki's model is further modified by the Egiazaroff equation, see section 3.9.3.

### 3.11.2 Suspended load

The suspended load is computed from the following equation

$$q_{si} = q \cdot C_{ai} \left[ \left(1 + \frac{1}{\kappa} \cdot \frac{u'_f}{V}\right) \Lambda_1 + \frac{1}{\kappa} \cdot \frac{u'_f}{V} \Lambda_2 \right] \quad (3.109)$$

where,

$q_s$  the suspended sediment load per unit width of the channel (m<sup>3</sup>/s/m)

$q$  the flow per unit width of the channel (m<sup>3</sup>/s/m) (=V·R)



$C_{ai}$ (the dimensionless) of above equation can be expressed as

$$C_{ai} = 0,025 \left\{ \frac{g(\xi_0)}{\xi_0} - G(\xi_0) \right\} \tag{3.110}$$

in which the functions are determined from

$$\xi_0 = \left( \frac{4}{3} \cdot \frac{\omega_0}{u_f} \right)$$

$$g(\xi_0) = \frac{1}{\sqrt{2\pi}} \exp(-\xi_0^2/2) \tag{3.111}$$

$$G(\xi_0) = \frac{1}{\sqrt{2\pi}} \int_{\xi_0}^{\infty} \exp(-\xi^2/2) d\xi$$

$\omega_0$  is determined from equation (3.133).

The calculation of  $\xi_0$  and  $g(\xi_0)$  is straight forward. The calculation of  $G(\xi_0)$  is made by using a table with values of the integral as a function of  $\xi_0$ . The table is shown below. The leftmost column shows values of  $\xi_0$  with one decimal. The top row show the second decimal. Hence the table gives  $G(\xi_0)$  for all values of  $\xi_0$  ranging from 0.00 to 3.69. Linear interpolation is made within the table. For values of  $\xi_0$  larger than 3.69 the value of  $G(\xi_0)$  is 0.9999.

Table 3.1 Ashida & Michiue model; Integral as function of  $\xi_0$  ('Ksi\_0')

Ksi_0	0.00	0.01	0.02	0.03	0.04	0.05	0.06	0.07	0.08	0.09
0.0	0,500 0	0,504 0	0,508 0	0,512 0	0,516 0	0,519 9	0,523 9	0,527 9	0,531 9	0,535 9
0.1	0,539 8	0,543 8	0,547 8	0,551 7	0,555 7	0,559 6	0,563 6	0,567 5	0,571 4	0,575 3
0.2	0,579 3	0,583 2	0,587 1	0,591 0	0,594 8	0,598 7	0,602 6	0,606 4	0,610 3	0,614 1
0.3	0,617 9	0,621 7	0,625 5	0,629 3	0,633 1	0,636 8	0,640 6	0,644 3	0,648 0	0,651 7
0.4	0,655 4	0,659 1	0,662 8	0,666 4	0,670 0	0,673 6	0,677 2	0,680 8	0,684 4	0,687 9
0.5	0,691 5	0,695 0	0,698 5	0,701 9	0,705 4	0,708 8	0,712 3	0,715 7	0,719 0	0,722 4
0.6	0,725 7	0,729 1	0,732 4	0,735 7	0,738 9	0,742 2	0,745 4	0,748 6	0,751 7	0,754 9



Table 3.1 Ashida & Michiue model; Integral as function of  $\xi_0$  ('Ksi\_0')

0.7	0,758 0	0,7611	0,764 2	0,767 3	0,770 4	0,773 4	0,776 4	0,779 4	0,782 3	0,785 2
0.8	0,788 1	0,791 0	0,793 9	0,796 7	0,799 5	0,802 3	0,805 1	0,807 8	0,810 6	0,813 3
0.9	0,815 9	0,818 6	0,821 2	0,823 8	0,826 4	0,828 9	0,831 5	0,834 0	0,836 5	0,838 9
1.0	0,841 3	0,843 8	0,846 1	0,848 5	0,850 8	0,853 1	0,855 4	0,857 7	0,859 9	0,862 1
1.1	0,864 3	0,866 5	0,868 6	0,870 8	0,872 9	0,874 9	0,877 0	0,879 0	0,881 0	0,883 0
1.2	0,884 9	0,886 9	0,888 8	0,890 7	0,892 5	0,894 4	0,896 2	0,898 0	0,899 7	0,901 5
1.3	0,903 2	0,904 9	0,906 6	0,908 2	0,909 9	0,9115	0,913 1	0,914 7	0,916 2	0,917 7
1.4	0,919 2	0,920 7	0,922 2	0,923 6	0,925 1	0,926 5	0,927 9	0,929 2	0,930 6	0,931 9
1.5	0,933 2	0,934 5	0,935 7	0,937 0	0,938 2	0,939 4	0,940 6	0,941 8	0,942 9	0,944 1
1.6	0,945 2	0,946 3	0,947 4	0,948 4	0,949 5	0,950 5	0,951 5	0,952 5	0,953 5	0,954 5
1.7	0,955 4	0,956 4	0,957 3	0,958 2	0,959 1	0,959 9	0,960 8	0,961 6	0,962 5	0,963 3
1.8	0,964 1	0,964 9	0,965 6	0,966 4	0,967 1	0,967 8	0,968 6	0,969 3	0,969 9	0,970 6
1.9	0,971 3	0,971 9	0,972 6	0,973 2	0,973 8	0,974 4	0,975 0	0,975 6	0,976 1	0,976 7
2.0	0,977 2	0,977 8	0,978 3	0,978 8	0,979 3	0,979 8	0,980 3	0,980 8	0,981 2	0,981 7
2.1	0,982 1	0,982 6	0,983 0	0,983 4	0,983 8	0,984 2	0,984 6	0,985 0	0,985 4	0,985 7
2.2	0,986 1	0,986 4	0,986 8	0,987 1	0,987 5	0,987 8	0,988 1	0,988 4	0,988 7	0,989 0
2.3	0,989 3	0,989 6	0,989 8	0,990 1	0,990 4	0,990 6	0,990 9	0,9911	0,991 3	0,991 6
2.4	09918	0,992 0	0,992 2	0,992 5	0,992 7	0,992 9	0,993 1	0,993 2	0,993 4	0,993 6
2.5	0,993 8	0,994 0	0,994 1	0,994 3	0,994 5	0,994 6	0,994 8	0,994 9	0,995 1	0,995 2
2.6	0,995 3	0,995 5	0,995 6	0,995 7	0,995 9	0,996 0	0,996 1	0,996 2	0,996 3	0,996 4
2.7	0,996 5	0,996 6	0,996 7	0,996 8	0,996 9	0,997 0	0,997 1	0,997 2	0,997 3	0,997 4





Table 3.1 Ashida & Michiue model; Integral as function of  $\xi_0$  ('Ksi\_0')

2.8	0,997 4	0,997 5	0,997 6	0,997 7	0,997 7	0,997 8	0,997 9	0,997 9	0,998 0	0,998 1
2.9	0,998 1	0,998 2	0,998 2	0,998 3	0,998 4	0,998 4	0,998 5	0,998 5	0,998 6	0,998 6
3.0	0,998 7	0,998 7	0,998 7	0,998 8	0,998 8	0,998 9	0,998 9	0,998 9	0,999 0	0,999 0
3.1	0,999 0	0,999 1	0,999 1	0,999 1	0,999 2	0,999 2	0,999 2	0,999 2	0,999 3	0,999 3
3.2	0,999 3	0,999 3	0,999 4	0,999 4	0,999 4	0,999 4	0,999 4	0,999 5	0,999 5	0,999 5
3.3	0,999 5	0,999 5	0,999 5	0,999 6	0,999 6	0,999 6	0,999 6	0,999 6	0,999 6	0,999 7
3.4	0,999 7	0,999 7	0,999 7	0,999 7	0,999 7	0,999 7	0,999 7	0,999 7	0,999 7	0,999 8
3.5	0,999 8	0,999 8	0,999 8	0,999 8	0,999 8	0,999 8	0,999 8	0,999 8	0,999 8	0,999 8
3.6	0,999 8	0,999 8	0,999 9	0,999 9	0,999 9	0,999 9	0,999 9	0,999 9	0,999 9	0,999 9

$\Lambda_1$  and  $\Lambda_2$  can be expressed by the following equations

$$\Lambda_1 = \left[ \frac{a}{h-a} \right]^z \int_{a/h}^1 \left[ \frac{1}{\eta} - 1 \right]^z d\eta \tag{3.112}$$

$$\Lambda_2 = \left[ \frac{a}{h-a} \right]^z \int_{a/h}^1 \ln \eta \left[ \frac{1}{\eta} - 1 \right]^z d\eta$$

where h is the water depth, a is the reference level at which the sediment concentration is taken (a= 0.05h), and z is an exponent determining the shape of the concentration profile,

$$z = \omega_0 / (1,2\kappa u_f') \tag{3.113}$$

in which  $\omega_0$  is the fall velocity,  $\kappa$  is the von-Karman constant (=0.4) and  $u_f'$  the friction velocity.

### 3.12 Ashida, Takahashi and Mizuyama model (ATM)

The Ashida, Takahashi and Mizuyama model is a bed load model. This model relates the bed load transport to effects of channel slope, the bottom shear stress and the critical shear stress for erosion. The model can be applied for uniform sediments as well as for the graded sediment transport model (GST)

of MIKE 11. Automatic updating of bed resistance according to the formulation by Engelund-Hansen (section 3.8.2) is optional.

The bed load transport equation (for uniform sediment) reads:

$$q_b = \sqrt{(s-1)gd^3} \cdot \frac{12-24\sqrt{l}}{\cos\theta} \cdot \tau_*^{(1,5-\sqrt{l})} \cdot \left(1 - \alpha^2 \frac{\tau_{*c}}{\tau_*}\right) \left(1 - \alpha \sqrt{\frac{\tau_{*c}}{\tau_*}}\right) \quad (3.114)$$

where:

$s$  is the relative density of sand,  $g$  is acceleration of gravity and  $d$  the sediment diameter (uniform sized or graded;  $d_i$ )

$l$  is the bed slope of channel ( $l = \tan(\theta) \Rightarrow \theta = \tan^{-1}(l)$ )

$\tau_*$  is the dimensionless shear stress

$\tau_{*c}$  is the dimensionless critical tractive force (shear stress)

$\alpha$  is a function of  $\tan(\theta)=l$  as defined in Table 3.2 below.

The dimensionless shear stress,  $\tau_*$ , is originally defined in the ATM-model as;

$$\tau_* = \frac{U_*^2}{(s-1) \cdot g \cdot d} \quad (3.115)$$

where:

$U_*$  is the friction velocity defined as;

$$U_* = \sqrt{g \cdot l_e \cdot R} \quad (3.116)$$

with  $l_e$  being the energy line gradient and  $R$  is the hydraulic radius

However, experiments with the above formulation revealed that the use of the energy line gradient in the expression of a governing variable in a fully dynamic model including morphological updates introduces a high risk of instabilities due to the potential locally very dynamic and varying variation of the energy line gradient. An alternative formulation for the calculation of the dimensionless shear stress based on bed resistance has therefore been implemented and replaces the original AMT-formulation.

The alternative formulation for the dimensionless shear stress,  $\tau_*$ , reads:

$$\tau_* = \frac{\bar{u}^2}{C^2 \cdot (s-1) \cdot d} \Leftrightarrow \tau_* = \frac{n^2 \cdot \bar{u}^2}{R^{1/3} \cdot (s-1) \cdot d} \quad (3.117)$$



where:

$\bar{u}$  is the average stream velocity

bed resistance is defined either by Chezy number,  $C$  or Mannings's  $n$

Table 3.2 Relationship between  $\tan(\theta)$  and  $\alpha$

$\tan(\theta) = l$	$\alpha$	$\alpha^2$
0.000	0.922	0.085
0.015	0.906	0.821
0.022	0.899	0.807
0.025	0.898	0.806
0.049	0.867	0.751
0.100	0.791	0.626



**NOTE:** if  $\tau^* \leq \tau_{*c}$  then  $q_b = 0$  !

If the ATM-model is applied for graded sediments, eq. (3.114) are adjusted to take into account the different sediment fractions. That is;  $d$  is replaced by  $d_i$ ,  $\tau^*$  is replaced by  $\tau_{*i}$  and  $\tau_{*c}$  is replaced by  $\tau_{*ci}$  (suffix 'i' being the different sediment fractions).

### Options for determination of dimensionless critical tractive force, $\tau_{*c}$

The dimensionless critical tractive force,  $\tau_{*c}$  is determined from  $\tau_{*cm}$ , the dimensionless critical tractive force (shear stress) corresponding to the average grain size  $d_m$ .

In case of graded sediments,  $\tau_{*ci}$  is determined from the Modified Egiazaroff Model (section 3.9.3) as a function of  $\tau_{*cm}$ .

For uniform sediments,  $\tau_{*c}$  is equal to,  $\tau_{*cm}$ .

Two options for  $\tau_{*cm}$  is available:

#### **Option 1: User-defined $\tau_{*cm}$ (constant for any average grain size $d_m$ )**

For this option,  $\tau_{*cm}$  is a constant value defined by the user in the MIKE 11 ST parameter file as the variable; 'Theta Critical' in the 'Transport Model' page of the sediment transport editor.

#### **Option 2: , $\tau_{*cm}$ calculated by Iwagaki's model**

For this option,  $\tau_{*cm}$  is calculated from Iwagaki's model (see section 3.9.2) as a function of the average grain size diameter.



## Options for the effect of channel slope

Eq. (3.114) includes the effect of channel slope  $l$  on the bed load. but ATM-model with  $l=0$  is also applied for steep rivers in many practical applications and therefore, different options are available for the channel slope:

Option 1 :  $l=0$ :

In this case eq.(3.114) with  $l=0$  and  $\alpha =0.922$  is used:

$$q_b = \sqrt{(s-1)gd^3} \cdot \frac{12}{\cos\theta} \cdot \tau_{*j}^{1.5} \cdot \left(1 - 0,85 \frac{\tau_{*ci}}{\tau_{*j}}\right) \left(1 - 0,922 \sqrt{\frac{\tau_{*ci}}{\tau_{*j}}}\right) \quad (3.118)$$

Option 2:  $l=Energy\ Grade$

In this case, eq. (3.114) is used with  $l$  as the local energy grade at each cross section.

Option 3:  $l = Channel\ bed\ slope$

In this case, eq. (3.114) is used with  $l$  as the local bed slope at each cross section.

## 3.13 Engelund & Fredsøe model

The sediment transport model presented by Engelund & Fredsøe (1976) /28/ gives a more detailed description of sediment transport and its relation to the flow resistance.

The total sediment transport is split up into bed load and suspended load and the sediment transport is calculated from the skin friction, i.e. the shear stress which is acting on the surface of the dunes, see section 3.8.2 Flow Resistance -  $\theta-\theta'$  Relationship (p. 237). It is, at present, doubtful whether the models which split the sediment load into bed load and suspended load are more reliable in determining the total transport than the transport formulae which consider the sediment transport as a whole.

It is, however, necessary to distinguish between suspended load and bed load, and to be able to estimate the variation of the sediment transport along the dunes if the river model is to be used to calculate the dimensions of the dunes. Separate computation of suspended load and bed load is also advantageous when calibrating models against measured suspended sediment transport rates. It seems reasonable to expect that future development will be concerned with this kind of model.



### 3.13.1 Bed Load

The velocity of the particles moving as bed load has been found to be:

$$u_{bs} = 10u_f' \left(1 - 0,7 \sqrt{\frac{\theta_c}{\theta}}\right) \quad (3.119)$$

where,

$u_{bs}$  is the velocity of bed load particles

$u_f'$  is the friction velocity

$\theta$  is a dimensionless bed shear stress

$\theta_c$  is the critical dimensionless bed shear stress (or Shields' parameter)

The number of moving surface particles per unit area which move is  $p/d$  where,  $d$  is the mean grain size of the bed material and  $p$  is the probability for the particles to move:

$$p = \left[ 1 + \left( \frac{\frac{\pi}{6}\beta}{\theta' - \theta_c} \right)^4 \right]^{-1/4} \quad (3.120)$$

$\theta'$  is the dimensionless skin friction, see section 3.8.2 Flow Resistance -  $\theta - \theta'$  Relationship (*p. 237*), and  $\beta$  is the dynamic friction coefficient, and is close to 1.  $p$  has been determined so that for moderate  $\theta$  values all of the bed shear stress,  $\tau$ , exceeding the critical value,  $\tau_c$ , is transferred to the bed through drag forces on the moving bed load particles. For high  $\theta$  values the limiting value for  $p$  is 1. By combining Equations (3.1) and (3.119) Engelund & Fredsøe found the following bed load function:

$$\Phi_b = 5 \left[ 1 + \left( \frac{\frac{\pi}{6}\beta}{\theta' - \theta_c} \right)^4 \right] (\sqrt{\theta'} - 0,7\sqrt{\theta_c}) \quad \text{and} \quad \Phi_b = \frac{q_b}{\sqrt{(s-1)gd^3}} \quad (3.121)$$



### 3.13.2 Suspended load

The suspended load  $q_s$  is found as the integral of the current velocity  $u$  and the concentration of suspended sediment  $c$ :

$$q_s = \int_a^D c u dy \quad (3.122)$$

In this equation  $a$  is the thickness of the bed layer which can be approximated by  $2d$  where,  $d$  is the grain diameter and  $D$  is the flow depth. The current velocity  $u$  at a distance  $y$  above bed level, is described by the logarithmic velocity profile:

$$u = 2,5 u_f' \ln \left( \frac{30y}{k} \right) \quad (3.123)$$

where,

$u_f'$  is the friction velocity and the equivalent sand roughness,  $k$ , is equal to  $2.5 d$ .

The concentration is calculated in accordance with the concentration profile derived by Rouse (1937):

$$c = c_a \left( \frac{D-y}{y} \frac{a}{D-a} \right)^z \quad (3.124)$$

where,

$c$  is concentration of suspended sediment (at  $y$  above bed)

$c_a$  is the concentration at the bed

$D$  is depth of water

$y$  is distance from bed level



$z$  is the Rouse number:  $z = w/(0.4u_f')$ .  $w$  is the settling velocity of the suspended material given by one of the following expressions depending on the grain size:

$$w = \begin{cases} \frac{1}{18} \frac{(s-1)gd^2}{v} & \text{for } d < 0,1 \text{ mm} \\ \frac{10v}{d} \left\{ \left[ 1 + \frac{0,01(s-1)gd^3}{v^2} \right]^{0,5} - 1 \right\} & \text{for } 0,1 \text{ mm} \leq d \leq 1,0 \text{ mm} \\ 1,1[(s-1)gd]^{0,5} & \text{for } 1,0 \text{ mm} < d \end{cases} \quad (3.125)$$

Only grains with a settling velocity smaller than  $0.8 u_f'$  can be carried in suspension and only these grains are considered in the calculation of the effective fall velocity. The grain-size distribution is assumed to have a logarithmic-normal distribution. The grain sizes not carried in suspension are subtracted from this distribution and the mean grain size of the remaining sediment is used in Equation (3.125).

The concentration  $c_a$  at  $y = 2d$  is, according to Engelund & Fredsøe, determined through dynamic considerations: for increasing values of  $\theta$  (the non-dimensional bed shear stress), the bed shear stress exceeding  $\theta_c$  cannot be transferred by the drag on the bed load particles alone. A part of the bed shear stress is transferred as a dispersive stress, i.e. through collisions between suspended particles close to the bed. The dispersive stress is described by the expressions developed by Bagnold (1954), /21/.

The total, non-dimensional bed shear stress corrected for the effect of dunes,  $\theta'$ , thus is made up of three terms; the critical shear stress, the drag on bed load particles and the dispersive stress from the suspended load:

$$\theta' = \theta_c + \frac{\pi}{6} \beta \rho + 0,027 s \theta' \lambda^2 \quad (3.126)$$

where,  $\rho$  is the probability of particles to move.

The linear concentration  $\lambda$  is related to  $c_a$  by:

$$c_a = \frac{0,65}{\left(1 + \frac{1}{\lambda}\right)^3} \quad (3.127)$$

With known reference concentration,  $c_a$ , and settling velocity,  $w$ , the integral Equation (3.122) can be evaluated with, for instance, the use of the diagrams presented by Einstein (1950), /25/. The integral cannot be expressed in



closed form and, during numerical simulations, it must be integrated numerically or, as in MIKE 11, an approximation must be applied.

### 3.14 Engelund & Hansen model

Engelund and Hansen (1967) /30/ presented a sediment transport formula derived from considerations of the work done by the flow on the sediment being transported. Although the formula was derived for a dune covered bed, it was found also to be applicable to the upper regime (plane bed and anti-dunes).

The Engelund & Hansen transport equation reads:

$$\Phi = 0,1 \frac{\theta^{5/2}}{f} \quad (3.128)$$

where,  $\theta$  is the dimensionless total bed shear stress (see also section 3.8.2 Flow Resistance -  $\theta$ - $\theta'$  Relationship ( $\rho$ . 237)) and  $\Phi$  is the dimensionless sediment transport rate:

$$\Phi = \frac{q_t}{\sqrt{(s-1)gd^3}} \quad (3.129)$$

$q_t$  is the total bed material transport per unit width and  $f$  is the friction factor, defined as:

$$f = 2 \frac{u_f^2}{u^2} \quad (3.130)$$

where,  $u_f$  and  $u$  are the friction and current velocities, respectively.

The friction factor may be determined through the calculations outlined in Flow Resistance sections 3.8.1 through 3.8.3.

### 3.15 Lane & Kalinske model

The Lane & Kalinske model implemented in MIKE 11 computes the suspended load based on the work by Lane & Kalinske /34/. Uniform as well as graded sediments can be modelled. The suspended sediment transport formula reads

$$q_s = q \cdot C_o \cdot \frac{P_s}{s \cdot 10^6} \quad (3.131)$$





where  $q$  is the flow rate per unit width of the river.  $C_0$  is determined by

$$C_0 = 5,55 \cdot \left[ \frac{1}{2} \cdot \frac{u_f'}{\omega_0} \exp \left\{ - \left( \frac{\omega_0}{u_f'} \right)^2 \right\} \right]^{1,61} \quad (3.132)$$

where  $u_f'$  is the friction velocity in, and  $\omega_0$  is the fall velocity which is determined by Rubey's equation

$$\omega_0 = \sqrt{(s-1)gd} \cdot \left( \sqrt{\frac{2}{3} + \frac{36\nu^2}{sgd^3}} - \sqrt{\frac{36\nu^2}{sgd^3}} \right) \quad (3.133)$$

in which  $\nu$  is the kinematic viscosity of water.

$P_s$  from equation (3.131) is determined by integration of the following equation

$$P_* = \int_{0,05}^1 \left\{ 1 + \frac{1}{\kappa\phi} (1 + 1n\eta) \right\} \exp \left( - \frac{15\omega_0}{u_f'} \eta \right) d\eta \quad (3.134)$$

where  $\phi = \frac{V}{u_f'}$  with  $V$  being the average cross sectional velocity and

$\kappa$  is the von-Karman constant (=0.4). In equation (3.134)  $d\eta$  is determined by

$$d\eta = (1-0.05)/\text{NUMBER\_OF\_ITERATIONS}$$

where the denominator is an integer value defined in the MIKE11.ini file under the sediment transport section where the following must be written:

[ST\_SIMULATION]

NUMBER\_OF\_ITERATIONS = 100

By default 100 iterations are used, but any integer value can be set by the user.

In case graded sediments are modelled, the suspended load is calculated for each fraction using the fraction grain diameter in the equations used. The total suspended load is the sum of the suspended loads from all fractions.



### 3.16 Meyer-Peter & Müller model

The Meyer-Peter & Müller model describes the bed load transport by relating the transport rate to the dimensionless shear stress acting on the grains. The dimensionless transport formula reads

$$\Phi_b = 8(\theta' - 0,047)^{1,5} \quad (3.135)$$

where

$\Phi_b$  is the dimensionless bed load transport

$\theta'$  is the dimensionless shear stress related to grains (skin friction)

The value of  $\theta'$  must exceed a critical parameter  $\theta_c$  before bed load transportation takes place. The absolute bed load transport per unit width of the river is obtained by

$$q_b = \Phi_b \sqrt{(s-1)gd^3}$$

where

$s$  is the relative density of sand (=2.65)

$g$  is the acceleration due to gravity

$d$  is the diameter of the grain

In MIKE 11 the transport computation is based on the dimensionless effective shear stress instead of the dimensionless skin friction. In this case the transport equation becomes

$$\mathbb{D}_b = 8(\theta_{eff} - 0,047)^{1,5} \quad (3.136)$$

where the dimensionless effective shear stress  $\theta_{eff}$  is defined by

$$\theta_{eff} = \frac{u_{eff}^2}{(s-1)gd} \quad (3.137)$$

with

$$u_{eff} = u'_f \cdot \left(\frac{n_b}{n}\right)^{0,75} \quad (3.138)$$

where

$u'_f$  is the bed friction velocity



$n$  is the resistance number

$n_b$  is defined by  $n_b = 0,0192 \cdot (d_{90})^{\frac{1}{6}}$  where  $d_{90}$  is the diameter of which 90% are finer.

The Meyer-Peter & Müller formula can only be applied for uniform sediments. The critical shear stress is computed by the principles of Iwagaki, see section 3.9.2, instead of the traditional Shield's criteria.

### 3.17 Sato, Kikkawa & Ashida model

The Sato, Kikkawa and Ashida model is a pure bed load model. The model relates the bed load transport to the bed friction velocity, the bed resistance, the bottom shear stress and the critical shear stress for erosion. The model can be applied for uniform sediments as well as for the graded sediment transport model (GST) of MIKE 11. Automatic updating of the bed resistance according to the formulation by Engelund (see page 3.8.2) is optional.

The bed load transport equation reads:

$$q_b = \frac{u'_f{}^3}{(s-1)g} \cdot \varphi(n) \cdot F\left(\frac{\tau_0}{\tau_c}\right) \quad (3.139)$$

where  $u'_f$  is the bed friction velocity,  $s$  is the relative density of sand and  $g$  the acceleration due to gravity.

The function  $\varphi(n)$  is obtained from

$$\varphi(n) = \begin{cases} 0,623, & n \geq 0,025 \\ 0,623 \cdot (40n)^{-3,5}, & n < 0,025 \end{cases} \quad (3.140)$$

where  $n$  is the Manning's roughness coefficient.

The last term in equation (3.139) represents a transition from no erosion to full bed load as a function of the relation between bed shear stress  $\tau_0$  ( $= u'_f{}^2 \cdot \rho$ ) and the critical shear stress  $\tau_c$  ( $= \theta_c \cdot (s-1)\rho g d$ ). The latter is obtained from the principles of Iwagaki (section 3.9.2) in the case of uniform sediments. If graded sediments are modelled, then the result from Iwagaki's model is further modified by the Egiazaroff equation (section 3.9.3). If graded sediments are modelled then the bed load of each sediment fraction is computed from equation (3.139), and the total bed load will be the sum of the fractional bed load transports.



## 3.18 Smart and Jaeggi model

Smart and Jaeggi (1983), /40/ presented a sediment transport formula which calculates the transport of coarse sediments in steep channels/ivers. The transport formulae is based on the original Meyer-Peter Müller equation, which was derived from laboratory experiments with non-uniform sediments of various densities and flume-slopes ranging from 0.04% to 2%.

The original Meyer-Peter Müller equation reads:

$$\phi = 8 \left[ \left( \frac{K_s}{K_r} \right)^{1,5} \theta - 0,047 \right]^{1,5} \quad (3.141)$$

where,

$\phi$  dimensionless sediment transport

$\theta$  dimensionless shear stress

$\frac{K_s}{K_r}$  corr.factor for bed form roughness

### 3.18.1 Revised transport formula

Through comparison of new laboratory experiments and the original Equation (3.141) it was found that the computed transport is seriously underestimated with slopes steeper than 3%. Smart and Jaeggi therefore proposed a new transport formulation based on Equation (3.141).

At higher slopes, grains in the bed have a slope induced height advantage of those grains immediately downstream of them and the critical shear stress is less than it would be for a flat bed. Shields parameter is therefore adjusted as a function of the slope to horizontal, Eq.(3.142):

$$\theta_c = \theta_{0cr} \cos \alpha \left( 1 - \frac{\tan \alpha}{\tan \beta} \right) \quad (3.142)$$

where,

$\theta_{0cr}$  Shields parameter

$\alpha$  Slope to horizontal of water surface or bottom level

$\beta$  Angle of repose of submerged bed material (33°)



Including non-uniformity of the sediment as well as the slope induced effect of the transport the revised equation - still based on laboratory experiments - reads:

$$\phi = 4 \left[ \left( \frac{d_{90}}{d_{30}} \right)^{0.2} I^{0.6} C \theta^{0.5} (\theta - \theta_{cr}) \right] \quad (3.143)$$

where,

$d_{90}$  90%-fractile of the sediment

$d_{30}$  30%-fractile of the sediment

$I$  Slope (water surface or bottom level)

$C$  Chezy resistance factor

Equation (3.143) is only recommended in the following ranges:

diameter > 0.4 mm

$(d_{90}/d_{30}) < 8.5$

$0.04\% < I < 20\%$

Concerning the available option of updating the bed resistance during a sediment transport simulation it is very important to notice, that there is NO formulation of updating the bed resistance built-in for the Smart and Jaeggi transport model.

However, to maintain the possibility of updating the bed resistance the formulation of the Engelund-Hansen model has been adopted. It is very important to note, that this formulation does not cover the wide range of grain diameter etc. as the Smart-Jaeggi formula does.

For that reason it would be advisable not to select the update bed resistance option for a Smart-Jaeggi sediment transport simulation. If used anyway the results should be analysed very carefully to check whether they are reliable or not.

### 3.18.2 MIKE 11 version

As an attempt to expand the possibilities for calibration of the sediment transport formula, Equation (3.143) has been implemented in MIKE 11 in such a way, that it is possible for the user to edit the coefficients and exponents in the transport equation.



The 'MIKE 11-equation' reads:

$$\phi = \text{co1} \left[ \left( \frac{d_{90}}{d_{50}} \right)^{\text{exp1}} I^{\text{exp2}} c^{\text{exp3}} \theta^{\text{exp4}} (\text{co2} \theta^{\text{exp4}} - \theta_{cr})^{\text{exp6}} \right] \quad (3.144)$$

### 3.19 van Rijn model

In the van Rijn transport models (/35/ and /37/) the sediment load is divided into bed load and suspended load according to the relative magnitudes of the bed shear velocity and the particle fall velocity. When the bed shear velocity exceeds the fall velocity then sediment is transported as both suspended and bed load. Bed load is considered to be transported by rolling and saltation and the rate is described as a function of saltation height. The suspended load is determined from the depth-integration of the product of the local concentration and flow velocity. The reference concentration is determined from the bed load transport.

#### 3.19.1 Bed load

In this model the bed load transport rate is computed from the product of particle velocity,  $u_{bs}$ , saltation height,  $\delta b$ , and the bed load concentration,  $c_b$ :

$$q_b = u_{bs} \delta b c_b \quad (3.145)$$

Expressions for the particle velocity and saltation height were obtained by numerically solving the equations of motion applied to a solitary particle. These expressions are given in terms of two dimensionless parameters which are considered to adequately describe bed load transport; a dimensionless particle diameter,  $D_*$ , and a transport stage parameter,  $T$  as defined below:

$$D_* = d_{50} \left[ \frac{s-1}{\nu^2} g \right]^{1/3} \quad (3.146)$$

This is similar to Acker's and White's  $D_{gr}$ , Equation (3.102) under Ackers and White model (p. 243).

$$T = \frac{(u'_g)^2 - (u'_{f,cr})^2}{(u'_{f,cr})^2} \quad (3.147)$$



$u'_g$  is the bed shear velocity, related to grains, and  $u'_{f,cr}$  is Shields critical bed shear velocity.  $u'_g$  is defined so that the influence of bed forms is eliminated since form drag does not contribute to bed load transport.  $u_g$  is given by:

$$u'_g = \frac{\sqrt{g}}{C'} u \quad (3.148)$$

where,

$u$  is the mean flow velocity

$C'$  is Chezy's coefficient related to skin friction

$C'$  is expressed as:

$$C' = 18 \log \left( \frac{R}{3d_{90}} \right) \quad (3.149)$$

where,

$R$  is the hydraulic radius (or resistance radius) related to the bed

$3d_{90}$  is considered to be the effective roughness height of the plane bed

The following expressions were determined for particle velocity and saltation height by applying the equations of motion to a solitary particle:

$$\frac{u_{bs}}{u'_f} = 9 + 2,6 \log(D_*) - 8 \left[ \frac{\theta_c}{\theta} \right]^{0,5} \quad (3.150)$$

This expression was determined by expressing the computed particle velocity as a function of flow conditions and sediment size ( $D_*$ ). A particle mobility,  $u_{bs}$ , was then defined as:

$$\frac{u_{bs}}{[(s-1)gd]^{0,5}} = 1,5 T^{0,6} \quad (3.151)$$

An expression for the saltation height,  $\delta b$ , is given by:

$$\frac{\delta b}{d} = 0,3 D_*^{0,7} T^{0,5} \quad (3.152)$$



An expression for the bed load concentration,  $c_b$ , is obtained from a rearrangement of Equation (3.145):

$$c_b = \frac{q_b}{u_{bs}} \delta b \quad (3.153)$$

Extensive analysis of flume measurements of bed load transport yielded the following expression for the bed load concentration:

$$\frac{c_b}{c_o} = 0,18 \frac{T}{D_*} \quad (3.154)$$

where,

$c_o$  is the maximum bed concentration (= 0.65).

Combining Equations (3.151), (3.152) and (3.154) gives the following expression for bed load transport:

$$\frac{q_b}{\sqrt{(s-1)gd_{50}^3}} = \frac{0,053 T^{2,1}}{D_*^{0,3}} \quad (3.155)$$

or from Equation (3.121):

$$\Phi_b = \frac{0,053 T^{2,1}}{D_*^{0,3}} \quad (3.156)$$

This relationship is valid for particles in the range 0.2 to 2.0 mm.

### 3.19.2 Suspended load

This method is based on the computation of a reference concentration determined from the bed load transport. Thus the reference concentration  $c_a$  is described as a function of the dimensionless particle diameter  $D_*$  and transport stage parameter  $T$ , (see Bed Load):

$$D_* = d_{50} \left[ \frac{(s-1)g}{v^2} \right]^{1/3} \quad (3.157)$$

$$T = \frac{(u'_g)^2 - (u'_{f,cr})^2}{(u'_{f,cr})^2} \quad (3.158)$$





where,

$u'_g$  is the bed shear velocity related to the grains

$u'_{f,cr}$  is the critical bed shear velocity

The reference concentration is defined for a reference level 'a' below which all sediment is considered to be transported as bed load. The reference level is approximated by:

$$a = 0,5H \quad (3.159)$$

where,

$H$  is the (known) bed form height

$$a = k \quad (3.160)$$

where,

$k$  is the equivalent sand roughness when the bed form dimensions are unknown or a minimum value of

$$a = 0,01D \quad (3.161)$$

where,

$D$  is water depth

The reference concentration is defined from:

$$q_b = c_b u_{bs} \delta_b = c_a u_a a \quad (3.162)$$

where,

$c_b$  is the bed concentration,

$u_{bs}$  is the velocity of bed load particles

$\delta b$  is the saltation height. Expressions for these parameters are given in Engelund & Fredsøe model, section 3.13.

$u_a$  is the effective particle velocity at reference level a. It is expressed as:

$$u_a = \alpha u_{bs}$$



From an examination of flume and field data a value for  $a$  of 2.3 was determined. Combining this value with the expressions for  $\delta b$  and  $c_b$  (as functions of  $D_*$  and  $T$ ) the following expression is obtained:

$$c_a = 0,015 \frac{d_{50} T^{1,5}}{a D_*^{0,3}} \quad (3.163)$$

The representative particle size of suspended load is generally finer than that of bed load. Van Rijn relates this particle size,  $d_s$  to the  $d_{50}$  and geometric standard deviation,  $\sigma_s$ , of the bed material:

$$\frac{d_s}{d_{50}} = 1 + 0,011(\sigma_s - 1)(T - 25) \text{ for } T < 25 \quad (3.164)$$

in which  $\sigma_s$  is given by:

$$\sigma_s = 0,5 \left( \frac{d_{84}}{d_{50}} + \frac{d_{50}}{d_{16}} \right) \quad (3.165)$$

This  $d_s$  value is then used to calculate fall velocity according to Equation (3.125). The threshold for the initiation of suspension can be determined from the actual flow conditions. Using the overall bed shear stress  $u_f$  the criterion implemented in the van Rijn model becomes:

$$\frac{u_f}{w} = \frac{u}{d_s}, \text{ for } 1 < d_s \leq 10 \quad (3.166)$$

and

$$\frac{u_f}{w} = 0,4, \text{ for } 10 < d_s \quad (3.167)$$

In describing the suspended load transport, van Rijn defines a suspension parameter  $Z$  which expresses the influence of the upward turbulent fluid forces and the downward gravitational forces.  $Z$  is defined as:

$$Z = \frac{w}{\beta \kappa u_f'} \quad (3.168)$$

where,

$u_f'$  is the over all bed shear velocity

$\kappa$  is von Karman's constant



$\beta$  is a coefficient related to the diffusion of sediment particles

An expression for  $\beta$  was derived as:

$$\beta = 1 + 2 \left[ \frac{W}{u_f'} \right]^2 \text{ for } 0,1 < \frac{W}{u_f'} < 1 \quad (3.169)$$

Many factors affect the suspension parameter  $Z$ , e.g. volume occupied by particles, reduction of fall velocity and damping of turbulence. These effects are grouped into a single correction factor  $\psi$ , which is used to define a modified suspension number  $Z'$  as shown:

$$Z' = Z + \psi \quad (3.170)$$

$\psi$  was found to be a function of the main hydraulic parameters:

$$\psi = 2,5 \left[ \frac{W}{u_f'} \right]^{0,8} \left[ \frac{c_a}{c_o} \right]^{0,4} \quad (3.171)$$

where,

$c_o$  is the maximum bed concentration (found to be 0.65)

The suspended load transport is expressed by Equation (3.122). By combining the expression describing the velocity and concentration profiles (Equations (3.123) and (3.124)) with the expressions for  $Z$  and  $\psi$  (Equations (3.170) and (3.171)) van Rijn derived the following expression:

$$q_s = FuDc_a \quad (3.172)$$

in which  $F$  is given by:

$$F = \frac{\left[ \frac{a}{D} \right]^{Z'} - \left[ \frac{a}{D} \right]^{1,2}}{\left[ 1 - \frac{a}{D} \right]^{Z'} [1,2 - Z']} \quad (3.173)$$

## 3.20 Nomenclature

reference level in calculation of suspended load

athickness of bed layer

Acritical flow mobility number in Ackers and White model



$A_i$ critical flow mobility number in Ackers and White model for class  $i$

$c$ concentration of suspended sediment

$c_d$ celerity of dune

$c_a$ reference sediment concentration

$c_b$ concentration of suspended sediment at the bed

$c_o$ maximum bed concentration

$c$ model parameter in Ackers and White model

$d$ grain size

$d_i$ representative grain size in class  $i$

$D$ total flow depth

$d_{med}$ representative grain size of total population

$D_g$ dimensionless grain diameter, Ackers and White model

$D'$ boundary layer thickness

$D^*$ dimensionless grain diameter, van Rijn Model

$d_s$ particle size of suspended sediment

$d_{XX}$ particle size than which  $XX\%$  is finer

$f$ function

$F$ Froude number

$F_{cg}$ mobility parameter for coarse material

$F_{fg}$ mobility parameter for fine material

$F_g$ general mobility parameter

$g$ acceleration due to gravity

$G_g$ general transport parameter

$h$ water elevation

$H$ total dune height

$k$ wave number of bed forms

$k$ equivalent sand roughness



$L$  dune length

$L_e$  equilibrium dune length

$l_o$  dune length, bed load only

$m$  model parameter in Ackers and White model

$n$  model parameter in Ackers and White model

$N$  number of classes in a graded sediment

$p$  probability for particles to move

$p_i$  percentage contribution in class  $i$

$p_{act,bed}$  percentage contributions of class  $i$  in active and parent layers, respectively

$q$  flow discharge per unit width

$q_b$  bed load transport rate

$q_{bt}$  transport rate at top of dune

$q_s$  suspended load transport rate

$q_t$  total load transport rate

$q_i$  total load transport rate in class  $i$

$s$  specific gravity of sediment

$qt_j^n$  sediment transport rate per unit of width at grid point  $j$  and time interval  $n$

$qt_{j,i}^n$  sediment transport rate per unit of width at grid point  $j$  and time interval  $n$  in class  $i$

$Qt_{j,i}^n$  sediment transport rate at grid point  $j$  and time interval  $n$   
(=  $Wqt_j^n$ )

$t$  parameter dependent on  $u$ ,  $h$ ,  $d$  (see Equation (3.95) in section 3.8.3 Flow Resistance - White et al. (p. 239).)

$T$  transport stage parameter, van Rijn model

$T_1$  average lifetime of a dune

$u$  mean flow velocity

$u_a$  velocity of bed load particles at reference level  $a$



$u_b$ near bed velocity

$u_{bs}$ velocity of bed load particles

$u_f, u_f'$ bed shear velocity or friction velocity

$U_{fcr}$ critical bed shear velocity

$u_g'$ bed shear velocity related to the grains

$w$ fall velocity

$W$ width (defined as  $A/R$  in code)

$X$ sediment transport, mass flux per unit mass flow rate

$y$ distance above bed level

$z$ local height of dune

$zR$ Rouse number

$Z$ bottom level above datum

$Zs$ suspension parameter

$Z'$ modified suspension number

$\Delta z$ change in bottom level

$Z_a$ depth of active layer

$\alpha$ velocity distribution coefficient

$\kappa$ von Karman's constant

$\beta$ dynamic friction coefficient

$\beta$ coefficient related to diffusion of sediment particles

$\delta$ spatial lag

$\varepsilon$ porosity of sediment

$\varepsilon$ eddy viscosity

$\lambda$ linear concentration related to  $c_a$

$C$ space centring coefficient

$\delta b$ saltation height

$\rho$ fluid density



$\theta$  dimensionless bed shear stress  
 $\theta$  time centring coefficient  
 $\theta_c$  critical dimensionless bed shear stress  
 $\theta_{ci}$  critical dimensionless bed shear stress for class  $i$   
 $\theta'$  dimensionless skin friction  
 $\theta_t$  dimensionless bed shear stress at dune top  
 $\tau$  bed shear stress  
 $\tau_c'$  critical bed shear stress  
 $\tau'$  skin friction  
 $\tau$  form drag  
 $\Phi$  dimensionless sediment transport rate  
 $\Phi_b$  dimensionless bed load sediment transport rate  
 $\Phi_s$  dimensionless suspended sediment load transport rate  
 $\Phi_t$  dimensionless total sediment transport rate  
 $\nu$  kinematic viscosity  
 $\psi$  correction factor

### 3.21 References

- /20/ Ackers, P. and White, W.R. (1973). "Sediment transport: new approach and analysis", Proc. ASCE, JHD, 99, HY11, pp. 2041-2060.
- /21/ Bagnold, R.A., 1954. "Experiments on gravity-free dispersion of large solid spheres in a Newtonian fluid under shear". Proc. R. Soc. London (A) 353.
- /22/ Challet, J.P. and Cunge, J.A., Simulation of unsteady flow in alluvial streams, Int. Symp. on river sedimentation March 24-29 1980, Chin. Soc. of Hydr. Eng., Beijing, China 1980.
- /23/ Deigaard, R. 1980. "Longitudinal and transverse sorting of grain sizes in alluvial rivers". Series Paper 26, Institute of Hydrodyn. & Hydr. Engrg., Technical University of Denmark.
- /24/ Egiazaroff, P.I., Calculation of non-uniform sediment concentration,



- Proc. ASCE HY 4, July 1965.
- /25/ Einstein, H.A., 1950. "The bed load function for sediment transportation in open channel flows". U.S. Dept. of Agriculture, Tech. Bulletin No. 1026.
- /26/ Engelund, F., 1966. "Hydraulic resistance of alluvial streams". ASCE, Vol. 92, No. Hy 2.
- /27/ Engelund, F., 1970. "Instability of erodible beds". 7. Fluid Mech., Vol. 42, pp. 225-44.
- /28/ Engelund, F. and Fredsøe, J., 1976. "A sediment transport model for straight alluvial channels". Nordic Hydrology, Vol. 7, No. 5.
- /29/ Engelund, F. and Fredsøe, J., 1982. "Hydraulic theory of alluvial rivers", Advances in Hydro Science, Vol. 13, pp. 187-215.
- /30/ Engelund, F. and Hansen, E., 1967. "A monograph on sediment transport in alluvial streams", Teknisk Forlag, Copenhagen.
- /31/ Fredsøe, J., 1979. "Unsteady flow in straight alluvial streams: Modifications of individual dunes". J. Fluid Mech., vol. 91, pp. 497-512.
- /32/ Fredsøe, J., 1979. "Dimensions of stationary dunes. Part 1. Low sediment transport rate". Prog. Rep. 49, Institute of Hydrodyn. & Hydr. Engrg., Technical University of Denmark.
- /33/ Fredsøe, J., 1982. "Shape and Dimensions of stationary dunes in rivers". ASCE, Vol. 108, No. Hy 8.
- /34/ Lane, E.W and Kalinske, A.A, 1941. "Engineering calculations of suspended sediment", Trans.Am.Geophys.Union, vol.22, pp. 603-607.
- /35/ Rijn, L.C. van, 1984a, "Part I: Bed load transport", J.Hyd.Eng., 110, 10 Oct.
- /36/ Ribberink, J.S, 1987, "Mathematical modelling of one-dimensional morphological changes in rivers with non-uniform sediment". Delft University of Technology, Report No. 87-2.
- /37/ Rijn, L.C. van, 1984b, "Part II: Suspended load transport", J. Hyd. Eng, 110, 11 Nov.
- /38/ Rouse, H., 1937. "Modern conceptions of the mechanics of fluid turbulence". Trans. ASCE, Vol. 102, pp. 463-543.
- /39/ Smart G.M., 1984. "Sediment transport formulae for steep chan-





- nels". Journal of Hydraulic Engineering, vol.110, No.3, March 1984.
- /40/ Smart, G.M. and Jaeggi, M.N.R. (1983): "Sediment Transport on Steep Slopes". Mitteilung nr. 64 of the Laboratory for Hydraulics, Hydrology and Glaciology at the Federal Technical University, Zurich.
- /41/ Vries, M. de (1981), Morphological Computations, Lecture Notes, (f10a, Delft University of Techn., Dept. of Civ.Eng., Fluid Mech. Group.
- /42/ White, W.R., Paris, E. and Bettess, R., 1979. "A new generation method for predicting the frictional characteristics of alluvial streams", Report No. IT 187, Hydr. Res. Station, Wallingford.





# RAINFALL-RUNOFF

## Reference





## 4 RR Reference Manual

This manual should be used when undertaking Rainfall-Runoff (RR) modelling applications. It provides a description of aspects which are encountered during the development, calibration and application of Rainfall Runoff models including detailed technical descriptions of the hydrological processes. Four different types of Rainfall-Runoff models are available:

1. **NAM:** A lumped, conceptual rainfall-runoff model, simulating the overland-, inter- flow, and base-flow components as a function of the moisture contents in four storages (see Section 4.1-4.11).
2. **UHM:** The Unit Hydrograph Module includes different loss models (constant, proportional) and the SCS method for estimating storm runoff (see Section 4.12).
3. **SMAP:** A monthly soil moisture accounting model (see section 4.13).
4. **Urban:** Two different model runoff computation concepts are available in the Rainfall Runoff Module for fast urban runoff.: A) Time/area Method and B) Non-linear Reservoir (kinematic wave) Method
5. **FEH:** Flood Estimation Handbook. A method for flood estimation in the UK.
6. **DRiFt (Discharge River Forecast):** A semi-distributed event model based on a geomorphologic approach.
7. **Combined:** The runoff from a number of catchments, constituting parts of a larger catchment, can be combined into a single runoff series. Each of the sub- catchments must be specified separately by name, model type, parameters etc. The combined catchment can be defined only after the sub-catchments have been created. The combined catchment is defined in the group for combined catchments, which is activated when selecting combined catchment. The runoff from the combined catchment is found by simple addition of the simulated flow from the sub-catchments.

Some of the features in the Rainfall Runoff package have been developed in cooperation with CTI Engineering, CO., Ltd., Japan. Amongst these are additional methods for Calculation of Runoff from catchments and Calculation of Mean Precipitation of basins (method of Thiessen polygons and Isohyetal Mapping).

The manual should be used in conjunction with the MIKE 11 User Manual.

### 4.1 NAM - Introduction

The NAM hydrological model simulates the rainfall-runoff processes occurring at the catchment scale. NAM forms part of the rainfall-runoff (RR) module of the MIKE 11 river modelling system. The rainfall-runoff module can either



be applied independently or used to represent one or more contributing catchments that generate lateral inflows to a river network. In this manner it is possible to treat a single catchment or a large river basin containing numerous catchments and a complex network of rivers and channels within the same modelling framework.

NAM is the abbreviation of the Danish "Nedbør-Afstrømnings-Model", meaning precipitation-runoff-model. This model was originally developed by the Department of Hydrodynamics and Water Resources at the Technical University of Denmark (/53/),.

A mathematical hydrological model like NAM is a set of linked mathematical statements describing, in a simplified quantitative form, the behaviour of the land phase of the hydrological cycle. NAM represents various components of the rainfall-runoff process by continuously accounting for the water content in four different and mutually interrelated storages. Each storage represents different physical elements of the catchment. NAM can be used either for continuous hydrological modelling over a range of flows or for simulating single events.

The NAM model can be characterised as a deterministic, lumped, conceptual model with moderate input data requirements. A description of the classification of hydrological models is given in Abbott and Refsgaard (1996), /43/. Refsgaard and Knudsen (1997), /55/ compare a number of different types of hydrological model, including the NAM model, in terms of both data requirements and model performance.

The NAM model is a well-proven engineering tool that has been applied to a number of catchments around the world, representing many different hydrological regimes and climatic conditions.

## 4.2 Data Requirements

The basic input requirements for the NAM model consist of:

- Model parameters
- Initial conditions
- Meteorological data
- Streamflow data for model calibration and validation

The basic meteorological data requirements are:

- Rainfall
- Potential evapotranspiration

In the case of snow modelling the additional meteorological data requirements are:



- Temperature
- Radiation (optional)

The NAM model also allows modelling of man-made interventions in the hydrological cycle in terms of irrigation and groundwater pumping. In this case time series of irrigation and groundwater abstraction rates are required.

In this section the meteorological and hydrological data are described. The model parameters and initial conditions are described in the subsequent sections.

#### 4.2.1 Meteorological data

##### Rainfall (mm)

The time resolution of the rainfall input depends on the objective of the study and on the time scale of the catchment response. In many cases daily rainfall values are sufficient, but in rapidly responding catchments where accurate representation of the peak flows is required, rainfall input on a finer resolution may be required. Rainfall data with any (variable) time increments can be specified in the rainfall input. The NAM model will then make the necessary interpolations according to the simulation time step. The rainfall data are treated as accumulated totals so the rainfall associated with any particular time is the rainfall volume since the last entered value.

##### Potential evapotranspiration (mm)

When daily time steps are used, monthly values of potential evapotranspiration are usually sufficient. In this case only minor improvements can be obtained by specifying daily values instead of monthly values. For small time steps, however, the diurnal variation of the evapotranspiration may be important. The evapotranspiration data are treated as accumulated totals where the evapotranspiration associated with any particular time is the evapotranspiration since the last entered value.

##### Temperature (C°)

Temperature data are required if snow accumulation and melt are included in the simulations. During the snow season, the time increments in the temperature data should reflect the length of the time step in the simulation, e.g. daily mean temperatures. The temperature data at a given time represents the average temperature since the last entered data.

##### Radiation (W/m<sup>2</sup>)

Actual incoming short wave radiation data can optionally be used as input in the extended snow module. The radiation data at a given time represents the average radiation since the last entered data.

##### Mean area weighting

The NAM model simulates the rainfall-runoff process in a lumped fashion so provision is given for combining meteorological data from different stations

within a single catchment or subcatchment into a single time series of weighted averages. The resulting time series will represent the mean area values of rainfall and potential evapotranspiration for a catchment.

The weights are user-defined and can be determined based e.g. on the Thiessen method. In the case of missing values the weighting procedure will redistribute the weights appropriately. Therefore, it is not necessary to specify weight combinations for all possible combinations of missing stations. Alternatively, the user can explicitly specify the weights when data are missing from one or more stations. A weight of “-1” is given to non-reporting stations, indicating missing data.

When rainfall data are available from stations with different reporting frequency, e.g. both daily and hourly stations, then the distribution in time of the average catchment rainfall may be determined using a weighted average of the high-frequency stations. It is possible to use all stations to determine the daily mean rainfall over the catchment and subsequently use the hourly stations to distribute this daily rainfall in time. Different weight combinations for different cases of missing values may be applied also to the calculation of the distribution in time.

## 4.2.2 Hydrological data

### Discharge (m<sup>3</sup>/s)

Observed discharge data at the catchment outlet are required for comparison with the simulated runoff for model calibration and validation. The discharge data at any particular time is the average discharge since the last entered data.

### Irrigation (mm)

If the irrigation module is included in the NAM simulation, an additional rainfall time series is required to provide information on the amount of irrigation water.

### Groundwater abstraction (mm)

When the effect of groundwater abstraction is expected to have a significant effect on the overall groundwater levels or catchment baseflow, pumping rates can be specified to account for these withdrawals. The groundwater abstraction data are treated as accumulated totals where the abstraction associated with any particular time is the abstraction since the last entered value.

## 4.3 Model Structure

A conceptual model like NAM is based on physical structures and equations used together with semi-empirical ones. Being a lumped model, NAM treats each catchment as a single unit. The parameters and variables represent, therefore, average values for the entire catchment. As a result some of the





model parameters can be evaluated from physical catchment data, but the final parameter estimation must be performed by calibration against time series of hydrological observations.

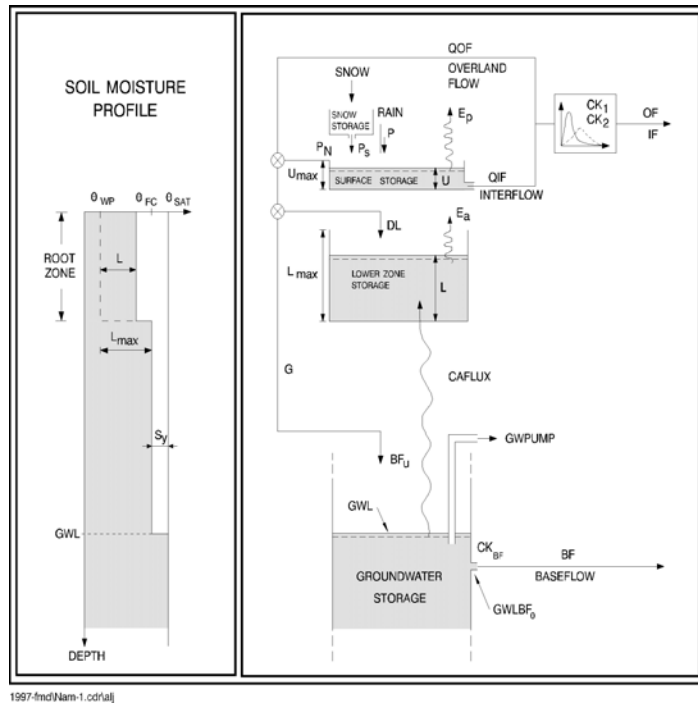


Figure 4.1 Structure of the NAM model.

The model structure is shown in Figure 4.1. It is an imitation of the land phase of the hydrological cycle. NAM simulates the rainfall-runoff process by continuously accounting for the water content in four different and mutually interrelated storages that represent different physical elements of the catchment. These storages are:

- Snow storage
- Surface storage
- Lower or root zone storage
- Groundwater storage

In addition NAM allows treatment of man-made interventions in the hydrological cycle such as irrigation and groundwater pumping.

Based on the meteorological input data NAM produces catchment runoff as well as information about other elements of the land phase of the hydrological cycle, such as the temporal variation of the evapotranspiration, soil moisture



content, groundwater recharge, and groundwater levels. The resulting catchment runoff is split conceptually into overland flow, interflow and baseflow components.

## 4.4 Basic modelling components

### 4.4.1 Surface storage

Moisture intercepted on the vegetation as well as water trapped in depressions and in the uppermost, cultivated part of the ground is represented as surface storage.  $U_{max}$  denotes the upper limit of the amount of water in the surface storage.

The amount of water,  $U$ , in the surface storage is continuously diminished by evaporative consumption as well as by horizontal leakage (interflow). When there is maximum surface storage, some of the excess water,  $P_N$ , will enter the streams as overland flow, whereas the remainder is diverted as infiltration into the lower zone and groundwater storage.

### 4.4.2 Lower zone or root zone storage

The soil moisture in the root zone, a soil layer below the surface from which the vegetation can draw water for transpiration, is represented as lower zone storage.  $L_{max}$  denotes the upper limit of the amount of water in this storage.

Moisture in the lower zone storage is subject to consumptive loss from transpiration. The moisture content controls the amount of water that enters the groundwater storage as recharge and the interflow and overland flow components.

### 4.4.3 Evapotranspiration

Evapotranspiration demands are first met at the potential rate from the surface storage. If the moisture content  $U$  in the surface storage is less than these requirements ( $U < E_p$ ), the remaining fraction is assumed to be withdrawn by root activity from the lower zone storage at an actual rate  $E_a$ .  $E_a$  is proportional to the potential evapotranspiration and varies linearly with the relative soil moisture content,  $L/L_{max}$ , of the lower zone storage

$$E_a = (E_p - U) \frac{L}{L_{max}} \quad (4.1)$$

### 4.4.4 Overland flow

When the surface storage spills, i.e. when  $U > U_{max}$ , the excess water  $P_N$  gives rise to overland flow as well as to infiltration.  $QOF$  denotes the part of



$P_N$  that contributes to overland flow. It is assumed to be proportional to  $P_N$  and to vary linearly with the relative soil moisture content,  $L/L_{max}$ , of the lower zone storage

$$QOF = \begin{cases} CQOF \frac{L/L_{max} - TOF}{1 - TOF} P_N & \text{for } L/L_{max} > TOF \\ 0 & \text{for } L/L_{max} \leq TOF \end{cases} \quad (4.2)$$

where

$CQOF$  is the overland flow runoff coefficient ( $0 \leq CQOF \leq 1$ )

$TOF$  is the threshold value for overland flow ( $0 \leq TOF \leq 1$ ).

The proportion of the excess water  $P_N$  that does not run off as overland flow infiltrates into the lower zone storage. A portion,  $\Delta L$ , of the water available for infiltration,  $(P_N - QOF)$ , is assumed to increase the moisture content  $L$  in the lower zone storage. The remaining amount of infiltrating moisture,  $G$ , is assumed to percolate deeper and recharge the groundwater storage.

#### 4.4.5 Interflow

The interflow contribution,  $QIF$ , is assumed to be proportional to  $U$  and to vary linearly with the relative moisture content of the lower zone storage.

$$QIF = \begin{cases} (CKIF)^{-1} \frac{L/L_{max} - TIF}{1 - TIF} U & \text{for } L/L_{max} > TIF \\ 0 & \text{for } L/L_{max} \leq TIF \end{cases} \quad (4.3)$$

where  $CKIF$  is the time constant for interflow, and  $TIF$  is the root zone threshold value for interflow ( $0 \leq TIF \leq 1$ ).

#### 4.4.6 Interflow and overland flow routing

The interflow is routed through two linear reservoirs in series with the same time constant  $CK_{12}$ . The overland flow routing is also based on the linear reservoir concept but with a variable time constant

$$CK = \begin{cases} CK_{12} & \text{for } OF < OF_{min} \\ CK_{12} \left( \frac{OF}{OF_{min}} \right)^{-\beta} & \text{for } OF \geq OF_{min} \end{cases} \quad (4.4)$$



where  $OF$  is the overland flow (mm/hour),  $OF_{min}$  is the upper limit for linear routing (= 0.4 mm/hour), and  $\beta = 0.4$ .

The constant  $\beta = 0.4$  corresponds to using the Manning formula for modelling the overland flow. Equation (4.4) ensures in practice that the routing of real surface flow is kinematic, while subsurface flow being interpreted by NAM as overland flow (in catchments with no real surface flow component) is routed as a linear reservoir.

#### 4.4.7 Groundwater recharge

The amount of infiltrating water  $G$  recharging the groundwater storage depends on the soil moisture content in the root zone

$$G = \begin{cases} (P_N - QOF) \frac{L/L_{max} - TG}{1 - TG} & \text{for } L/L_{max} > TG \\ 0 & \text{for } L/L_{max} \leq TG \end{cases} \quad (4.5)$$

where

$TG$  is the root zone threshold value for groundwater recharge ( $0 \leq TG \leq 1$ ).

#### 4.4.8 Soil moisture content

The lower zone storage represents the water content within the root zone. After apportioning the net rainfall between overland flow and infiltration to groundwater, the remainder of the net rainfall increases the moisture content  $L$  within the lower zone storage by the amount  $\Delta L$

$$\Delta L = P_N - QOF - G \quad (4.6)$$

#### 4.4.9 Baseflow

The baseflow  $BF$  from the groundwater storage is calculated as the outflow from a linear reservoir with time constant  $CK_{BF}$

### 4.5 Extended groundwater components

#### 4.5.1 Drainage to or from neighbouring catchments

Local geological conditions may cause part of the infiltrating water to drain to neighbouring catchments. In NAM this loss of water can be described by specifying the ratio of the groundwater catchment area to the topographical



catchment area,  $C_{area}$ , with a value less than one. In this case the proportion  $(1-C_{area})$  of the recharge  $G$  is drained to neighbouring catchments. Similarly, water may be drained from neighbouring catchments, implying an increased groundwater recharge in the catchment ( $C_{area} > 1$ ).

#### 4.5.2 Lower groundwater storage

For a better description of the baseflow, an additional (lower) groundwater storage can be defined. In this case the upper groundwater storage provides the fast responding component of the baseflow, whereas the lower storage usually has a slower response. The recharge to the lower storage is given as a proportion  $CQ_{LOW}$  of the total recharge  $G$ . The routing from the lower storage is described by a linear reservoir with time constant  $CK_{LOW}$ .

#### 4.5.3 Shallow groundwater reservoir description

The groundwater level is calculated from a continuity consideration accounting for recharge  $G$ , capillary flux  $CAFLUX$ , net groundwater abstraction  $GWPUMP$ , and baseflow  $BF$ . The inclusion of capillary flux and groundwater pumping are optional. The groundwater storage can be treated in two different ways, either as a simple linear reservoir as described in Section 4.4.9 Baseflow (p. 284) or as a shallow groundwater reservoir.

The shallow groundwater reservoir description is appropriate for lowland catchments with little topographical variation and the potential for water logging. The baseflow is given by

$$BF = \begin{cases} (GWL_{BF0} - GWL) S_Y (CK_{BF})^{-1} & \text{for } GWL \leq GWL_{BF0} \\ 0 & \text{for } GWL > GWL_{BF0} \end{cases} \quad (4.7)$$

where  $S_Y$  is the specific yield of the reservoir,  $GWL$  is the groundwater table depth, and  $GWL_{BF0}$  is the maximum groundwater table depth, which causes baseflow.

The parameter  $GWL_{BF0}$  can be interpreted as the distance between the average ground level of the catchment to the water level of the river. Due to the variation in the river water level throughout the year  $GWL_{BF0}$  can be given a significant annual variation.

#### 4.5.4 Capillary flux

The capillary flux  $CAFLUX$  of water from the groundwater to the lower zone storage is assumed to depend on the depth of the groundwater table below

the ground surface,  $GWL$ , as well as on the relative moisture content,  $L/L_{max}$ , of the lower zone storage

$$CAFLUX = \sqrt{1 - L/L_{max}} \left( \frac{GWL}{GWL_{FL1}} \right)^{-\alpha} \text{ (mm/day)} \quad (4.8)$$

$$\alpha = 1,5 + 0,45 GWL_{FL1}$$

where  $GWL_{FL1}$  is the groundwater table depth at which the capillary flux is 1 mm/day when the lower zone storage is completely dry. Equation (4.8) provides a good fit to the theoretical relationship between the capillary flux, the depth to the water table and the soil moisture content pro

## 4.6 Snow module

Snow accumulation and melt are important hydrological processes in river basins where the snow pack acts as a storage in which precipitation is retained during the cold season and subsequently released as melt water during the warmer parts of the year.

The snow melt component of the runoff is incorporated as an integrated module within NAM. This component is optional and temperature data is only required if the snow routine is selected. Normally the precipitation enters directly into the surface storage. However, during cold periods precipitation is retained in the snow storage from which it is melted in warmer periods. Two different models can be applied; a simple lumped calculation or a more general approach that divides the catchment into a number of altitude zones with separate snow melt parameters, temperature and precipitation input for each zone.

### 4.6.1 Accumulation and melting of snow

Several investigations (e.g. /58/) have shown that the shift between precipitation in the form of rain and snow usually takes place when the air temperature is within a narrow interval close to 0° C. In the snow module it is assumed that the precipitation falls as rain when the air temperature is above a certain base temperature level,  $T_0$ , which can be specified by the user.

The snowmelt QS is calculated using a degree-day approach

$$QS = \begin{cases} C_{snow}(T - T_0) & \text{for } T > T_0 \\ 0 & \text{for } T \leq T_0 \end{cases} \quad (4.9)$$

where  $C_{snow}$  is the degree-day coefficient. The generated melt water is retained in the snow storage as liquid water until the total amount of liquid



water exceeds the water retention capacity of the snow storage. The excess melt water  $P_S$  is routed to the NAM model where it contributes to the surface storage. The excess melt water contribution  $P_S$  to NAM is

$$P_S = \begin{cases} Q_{melt} & \text{for } WR \geq C_{wr}S_{snow} \\ 0 & \text{for } WR < C_{wr}S_{snow} \end{cases} \quad (4.10)$$

where  $WR$  is the water retention in the snow storage,  $C_{wr}$  is the water retention coefficient, and  $S_{snow}$  is the snow storage. The new snow storage is calculated by subtracting the excess melt water  $P_S$  from the snow storage.

The rain fraction is added as liquid water and is retained in the snow storage if the total liquid water content of the snow pack is below its water retaining capacity. When the air temperature is below  $T_0$ , the liquid water content in the snow storage freezes with rate  $C_{snow}$ . Evaporation from the snow pack is neglected.

## 4.6.2 Altitude-distributed snowmelt model

### Introduction

In mountainous areas temperature, precipitation and snow cover often vary significantly within a single catchment. The runoff simulation for such areas can be improved by dividing the catchment into smaller zones and maintain individual snow storage calculations in each zone.

The altitude-distributed snow model calculates melt water in a number of altitude zones using the degree-day approach. Since in many cases the hydro-meteorological information from mountain basins is quite sparse, the module also includes facilities for distribution of the meteorological information with altitude.

### Structure of the altitude-distributed snowmelt module

The snow melt module allows the user to define a number of altitude zones within a NAM catchment and adjust the snow melt parameters and the temperature and precipitation input to the model for each zone. The snow melt module maintains individual snow storages and calculates accumulation and melting of snow for each altitude zone. The simulated melt water from all zones is subsequently superposed and routed through the NAM model as illustrated in Figure 4.2. This implies that the same model parameters for infiltration, runoff and groundwater routing are applied for all altitude zones. Such an approach will be appropriate for the large majority of mountain catchments.

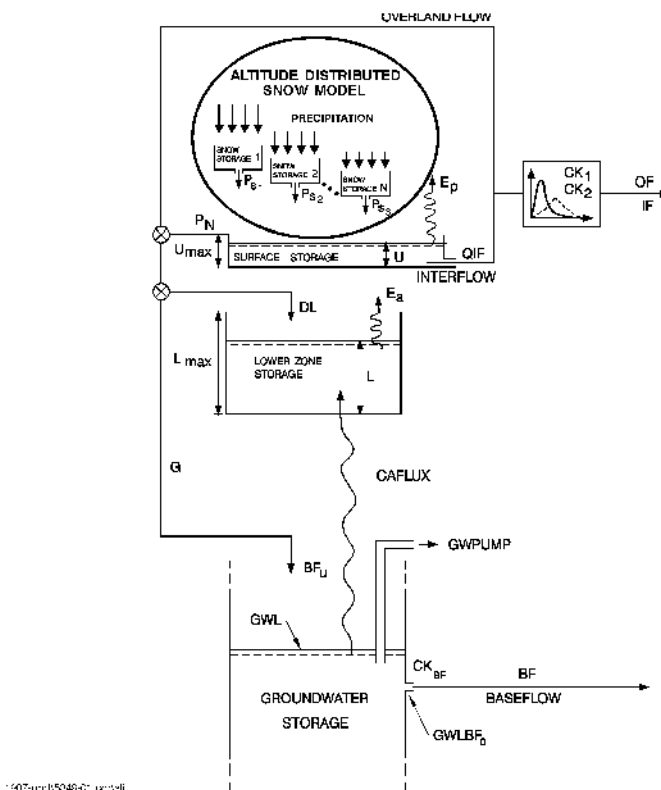


Figure 4.2 Structure of the NAM model with extended snow module.

In special cases where differentiation is needed also in the other parameters the catchment in question can be divided into two or more sub-catchments. The total simulated discharge is then found by accumulating the simulated discharge from the different sub-catchments using the combined catchment approach in the MIKE 11 RR editor.

In the altitude-distributed snow model, snow melting only takes place from the snow-covered part of each zone. When the water equivalent of the snow pack falls under a user-specified value (minimum storage for full coverage), the area coverage will be reduced linearly with the snow storage in the zone.

Snow will not necessarily melt on the location where it falls. Due to wind transport the snow accumulation at wind exposed sites may often be significantly smaller than at locations well sheltered against wind. Wind exposed conditions are often present at higher altitudes where vegetation is sparse and wind velocities generally high. Furthermore, for the higher parts of mountain ranges, steep slopes having a limited snow storage capacity will often dominate. Snow storage in excess of this capacity will at such locations generate avalanches which transport the snow to lower altitudes. Hence, some of the snow falling on wind exposed and/or steep highlands may not melt on the location but be deposited and melting at lower altitudes. To account for such re-distribution of snow and avoid unrealistic accumulation of snow in the cold





upper zones a user specified upper limit of the snow storage in the individual zones has been introduced in the model. Snow storage exceeding this value will be transferred to the neighbouring lower zone.

## Adjustment of temperature and precipitation to altitude zones

The altitude-distributed snow model operates with three meteorological reference time series; precipitation, temperature and potential evapotranspiration. In order to account for the large variations in precipitation and temperature with altitude the reference series can be adjusted for each altitude zone in two different ways:

- lapse rate corrections
- individual correction factors applied for each zone

### Lapse rate corrections

The lapse rate correction approach is a very simple but powerful way of adjustment in which the temperature and the precipitation are assumed to vary linearly with the altitude. The only input data required are the average altitude of the various zones, a reference altitude of the time series, and the lapse rates. The temperature lapse rates, however, are known to be quite variable, ranging from high values under dry conditions to lower values under wet conditions. Hence, in the model it is possible to specify two different temperature lapse rates to be used during dry and wet weather conditions, respectively. The model applies the “wet” lapse rate during days with precipitation and the “dry” lapse rate during the rest of the time.

The temperature in each zone is adjusted by the following formula:

$$T_{zone} = \begin{cases} T_{ref} + (H_{zone} - H_{ref})\beta_{dry} & \text{for } P = 0 \\ T_{ref} + (H_{zone} - H_{ref})\beta_{wet} & \text{for } P > 0 \end{cases} \quad (4.11)$$

where

$T_{zone}$  temperature in the considered zone

$T_{ref}$  temperature at the reference temperature station

$H_{zone}$  average height in the zone

$H_{ref}$  height at the reference temperature station

$b_{dry}$  temperature lapse rate for dry conditions

$b_{wet}$  temperature lapse rate for wet conditions



The precipitation in each altitude zone is calculated from the precipitation at the reference station:

$$P_{zone} = P_{ref}(1 + (H_{zone} - H_{ref})\alpha) \quad (4.12)$$

where

$P_{ref}$  precipitation at the reference precipitation station

$H_{ref}$  height at the reference precipitation series

$\alpha$  precipitation lapse rate

### Individual correction factors applied for each zone

In this case corrections have to be specified by the user for each altitude zone. This method requires more input but also offers a larger flexibility. The corrected meteorological series are calculated using the formulae:

$$T_{zone} = \begin{cases} T_{ref} + T_{cor,zone,dry} & \text{for } P = 0 \\ T_{ref} + T_{cor,zone,wet} & \text{for } P > 0 \end{cases} \quad (4.13)$$

$$P_{zone} = P_{ref}(1 + P_{cor,zone}) \quad (4.14)$$

where  $T_{cor,zone,wet}$  and  $P_{cor,zone,dry}$  are the actual temperature corrections for wet and dry conditions, respectively, and  $P_{cor,zone}$  is the relative precipitation correction.

If it is not possible to represent the meteorological conditions in the catchment by adjustment of one series only, the catchment may be divided into smaller sub-catchments in which one series will be representative. The discharges for the individual sub-catchments are then superposed using the combined catchment approach in the MIKE 11 RR editor.

## 4.6.3 Extended components

### Seasonal variation of degree-day coefficient

The simple degree-day approach for calculating snow melt cf. (4.9) can be extended by using a seasonal variation of the degree-day coefficient  $C_{snow}$ . This variation reflects in a conceptual way the seasonal variation of the incoming short wave radiation and the variation in the albedo of the snow surface during the snow season. The albedo is very high (about 0.8) for new, cold snow falling in the beginning of the accumulation season and then decreases with the age of the snow (to a minimum value of about 0.3 in the end of the season).



## Radiation

The melting effects caused by the absorbed short wave radiation can be explicitly modelled. In this case an additional snow melting is calculated as

$$\Delta QS = C_{rad}R \quad (4.15)$$

where  $C_{rad}$  is the radiation coefficient, and  $R$  is the incoming short wave radiation. The total amount of snow melt is calculated as the sum of the snow melt rates given by (4.9), (4.15), and (4.16) (optional), respectively.

## Condensation of humid air and heat contribution from rainfall

The melting effects from condensation of humid air on the snow surface and the advective heat transferred to the snow pack by precipitation can be explicitly modelled. The effects are calculated as an additional snowmelt

$$\Delta QS = C_{rain}P(T - T_0) \quad (4.16)$$

where  $C_{rain}$  is a degree-day coefficient, and  $P$  is the rainfall. The total amount of snow melt is calculated as the sum of the snow melt rates given by (4.9), (4.15) (optional), and (4.16), respectively.

## 4.7 Irrigation module

### 4.7.1 Introduction

Minor irrigation schemes within a catchment will normally have negligible influence on the catchment hydrology, unless transfer of water over catchment boundaries is involved. Large schemes, however, may significantly affect the runoff and the groundwater recharge through local increases in evapotranspiration and infiltration as well as through operational and field losses.

The irrigation module of NAM may be applied to describe the effect of irrigation on the following aspects:

- The overall water balance of the catchment. This will be affected mainly by the increased evapotranspiration and by possible external water sources for irrigation.
- Local infiltration and groundwater recharge in irrigated areas.
- The distribution of catchment runoff amongst different runoff components (overland flow, interflow, baseflow). This may be influenced by the increased infiltration in irrigated areas as well as by local abstraction of irrigation water from groundwater or streams.

For each irrigation area within the catchment a NAM subcatchment is defined with individual model parameters. The non-irrigated areas are modelled by defining a general NAM subcatchment. The total simulated discharge is then found by accumulating the simulated discharge from the different sub-catchments using the combined catchment approach in the MIKE 11 RR editor.

## 4.7.2 Structure of the irrigation module

The structure of the irrigation module is illustrated in Figure 4.3.

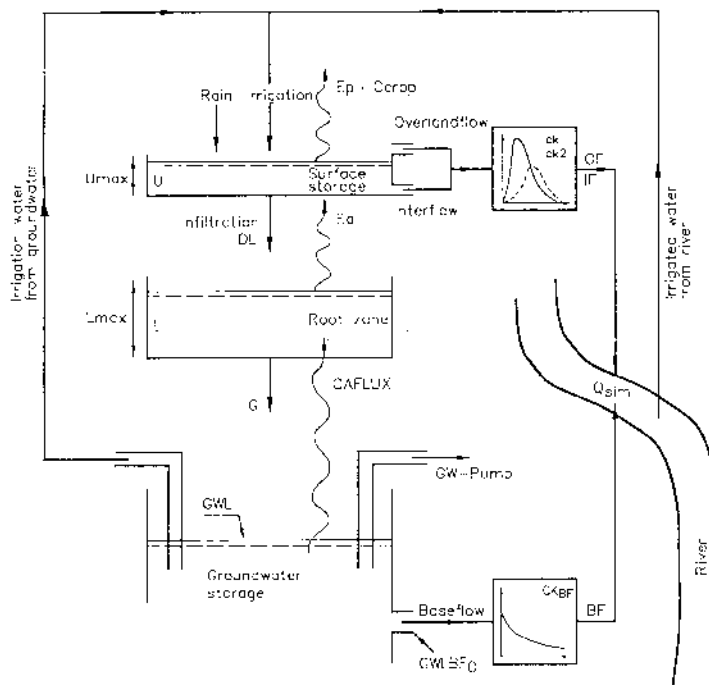


Figure 4.3 Structure of the NAM irrigation module.

Water supplied to the surface storage in irrigated areas will be a sum of precipitation  $P$  and irrigation water  $P_{ir}$ . The potential evapotranspiration may vary with crop type and the stage of growth. The irrigation module accounts for this by allowing the user to specify monthly varying crop coefficients  $C_{crop}$  for each irrigation area. The potential evapotranspiration for a specific crop is given by

$$E_{p, crop} = C_{crop} E_p \quad (4.17)$$

where  $E_p$  is the reference time series of potential evapotranspiration.



Infiltration  $I$  is taken directly from the surface storage to the lower zone and groundwater storages and is calculated as a function of the moisture content in the lower zone  $L$

$$I = \begin{cases} k0_{inf}L_{max}/L & \text{for } k0_{inf}L_{max}/L < U \\ U & \text{for } k0_{inf}L_{max}/L \geq U \end{cases} \quad (4.18)$$

where  $k0_{inf}$  is an infiltration factor describing the infiltration rate at field capacity (i.e.  $L = L_{max}$ ).

A portion  $G$  of the infiltration is assumed to percolate deeper and recharge the groundwater storage. This portion is, as in the general NAM model, calculated as a function of the conditions in the lower zone storage

$$G = \begin{cases} I \frac{L/L_{max} - TG}{1 - TG} & \text{for } L/L_{max} > TG \\ 0 & \text{for } L/L_{max} \leq TG \end{cases} \quad (4.19)$$

where  $TG$  is the root zone threshold value for groundwater recharge.

The remaining part  $\Delta L$  is assumed to increase the moisture content in the lower zone

$$\Delta L = I - G \quad (4.20)$$

If the maximum surface storage  $U_{max}$  is exceeded, the general NAM model diverts the excess water into overland flow ( $QOF$ ) and infiltration. In the irrigation module infiltration has been accounted for as described above, and hence the excess water is added directly to overland flow.

Irrigation water can be abstracted from three different sources. The amount of water taken from each source type is determined by specifying fixed percentages of  $P_{ir}$  for each source type:

- local groundwater ( $PC_{lgw}$ )
- local river ( $PC_{lr}$ )
- external river ( $PC_{extr}$ )

The term "local" means within the actual NAM catchment. If irrigation water is abstracted from local groundwater, it will be subtracted from the groundwater storage and the groundwater level will then be reduced with the amount

$$\Delta GWL = \frac{\Delta t PC_{lgw} P_{ir}}{S_Y} \quad (4.21)$$



where  $S_Y$  is the specific yield, and  $\Delta t$  is the time step used in the calculations.

If the water is abstracted from a local river, it will be subtracted from the calculated runoff

$$\Delta Q_{sim} = \Delta t PC_{ir} P_{ir} \quad (4.22)$$

If the water is imported from a river outside the NAM catchment (external), no subtractions are made.

A part of the water diverted for irrigation will be lost on its way to the fields. The losses may include evaporation and seepage from channels, illegal off-takes, and operational losses (i.e. water that is diverted to the irrigation area but is not being utilised). In the irrigation module, the user may specify percentages of the irrigation water  $P_{ir}$  that is lost, i.e.

- evaporation losses ( $PC_{evap}$ )
- seepage losses ( $PC_{gw}$ )
- operational losses contributing to overland flow ( $PC_{of}$ )

The losses may vary in time on a monthly basis.

Due to the different losses the irrigation water is reduced with the amount

$$\Delta P_{ir} = P_{ir}(PC_{evap} + PC_{gw} + PC_{of}) \quad (4.23)$$

The operational losses yields an increase in the overland flow

$$\Delta OF = \Delta t PC_{of} P_{ir} \quad (4.24)$$

The seepage losses contributes to an increase in the groundwater level

$$\Delta GWL = \frac{\Delta t PC_{gw} P_{ir}}{S_Y} \quad (4.25)$$

## 4.8 Model parameters

This section provides a short description of the model parameters, their physical interpretation and importance along with suggestions for parameter adjustments in the calibration.



## 4.8.1 Surface and root zone parameters

### Maximum water content in surface storage $U_{max}$

$U_{max}$  [mm] defines the maximum water content in the surface storage. This storage is interpreted as including the water content in the interception storage (on vegetation), in surface depression storages, and in the uppermost few cm's of the ground. Typical values of  $U_{max}$  are in the range 10-20 mm.

One important characteristic of the model is that the surface storage must be at its maximum capacity, i.e.  $U \geq U_{max}$  before any excess water,  $P_N$ , occurs. In dry periods, the amount of net rainfall that must occur before any overland flow occurs can be used to estimate  $U_{max}$ .

### Maximum water content in root zone storage $L_{max}$

$L_{max}$  [mm] defines the maximum water content in the lower or root zone storage.  $L_{max}$  can be interpreted as the maximum soil moisture content in the root zone available for the vegetative transpiration. Ideally,  $L_{max}$  can then be estimated by multiplying the difference between field capacity and wilting point of the actual soil with the effective root depth. The difference between field capacity and wilting point is referred to as the available water holding capacity (AWHC). For estimation of AWHC, moisture contents for different soil types at pF-value 2.5, corresponding approximately to field capacity, and pF-value 4.2, corresponding to wilting point are shown in Table 4.1

It should be noted that  $L_{max}$  represents the average value for an entire catchment, i.e. an average value for the various soil types and root depths of the individual vegetation types. Hence,  $L_{max}$  cannot in practice be estimated from field data, but an expected interval can be defined.

Since the actual evapotranspiration is highly dependent on the water content of the surface and root zone storages,  $U_{max}$  and  $L_{max}$  are the primary parameters to be changed in order to adjust the water balance in the simulations. In the preliminary stages of the model calibration, it is recommended to fix the relation between  $U_{max}$  and  $L_{max}$ , leaving only one storage parameter to be estimated. As a rule,  $U_{max} = 0.1L_{max}$  can be used unless special catchment characteristics or hydrograph behaviour indicate otherwise.

Table 4.1 Moisture content in  $\text{cm}^3/\text{cm}^3$  at (effective) saturation ( $\theta_s$ ) and at pF-values of 2.5( $\theta_{2.5}$ ) and 4.2( $\theta_{4.2}$ ), for eleven textural classes and from three sources: (1) Rawls et al. (1982),/54/; (2) Cosby et al. (1984),/46/; (3)

Rijtema (1969), /57/.

Soil texture	$\theta_s$			$\theta_{2.5}$			$\theta_{4.2}$		
	(1)	(2)	(3)	(1)	(2)	(3)	(1)	(2)	(3)
Sand	0.417	0.339	0.350-0.395	0.091	0.086	0.021-0.140	0.033	0.021	0.012-0.042
Loamy Sand	0.401	0.421	0.301-0.470	0.125	0.148	0.131-0.328	0.055	0.059	0.060-0.105
Sandy Loam	0.412	0.434	0.504-0.463	0.207	0.225	0.169-0.249	0.094	0.099	0.061-0.087
Loam	0.434	0.439	0.503	0.270	0.289	0.272	0.117	0.137	0.098
Silt Loam	0.486	0.476	0.509	0.330	0.364	0.309	0.133	0.175	0.092
Sandy Clay Loam	0.330	0.404	0.432	0.255	0.254	0.303	0.148	0.142	0.180
Clay Loam	0.390	0.465	0.445	0.318	0.343	0.380	0.197	0.212	0.255
Silty Clay Loam	0.432	0.464	0.475	0.366	0.385	0.325	0.208	0.246	0.185
Sandy Clay	0.321	0.406	-	0.339	0.294	-	0.239	0.204	-
Silty Clay	0.423	0.468	0.507	0.387	0.376	0.435	0.250	0.258	0.257

## Overland flow runoff coefficient $CQOF$

$CQOF$  is a very important parameter, determining the extent to which excess rainfall runs off as overland flow and the magnitude of infiltration.

$CQOF$  is dimensionless with values between 0 and 1. Physically, in a lumped manner, it reflects the infiltration and also to some extent the recharge conditions. Small values of  $CQOF$  are expected for a flat catchment having coarse, sandy soils and a large unsaturated zone, whereas large  $CQOF$ -values are expected for catchments having low, permeable soils such as clay or bare rocks.  $CQOF$ -values in the range 0.01-0.90 have been experienced.

It should be noted that during periods where the groundwater table is at the ground surface the model excludes the infiltration component, and hence  $CQOF$  becomes redundant.

## Time constant for interflow $CKIF$

$CKIF$  [hours] determines together with  $U_{max}$  the amount of interflow ( $(CKIF)^{-1}$  is the quantity of the surface water content  $U$  that is drained to interflow every hour). It is the dominant routing parameter of the interflow because  $CKIF \gg CK_{12}$ .

Physical interpretation of the interflow is difficult. Since interflow is seldom the dominant streamflow component,  $CKIF$  is not, in general, a very important parameter. Usually,  $CKIF$ -values are in the range 500-1000 hours.

## Time constant for routing interflow and overland flow $CK_{12}$

The time constant for routing interflow and overland flow  $CK_{12}$  [hours] determines the shape of hydrograph peaks. The value of  $CK_{12}$  depends on the size of the catchment and how fast it responds to rainfall. Typical values are in the range 3-48 hours.

The time constant can be inferred from calibration on peak events. If the simulated peak discharges are too low or arriving too late, decreasing  $CK_{12}$  may correct this, and vice versa.





## Root zone threshold value for overland flow $TOF$

$TOF$  is a threshold value for overland flow in the sense that no overland flow is generated if the relative moisture content of the lower zone storage,  $L/L_{max}$ , is less than  $TOF$ . The behaviour of the threshold value is illustrated in Figure 4.4. Similarly, the root zone threshold value for interflow  $TIF$  and recharge  $TG$  act as threshold values for generation of interflow and recharge, respectively.

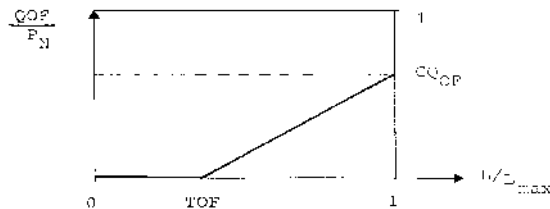


Figure 4.4 Generation of overland flow.

Physically, the three threshold values should reflect the degree of spatial variability in the catchment characteristics, so that a small homogeneous catchment is expected to have larger threshold values than a large heterogeneous catchment.

For catchments with alternating dry and wet periods, the threshold values determine the onset of the flow components in the periods where the root zone is being filled up. This can be used in model calibration. It should be noted that the threshold values have no importance in wet periods. The significance of the threshold value varies from catchment to catchment and is usually larger in semi-arid regions.

In areas with alternating dry and wet seasons,  $TOF$  can be estimated on the basis of situations where even very heavy rainfall does not give rise to the quick response of the overland flow component. The parameter has an impact only during the first, few weeks of the wet season. Values of  $TOF$  in the range 0-0.7 have been experienced.

## Root zone threshold value for interflow $TIF$

The root zone threshold value for interflow has the same function for interflow as  $TOF$  has for the overland flow. It is usually not a very important parameter, and it can in most cases be given a value equal to zero.



## 4.8.2 Groundwater parameters

### Baseflow time constant $CK_{BF}$

The time constant for baseflow,  $CK_{BF}$  [hours], determines the shape of the simulated hydrograph in dry periods. According to the linear reservoir description the discharge in such periods is given by an exponential decay.  $CK_{BF}$  can be estimated from hydrograph recession analysis.  $CK_{BF}$ -values in the range 500-5000 hours have been experienced.

If the recession analysis indicates that the shape of the hydrograph changes to a slower recession after a certain time, an additional (lower) groundwater storage can be added to improve the description of the baseflow.

### Root zone threshold value for groundwater recharge $TG$

The root zone threshold value for recharge has the same effect on recharge as  $TOF$  has on the overland flow. It is an important parameter for simulating the rise of the groundwater table in the beginning of a wet season.

### Recharge to lower groundwater storage $CQ_{LOW}$

In some cases the shape of the hydrograph recession changes to a slower recession after a certain period. To simulate this, a lower groundwater storage may be included. The parameter  $CQ_{LOW}$  determines the proportion of the recharge that percolates to the lower groundwater storage.  $CQ_{LOW}$  together with  $CK_{low}$  can be estimated from hydrograph recession analysis.

### Time constant for routing lower baseflow $CK_{low}$

The baseflow from the lower groundwater storage is modelled using a linear reservoir with time constant  $CK_{low}$  [hours]. The time constant can be estimated from hydrograph recession analysis. Usually,  $CK_{low}$  is larger than  $CK_{BF}$ .

### Ratio of groundwater catchment to topographical catchment area $C_{area}$

Drainage to or from neighbouring catchments can be modelled by specifying a value of  $C_{area}$  different from 1.  $C_{area}$  specifies the amount of recharge  $G$  that is being drained. If  $C_{area} < 1$ , part of the recharge,  $(1-C_{area})G$ , is drained to another catchment, whereas for  $C_{area} > 1$ , the amount  $(C_{area}-1)G$  is added to the catchment recharge.

### Maximum groundwater depth causing baseflow $GWL_{BF0}$

The maximum depth to the groundwater table for which baseflow occurs,  $GWL_{BF0}$  [m], represents the outflow level of the groundwater reservoir given as the distance between the average ground level of the catchment and the minimum level of the river to which it drains. In low, flat areas the annual vari-



ation of this distance may be of importance and the facility to allow  $GWL_{BF0}$  to vary seasonally is provided in NAM.

$GWL_{BF0}$  and the specific yield  $S_Y$  can be calibrated by comparing the simulated groundwater level with observations.

### Specific yield $S_Y$

Values of the specific yield for the groundwater storage may often be assessed from hydrological data e.g. pump tests. Alternatively,  $S_Y$ -values can be estimated from the literature for different soil types. Small values are found for clay (0.01-0.1) and high values for sand (0.1-0.3).

### Groundwater depth for unit capillary flux $GWL_{FL1}$

$GWL_{FL1}$  [m] is the depth to the groundwater table which yields an upward capillary flux of 1 mm/day when the moisture content of the upper soil layers is at wilting point, i.e.  $L = 0$ . This parameter will depend on the soil type, and values for 20 soil types according to Rijtema (1969), /57/ are listed in Table 4.2.

Table 4.2 Depth to the groundwater table corresponding to a capillary flux of 1 mm/day for 20 soil types

Soil type	$GWL_{FL1}$ [m]
1. Coarse sand	0.5
2. Medium coarse sand	0.6
3. Medium fine sand	0.9
4. Fine sand	1.5
5. Humus loamy medium coarse sand	1.2
6. Light loamy medium coarse sand	0.7
7. Loamy medium coarse sand	0.5
8. Loamy fine sand	1.7
9. Sandy loam	0.7
10. Loess loam	1.5
11. Fine sandy loam	2.5
12. Silty loam	2.8
13. Loam	1.9
14. Sandy clay loam	2.2



Table 4.2 Depth to the groundwater table corresponding to a capillary flux of 1 mm/day for 20 soil types

Soil type	GWL <sub>FL1</sub> [m]
15. Silty Clay Loam	1.8
16. Clayey Loam	1.0
17. Light clay	2.9
18. Basin clay	0.4
19. Silty clay	1.4
20. Peat	0.6

### 4.8.3 Snow module parameters

#### Degree-day coefficient $C_{snow}$

The snow melts at a rate defined by the degree-day coefficient  $C_{snow}$  [mm /°C/day]. A seasonal variation of  $C_{snow}$  can be defined in order to account for the seasonal variations of the incoming short wave radiation and the albedo of the snow surface. Typical values of  $C_{snow}$  are in the range 2-4 mm/°C/day.

#### Base temperature (snow/rain) $T_0$

The precipitation is assumed to fall as snow if the temperature is below the base temperature  $T_0$  [°C]. For temperatures above  $T_0$  the snow in the snow storage is melting. The base temperature is usually close to zero degrees Celsius.

#### Radiation coefficient $C_{rad}$

The radiation coefficient  $C_{rad}$  [m<sup>2</sup>/W/mm/day] determines the rate of snow melting caused by the absorbed short wave radiation.

#### Rainfall degree-day coefficient $C_{rain}$

The rainfall degree-day coefficient  $C_{rain}$  [mm/mm/°C/day] determines the rate of snow melting caused by condensation of humid air on the snow surface and the advective heat transferred to the snow pack by precipitation.



## 4.8.4 Irrigation module parameters

### Infiltration factor $KO_{inf}$

$KO_{inf}$  [mm/day] is the infiltration factor which, together with the moisture content in the upper and root zone storages, determines the amount of water infiltrating from the surface to the root zone and groundwater storage.

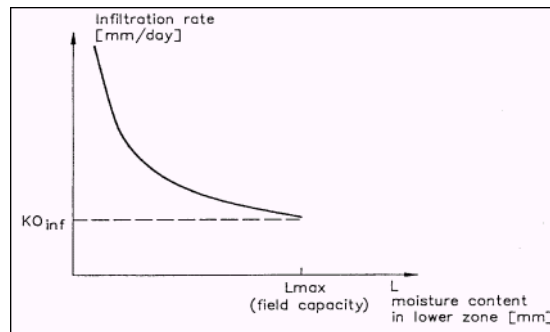


Figure 4.5 Infiltration rate as a function of the moisture content in the root zone.

In Figure 4.5 the infiltration rate is shown as a function of the moisture content in the root zone.  $KO_{inf}$  is strongly dependent on the soil type and is large for sandy soils and small for clayey soils.

When irrigation water is supplied, the root zone will often be close to saturation. Under such conditions the infiltration rate  $KO_{inf}$  may converge to the saturated hydraulic conductivity of the soil ( $K_s$ ). As a guideline  $K_s$ -values for different soil types, as estimated by various authors, are presented in Table 4.3.

When the root zone is only partly saturated, the flow dynamics become very complicated and are not properly described in a lumped model like NAM. Furthermore, the soil preparation may have a significant influence on the soil hydraulic conductivity.

### Crop coefficients and irrigation losses

The crop coefficients account for the fact that potential evapotranspiration is dependent of the crop type and the stage of growth. This is achieved by multiplying the input time series of potential evapotranspiration with the crop coefficient. For dry uncropped soils, the crop coefficient will tend to zero while well cropped fields reaching full growth potential could have crop coefficients greater than 1. Further information about how to estimate the crop coefficients is given in /47/. Monthly values of crop coefficients can be specified.

The monthly magnitude and distribution of losses to evaporation, seepage, and overland flow should correspond to the design values of the irrigation scheme unless observations have shown a different distribution.

**Table 4.3** Values of saturated hydraulic conductivity  $K_s$  for eleven textural classes from six sources (1) Li et al. (1976), /49/; (2) Brakensiek (1979), /44/; (3) Brakensiek et al. (1981), /45/; (4) McCuen et al. (1981), /51/; (5) Cosby et al. (1984), /46/; (6) Rijtema (1969), /57/. The ratio between the largest and the smallest estimate has been calculated for columns 1-5 and 1-6, respectively.

Soil texture	$K_s$ [cm/min]						Ratio (max/min)	
	(1)	(2)	(3)	(4)	(5)	(6)	Col 1-5	Col 1-6
Sand	1.056	0.38	0.504	0.410	0.28	0.035-0.78	3.8	13
Loamy Sand	0.938	0.64	1.318	1.316	0.0003-0.080	0.018	16.5	4393
Sandy Loam	0.208	0.10	0.315	0.299	0.0083-0.031	0.0115	10.1	38
Loam	0.0417	0.019	0.109	0.100	0.020	0.0035	5.7	31
Silt Loam	0.0432	0.0085	0.027	0.027	0.0066	0.0045	6.5	9.6
Sandy Clay Loam	0.0378	0.026	0.082	0.079	0.026	0.0163	3.1	5
Clay Loam	0.0147	0.0054	0.064	0.061	0.015	0.0007	11.9	91
Silty Clay Loam	0.0102	0.020	0.019	0.018	0.012	0.0010	2.0	20
Sandy Clay	0.0130	0.0050	-	0.021	0.043	-	8.6	8.6
Silty Clay	0.0062	0.0065	0.039	0.030	0.008	0.0009	6.3	43
Clay	0.0077	0.0078	0.020	0.018	0.0002-0.0058	0.0024	3.4	100

## 4.9 Initial conditions

The initial conditions required by the NAM model consist of the initial water contents in the surface and root zone storages, together with initial values of overland flow, interflow, and baseflow.

If a lower groundwater reservoir is specified, the initial baseflow from both the upper and the lower reservoir should be specified. If the snow module is included, the initial value of the snow storage should be specified.

If a simulation commences at the end of a dry period, it is often sufficient to set all initial values to zero, except the water content in the root zone and the baseflow. The water content in the root zone should be about 10-30% of the capacity and the baseflow should be given a value close to the observed discharge.

Improved estimates of the initial conditions may be obtained from a previous simulation, covering several years, by noting the appropriate moisture contents of the root zone and baseflow at the same time of the year as the new simulation will start.

In general it is recommended to disregard the first 3-6 months of the NAM simulation in order to eliminate the influence of erroneous initial conditions.

## 4.10 Model calibration

In the NAM model the parameters and variables represent average values for the entire catchment. While in some cases a range of likely parameter values can be estimated, it is not possible, in general, to determine the values of the NAM parameters on the basis of the physiographic, climatic and soil physical



characteristics of the catchment, since most of the parameters are of an empirical and conceptual nature. Thus, the final parameter estimation must be performed by calibration against time series of hydrological observations.

#### 4.10.1 Calibration objectives and evaluation measures

The following objectives are usually considered in the model calibration

1. A good agreement between the average simulated and observed catchment runoff (i.e. a good water balance)
2. A good overall agreement of the shape of the hydrograph
3. A good agreement of the peak flows with respect to timing, rate and volume
4. A good agreement for low flows

In this respect it is important to note that, in general, trade-offs exist between the different objectives. For instance, one may find a set of parameters that provide a very good simulation of peak flows but a poor simulation of low flows, and vice versa.

In the calibration process, the different calibration objectives 1-4 should be taken into account. If the objectives are of equal importance, one should seek to balance all the objectives, whereas in the case of priority to a certain objective this objective should be favoured.

For a general evaluation of the calibrated model, the simulated runoff is compared with discharge measurements. For individual calibration of the groundwater parameters, the simulated average groundwater level can be compared with groundwater level measurements in the catchments.

Both graphical and numerical performance measures should be applied in the calibration process. The graphical evaluation includes comparison of the simulated and observed hydrograph, and comparison of the simulated and observed accumulated runoff. The numerical performance measures include the overall water balance error (i.e. the difference between the average simulated and observed runoff), and a measure of the overall shape of the hydrograph based on the coefficient of determination or Nash-Sutcliffe coefficient (152)

$$R^2 = 1 - \frac{\sum_{i=1}^N [Q_{obs,i} - Q_{sim,i}]^2}{\sum_{i=1}^N [Q_{obs,i} - \bar{Q}_{obs}]^2} \quad (4.26)$$

where  $Q_{sim,i}$  is the simulated discharge at time  $i$ ,  $Q_{obs,i}$  is the corresponding observed discharge, and  $\bar{Q}_{obs}$  is the average observed discharge. A perfect match corresponds to  $R^2 = 1$ .

An exact agreement between simulations and observations must, however, not be expected. The goodness-of-fit of the calibrated model is affected by different error sources, including

1. Errors in meteorological input data
2. Errors in recorded observations
3. Errors and simplifications inherent in the model structure
4. Errors due to the use of non-optimal parameter values

In model calibration only error source (4) should be minimised. In this respect it is important to distinguish between the different error sources since calibration of model parameters may compensate for errors in data and model structure. For catchments with a low quantity or quality of data, less accurate calibration results may have to be accepted.

Satisfactory calibrations over a full range of flows usually require continuous observations of runoff for a period of 3-5 years. Runoff series of a shorter duration, however, will also be useful for calibration, although they do not ensure an efficient calibration of the model. For a proper evaluation of the reliability and hydrological soundness of the calibrated model it is recommended to validate the model on data not used for model calibration (split-sample test). Some general aspects related to calibration and validation of hydrological models are described in Refsgaard and Storm (1996), /56/.

#### 4.10.2 Manual calibration

The process of model calibration is normally done either manually or by using computer-based automatic procedures. In this section a manual calibration strategy for the NAM model is outlined. Application of an automatic optimisation routine for calibration of the basic NAM model is described in the subsequent section.

In manual calibration, a trial-and-error parameter adjustment is made until satisfactory results are obtained. It is recommended, especially for the less experienced users, to change only one parameter between each trial, so that the effect of the change can be easily discerned. The manual calibration strategy outlined below is based on the different rainfall-runoff process descriptions for calibration of the relevant model parameters, i.e. the parameters that mostly affect the considered process description (see also Section 4.8 Model parameters (p. 294)).

A calibration usually commences by adjusting the water balance in the system. The total evapotranspiration over a certain period should correspond to the accumulated net precipitation minus runoff. The evapotranspiration will





increase when increasing the maximum water contents in the surface storage  $U_{max}$  and the root zone storage  $L_{max}$ , and vice versa.

The peak runoff events are caused by large quantities of overland flow. The peak volume can be adjusted by changing the overland flow runoff coefficient ( $CQOF$ ), whereas the shape of the peak depends on the time constant used in the runoff routing ( $CK_{12}$ ).

The amount of base flow is affected by the other runoff components; a decrease in overland flow or interflow will result in a higher baseflow, and vice versa. The shape of the baseflow recession is a function of the baseflow time constant ( $CKBF$ ). If the baseflow recession changes to a slower recession after a certain time, a lower groundwater reservoir should be added, including calibration of  $CQ_{low}$  and  $CK_{low}$ .

Initially, the root zone threshold values  $TOF$ ,  $TIF$  and  $TG$  can be set to zero. After a first round of calibration of the parameters  $U_{max}$ ,  $L_{max}$ ,  $CQOF$ ,  $CK_{12}$  and  $CKBF$ , the threshold parameters can be adjusted for further refinement of the simulation results.

For individual calibration of the groundwater parameters  $GWL_{BF0}$  and  $S_y$ , the simulated groundwater level is compared to observed groundwater levels. Inclusion of the shallow groundwater reservoir description is important in low-land areas, as found e.g. in swamps or river delta areas, where the groundwater table may reach the ground surface during the wet season.

The snow module parameters are calibrated against periods with snowmelt runoff.

### 4.10.3 Automatic calibration routine

For calibration of the basic NAM model, including the 9 model parameters listed in , an automatic optimization routine is available. The automatic calibration routine is based on a multi-objective optimization strategy in which the four different calibration objectives given above can be optimised simultaneously.

#### Multi-objective calibration measures

In automatic calibration, the calibration objectives have to be formulated as numerical goodness-of fit measures that are optimised automatically. For the four calibration objectives defined above the following numerical performance measures are used:

1. Agreement between the average simulated and observed catchment runoff: overall volume error.
2. Overall agreement of the shape of the hydrograph: overall root mean square error (RMSE).



3. Agreement of peak flows: average RMSE of peak flow events.
4. Agreement of low flows: average RMSE of low flow events.

### Overall volume error

$$F_1(\theta) = \left| \frac{1}{N} \sum_{i=1}^N [Q_{obs,i} - Q_{sim,i}(\theta)] \right| \quad (4.27)$$

where

$Q_{obs,i}$  is the observed discharge at time  $i$

$Q_{sim,i}$  is the simulated discharge at time  $i$

$\theta$  is the set of model parameters to be calibrated

$N$  is the number of time steps in the calibration period

### Overall RMSE

$$F_2(\theta) = \left[ \frac{1}{N} \sum_{i=1}^N [Q_{obs,i} - Q_{sim,i}(\theta)]^2 \right]^{1/2} \quad (4.28)$$

The coefficient of determination in Eq. (4.26) is a transformed and normalised measure of the overall RMSE (normalised with respect to the variance of the observed hydrograph). Thus, minimisation of (4.28) corresponds to maximising  $R^2$ .

### Average RMSE of peak flow events

$$F_3(\theta) = \frac{1}{M_p} \sum_{j=1}^{M_p} \left[ \frac{1}{n_j} \sum_{i=1}^{n_j} [Q_{obs,i} - Q_{sim,i}(\theta)]^2 \right]^{1/2} \quad (4.29)$$

where  $M_p$  is the number of peak flow events in the calibration period, and  $n_j$  is the number of time steps in event no.  $j$ . Peak flow events are defined as periods where the observed discharge is above a given (user-specified) threshold level.

### Average RMSE of low flow events

$$F_3(\theta) = \frac{1}{M_l} \sum_{j=1}^{M_l} \left[ \frac{1}{n_j} \sum_{i=1}^{n_j} [Q_{obs,i} - Q_{sim,i}(\theta)]^2 \right]^{1/2} \quad (4.30)$$



where  $M_j$  is the number of low flow events in the calibration period. Low flow events are defined as periods where the observed discharge is below a given (user-specified) threshold level.

## Optimization algorithm

The multi-objective optimization problem can be formulated as follows

$$\min \{F_1(\theta), F_2(\theta), F_3(\theta), F_4(\theta)\}, \theta \in \Theta \quad (4.31)$$

The optimization problem is said to be constrained in the sense that  $\theta$  is restricted to the feasible parameter space  $\Theta$ . The parameter space is defined as a hypercube by specifying lower and upper limits on each parameter. These limits should be chosen according to physical and mathematical constraints in the model and from modelling experiences.

The solution of (4.31) will not, in general, be a single unique set of parameters but will consist of the so-called Pareto set of solutions (non-dominated solutions), according to various trade-offs between the different objectives. The concept of Pareto optimality implies that the entire parameter space  $\Theta$  can be divided into “good” (Pareto optimal) and “bad” solutions, and none of the “good” solutions can be said to be “better” than any of the other “good” solutions. A member of the Pareto set will be better than any other member with respect to some of the objectives, but because of the trade-off between the different objectives it will not be better with respect to other objectives.

In practical applications, the entire Pareto set may be too expensive to calculate, and one is only interested in part of the Pareto optimal solutions. To estimate only a single point of the Pareto front a single-objective optimization problem is defined that aggregates the different objective functions  $F_1(\theta) - F_4(\theta)$ . The applied aggregate measure is the Euclidian distance

$$F_{agg}(\theta) = [(F_1(\theta) + A_1)^2 + (F_2(\theta) + A_2)^2 + (F_3(\theta) + A_3)^2 + (F_4(\theta) + A_4)^2]^{1/2} \quad (4.32)$$

where  $A_i$  are transformation constants. A balanced aggregated measure is defined by assigning transformation constants in (4.32) such that the different objectives have equal weight in the optimization. The transformation constants are automatically calculated based on the initially generated population of parameter sets in the optimization loop (/50/).

The optimal parameter set is found by minimising (4.32) with respect to  $\theta$ . Optimization is performed automatically using the shuffled complex evolution (SCE) algorithm (/48/). The SCE method is a global search method in the sense that it is especially designed for locating the global optimum of the objective function and not being trapped in local optima. A detailed descrip-

tion of the algorithm is given in /48/. Implementation and testing of the algorithm for automatic calibration of the NAM model is described in /50/.

## User specifications

Specifications for the NAM auto-calibration module include:

- Calibration parameters
- Range of calibration parameters
- Objective functions
- Stopping criterion

### Calibration parameters

The automatic calibration routine includes the 9 model parameters shown in . The user specifies the subset of these parameters that should be calibrated automatically.

### Range of calibration parameters

For the subset of NAM parameters to be calibrated automatically the user specifies the hypercube search space, i.e. lower and upper bounds on each parameter. The range of the different parameters should reflect the prior knowledge of experienced values for the type of catchment being considered. Default limits based on physical and mathematical model constraints and experienced values for a range of different catchments are provided in Table 4.4.

Table 4.4 Calibration parameters and default hypercube search space

Parameter	Unit	Lower bound	Upper bound
$U_{\max}$	[mm]	5	35
$L_{\max}$	[mm]	50	400
CQOF	[-]	0	1
CKIF	[hours]	200	2000
$CK_{12}$	[hours]	3	72
TOF	[-]	0	0.9
TIF	[-]	0	0.9
TG	[-]	0	0.9
$CK_{BF}$	[hours]	500	5000



### Objective functions

The user can specify any combination of the 4 objective functions: (1) overall water balance error, (2) overall RMSE, (3) peak flow RMSE, and (4) low flow RMSE. For the peak and low flow RMSE the user should specify the threshold levels for defining peak and low flow events, respectively.

The choice of objective functions should reflect the objective of the model simulation. For general hydrological studies, the overall water balance error and overall RMSE is normally applied. If focus of the study is on high or low flows, the peak or low flow RMSE should be included. It is not advised to use only the water balance error for optimisation, since this may provide an unrealistic model calibration.

### Stopping criterion

The stopping criterion for the optimisation algorithm is the maximum number of model evaluations. The appropriate number of model evaluations depends primarily on the number of calibration parameters and the complexity of the model (interaction between model parameters). A large number of model evaluations are, in general, needed for a complex model with many parameters. This requirement should be balanced against the computing time. For a model calibration that includes all 9 parameters, a maximum number of model evaluations in the range 1000-2000 normally ensures an efficient calibration.

Besides the user-defined stopping criterion, the optimisation algorithm includes a parameter convergence criterion. In this case the optimisation algorithm stops if the entire population of parameter sets in an optimisation loop have converged into the same parameter values.

## 4.11 NAM - References

- /43/ Abbott, M.B. and J.C. Refsgaard (eds) (1996), Distributed Hydrological Modelling, Kluwer Academic Press, The Netherlands, 321 p.
- /44/ Brakensiek, D.L. (1979), Comments on 'Empirical Equations for some soil Hydraulic Properties' by Roger B. Clapp and George M. Hornberger, Water Resources Research, 15 (4), 989-990.
- /45/ Brakensiek, D.L., Engleman, R.L. and Rawls, W.J. (1981), Variation within texture classes of soil water parameters, Trans. ASAE, 24, 335-339.
- /46/ Cosby, B.J., Hornberger, G.M., Clapp, R.B. and Ginn, T.R. (1984), A statistical exploration of the relationships of soil moisture characteristics to the physical properties of soils, Water Resources Research, 20 (6), 682-690.
- /47/ Doorenbos, J. and W.O. Pruitt (1977), Guidelines for Predicting Crop Water Requirements. FAO Irrigation and Drainage paper No.



## 24. Food and Agricultural Organization of the United Nations.

- /48/ Duan, Q., Sorooshian, S., Gupta, V. (1992), Effective and efficient global optimization for conceptual rainfall-runoff models, *Water Resources Research*, 28(4), 1015-1031.
- /49/ Li, R.-M., Stevens, M.A. and Simons, D.B. (1976), Solutions to Green-Ampt infiltration equations, *J. Irrig. and Drain. Div., Amer. Soc. Civil. Eng.*, 102 (IR2), 239-248.
- /50/ Madsen, H. (1999), Automatic calibration of a conceptual rainfall-runoff model using multiple objectives, *Journal of Hydrology*, Submitted.
- /51/ McCuen, R.H., Rawls, W.J. and Brakensiek, D.L. (1981), Statistical analysis of the Brooks-Corey and Green-Ampt parameters across soil textures, *Water Resources Research*, 17, 1005-1013.
- /52/ Nash, I.E. and Sutcliffe, I.V. (1970), River flow forecasting through conceptual models, Part I, *Journal of Hydrology*, 10, 282-290.
- /53/ Nielsen, S.A. and E. Hansen (1973), Numerical simulation of the rainfall runoff process on a daily basis, *Nordic Hydrology*, 4, 171-190.
- /54/ Rawls, W.J., Brakensiek, D.L. and Saxton, K.E. (1982), Estimation of soil water properties, *Transactions of the ASAE*, 25, 1316-1320.
- /55/ Refsgaard, J.C. and J. Knudsen (1997), Operational validation and intercomparison of different types of hydrological models. *Water Resources Research*, 32(7), 2189-2202.
- /56/ Refsgaard, J.C. and Storm, B. (1996), Construction, calibration and validation of hydrological models, In: *Distributed Hydrological modelling* (eds. M.B. Abbott and J.C. Refsgaard), Kluwer Academic Press, The Netherlands, 41-54.
- /57/ Rijtema, P.E. (1969), Soil moisture forecasting, *Nota 513*, Instituut voor Cultuurtechniek en Waterhuishouding, Wageningen, The Netherlands.
- /58/ U.S. Army Corps of Engineers (1956), *Snow hydrology: Summary report on snow investigations*.



## 4.12 UHM

### 4.12.1 Introduction

The present UHM module simulates the **runoff from single storm events** by the use of the well known unit hydrograph techniques and constitutes an alternative to the NAM model for flood simulation in areas where no stream-flow records are available or where unit hydrograph techniques have already been well established. The module calculates simultaneously the runoff from several catchments and includes facilities for presentation and extraction of the results. The output from the module can further be used as lateral inflow to the advanced hydrodynamic module in MIKE 11.

In the unit hydrograph module the excess rain is calculated assuming that the losses to infiltration can be described as a fixed initial and constant loss, a proportional loss (the rational method) or by the SCS curve number method.

The excess rainfall is routed to the river by unit hydrograph methods. The module includes the SCS-dimensionless hydrographs as well as facilities for establishing and management of databases with user defined unit hydrographs and time series of recorded rainfall and streamflow.

### Storage function method

#### Basic equation

The continuity equation and momentum equation are given by:

$$A \frac{dS_i}{dt} = f r_{ave} A - Q_i \quad (4.33a)$$

$$S_i = K Q_i^P \quad (4.33b)$$

where:

$S_i$  apparent basin storage.

$Q_i$  direct runoff from a basin with consideration of the time of delay (except for base flow) .

$T_i$  time of delay.

$K, P$  constants.

$f$  coefficient of inflow.

$r_{ave}$  mean rainfall of river basin.

$A$  catchment area.



### Numerical solution

Equation (4.33a) is approximated as follows:

$$S_{i,t+\Delta t} - S_{i,t} = \left( r_{t+\Delta t} - \frac{q_{i,t} - q_{i,t+\Delta t}}{2} \right) \quad (4.34a)$$

$$Kq_{i,t+\Delta t}^P - Kq_{i,t}^P = \left( r_{t+\Delta t} - \frac{q_{i,t} - q_{i,t+\Delta t}}{2} \right) \quad (4.34b)$$

which by rearranging gives

$$2 \frac{K}{\Delta t} q_{i,t+\Delta t}^P + q_{i,t+\Delta t} - 2 \left( r_{t+\Delta t} - \frac{q_{i,t}}{2} + \frac{K}{\Delta t} q_{i,t}^P \right) = 0 \quad (4.34c)$$

where:

$r_{t+\Delta t}$  rainfall intensity at the time  $t+\Delta t$ .

$q_{i,t}$  runoff at the time  $t$  ( $Q/A$ ).

$s_{i,t}$  apparent storage at the time  $t$ .

$\Delta t$  time step.

Work out equation (4.34c) numerically using:

$$C = r_{t+\Delta t} - \frac{q_{i,t}}{2} + \frac{K}{\Delta t} q_{i,t}^P \quad (4.35a)$$

$$\text{and} \quad (4.35b)$$

$$x = q_{i,t+\Delta t} \quad (4.35c)$$

Thus equation (4.34c) now reads

$$2 \frac{K}{\Delta t} x^P + x - 2C = 0 \quad (4.36)$$

which is solved with respect to  $x$ .





## Quasi-linear function method

### Basic equation

Generating rational formula, rectangle unit hydrograph as follows is available.

$$U(\tau) = \begin{cases} 0 & \text{for } \tau < 0, \tau < t_c \\ \frac{1}{t_c} & \text{for } 0 < \tau < t_c \end{cases} \quad (4.37)$$

Or, moving average process as follows, by the time of flood concentration ( $t_c$ ).

$$q(\tau) = \frac{1}{t_c} \int_{t-t_c}^t r_e(\tau) d\tau \quad (4.38)$$

Using a kinematic wave method  $t_c$  is given by:

$$t_c = \left( \frac{L r_e^{1-m}}{\alpha} \right)^{1/m} \quad (4.39)$$

$L$  is the physical length of the slope,  $\alpha$ ,  $m$  are constants.

The relation between the water depth on the slope ( $h$ ) and the unit discharge ( $q$ ) is given by

$$q = \alpha h^m \quad (4.40)$$

The term  $m$  is 3 for laminar flow and 5/3 for Manning type flow.

Take  $S$  as the physical average grade of the slope,  $N$  as the equivalent roughness of Manning type.

$$\alpha \propto \frac{\sqrt{S}}{N} \quad (4.41a)$$

$$t_c \propto L^{1/m} N^{1/m} S^{-1/2m} r_e^{1/m-1} \quad (4.41b)$$

Kadoya and others get the following experimental equation:

$$t_c = CA^{0,22} r_e^{-0,35} \quad (4.42)$$



If the flood term  $t_c$  is fixed, the runoff hydrograph can be computed by equation (4.37). However the outflow would be zero if it passes  $t_c$ . Therefore, a logarithmic unit hydrograph given by

$$U(\tau) = \begin{cases} 0 & \text{for } \tau < 0 \\ \frac{1}{k} e^{-\tau k} & \text{for } 0 < \tau \end{cases} \quad (4.43)$$

where  $k = t_c/2$  (by Yoshino) is used.

### Numerical solution

The term  $k$  in the storage equation is given using time of flood concentration  $t_c$  by kadoya. Thus the equations to solve are given by

$$\frac{dS}{dt} = r_e - q \quad (4.44a)$$

$$S = kq \quad (4.44b)$$

where  $k = t_c/2$  and  $t_c$  is given by equation (4.42).

## Nakayasu method

### Basic equation

The unit hydrograph equation is given by

$$q(t) = \sum_{j=0}^{''} r_e(t-j\Delta t)h(j\Delta t) \quad (4.45)$$

where:

$q(t)$  Runoff height at time  $t$ .

$r_e(t)$  Effective rainfall intensity in time interval

$h(t)$  Unit hydrograph

$\Delta t$  Time interval

### Solution

The maximum discharge is given by

$$Q_{\max} = \frac{AR_0}{0,3T_1 + T_{0,3}} \quad (4.46)$$



The increasing curve in the unit hydrograph is given by

$$\frac{Q_d}{Q_{\max}} = \left( \frac{t}{T_1} \right)^{2,4} \quad (4.47)$$

The decreasing curve in the unit hydrograph leads

$$\frac{Q_d}{Q_{\max}} = \begin{cases} 0,3^{(t-T_1)/T_{0,3}} & \text{for } 1 \geq \frac{Q_d}{Q_{\max}} > 0,3 \\ 0,3^{(t-T_1+0,5T_{0,3})/1,5T_{0,3}} & \text{for } 0,3 \geq \frac{Q_d}{Q_{\max}} > 0,3^2 \\ 0,3^{(t-T_1+0,5T_{0,3})/2,0T_{0,3}} & \text{for } 0,3^2 \geq \frac{Q_d}{Q_{\max}} \end{cases} \quad (4.48)$$

where:

$Q_{\max}$  Maximum discharge in unit hydrograph.

$Q_d$  Unit hydrograph.

$A$  Catchment area.

$R_0$  Rainfall intensity.

$T_1$  Constant.

$T_{0,3}$  Constant.

#### 4.12.2 The Loss Model

During a storm a part of the total rainfall infiltrates the soil. Large parts of the infiltration evaporates or reaches the river a long time after the end of storm as baseflow. Hence in event models as the present one, it is reasonable to describe the major part of the infiltration as loss. The amount of rain actually reaching the river, i.e. the total amount of rainfall less the loss is termed the excess rainfall.

The unit hydrograph module includes **three optional methods** for calculation of the excess rainfall. They are all lumped models considering each catchment as one unit and hence the parameters represent average values for the catchment.

All the methods include an areal adjustment factor accounting, to some extent, for non uniform distribution the precipitation over the catchment.



## Proportional Loss (The rational method)

In this method the losses are assumed to be proportional to the rainfall rate and thus the excess rainfall is given by:

$$P_{excess} = a * A_f * P \quad (4.49)$$

where:

$P_{excess}$  Excess rainfall (mm/hr).

$a$  User defined run-off coefficient between 0 and 1.

$A_f$  Areal adjustment factor.

$P$  Rainfall (mm/hr).

## Fixed Initial Loss and Constant Loss

Following this method no excess rainfall will be generated before a user specified initial loss demand has been met. Subsequently excess rainfall will be generated whenever rainfall rate exceeds a specified constant loss rate i.e.

where:

$$P_{excess} = \begin{cases} 0 & ; \text{for } P_{sum} < I_a + I_c \cdot dt \\ A_f * P \cdot I_c & ; \text{for } P_{sum} > I_a \end{cases} \quad (4.50)$$

$P_{excess}$  Excess rainfall (mm/hr).

$P_{sum}$  Accumulated precipitation since start of storm event (mm).

$I_a$  User defined Initial loss (mm)

$I_c$ : User defined constant loss rate (mm/h)

$A_f$  Areal adjustment factor

$P$  Rainfall (mm/hr)

$dt$  Calculation time step (hr)



To some extent this method accounts for the losses being highest at the start of the storm.

## The SCS Loss Method

The U.S. Soil Conservation Service (SCS), /59/, developed this method for computing losses from storm rainfall in 1972.

For the storm as a whole, the depth of excess precipitation or direct runoff ( $P_e$ ) is always less than or equal to the depth of precipitation  $P$ ; likewise, after runoff begins, the additional depth of water retained in the watershed,  $F_a$ , is less than or equal to some potential maximum retention  $S$  (see Figure 4.6). There is some amount of rainfall  $I_a$ , (initial loss before ponding) for which no runoff will occur, so the potential runoff is  $P - I_a$ .

The hypothesis of the SCS method is that the ratios of the two actual to the two potential quantities are equal, that is

$$\frac{F_a}{S} = \frac{P_e}{P - I_a} \quad (4.51)$$

From the continuity principle

$$P = P_e + I_a + F_a \quad (4.52)$$

Combining equations (4.51) and (4.52) gives

$$P_e = \frac{(P - I_a)^2}{P - I_a + S} \quad (4.53)$$

which is the basic equation for computing the depth of excess rainfall or direct runoff from a storm by the SCS method.

By study of results from many small experimental watersheds, an empirical relation was developed.

$$I_a = 0.2S \quad (4.54)$$

Combining equations (4.53) and (4.54) the basic equation used in this model is derived.

$$P_e = \frac{(P - 0.2S)^2}{P + 0.8S} \quad (4.55)$$

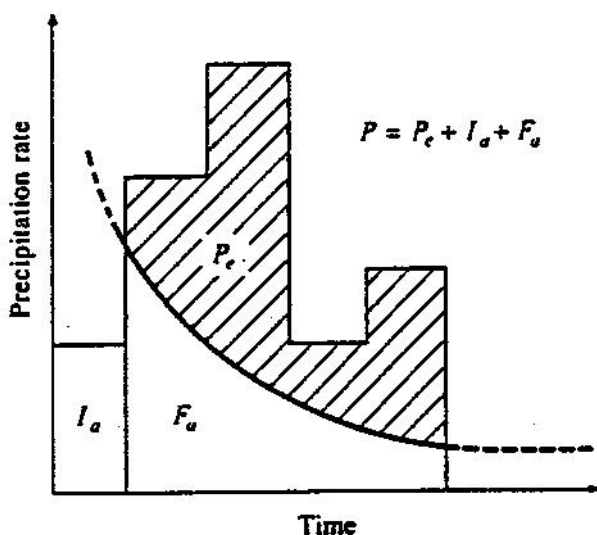


Figure 4.6 Variables in the SCS method of rainfall abstractions:  $I_a$  = initial abstraction,  $P_e$  = accumulated excess rain,  $F_a$  = continuing abstraction,  $P$  = total rainfall.

The potential maximum retention  $S$  is calculated from a dimensionless curve number (CN) using the empirical formula derived by SCS on the basis of rainfall runoff analyses of a large number of catchments.

$$S = \left( \left( \frac{1000}{CN} \right) - 10 \right) \cdot 25.4 \text{ (mm)} \quad (4.56)$$

The curve number depends on the soil type, the land use and the antecedent moisture condition (AMC) at the start of the storm.

CN varies between 0, resulting in no runoff, and 100 which generates an excess rain equal to the rainfall. For natural catchments normally  $50 < CN < 100$ .

The model operates with three different antecedent moisture conditions namely:

AMC(I) : Dry conditions close to wilting point.



AMC(II) : Average wet conditions close to field capacity.

AMC(III): Wet conditions close to saturation.

For each calculation time step the excess rainfall is calculated as the difference between the accumulated excess rainfall  $P_e$  at the start and the end of the time step.

Table 4.5 Correlation between SCS Curve numbers and the antecedent moisture condition as given in /59/.

Antecedent moisture conditions								
II	I	III	II	I	III	II	I	III
0	0	0	34	18	54	68	48	84
1	0	3	35	18	55	69	50	84
2	1	5	36	19	56	70	51	85
3	1	8	37	20	57	71	52	86
4	2	10	38	21	58	72	53	86
5	2	13	39	21	59	73	54	87
6	2	15	40	22	60	74	55	88
7	3	17	41	23	61	75	57	88
8	3	18	42	24	62	76	58	89
9	4	20	43	25	63	77	59	89
10	4	22	44	25	64	78	60	90
11	4	24	45	26	65	79	62	91
12	5	25	46	27	66	80	63	91
13	5	27	47	28	67	81	64	92
14	6	28	48	29	68	82	66	92
15	6	30	49	30	69	83	67	93
16	7	31	50	31	70	84	68	93
17	7	33	51	31	70	85	70	94
18	8	34	52	32	71	86	72	94
19	8	36	53	33	72	87	73	95
20	9	37	54	34	73	88	75	95
21	10	38	55	35	74	89	76	96
22	10	39	56	36	75	90	78	96
23	11	41	57	37	75	91	80	97
24	11	42	58	38	76	92	81	97
25	12	43	59	39	77	93	83	98
26	13	44	60	40	78	94	85	98
27	13	46	61	41	78	95	87	98
28	14	47	62	42	79	96	89	99
29	14	49	63	43	80	97	91	99
30	15	50	64	44	81	98	94	99
31	16	51	65	45	82	99	97	100
32	16	52	66	46	82	100	100	100
33	17	53	67	47	83			

The SCS method was developed on the basis of daily rainfall and consequently the program considers the beginning of a new 24 hour period as the start of a new storm event i.e.

- Each 24 hour AMC is updated by one class for each 16 mm rain fallen during the simulation period.
- CN and S are recalculated in correspondence with the updated AMC. Conversion of CN due to AMC is done using Table 4.5.
- The accumulated rainfall amount Pe is reset to zero.

## Nakayasu

The governing equations are given by

$$SRe = \alpha SR^\beta \text{ for } SR \leq R_{sa} \quad (4.57a)$$

$$Re = SR - R_{sa} + \alpha R_{sa}^\beta \text{ for } SR > R_{sa} \quad (4.58a)$$

where:

$Re$  Effective rainfall.

$SR$  Cumulative rainfall.

$R_{sa}$  Saturation rainfall.

$\alpha, \beta$  Constants.

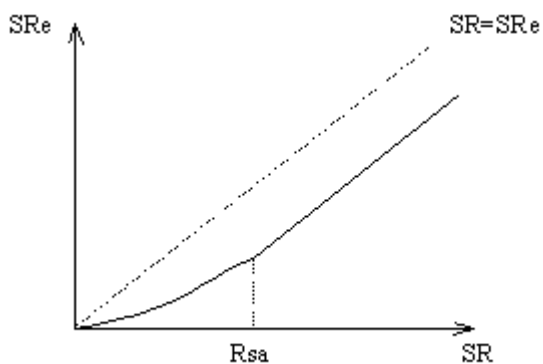


Figure 4.7 The effective cumulative rainfall as a function of the cumulative rainfall.





## $f_1$ - $R_{sa}$

The governing equation is given by

$$Re = \begin{cases} f_1 R & \text{for } 0 < SR \leq R1_{sa} \\ f_2 R & \text{for } R1_{sa} < SR \leq R2_{sa} \\ f_3 R & \text{for } R2_{sa} < SR \end{cases} \quad (4.59)$$

where:

$Re$  Effective rainfall.

$SR$  Cumulative rainfall.

$R_{sa}$  Saturation rainfall.

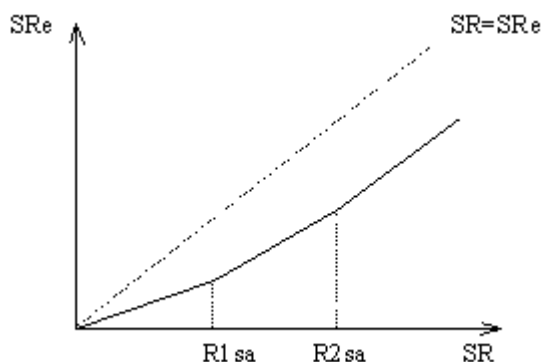


Figure 4.8 The effective cumulative rainfall as a function of the cumulative rainfall.

### 4.12.3 The Unit Hydrograph Routing Model

#### Basic Assumptions

The unit hydrograph method is a simple linear model that can be used to derive the resulting hydrograph from any amount of excess rainfall.

The unit hydrograph is the unit pulse response function of a linear hydrological system, i.e. the direct runoff hydrograph resulting from one unit of excess rain with the duration,  $t_r$ .

The following basic assumptions are inherent in this model:

- The excess rainfall has a constant intensity within the effective duration.

- The excess rainfall is uniformly distributed over the whole catchment area.
- The base time of the direct runoff hydrograph resulting from an excess rain with a given duration is constant.
- The ordinates of all direct runoff hydrographs of a common base time are directly proportional to the total amount of excess rain represented by each hydrograph.
- The principle of superposition applies to hydrographs resulting from continuous and/or isolated periods of uniform-intensity excess rain as illustrated on (see Figure 4.9).
- For a given catchment, the hydrograph resulting from a given excess rainfall reflects the unchanging conditions of the catchment.

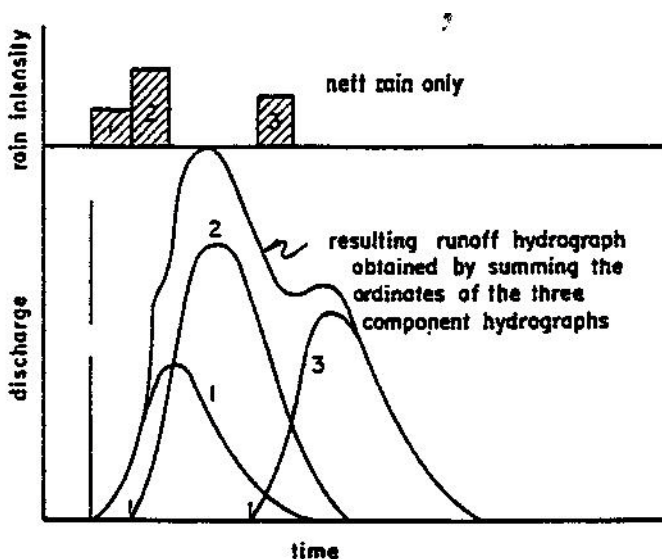


Figure 4.9 Principle of superposition applied to hydrographs.

Under natural conditions the above assumptions cannot be perfectly met. However in many cases the hydrological conditions come close enough to the above assumptions to generate satisfactory results. A more detailed discussion of the above assumptions can be found in /60/.

### Principle of calculation

In accordance with the principle of superposition, the model for each calculation time step determines the responding hydrograph to the excess rainfall, as generated by the loss model during this time step, and add the response to the flow contributions generated in previous time steps.

## Types of unit hydrographs

A unit hydrograph can be characterized by the duration of the unit rainfall ( $t_r$ ) resulting in the hydrograph and the lag time ( $t_l$ ) defined as the time difference between the centre of the unit rainfall event and the runoff peak.

From these two characteristics the time to peak ( $T_p$ ), i.e. the time from the start of the storm event until the occurrence of peak runoff can be calculated as:

$$T_p = t_r/2 + t_l \quad (4.60)$$

In reality the unit hydrograph of a given catchment is unique. However, large efforts have been put in development of synthetic unit hydrographs which are more or less generally applicable. Two such hydrographs namely the SCS triangular unit hydrograph and the SCS dimensionless hydrograph (see Figure 4.10) are pre-specified in the model.

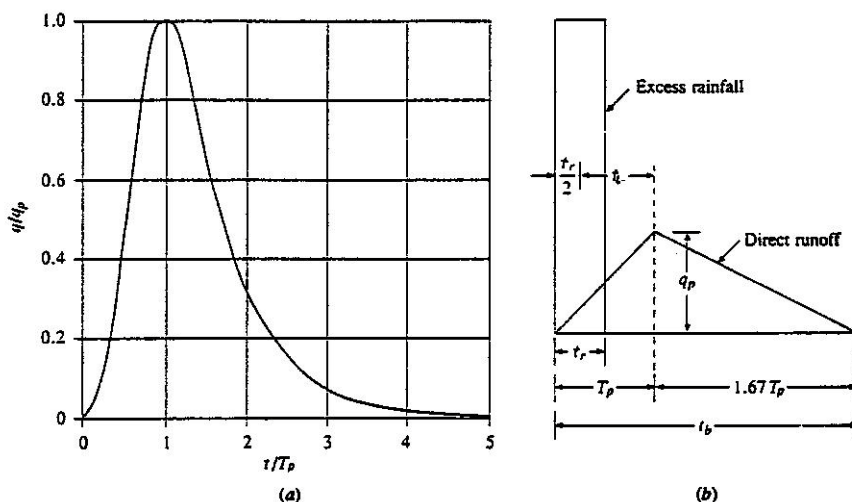


Figure 4.10 Soil Conservation Service Synthetic Hydrographs. (a) Dimensionless hydrograph. (b) Triangular hydrograph.

The user can either use one of these or choose to apply a user defined hydrograph from the unit hydrograph data base.

The model supports three types of user defined hydrographs:

1. Dimensionless hydrographs specified as the flow divided by the peak flow ( $q/q_p$ ) as a function of the time divided by the time to peak ( $T/T_p$ ).
2. Catchment specific hydrographs which are entered in dimensions and with correspondent unit rain duration,  $t_r$ .



### 3. Instantaneous unit hydrographs derived by the time-area method.

Instantaneous unit hydrographs are automatically converted to hydrographs, i.e. 'dt'-hour-hydrographs with a unit rain duration equal to the calculation time step (dt) after the formula:

$$qdt(t) = (q(t) + q(t-dt)) / 2 \quad (4.61)$$

where:

qdt(t) Ordinate at time = t of the 'dt'-hour-hydrograph.

q(t) Ordinate at time = t of the instantaneous hydrograph.

t Actual calculation time.

dt Calculation time step.

The present version of the program does not include a facility for deconvolution of hydrographs and hence non instantaneous unit hydrographs are assumed to originate from a unit rain of duration equal to the time step.

The user must specify the lag time to be used in a given the calculation. The program will then scale the applied hydrograph accordingly ensuring that the area under the curve is unity.

## Lag time

The lag time can either be specified directly or may be calculated from catchment characteristics using the standard SCS formula:

$$t_l = \left( L * 3.28 * 10^3 \right)^{0.8} * \left( 1000 / CN - 9 \right)^{0.7} / \left( 1900 * Y^{0.5} \right) \quad (4.62)$$

where:

t<sub>l</sub> Lag time in hours.

L Hydraulic length of the catchment in km.

CN SCS curve number.

Y Average catchment slope in per cent.

A unit-hydrograph derived from a time-area curve is considered catchment specific. consequently specification of arbitrary lag times are not allowed if the time-area method is applied. The program will simply use the lagtime implicitly given by the time-area curve.



The time-area method in the UHM-model performs a pure translation of the excess rainfall hydrograph via the drainage network, described using the channel travel time. This results in an outflow hydrograph that ignores watershed storage effects.

#### 4.12.4 Kinematic wave hydrograph methods

Runoff models are classified into two groups; a distributed one and a lumped one. The kinematic wave model is typically of the distributed one.

In the kinematic wave model, catchment area is considered to be composed of channels and slopes. The hydraulic equations are applied to slope and river channel, and solved by using kinematic wave theory. As the result, characteristics of the runoff process such as the time of concentration and flow resistance are theoretically described.

##### Basic equations

Equations of motion and continuity of an open channel flow are

$$\frac{1}{g} \frac{\partial v}{\partial t} + \frac{v}{g} \frac{\partial v}{\partial x} + \frac{\partial h}{\partial x} + I_e = \frac{v}{gA} (I - F) \quad (4.63)$$

and

$$\frac{\partial A}{\partial t} + \frac{\partial Q}{\partial x} = I - F \quad (4.64)$$

where,  $g$ : gravitational acceleration,  $v$ : velocity,  $t$ : time,  $h$ : depth,  $x$ : distance,  $z$ : bed elevation,  $I_e$ : energy gradient,  $A$ : cross-sectional area,  $I$ : inflow rate,  $F$ : outflow rate and  $Q$ : discharge of the channel.

Generally, the first terms of the left-hand side and the right-hand side of Eq. (4.63) are negligibly small. In the case that the channel is relatively steep, the second and the third terms of the left-hand side of Eq. (4.63) are much smaller than the fourth one. Therefore, this equation is simplified as

$$\frac{\partial z}{\partial x} + I_e = 0 \quad (4.65)$$

##### Modelling Hill slope:

##### Kinematic wave equations on a slope

On a slope as illustrated in Figure 4.11,  $A=Bh$ ,  $Q=Bq$ ,  $I=Brcos\theta$  and  $F=Bfcos\theta$ , where,  $B$ : width of the slope,  $q$ : discharge per unit width,  $r$ : rainfall intensity,  $f$ : infiltration rate, and  $\theta$ : slope angle.

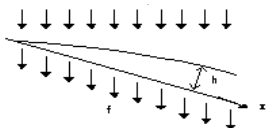


Figure 4.11 Illustration of slope for kinematic wave equation

Eq. (4.64) is rewritten as

$$\frac{\partial h}{\partial t} + \frac{\partial q}{\partial x} = (r - f) \cos \theta \quad (4.66)$$

If we apply Manning's equation to Eq. (4.65) we obtain

$$v = k_s q^p, \quad k_s = \left( \frac{n}{\sqrt{\sin \theta}} \right)^p \quad \text{and } p = 0.6 \quad (4.67)$$

where,  $n$ : roughness coefficient.

Substituting (4.67) into eq. (4.66) yields

$$k_s p q^{p-1} \frac{\partial q}{\partial t} + \frac{\partial q}{\partial x} = r_e \quad (4.68)$$

where,  $r_e = (r-f)\cos\theta$  : effective rainfall intensity.

Characteristic curve expression of Eq. (4.68) is

$$\frac{dt}{k_s p q^{p-1}} = \frac{dx}{l} = \frac{dq}{r_e} \quad (4.69)$$

From the above equation, we obtain

$$\frac{dx}{dt} = \frac{l}{k_s p} q^{1-p} \quad (4.70)$$

$$\frac{dq}{dx} = r_e \quad (4.71)$$

and

$$\frac{dq}{dt} = \frac{l}{k_s p} q^{1-p} r_e \quad (4.72)$$



## Rectangular slope model

If a basin is considered to be rectangular, slope length is a constant

Equation (4.72) is integrated as below:

$$q(x + \Delta x, t + \Delta t) = \left( q^p(x, t) + \frac{1}{k_s} \int_t^{t+\Delta t} r_e dt \right)^{1/p} \quad (4.73)$$

Relation between  $\Delta x$  and  $\Delta t$  is given by Eqs. (4.70) and (4.71) as

$$\left. \begin{aligned} \Delta x &= \frac{q(x + \Delta x, t + \Delta t) - q(x, t)}{r_e} && ; r_e > 0 \\ \Delta x &= \frac{\Delta t}{k_s p q^{p-1}(x, t)} && ; r_e = 0 \end{aligned} \right\} \quad (4.74)$$

By substituting  $\Delta x=l$  and  $\Delta t=T$  into Equation (4.73), discharge at the end of a slope is obtained as

$$q(l, t) = \left( \frac{1}{k_s} \int_{t-T}^t r_e(\tau) d\tau \right)^{1/p} \quad (4.75)$$

where,  $l$ : slope length and  $T$ : time of concentration.

## Distributed slope length model

Generally, shape of a basin is not rectangular, but slope length likely to distributes log-normally. In this model, logarithmic normal distribution of slope length is assumed.

Integration of Eq. (4.70) yields

$$l = \frac{1}{k_s p} \int_{t-T}^t q^{1-p} d\tau \quad (4.76)$$

Runoff intensity from a basin,  $q_*$ , is defined as

$$q_*(t)A = \int_0^L q(l, t) dx \quad (4.77)$$

where,  $A$ : catchment area and  $L$ : channel length

In the case that the effective rainfall intensity is constant and continues over a long period of time, i.e.  $r_e(t) = r_0$ ;  $0 \leq t < \infty$ , integration of Eq. (4.71) yields

$$q(l, t) = l r_0 \text{ and } q_*(t)A = \int_0^L l r_0 dx$$



As  $q_*(t)=r_0$  in this case we obtain

$$A = \int_0^L l r dx \quad (4.78)$$

and

$$dA = l dx = A f(l) dl \quad (4.79)$$

where  $f(l)$ : density function of slope length.

Substituting Eq. (4.79) into Eq. (4.77) we obtain

$$q_*(t) = \int_0^L \frac{q(l, t)}{A} dx = \int_0^\infty q(l, t) \frac{f(l)}{l} dl \quad (4.80)$$

If we use log-normal distribution function for the density function of slope length, then  $X=\log(l)$ ,  $f(l)dl=F(X)dX$  and

$$F(X) = \frac{1}{\sqrt{2\pi}S} \exp\left(-\frac{(X-X_m)^2}{2S^2}\right) \quad (4.81)$$

where,  $X_m=\log_{10} l_m$ ,  $l_m$ : mean slope,  $S$ :  $\log_{10}\sigma$  and  $\sigma$ : standard deviation of slope length.

Substitution of Eq. (4.81) into Eq. (4.80) yields

$$\begin{aligned} q_*(t) &= \int_0^\infty q(l, t) \frac{f(l)}{l} dl \quad (4.82) \\ &= \exp\left(-cX_m + \frac{(cS)^2}{2}\right) \int_{-\infty}^\infty \frac{q(l, t)}{\sqrt{2\pi}S} \exp\left[-\frac{\{X - (X_m - cS^2)\}^2}{2S^2}\right] dx \end{aligned}$$

#### 4.12.5 Calculation time step

As no deconvolution of the unit hydrographs stored in the database is performed by the model the user must make sure that the specified calculation time step correspond to the unit rain duration for the unit hydrograph, if a user defined hydrograph is selected.

If the SCS hydrographs are used /60/ suggest the time step to be selected as 22% of the lag time and that it should not exceed 27% of the lag time.





## 4.12.6 UHM - References

- /59/ SCS, National Engineering Handbook, Section 4, Hydrology, Soil Conservation Service, U.S. Department of Agriculture, 1972.
- /60/ Chow, V.T., David R. Maidment, Larry W. Mays. Applied Hydrology. McGraw-Hill Book Company, 1988.

## 4.13 SMAP

### 4.13.1 Introduction

SMAP is a hydrological rainfall-runoff simulation model of the lumped conceptual type. The model continuously accounts for the moisture storage in the root zone and in the groundwater of catchment as well as the inter actions between these two storages and their influence on the catchment evaporation and runoff.

Just like other continuously moisture accounting rainfall runoff models SMAP needs continuous series of rainfall and potential evapotranspiration from the whole simulation period as input and in addition observed monthly discharges from a period of four to eight years for calibration.

Unlike the NAM model SMAP has been designed to operate on the basis of monthly data. This may save data collection and preprocessing work and may therefore be an advantage in studies where a daily resolution of the output is not required. the model requires calibration against monthly discharges for four to ten year period.

### 4.13.2 SMAP model equations

SMAP describes the various water exchange processes taking place in a catchment by largely simplified mathematical equations. These equations includes the following five parameters which, when they have been properly calibrated, together reflects the hydrological characteristics of the catchment in question.

The model parameters are:

- Max storage in the root zone (The saturation capacity of the soil storage) (SAT)
- The control exponent of the Evapotranspiration (E1)
- The control exponent of surface runoff (E2)
- The recharge coefficient of the groundwater level (CREC)
- The recession time constant of the groundwater reservoir (CK)



- The following parameters are necessary to define the initial conditions for the model:
- The initial rate of content of water in the soil (RSOL initial)
- The base flow outflow from the catchment by the start of the simulation period (Qbin)

Qbin will in the model be used to calculate the initial storage in the groundwater reservoir from the formula:

$$RSUB_1 = (Q_{BIN} \cdot T) / S \cdot (1 - CK) \quad (4.83)$$

where

S Surface of the catchment in km<sup>2</sup>.

T Number of seconds in the month.

Figure 4.12 shows the schematics of the SMAP model and indicates how the reservoirs are linked up.

The two linear reservoirs represent the soil moisture and the groundwater reservoir respectively.

The degree of moisture saturation in the root zone is described by the equation:

$$TU = RSOL/SAT \quad (4.84)$$

where

RSOL Level in mm of the soil storage

SAT Saturation level in mm of the basin.

In each time step a fraction of the rain water is routed instantaneously to the river as surface runoff, While the remaining part of the rainfall feeds the root zone storage. The surface runoff is calculated as:

$$OF = P \cdot TU^{E2} \quad (4.85)$$

where

OF Surface runoff in mm

P Precipitation in mm

The parameter E2 is a coefficient control of the surface runoff.



In the soil storage, part of the stored water is extracted as evaporation. SMAP calculates this actual evapotranspiration from the potential evapotranspiration and the saturation degree of the root zone

$$E_a = E_p * TU^{E1} \quad (4.86)$$

where

$E_a$  Actual evaporation in mm

$E_p$  Potential evapotranspiration in mm

$E1$  Parameter controlling the surface evaporation

The recharge of the groundwater reservoir (groundwater level) is deduced from the root zone storage. The recharge is a function of the saturation degree of the rootzone and the crec parameter:

$$REC = RSOL * TU^4 * CREC \quad (4.87)$$

where

REC Recharge in mm

CREC Recharge coefficient of the groundwater level

The groundwater reservoir is a normal linear reservoir with a time constant CK.

The water balance for the root zone and groundwater storages carried out for each calculation time step follows the equations:

$$RSUB_{(i+1)} = RSUB_i + REC - BF \quad (4.88)$$

$$RSOL_{(i+1)} = RSOL_i + P - E_a - OF - REC \quad (4.89)$$

where  $i$  and  $i+1$  signifies values at two consecutive time steps. And where RSOL and RSUB are the contents of the root zone and groundwater storages.

The total discharge from the catchment is the sum of the surface runoff and the base flow (BF) sum of the surface discharge ES and the basic discharge EB result in the output at the control point of the basin, which is:

$$Q = (ES + EB) \text{ (mm)} \quad (4.90)$$

The water contents of the two reservoirs are updated every time step on the basis of the calculated surface runoff, groundwater recharge, actual evaporation and base flow. Since no iterations are carried out in the model the results

depend on the calculation selected time step. DHI has found that running the model with daily time steps even with monthly input improves significantly the model performance.

The entry data are: precipitation (mm/month), evaporation (mm/month), the monthly mean discharge ( $\text{m}^3/\text{s}$  or  $\text{Hm}^3$ ) which will allow the model calibration.

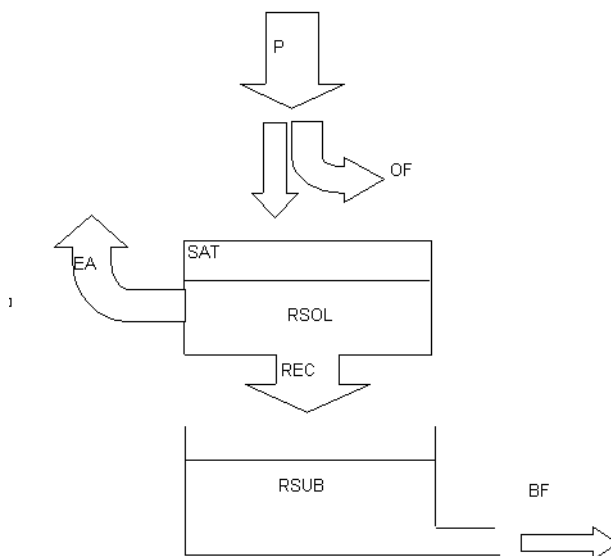


Figure 4.12 Schematics of the SMAP mode

## 4.14 Urban

### 4.14.1 Introduction

Two different urban runoff computation concepts are available in the Rainfall Runoff Module as two different runoff models:

Model A) Time/area Method

Model B) Non-linear Reservoir (kinematic wave) Method

The two used concepts are the same methods as used in the MOUSE, see MOUSE Surface Runoff models, Reference Manual.



## 4.14.2 Urban, model A, Time/area Method

### Introduction

The concept of Urban Runoff Model A is founded on the so-called "Time-Area" method. The runoff amount is controlled by the initial loss, size of the contributing area and by a continuous hydrological loss.

The shape of the runoff hydrograph is controlled by the concentration time and by the time-area (T-A) curve. These two parameters represent a conceptual description of the catchment reaction speed and the catchment shape.

### Hydrological Parameters

**Initial Loss** - defines the precipitation depth, required to start the surface runoff. This is a one-off loss, comprising the wetting and filling of catchment depressions. During dry period, the initial storage capacity is increased with the evaporation rate until the initial storage capacity is back to the initial loss capacity. The evaporation rate is specified as a timeseries or alternatively set equal to 0.05 mm/h.

**Hydrological Reduction** - runoff reduction factor, accounts for water losses caused by e.g. evapo-transpiration, imperfect imperviousness, etc. on the contributing area.

**Time/Area Curve** - accounts for the shape of the catchment lay-out, determines the choice of the available T/A curve to be used in the computations.

Three pre-defined types of the T/A curves are available:

- 1 - rectangular catchment
- 2 - divergent catchment
- 3 - convergent catchment

**Concentration Time** - defines the time, required for the flow of water from the most distant part of the catchment to the point of outflow.

### Runoff computation

The continuous runoff process is discretised in time by the computational time step  $\Delta t$ . The assumption of the constant runoff velocity implies the spatial discretisation of the catchment surface to a number of cells in a form of concentric circles with a centre point at the point of outflow. The number of cells equals to:

$$n = \frac{t_c}{\Delta t} \quad (4.91)$$

where:

$t_c$ : concentration time

$\Delta t$ : simulation time step

MIKE 11 calculates the area of each cell on the basis of the specified time-area curve. The total area of all cells is equal to the specified impervious area.

A time-area curve characterises the shape of the catchment, relating the flow time i.e. concentric distance from the outflow point and the corresponding catchment sub-area. There are three pre-defined time/area curves available in MIKE 11. Irregularly shaped catchments can be more precisely described by the user-specified T/A curves.

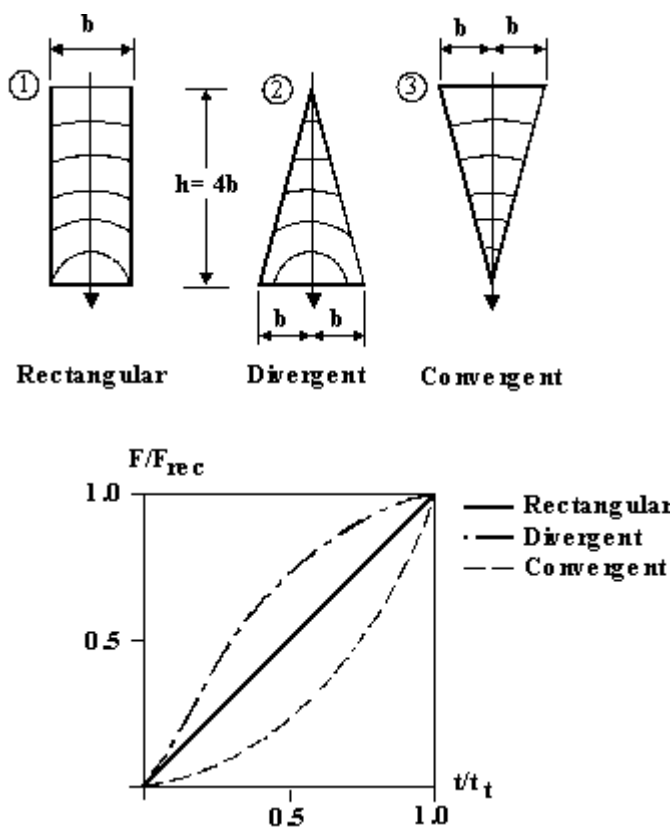


Figure 4.13 The three pre-defined time/area curves available in MIKE 11

The runoff starts after the rain depth has exceeded the specified initial loss for the catchment. The runoff stops when the accumulated rain depth on the



whole catchment surface regresses below the specified initial loss for the catchment.

At every time step after the start of the runoff, the accumulated volume from a certain cell is moved to the downstream direction. Thus, the actual volume in the cell is calculated as a continuity balance between the inflow from the upstream cell, the current rainfall (multiplied with the cell area) and the outflow to the downstream cell. The outflow from the most downstream cell is actually the resulting surface runoff hydrograph.

To account for the specified hydrological reduction, the runoff from the impervious surface is reduced by the catchment's hydrological reduction factor.

### 4.14.3 Urban, model B, Non-linear Reservoir (kinematic wave) Method

#### Introduction

The concept of surface runoff computation of Urban Runoff Model B is founded on the kinematic wave computation. This means that the surface runoff is computed as flow in an open channel, taking the gravitational and friction forces only. The runoff amount is controlled by the various hydrological losses and the size of the actually contributing area.

The shape of the runoff hydrograph is controlled by the catchment parameters length, slope and roughness of the catchment surface. These parameters form a base for the kinematic wave computation (Manning equation).

#### Model Specific Data

**Length** - conceptually, definition of the catchment shape, as the flow channel. The model assumes a prismatic flow channel with rectangular cross section. The channel bottom width is computed from catchment area and length.

**Slope** - average slope of the catchment surface, used for the runoff computation according to Manning.

**Surface type areas** - fractions of the catchment surface belonging to different surface types:

- impervious steep
- impervious flat
- pervious -small impermeability
- pervious - medium impermeability
- pervious - large impermeability

The model applies different hydrological parameters for each of the surface types.



## Hydrological Parameters

**Wetting loss** - one-off loss, accounts for wetting of the catchment surface.

**Storage loss** - one-off loss, defines the precipitation depth required for filling the depressions on the catchment surface prior to occurrence of runoff.

**Start infiltration** - defines the maximum rate of infiltration (Horton) for the specific surface type.

**End infiltration** - defines the minimum rate of infiltration (Horton) for the specific surface type.

**Horton's Exponent** - time factor "characteristic soil parameter". Determines the dynamics of the infiltration capacity rate reduction over time during rainfall. The actual infiltration capacity is made dependent of time since the rainfall start only.

**Inverse Horton's Equation** - time factor used in the "inverse Horton's equation", defining the rate of the soil infiltration capacity recovery after a rainfall, i.e. in a drying period.

**Manning's number** - Describes roughness of the catchment surface, used in hydraulic routing of the runoff (Manning's formula).

## Runoff computations

The model computations are based on the volume continuity and the kinematic wave equations.

The first step is the calculation of effective precipitation intensity. The effective precipitation intensity is the precipitation which contributes to the surface runoff.

Next, the hydraulic routing, based on the kinematic wave formula (Manning) and volume continuity is applied. The sketch with schematics of the model computation is shown in Figure 4.13.



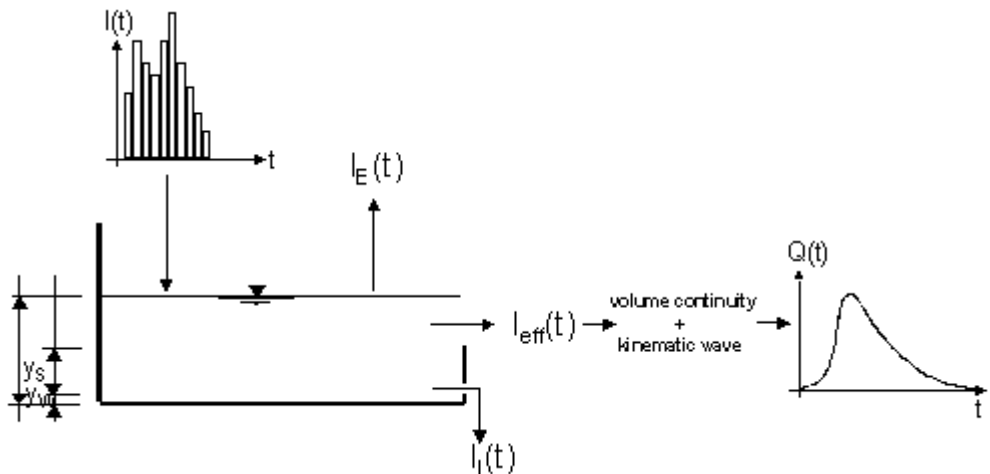


Figure 4.14 The simulated processes in the Surface runoff model B.

## Computing effective precipitation

The simulated hydrologic processes account for various losses calculated - evaporation, wetting, infiltration and surface storage - according to the conventions and equations presented below. The remaining precipitation is called effective precipitation, defined generally as:

$$I_{eff}(t) = I(t) - I_E(t) - I_W(t) - I_I(t) - I_S(t)$$

$$I_{eff} \geq 0 \quad (4.92)$$

where,

$I(t)$  Actual precipitation at time  $t$ ,

$I_E(t)$  Evaporation loss at time  $t$ . It should be noted that the

Evaporation loss for the catchment is accounted only if it has been specified as input timeseries

$I_W(t)$  Wetting loss at time  $t$ ,

$I_I(t)$  Infiltration loss at time  $t$ ,

$I_S(t)$  Surface Storage loss at time  $t$ .



The individual terms in the loss equation are fundamentally different, as some terms are continuous where others are discontinuous. If the calculated loss is negative, it is set to zero.

The actual precipitation,  $I(t)$ , is assumed to be uniformly distributed over the individual catchments. Otherwise, it may vary as a random time function.

The evaporation,  $IE(t)$ , is a continuous loss that is normally of less significance for single event simulations. However, on a long-term basis, evaporation accounts for a significant part of hydrological losses. If included in the computation, the evaporation is the first part subtracted from the actual precipitation, according to the following:

$$I_E(t) = \begin{cases} I_{PE}(t) & \text{for } (I(t) \geq I_{PE}(t)) \text{ OR } (y(t) > 0) \\ I(t) & \text{for } (I(t) < I_{PE}(t)) \text{ AND } (y(t) = 0) \end{cases} \quad (4.93)$$

where:

$I(t)$  Actual precipitation at time  $t$ ,

$IE(t)$  Evaporation loss at time  $t$ .

$I_{PE}(t)$  Potential evaporation at time  $t$ ,

$y(t)$  Accumulated depth at time  $t$ .

The wetting,  $I_W(t)$ , is a discontinuous loss. When precipitation starts, a part of the precipitation is used for wetting of the surface if the surface is initially dry. The model assumes that the precipitation remaining after subtraction of the evaporation loss is used for wetting of the catchment surface. When the surface is wet, the wetting loss,  $I_W$ , is set to zero. This is summarised in the following expression:

$$I_W(t) = \begin{cases} I(t) - I_E(t) & \text{for } y(t) < y_w \\ 0 & \text{for } (I(t) \leq I_E(t)) \text{ OR } (y(t) \geq y_w) \end{cases} \quad (4.94)$$

where:

$I(t)$  Actual precipitation at time  $t$ ,

$IE(t)$  Evaporation loss at time  $t$ .

$I_W(t)$  Wetting loss at time  $t$ ,



$y_W$  Wetting depth,

$y(t)$  Accumulated depth at time  $t$ .

The infiltration,  $I(t)$ , is the water loss to the lower storage caused by the porosity of the catchment surface. It is assumed that the infiltration starts when the wetting of the surface has been completed. The infiltration loss is calculated according to the following relations:

$$I(t) = \begin{cases} I_H(t) & \text{for } (y(t) \geq y_W) \text{ AND } (I(t) - I_E(t) - I_W(t) \geq I_H(t)) \\ I(t) - I_E(t) - I_W(t) & \text{for } (I(t) - I_E(t) - I_W(t)) < I_H(t) \\ 0 & \text{for } y(t) < y_W \end{cases} \quad (4.95)$$

where:

$I(t)$  Infiltration loss at time  $t$ .

$I_H(t)$  Horton's infiltration at time  $t$  (see below),

$y_W$  Wetting depth,

$y(t)$  Accumulated depth at time  $t$ .

The infiltration is a complex phenomenon, dependent on the soil porosity, moisture content, groundwater level, surface conditions, storage capacity, etc. The model calculates the infiltration loss capacity using the well-known Horton's equation:

$$I_H(t) = I_{\min} + (I_{\max} - I_{\min}) \cdot e^{-kat} \quad (4.96)$$

where:

$I_H(t)$  Infiltration loss calculated according to Horton

$I_{\max}$  Maximum infiltration capacity (after a long dry period),

$I_{\min}$  Minimum infiltration capacity (at full saturation),

$t$  Time since the start of the reduction process,

$ka$  Time factor (characteristic soil parameter) for wetting conditions.



In the dry period following the rainfall, the infiltration capacity is gradually recovered to the initial value, using an inverse form of the Horton's equation:

$$I_H(t) = I_{IT} + (I_{I_{\max}} - Q_{IT}) \cdot e^{-1/kht} \quad (4.97)$$

where:

$I_H(t)$  Infiltration loss capacity calculated according to Horton,

$I_{I_{\max}}$  Maximum infiltration capacity (after a long dry period),

$I_{IT}$  Infiltration capacity at the threshold between the wetting and drying period

$t$  Time since the start of the recovery process,

$kh$  Time factor (characteristic soil parameter) for drying conditions.

The surface storage.  $IS(t)$ , is the loss due to filling the depressions and holes in the terrain. The model begins with the surface storage calculation after the wetting process is completed. The surface storage is filled only if the current infiltration rate is smaller than the actual precipitation intensity reduced by evaporation. The actual surface storage loss is calculated according to the following:

$$IS(t) = \begin{cases} I(t) - I_E(t) - I_W(t) - I(t) & \text{for } y(t) \leq (y_W + y_S) \\ 0 & \text{for } y(t) > (y_W + y_S) \end{cases} \quad (4.98)$$

where:

$I(t)$  Precipitation intensity at time  $t$ ,

$IS(t)$  Surface storage loss at time  $t$ ,

$I_I(t)$  Infiltration loss at time  $t$ ,

$I_W(t)$  Wetting loss at time  $t$ ,

$I_E(t)$  Evaporation loss at time  $t$ ,

$y_W$  Wetting depth,

$y_S$  Surface storage depth,

$y(t)$  Accumulated depth at time  $t$ .



## The Surface Runoff routing

The runoff starts when the effective precipitation intensity is larger than zero. The hydraulic process is described with the kinematic wave equations for the entire surface at once. This description assumes uniform flow conditions on the catchment surface, i.e. equal water depth over the entire surface of certain category.

This type of runoff model is also called a non-linear reservoir model.

The surface runoff at time  $t$  is calculated as:

$$Q(t) = M \cdot B \cdot I^{1/2} \cdot y_R(t)^{5/3} \quad (4.99)$$

where:

$M$  Manning's number,

$B$  Flow channel width, computed as:

$B = A / L$

$I$  Surface slope,

$y_R(t)$  Runoff depth at time  $t$ .

The depth  $y_R(t)$  is determined from the continuity equation:

$$I_{eff}(t) \cdot A - Q(t) = \frac{dy_R}{dt} \cdot A \quad (4.100)$$

where:

$I_{eff}$  Effective precipitation,

$A$  Contributing catchment surface area,

$dt$  Time step,

$dy_R$  Change in runoff depth.

## Impact of Catchment Surface Type on Computations of Losses

Surface Runoff Model B distinguishes between up to 5 different catchment surface types. This is practically handled by the model so that the individual catchment is split into up to five sub-catchments, each with the area according to the specified percentages for specific surface categories.

For each surface type, only relevant processes are simulated. The model treats every area with different surface category as a sub-catchment, and the runoff computations are performed individually. The total runoff from the entire catchment is obtained then as a sum of runoffs from up to five different sub-catchments.

## 4.15 DRiFt

### 4.15.1 Introduction

DRiFt (Discharge River Forecast), a semi-distributed event model based on a geomorphologic approach, is presented. This model is focused on the efficient description of the drainage system in its essential parts: hillslopes and channel networks are addressed with two kinematic scales, which determine the base of the geomorphologic response of the basin. The geomorphologic module is coupled with a distributed representation of soil infiltration properties, while the rainfall event is schematized with its variability in time and space. The runoff volume is routed with a time variant TUH (T-hour Unit Hydrograph) technique, which takes into account the runoff production variability. Parameters calibration and validation has to be carried out using different intense rainfall events in different size basins. This robust and parsimonious model is able to predict consistently the main features of the hydrograph; the observed parameter invariance with basin size and rainfall intensity within a homogeneous region allows the reliable utilization for engineering purposes as well as for flood forecasting, especially in regions where many small non-gauged basins are present.

The development of DRiFt has been made by CIMA - Centro di ricerca Inter-universitario in Monitoraggio Ambientale - a research institution of the Universities of Genoa and Basilicata (Italy), in cooperation with ACROTEC S.r.l..

### 4.15.2 Model structure

The model frame is quite simple and it is focused on the main characteristics of the hydrograph: peak and time to peak. Its parameters must be evaluated by fitting computed hydrographs to observed ones, placing this model in the calibrated parameters models category.

The parameters have an intuitive and direct physical meaning; it is therefore possible to control their values after the calibration. This is important because it simplifies the validation procedure, but, moreover, because it shows the goodness of the processes schematisation. This schematisation takes into account the spatial variation of inputs such as rainfall, morphologic, geological and anthropic characteristics of the basin, but it is lumped in parameters, which represent characteristic values all over the catchment. The model outputs can be obtained in a given location wherever in the catchment. From a technical point of view this is the main feature of the model, as it conceals



most of the advantages of both distributed and lumped models. The geomorphologic filter, described in detail in section “Morphological parameters”. The morphological parameters:  $AS^k$  and  $k$ , is used to distinguish hillslopes and channel network starting from a space-filling representation of the drainage system directly obtainable from Digital Elevation Models (DEM). The routing time of each site in the basin is evaluated assigning different typical velocity values in each pixel pertaining to the basin and classified as hillslope or channel. The two velocities,  $v_h$  and  $v_c$ , used to describe the flow routing process in each of the two components of the drainage system are assumed constant; they maintain a physical meaning as the average velocities on hillslopes and in channel network, related to a particular range of discharge, and to the particular class of basin considered.

The Instantaneous Unit Hydrograph (IUH) technique (Sherman, 1932), used to determine the basin response is applied with some differences with respect to the classical procedure. Here in fact, the runoff generation is computed in each pixel of the basin at any time step considering the soil infiltration capacity heterogeneity and the rainfall field variability. This leads to a time variant unit response of the basin allowing a better representation of the real basin behaviour excited by a particular rainfall distribution.

Schematically, discharge at any location along the drainage network is represented by the expression:

$$Q(t) = \int_B M\left(t - \frac{d_h(x)}{v_h} - \frac{d_c(x)}{v_c}, x\right) dx \quad (4.101)$$

where  $B$  is the drainage basin above the specified location,  $M(t,x)$  is the runoff rate at time  $t$  and location  $x$ ,  $d_h(x)$  denotes the distance from  $x$  to the closest stream channel and  $d_c(x)$  denotes the distance from  $x$  to the outlet of the basin specified by the region  $B$ . The runoff rate  $M(t,x)$  is computed from the rainfall rate  $P(t,x)$  using the Soil Conservation Service method (SCS, 1972) with the Curve Number parameters locally defined, according to lithology, soil type, land cover and use (see UHM model, paragraph 4.12).

### Range of applicability of the model.

Typical environments for DRiFt applications are steep and relatively small mountainous catchments, where the draining network is clearly definable.

The model is also suitable to describe hortonian dominated hydrological environments, in general where the catchments' size does not exceed 3000-4000 km<sup>2</sup>.

Moreover, the use of DRiFt should be avoided for those basins where subsurface and base flows are relevant. In particular, presence of karsts phenomena might strongly affect the runoff behaviour, modifying groundwater contributions not considered by the model.



Caution is also required in using parameters derived in one hydrological regime for prediction in another region. It is evident that the relative importance and even nature of hydrological processes vary between countries, and from one region to another in the same country. Therefore an “ad hoc” calibration is needed when the hydrological environment changes significantly.

### 4.15.3 Data requirements

The basic input requirements for the DRiFt model consists of:

- Digital Elevation Model (DEM)
- Model parameters
- Rainfall data
- Streamflow data for model calibration and validation

Information of the previous days precipitation are also required in order to estimate the antecedent soil moisture content.

#### Digital Elevation Model (DEM)

The increasing availability of Digital Elevation Models (DEMs), with the associated possibility of extracting the drainage structure from these representations, is one of the most important advances in both morphologic and hydrologic studies.

DEMs allow to consider the actual morphology of the basin from a topological point of view.

Hillslopes are areas of topographic divergence, valleys are areas of topographic convergence. Channels appear within areas of topographic convergence but are not defined by curvature alone. It is customary (Dietrich et al., 1992) to consider topographic concavity of a site as necessary but not sufficient condition for canalization to occur. The stream or channel network is made up of well-defined banks and sources, the valleys or drainage network are defined on the basis of basin morphometry.

From the availability of accurate DEM data, the convergence (divergence) of topography at any point of the landscape can be measured (see, e.g., Rodríguez-Iturbe and Rinaldo, 1997) and several criteria for the determination of the channelled part of a DEM have been proposed. Anyway, while criteria using topographic convergence are particularly effective when applied to high resolution DEMs, they become meaningless for coarser DEMs, still suitable for hydrologic applications.

The channelled draining network identification is carried out here through a filtering procedure based on an area-slope threshold.

This allows the utilization of a wide range of DEM resolution.





DRiFt was tested on different DEM resolution giving acceptable results in any tested conditions.

However, some studies proved the suitability of the DEM resolution from 225m x 225m to 40m x 40m resolution for hydrologic modeling purposes in the environment analyzed (Molnár and Julien, 2000; Giannoni, 2001) and this is also the suggested range for DRiFt applications.

## Model parameters

The model makes use of five parameters. The threshold value  $AS^k$  and  $k$  are addressed to describe the geo-morphology of the environment where the model is applied. Both of them have a long literature background (see, e.g., Roth et al., 1996) with regard to morphologic studies.

Two other parameters are used to determine the time scale of the geomorphologic hydrograph. They are two characteristic velocities, one for the hillslope links and the other for the channel paths.

The last parameter describes the antecedent soil moisture conditions. It is obviously an event sensitive parameter and has to be introduced by the operator any time a simulation is performed. The evaluation of this parameter refers to the rainfall cumulate in the period preceding the event.

### The morphologic parameters: $AS^k$ and $k$

The hypothesis that in a drainage channel the quantity  $AS^k$  is approximately constant, or at least greater than a threshold value (Montgomery and Dietrich, 1988, 1992)], is used to develop a threshold criterion able to discriminate between different transport mechanisms, i.e. between channeled and non-channeled paths.

The  $k$  exponent of the threshold expression is substantially responsible for drainage density redistribution within the basin. This parameter assigns different importance to the slope, magnifying the influence of high slope values in steep zones, acting oppositely in flat areas. The value of  $k$  is derived from empirical power law relationships that describe the scaling of geometric hydraulic variables (Leopold et al., 1964; Flint, 1974). One of such relationships links slope and discharge,  $Q$ , in the form  $S \propto Q^z$  while a common relationship between discharge and contributing area is  $S \propto Q^x$ . Combining these, (Flint, 1974) gives  $S \propto A^{xz}$ , or :

$$AS^{-\frac{1}{xz}} = \text{constant} \quad (4.102)$$

The way in which a natural drainage system respond to systematic spatial and temporal variability of rainfall by adjusting widths, depths, gradients, and its drainage network shape is embedded in these relationships, together with a tendency to quasi-equilibrium, expressed by the observation that the product  $xz$  tends to be constant (Flint, 1974).

To apply this filtering procedure, the slope may be computed as the ratio of the difference in elevation between two adjacent cells and their relative distance. Dealing with flows, this is usually calculated in the downward direction. Here, in order to minimize DEM sampling errors, a “quasi-local” slope (Giannoni et al., 2000a) is computed taking into account all relative up and downstream cells, as the following scheme;

$$S_i = \frac{1}{n+1} \sum_{k=1}^n \frac{z_k^{upstream} - z_i}{l_{ki}} + \frac{z_i - z^{downstream}}{l_i} \quad (4.103)$$

where  $S_i$  slope in the cell under study  $i$ ;  $z_k^{upstream}$  level of the cell draining to the cell under study;  $z^{downstream}$  level of the cell towards the cell under study drains to.

The quantity  $AS^k$  is then locally computed, and the cells with a local  $AS^k$  value greater than the chosen threshold are assumed to represent the initiation of the effective channeled structure. When a channel is found it is traced to the outlet following the maximum slope direction. In rainfall-runoff modeling, the identification of channel head points assumes a foremost significance with regard to the agreement between simulated and recorded hydrographs. This allows the identification of a threshold value supported by empirical evidence and recorded discharge data. The threshold calibration procedure is described in section “Morphological parameters”.

### Kinematic parameters

Constant velocities are assumed for each of the two components of the drainage system even if variable transfer velocities might be associated to the different elements that contribute to the transport of water as function of local properties (e.g. land use, roughness, local slope). On the hillslope portion of the flow path, the use of a single velocity value is justified by the available information, which are usually characterized by a low detail, not suitable to describe a flow velocity relationship able to consider the wide variety of natural characteristics and the complex processes that take place on these elements.

A different situation is found in the channel part of the flow path, where it could be possible to link velocity values with the local characteristics of the drainage network. The kinematic parameters, i.e. flow velocities on hillslope and in the drainage network, can be interpreted from two different points of view: as lumped hydrological parameters or as an approximation of local hydraulic variables. In the present work they are intended as hydrological parameters, even if they maintain their physical implication as average value for velocities in the channel and on the hillslope paths related to a particular class of events and, therefore, to a particular range of discharge.

### Runoff excess: the Soil Conservation Service method

The Soil Conservation Service (1972) developed a method for computing rainfall abstractions. For the storm as a whole, excess precipitation depth or direct runoff  $P_e$  is always less than or equal to the precipitation depth; likewise, after runoff begins, the additional depth of water retained in the watershed,  $F_a$ , is less than or equal to some potential maximum retention  $S$  (see Figure 4.15). There is some amount of rainfall  $I_a$  (initial abstraction before ponding) for which no runoff will occur, so the potential runoff is  $P - I_a$ .

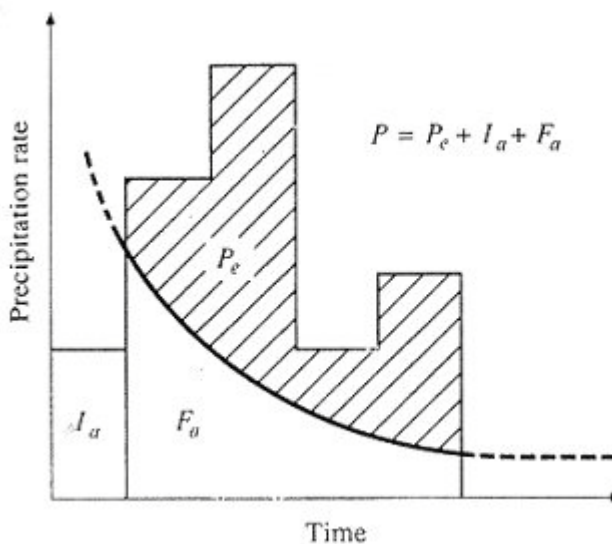


Figure 4.15 SCS abstraction scheme

The hypothesis of the SCS method is that the ratios of the two actual to the two potential quantities are equal, that is

$$\frac{F_a}{S} = \frac{P_e}{P - I_a} \quad (4.104)$$

From the continuity principle

$$P = P_e + I_a + F_a \quad (4.105)$$

Combing (4.104) and (4.105) to solve for  $P_e$  gives:

$$P_e = \frac{(P - I_a)^2}{P - I_a + S} \quad (4.106)$$



which is the basic equation for computing the depth of excess rainfall or direct runoff from a storm by the SCS method. By study of results from many small experimental watersheds, an empirical relation was developed for the initial abstraction as:

$$I_a = 0,2 S \tag{4.107}$$

On this basis

$$P_e = \frac{(P - 0,2 S)^2}{P + 0,8 S} \tag{4.108}$$

Plotting the data for P and P<sub>e</sub> for many watersheds, the SCS found curves of the type shown in Figure 4.16. To standardize these curves, a dimensionless curve number CN is defined such that 0 ≤ CN ≤ 100. For impervious and water surfaces CN=100.

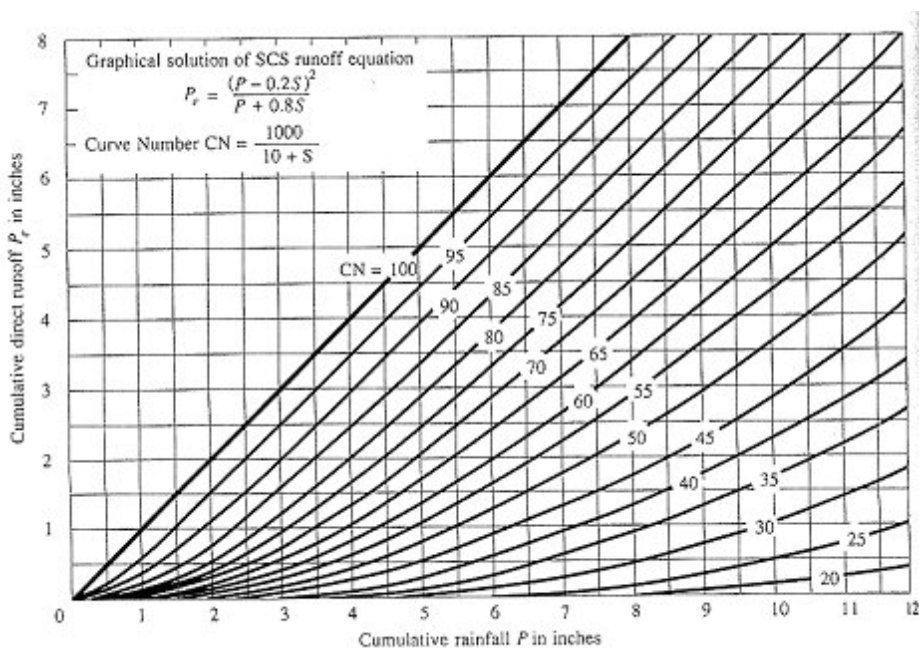


Figure 4.16 Cumulative direct runoff (SCS method)

The CN and S are related by

$$S = \frac{25000}{CN} - 250 \tag{4.109}$$



where  $S$  is in millimeter. The curve numbers shown in Figure 4.16 apply for normal antecedent moisture conditions (AMC II).

For dry conditions (AMC I) or wet conditions (AMC III), equivalent curve number can be computed by:

$$CN(I) = \frac{4,2 \, CN(II)}{10 - 0,058 \, CN(II)} \quad (4.110)$$

$$CN(III) = \frac{23 \, CN(II)}{10 + 0,13 \, CN(II)} \quad (4.111)$$

### Application of the Curve Number method to the model

At this point, only the total depth of excess rainfall or direct runoff during a storm has been computed. By extension of the previous method, the time distribution of abstractions  $F_a$  within a storm, thus the relative time distribution of excess rainfall, can be found. Solving for  $F_a$  from equations (4.104) and (4.105),

$$F_a = \frac{S(P - I_a)}{P - I_a + S} \quad ; P \geq I_a \quad (4.112)$$

Differentiating, and noting that  $I_a$  and  $S$  are constants,

$$\frac{dF_a}{dt} = \frac{S^2 \, dP/dt}{(P - I_a + S)^2} \quad (4.113)$$

As  $P \rightarrow \infty$ , ( $dF_a/dt \rightarrow 0$ ) as required, but the presence of  $dP/dt$  (rainfall intensity) in the numerator means that as the rainfall increases, the rate of retention of water within the watershed tends to increase. This property of the SCS method may not have a strong physical basis. To compute  $F_a$  and thus  $P_e = (1 - F_a)$  it is sufficient to discretize (4.113). In the model this procedure is applied to each pixel that is separately treated on the basis of local soil, land use and urbanization characteristics, summarized in the local CN value. In this way the physical description capacity of the model is increased.

It is necessary to add some more explanations. It is assumed that after the rainfall is filtered by the CN method and has become net rainfall  $P_e$ , all this volume is routed to the channel. This is not completely true; it is a simplification justified by the large number of pixels and the relatively long period considered. In reality it may happen that the runoff generated in one pixel will infiltrate during its route to the channel network in another pixel. This part of the runoff, coming from upstream, increases the saturation of this pixel. In

this way runoff generation increases and, taken as an average process, this pixel releases what was absorbed by the pixels above. This could change the distribution of routing times locally, but not so strongly to make one think that it is worth-while to take into account the possibility of modelling this process too.

## Rainfall input

Rainfall data input can be inserted in several way into DRiFt. With respect of the availability of data and the morphology, the user may choose among four different options corresponding to different levels of interpretation of precipitation processes. Here the possible alternatives are explained.

### Uniform and constant

A constant value of rainfall rate (mm/h) is assumed all around the catchment. Many features of the precipitation field, such as spatial and temporal variability, are not represented with this approach, denying to exploit all the model potentiality. The use of this option should be therefore limited to small catchments and brief events. Moreover, in this way quick simulation can be performed to check out the order of magnitude of results.

### Uniform and time-varying

A rainfall rate time series is assumed for the whole basin.

The time resolution of the rainfall input is strictly connected to basin size. Usually hourly rainfall rate are suitable, but in very small catchment a finer resolution may be required.

In this case spatial variability is still unpreserved. Unfortunately a widespread rainfall cannot be representative of the real precipitation field, especially for those environments usually subjected to convective precipitation regimes.

### Distributed

Time varying precipitation maps can be inserted directly into DRiFt. Rainfall rate values vary from pixel to pixel at each time step allowing to reproduce the spatial heterogeneity of rainfall.

Example of this kind of areal information are observation from remote sensors such as radar and satellite.

### Precipitation maps from raingauges

In most common cases, bi-dimensional time-varying precipitation maps are not available and must be created from raingauges' measurements. These punctual precipitation measurements can be processed in order to extrapolate the rainfall distribution.

The computational routines implemented in DRiFt correspond to two classical interpolation methods: *Thiessen polygons* method and *Inverse squared distance* method.



### *Thiessen polygons method*

This method assumes that at any point in the watershed the rainfall is the same as that at the nearest gage so the depth recorded at a given gage is applied out to a distance halfway to the next station in any direction. Some gages are therefore considered more representative of the area in question than others. Areas corresponding to each gage are determined through the construction of Thiessen polygon network, where the polygon boundaries are formed by the perpendicular bisectors of the lines joining adjacent gages.

### *Inverse squared distance method*

A new rainfall value at an unknown point is calculated as a linear weighted combination of sample values within a local neighborhood of the point being estimated. The weight of a sample point is assigned according to the inverse of its squared distance to the point being estimated. The closer the sample value, the greater the assigned weight.

The sample points in the immediate proximity are assigned higher weights in the interpolation because they are more likely to have similar values.

$$P = \frac{\sum_{i=1}^N \frac{P_i}{d_i^2}}{\sum_{i=1}^N \frac{1}{d_i^2}} \quad (4.114)$$

Where  $P_i$ : sample values;  $d_i$ : Euclidian distances from sample points to the point being estimated;  $n$ : number of sample points.

Sample points need to be selected within a neighborhood to compute the unknown rainfall at a specified location.

The computational routine is created in such a way that a new area of influence are re-constructed whenever there is a change in measurements availability, such as when data is missing from one of the gages.

The precipitation time step is the temporal resolution that maps will be created with.

In order to exploit the whole available information, it is recommended to set the precipitation time step on the same value of raingauges measurements resolution. Anyway, if temporal variations are not significant, cumulative maps may be introduced with a coarser resolution, speeding up the process computational time. A finer resolution does not improve the data input accuracy and slows down the computational time.



## 4.15.4 Model calibration

### Morphological parameters

The morphological exponent  $k$  calibration should be performed, modifying, only if necessary, typical values suggested in literature (see below “range and typical values” session).

Once  $k$  has been set, the value of  $AS^k$  is quantitatively defined in order to produce a network as natural as possible. The threshold value is therefore tested against four different and nearly independent criteria.

These criteria are here briefly summarized:

#### 1) Graphic control

The accuracy of the derived network must be checked through a comparison with the blue lines cartography, even if they are a poor representation of the actual channel network (Montgomery and Foufoula-Georgiou, 1993), and with any other source of knowledge for the basin under analysis. This subjective criterion gives a first idea of the order of magnitude of the threshold value. However, its main use is to avoid gross mistakes in the network identification due to DEM errors (e.g., false junctions, missing branches) that might alter the hydrologic response.



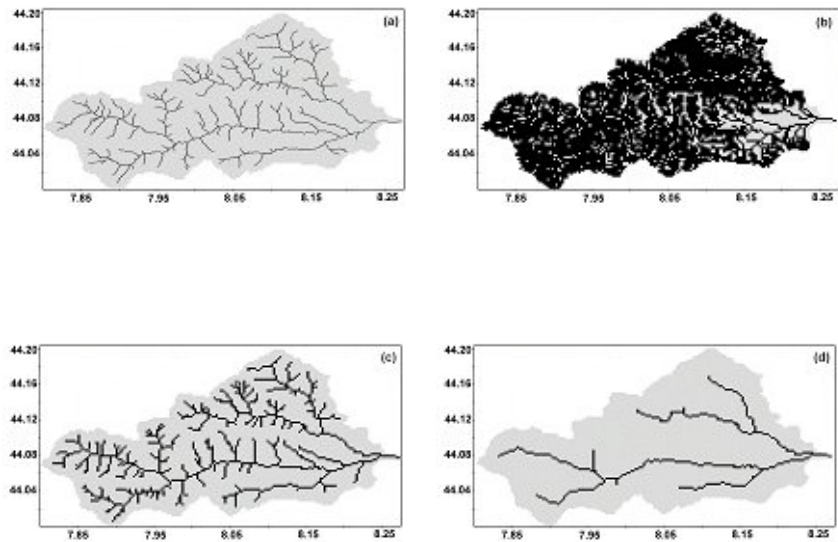


Figure 4.17 Comparison between (a) cartography blue lines and the DEM derived network with different thresholds: (b)  $AS^k=10^4 \text{ m}^2$ ; (c)  $AS^k=10^5 \text{ m}^2$ ; (d)  $AS^k=10^6 \text{ m}^2$ , Centa River basin. Geographic coordinates are in Longitude east and Latitude north.

## 2) Hillslopes and channel percentages

Following the theory on which this procedure is based, the quantity  $AS^k$ , locally estimated in the channeled network, is expected to be constant, and greater than a specific channelization threshold. The percentage of channel cells is thus expected to asymptotically reach a quasi-stable value when the reference threshold is increased and then to drop dramatically, due to the river network vanishing, when the correct channelization threshold value is exceeded (Roth et al., 1996). Obviously, the constancy of the quantity  $AS^k$  is not strictly respected in nature; however, an asymptotic trend in the vicinity of the threshold value is observable (Giannoni et al., 2000a).

It is therefore fundamental to identify where the region of stability begins and to select a representative value of the threshold for this region. Operatively, this value is better marked out using the second derivative of the channel/hillslope percentage vs.  $AS^k$ : when the curves representing the channel/hillslope percentage reach their asymptotic behavior, first and second derivative are almost null; consequently, the modifications of the network for correspondent modification of the thresholds are negligible, and so are the repercussions on the hydrologic response.

An example is exposed in Figure 4.18

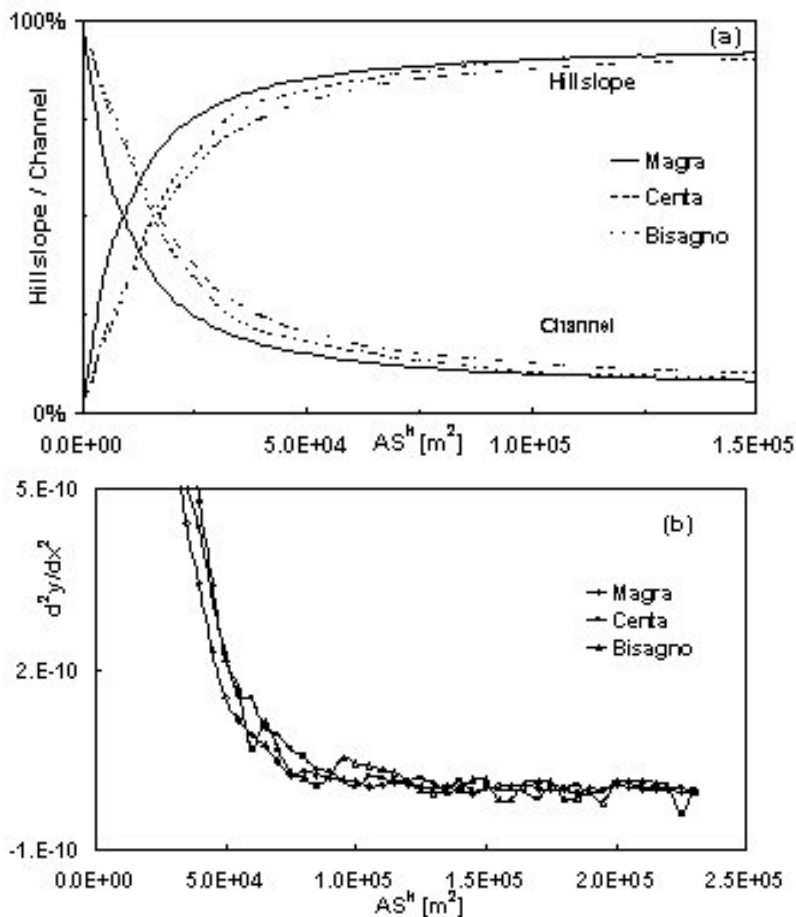


Figure 4.18 (a) Hillslope and channel percentages as function of the threshold value for Magra, Centa and Bisagno. The three drainage networks present a similar behavior: a rapid conversion of hillslope cells into channel cells in the zone of low threshold values and an asymptotic trend when higher values are reached. (b) Second derivative of the hillslope percentages vs.  $AS^k$ .

### 3) Hillslope's length frequency distribution

The hillslope's length frequency distribution is expected to be heterogeneous, in accordance with observations (e.g., Wyss, 1988), and well described by a gamma function (e.g., Gyasi-Agyei et al., 1996). To test the accordance between theoretic distributions and observed frequencies a non-parametric test, as the Kolmogorov-Smirnov test, is proposed.

**Example:** The results for different orders of magnitude of the threshold value are analyzed for some Ligurian basins. In Figure 4.19 an example of the Kolmogorov-Smirnov test for the Bisagno basin is shown. The hill-slope lengths distribution for  $AS^k = 10^4$  m<sup>2</sup> and  $AS^k = 10^6$  m<sup>2</sup> badly fail the test, while the dis-

tribution for  $AS^k = 10^5 \text{ m}^2$  shapes the theoretic gamma. The discrepancies are mostly due to the digital representation of the hillslope paths, that allows only discrete travel times values. This is particularly true for small values, where the step-like behavior of the empirical function is more evident.

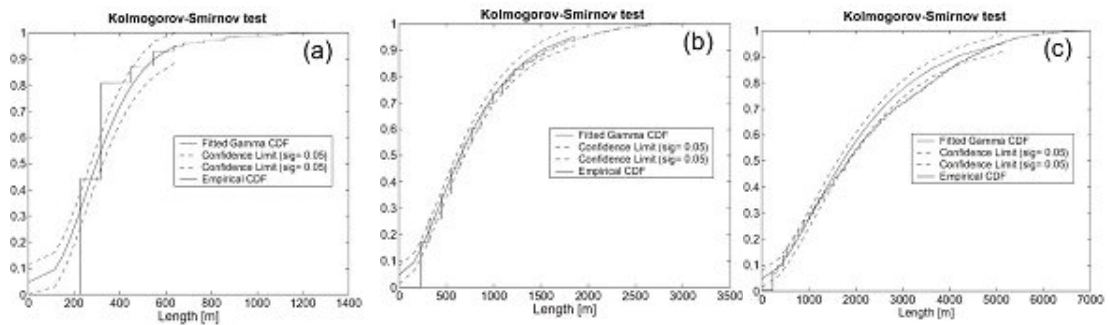


Figure 4.19 Kolmogorov-Smirnov test for cumulative hillslope lengths frequency distribution for three different threshold values: (a)  $AS^k = 10^4 \text{ m}^2$ ; (b)  $AS^k = 10^5 \text{ m}^2$ ; (c)  $AS^k = 10^6 \text{ m}^2$ , Bisagno basin. The curve in (b) gives the best approximation of the expected gamma function.

#### 4) Hillslope's length spatial distribution

In steep basins, the differences between mountain and valley hillslopes are quite strong. If hillslope lengths were constant over the entire basin, they would not converge on a proper basin response because of a lack in the morphologic variability description. The hillslope elements are not randomly joint to the channel: a heterogeneous distribution of hillslope lengths, corresponding to a well-defined spatial distribution over the territory, is expected.

Figure 4.20 depicts the hillslope lengths of the Centa basin, which confirms the intuitive idea that short mountain hillslopes are connected to longer channel network paths, while long hillslopes are usually located not far from the outlet.

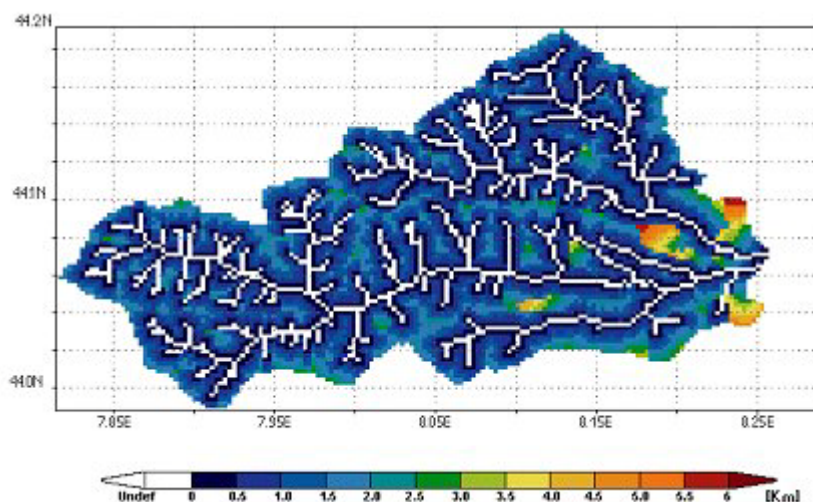


Figure 4.20 Hillslope lengths spatial distribution, Centa basin. Short mountain hillslopes are connected to longer channel network paths, while long hillslopes are usually located not far from the outlet.

### Range and typical values

In Flint's work (Flint, 1974) the exponent  $k = -(1/xz)$  takes values in the range from 1.2 to 2.7 with an average of 1.7. The scaling of link slope with contributing area was investigated by Tarboton et al. (1989): a  $k$  value equal to 1.67 is estimated from contributing area-slope plots with reference to DEM derived networks. Fiorentino et al. (1993) estimated  $k=1.75$  from an entropy-based morphologic analysis of river basin network. Rodríguez-Iturbe et al. (1992) introduce three principles of optimality for drainage networks; a  $k$  value equal to 2 is derived assuming both a linear relation between mean annual discharge and contributing area, i.e.  $x=1$ , and a constant flow velocity through the network. These assumptions were relaxed by Molnár and Ramírez (1998): a  $k=1.6$  value is estimated for optimal combinations of channel downstream hydraulic geometry and basin topography for natural drainage systems.

On the basis of the previous considerations, the value 1.7 is assumed as a suitable estimate for the  $k$  parameter. Values of  $k$  within the 1.6-1.75 range do not produce considerable differences in the values of the others parameters of the model, as obtained from the complete calibration procedure. The validity of this assumption is qualitatively confirmed by the graphic comparison between the filtered network drainage density distribution and the blue lines, presented in the previous section (Figure 4.17).



On this basis, range and typical values of morphologic parameters are summarized in Table 4.6.

Table 4.6 Range and typical values of morphologic parameters

	Range		Typical values	
	Lower bound	Upper bound	DEM (40mx40m)	DEM (225mx225)
k	1.3	2	1.7	1.7
AS <sup>k</sup>	10 <sup>2</sup>	10 <sup>6</sup>	10 <sup>4</sup>	10 <sup>5</sup>

## Kinematic parameters

The estimation of kinematic parameters has to be performed using different recorded hydrographs in several hydrometric stations, paying particular attention on correctly reproducing the peak discharge value,  $Q_p$ , and the time when this peak is experienced,  $t_p$ . Another important issue, that calibration should care for, is consistency of surface runoff volume. The model does not manage the infiltrated part of the rainfall: the shape of the hydrograph is often not preserved, especially in its tail. However, for in the environments that the model intend to analyze, this has a minor role in the characterization of the hydrograph peak.

A sensivity analysis showed that an increase in hillslope velocity lead to a reduction of the hydrograph base and consequently to an increase in the discharge peak value. The same trend is observed increasing the channel velocity, while the ratio between the two velocity affects the basic characteristics of the hydrograph shape, such as skewness, rising limb, tail.

### Range and typical values

A deep analysis over the Tanaro region (North Italy) was chosen to identify three typical set of kinematic parameters representing its morphological variability. The region, in fact, includes a mountain zone characterized by very steep catchments, a pede-mountain part and a valley alluvial part. The average velocities decrease from steep mountain sub-catchments to valley basins both on hillslopes and channels. Their values (see Table 4.7) maintain always a physical meaning with regard to the morphology considered (Giannoni et al., 2003) supporting the conviction of a good description capacity of the catchment system offered by the model.



Table 4.7 Kinematic parameters range and typical values for Tanaro basin.

	Range		Typical values (for Tanaro basin)		
	Lower bound	Upper bound	Mountain	Pede-mountain	Valley
$V_{\text{channel}}$ [m/s]	0.1	10	2.5	2.2	1.5
$V_{\text{hillslopes}}$ [m/s]	0.001	1	0.16	0.16	0.12

This corroborates the idea that the model includes the relevant processes that contribute to form the hydrologic response at the basin scale, at least in respect to severe rainfall events in small to medium size catchments in the Mediterranean environment.

## Curve Number

Curve numbers have been tabulated by the Soil Conservation Service on the basis of soil type and land use. Four soil groups are defined:

Group A: Deep sand, deep loess, aggregated silt

Group B: Shallow loess, aggregated silts

Group C: Clay loams, shallow sandy loam, soils low in organic content, and soils usually high clay

Group D: Soils that swell significantly when wet, heavy plastic clays, and certain saline soils

The values of CN for various land uses on these soil types are given in Table 4.8. For a watershed made up of several soil types and land uses, a composite CN can be calculated.



Table 4.8 Runoff coefficient for different condtions (AMCII)

**Runoff curve numbers for selected agricultural, suburban, and urban land uses (antecedent moisture condition II,  $I_a = 0.2S$ )**

Land Use Description	Hydrologic Soil Group			
	A	B	C	D
Cultivated land <sup>1</sup> : without conservation treatment	72	81	88	91
with conservation treatment	62	71	78	81
Pasture or range land: poor condition	68	79	86	89
good condition	39	61	74	80
Meadow: good condition	30	58	71	78
Wood or forest land: thin stand, poor cover, no mulch	45	66	77	83
good cover <sup>2</sup>	25	55	70	77
Open Spaces, lawns, parks, golf courses, cemeteries, etc.				
good condition: grass cover on 75% or more of the area	39	61	74	80
fair condition: grass cover on 50% to 75% of the area	49	69	79	84
Commercial and business areas (85% impervious)	89	92	94	95
Industrial districts (72% impervious)	81	88	91	93
Residential <sup>3</sup> :				
Average lot size	Average % impervious <sup>4</sup>			
1/8 acre or less	65	77	85	90
1/4 acre	38	61	75	83
1/3 acre	30	57	72	81
1/2 acre	25	54	70	80
1 acre	20	51	68	79
Paved parking lots, roofs, driveways, etc. <sup>5</sup>	98	98	98	98
Streets and roads:				
paved with curbs and storm sewers <sup>5</sup>	98	98	98	98
gravel	76	85	89	91
dirt	72	82	87	89

<sup>1</sup>For a more detailed description of agricultural land use curve numbers, refer to Soil Conservation Service, 1972, Chap. 9

<sup>2</sup>Good cover is protected from grazing and litter and brush cover soil.

<sup>3</sup>Curve numbers are computed assuming the runoff from the house and driveway is directed towards the street with a minimum of roof water directed to lawns where additional infiltration could occur.

<sup>4</sup>The remaining pervious areas (lawn) are considered to be in good pasture condition for these curve numbers.

<sup>5</sup>In some warmer climates of the country a curve number of 95 may be used.

Since the SCS method was developed in the USA, attention must be paid adapting this method to a different application field. In fact, it is an empirical method and the large number of experiments that give it reliability were made in a country with its own specific morphology and particular kind of precipita-



tion. It is therefore not sure that CN values and classifications furnished by the SCS fit every case of study.

### Initial condition

The CN method allows the use of different antecedent soil moisture conditions. The program gives the user the possibility of choosing dry, normal or wet conditions at the beginning of each event studied. This is a critical issue, because the moisture content of the soil before a rainfall event has a direct effect on infiltration and thus on runoff .

It is not easy to choose the initial conditions, because many factors concur to make the wetting and drying process very complicated. There is no fixed rule able to identify for one event whether antecedent conditions are wet, normal or dry. Each case is different from one another. In general one should consider how long the interval is between two consequent precipitations, vegetal coverage, soil composition, season and all other aspects that affect the evapotranspiration process.

However some indicative tables exist for the range of antecedent moisture conditions for each class; the one the proposed by Chow (1988) is given below (Table 4.9).

Table 4.9 Suggested classification of antecedent soil moisture classes. (Source: Soil Conservation Service, 1972, table4.2, p.4.12.)

AMC	Total 5-day antecedent rainfall (mm)	
	Dormant season	Growing season
Type I	< 13	< 35
Type II	13 - 28	35-53
Type III	> 28	> 53

#### 4.15.5 DRiFt references

Chow V. T., D. R. Maidment, and L. W. Mays, Applied Hydrology, McGraw Hill, New York, 1988, 572.

Dietrich W. E., C. Wilson, D. R. Montgomery, J. McKean, and R. Bauer, Erosion thresholds and land surface morphology, Geology, 20, 675-679, 1992.

Fiorentino, M., P. Claps, and V. P. Singh, An entropy-based morphological analysis of river basin networks, Water Resour. Res., 29(4), 1215-1224, 1993.

Flint, J. J., Stream gradient as a function of order, magnitude and discharge. Water Resour. Res., 10(5), 969-973, 1974.





- Giannoni, F., G. Roth, and R. Rudari, A Semi - Distributed Rainfall - Runoff Model Based on a Geomorphologic Approach, *Physics and Chemistry of the Earth*, 25/7-8, 665-671, 2000a.
- Giannoni F., Morphologic analysis of natural drainage networks targeted to the characterization of the hydrologic response, Ph. D Thesis, Università della Basilicata, 2001.
- Giannoni F., G. Roth, and R. Rudari, Can the behaviour of different basins be described by the same model's parameter set? A geomorphologic framework, *Physics and Chemistry of the Earth*, 28(6-7), 289-295, 2003.
- Gyasi-Agyei, Y., F. P. De Troch, and P. A. Troch, A dynamic hillslope response model in a geomorphology based rainfall-runoff model, *J. Hydrol.*, 178, 1-18. 1996.
- Leopold, L. B., M. G. Wolman, and J. P. Miller, *Fluvial Processes in Geomorphology*, W. H. Freeman, New York, 1964.
- Molnár, D. K., and P. Y. Julien, Grid-Size effects on surface runoff modeling, *J. Hydr. Engrg.*, ASCE, 5(1), 8-16, 2000.
- Molnar, P., and J. A. Ramírez, Energy dissipation theories and optimal channel characteristics of river networks, *Water Resour. Res.*, 34(7), 1809-1818, 1998.
- Montgomery, D. R., and W. E. Dietrich, Where do channels begin?, *Nature*, 336, 232-234, 1988.
- Montgomery, D. R., and W. E. Dietrich, Channel initiation and the problem of landscape scale, *Science*, 225, 826-830, 1992.
- Montgomery, D. R., and E. Foufoula-Georgiou, Channel network sources representation using digital elevation model, *Water Resour. Res.*, 29(12), 3925-3934, 1993.
- Rodríguez-Iturbe, I., A. Rinaldo, R. Rigon, R. L. Bras, A. Marani, and E. Ijjasz-Vasquez, Energy dissipation, runoff production, and the three-dimensional structure of river basins, *Water Resour. Res.*, 28(4), 1095-1103, 1992.
- Rodríguez-Iturbe, I., and A. Rinaldo, *Fractal river basins: chance and self-organization*, Cambridge University Press, 1997.
- Roth, G., P. La Barbera, and M. Greco, On the description of the basin drainage structure, *J. Hydrol.*, 187, 119-135, 1996.
- SCS National Engineering handbook, "Section 4: Hydrology", Soil Conservation Service, USDA, Washington, D.C., 1972.
- Sherman, L. K., Streamflow from rainfall by the unit hydrograph method, *Eng. News Rec.*, 108, 501-505, 1932.



Tarboton, D. G., R. L. Bras, and I. Rodríguez-Iturbe, Scaling and elevation in river networks, *Water Resour. Res.*, 25(9), 2037-2051, 1989.

Wyss, J. D., Hydrologic modelling of New England river basins using radar rainfall data, M. S. thesis, Dep. of Meteor., 164 pp., Mass. Inst. Of Technol., Cambridge, 1988.



# FLOOD FORECASTING

Reference





## 5 FF Reference Manual

This manual should be used when undertaking flood forecasting (FF) modelling applications. It provides a description of aspects which are encountered during the development, calibration and application of FF models. The manual should be used in conjunction with the MIKE 11 User Guide.

### 5.1 Introduction

The demand for means to mitigate the impact of flooding has increased in many parts of the world in recent years, especially where major urban development in the flood plains has taken place.

Flood forecasting systems, producing real-time forecasts of river flows and levels, provide a cost-effective solution to many flood management problems. In addition, the environmental impact of implementing flood forecasting and warning systems is considerably less than many other flood control measures.

Such flood forecasting systems provide

- predictions of the inflow to flood control reservoirs, polders, etc. This will enable reservoir operations that prevent or reduce flooding in the downstream reaches while avoiding unnecessary waste of water resources.
- warnings to local authorities and the affected population of the expected levels and extent of flood inundation

It is very important that the system is able to produce accurate, reliable and timely forecasts as major decisions on reservoir operations, evacuation of people, etc. will be based on this information.

Inland flooding may occur due to heavy rainfall in the local catchment area, increasing inflow at upstream boundaries or as a combination of the two. Real-time flood forecasting therefore requires adequate descriptions of the rainfall-runoff process and of the flow in rivers and channels and thus also real-time information on precipitation and river conditions in the area.

The MIKE 11 Flood Forecasting module (MIKE 11 - FF) is designed to perform the calculations required to predict the variation in discharges and water levels in a river system as a result of catchment rainfall and inflow/outflow through boundaries in the river system.

An automatic updating (data assimilation) routine is included in MIKE 11 - FF. In real-time forecasting the simulated discharge/water level generally deviates from the measured discharge/water level. In order to obtain the maximum benefit of the real-time measurements in the forecasts, some kind of updating of the forecasting model is required. Updating consists of condition-



ing the model predictions to the observed data prior to the Time of Forecast (ToF).

The accuracy of the forecasts will depend on the accuracy of the boundary and rainfall forecasts, the model (calibration and structure) and the efficiency of updating routine. The advantages of applying real-time updating to provide accurate flood forecasting are widely recognised (/62/).

MIKE 11 - FF constitute an add on module to MIKE 11, and should be installed along with the hydrodynamic model HD and the rainfall-runoff model NAM.

MIKE 11 FF is designed to minimise the amount of information to be given by the operational forecaster. This is important for real-time applications where reliability and fast performance are crucial.

MIKE 11 - FF has been applied to operational real-time flood forecasting since 1985. Very large applications have been setup for river systems in India and Bangladesh.

MIKE 11 FF can be used in connection with either a manually based or a fully automatic data collection and processing (SCADA) system.

## 5.2 Updating Procedure

Accurate forecasting requires that the rainfall-runoff model as well as the hydrodynamic model are well calibrated on historical data i.e. that they are able to simulate the water flow very accurately up to the time of forecast. Deviations between measured and simulated water levels/discharges will never the less often occur, and it is important that these errors are corrected before forecasts are calculated.

Differences in the simulated and observed discharges prior to the time of forecast (ToF) can be attributed to four sources:

1. Errors in the model input data such as precipitation, evaporation, and temperature.
2. Errors in the model parameters due to data limitations, sub-optimal calibrations, etc.
3. Errors in the output variables due to the uncertainty in the rating curves and other uncertainties arising from the measurement process.
4. Errors in the model structure due to lumping, inappropriate conceptualisation of the flood-producing processes, etc.

Forecast updating procedures can be classified according to whether the input variables, state variables, model parameters or output variables are modified. A thorough discussion of the merits and disadvantages of different updating schemes is provided in Refsgaard, 1997 (/61/). Since the start of



DHI's commercial flood forecasting activities in the early 1980's (/63/, /64/, /65/), the importance of incorporating updating procedures for real-time forecasting was recognised. In the WMO project "Simulated Real-Time Intercomparison of Hydrological Models" DHI submitted two models both based on the NAM model; NAMS11, the predecessor of MIKE 11 FF, and NAMKAL where NAM was formulated in state space form and built into an extended Kalman filter updating. The NAMS11 used output updating based on a error prediction algorithm while NAMKAL provided state variable updating based on the extended Kalman filter.

DHI's NAMS11 showed the best overall results with a ranking of No. 1-2 in the Bird Creek catchment and No. 2-3 in the Orgeval catchment. However it was noted that there was scope for improvement particularly in the case of phase errors. A new procedure that implemented these improvements was implemented in the MIKE 11 FF module in 1989, Rungø et al., 1989, (/66/). As a result the standard updating procedure provided by MIKE 11 FF is an improved error correction routine (output updating) capable of distinguishing between phase and amplitude errors.

Two unique features MIKE 11 FF'S updating procedure must be emphasised.

1. Updating can be carried out directly on either water level or discharge. Many traditional forecast models based on a purely hydrological approach allow updating only on discharge. These discharges are derived from water levels using rating curves which are subject to uncertainties due to measurement errors, loop effects, etc. Direct updating on water levels improves the forecast accuracy significantly.
2. It allows correction of both amplitude errors and phase errors. While traditional updating procedures perform quite well where the deviations arise from amplitude or volume errors they generally perform poorly in the case of phase error. Such phase errors may arise from the variable wave speeds for flooding over bank levels or the position and path of storm relative to the catchment outlet.

The two types of errors are illustrated below.

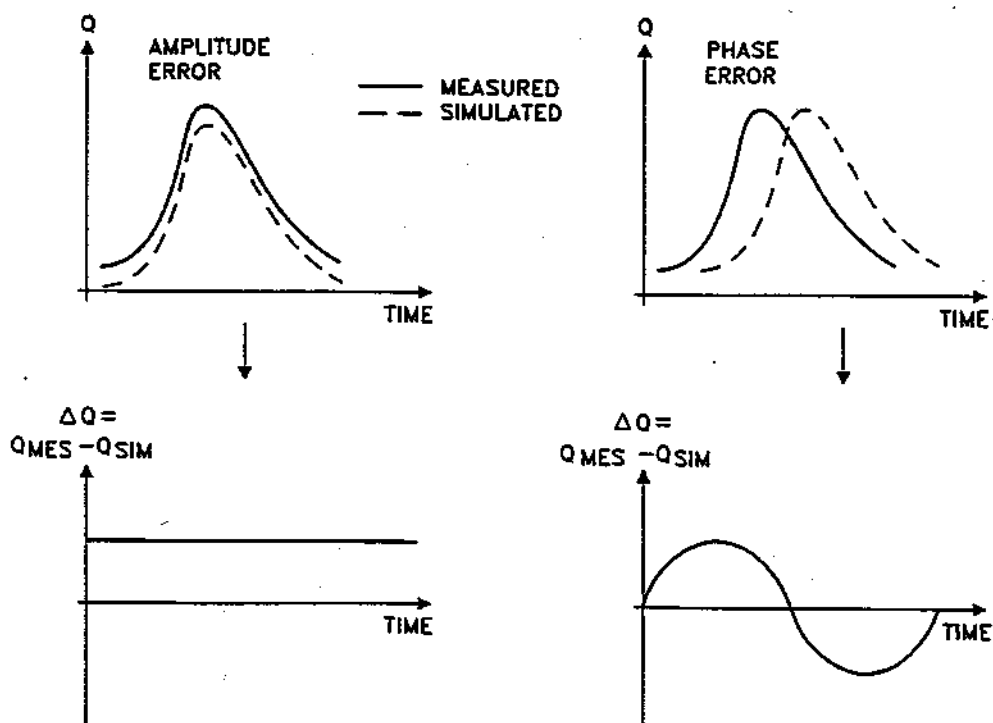


Figure 5.1 Illustration of amplitude and phase error.

The updating procedure distinguishes between the two error types and make corrections accordingly by minimizing the objective function given below:

$$\sum_{i=1}^n F_i \left[ M_i - \left\{ S_i + A_e + \frac{\Delta S}{\Delta t} P_e \right\} \right]^2 + \alpha Q_p^2 |P_e| \quad (5.1)$$

where

$A_e$  amplitude error ( $m^3/s$ )

$P_e$  phase error (s)

$M$  measured discharge ( $m^3/s$ )

$S$  simulated discharge ( $m^3/s$ )

$F$  weighting factor





$n$  number of values taken into account

$\Delta S(S_{i+1} - S_i)$

$\Delta t$  time step (s)

$\alpha$  phase factor ( $s^{-1}$ )

$Q_p$  typical peak discharge ( $m^3/s$ )

The minimum is found by differentiating the equation with respect to  $A_e$  and  $P_e$ , and solving these two equations.

A time series of correction discharge is generated on the basis of the identified errors, and introduced as a lateral inflow/outflow to the river at an update point or reach.

These corrections are typically made at several locations in the river system, where real-time data are available. This will ensure that the simulated flow upstream of forecast points is as correct as possible at Time of Forecast (TOF), and this will improve the accuracy of the forecasts.

Deviations found at TOF are likely to persist for some time in the forecast period. Corrections are therefore continued after TOF, but gradually reduced according to a first order decay, as illustrated in Figure 5.2 below.

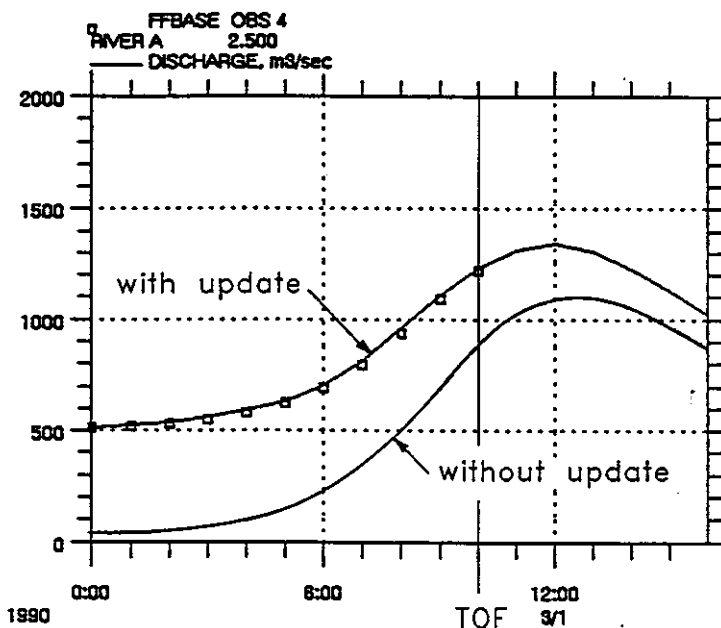


Figure 5.2 The updating ensures that the simulations are as close to the observations as possible up to the time of forecast. Corrections are continued, but gradually reduced, in the forecast period.

The updating procedure uses a number of parameters that should be found from calibration, using historical peak events.

The purpose of the calibration of the update parameters is to distinguish correctly between deviations in time (phase errors) and deviations in volume (amplitude errors). Only by a correct determination of phase and amplitude errors, will the correction discharge calculated for the forecasting period will be correct.

A detailed calibration of parameters should be carried out for each update location.

During calibration the available information stored in the TRF result file should be utilized. The result file contains the following information for all update points:

- Phase error after each update iteration
- Amplitude error after each update iteration
- Discharge after each update iteration
- Summation of correction discharge after each update iteration



- Simulated time series of water level and discharges after each update iteration

Prior to the calibration of the updating parameters, the observed and simulated hydrographs at the updating location should be examined. The purpose is to determine the phase and amplitude errors which are straightforward to identify from the hydrographs. The results from this evaluation should be compared with the simulated updating results obtained when calibrating the updating parameters.

### Max Phase Error

Corresponds to the largest deviation in time that will be identified as a phase error. If the updating determines a larger phase error it is automatically reduced to this value.

Used to limit the interpretation of errors as phase errors. Should only rarely be a limiting factor. If the calculated phase error often reaches this value, the Analysis Period (AP) should be decreased or the value of Alpha increased. In the first calibration the value of Max Phase Error can be set equal to AP.

### Analysis period (AP)

This is the number of hours back in time from time of forecast that simulated and observed flow should be compared. This should as a minimum be larger than the duration of a peak. When hotstarting, analysis will be made for the full analysis period, i.e. including results of the previous simulation.

The order of magnitude will typically be days in very slow responding river systems down to a few hours in very flashy river systems. The AP must be large enough for detection of phase errors.

### Time constant in analysis period

Recent deviations between simulated and observed flow may be given more weight than those occurring earlier, using first order decay. The time constant determines the reduction of the weighting factor back in time. It should be of the same order of magnitude as the length of the analysis period.

To be used in river systems with very low correlation.

### Time constant in forecast period

The errors found at Time of Forecast are assumed to be gradually reduced during the forecast period following a first order decay given by this time constant.

A small time constant will rapidly reduce the calculated correction discharge during the forecast period. The calibration will show if this is necessary. In the first calibration the value can be set equal to AP.



### Adjust factor

The effect of the updating may be generally reduced by specifying an adjustment factor less than 1.0. This is used e.g. at locations where observations are not considered reliable.

### Alpha and Typical Peak Value

The Alpha parameter is used in the last term of equation (5.1) to set a reasonable limit for the extent to which the updating interprets deviations as phase errors. In case of hydrographs with very small slopes the deviations can often be misinterpreted as phase errors. Initially, Alpha should be set to 0.001 and the Typical Peak Value should be determined from the observed hydrograph. If the calibration results show poor distinction between phase and amplitude errors, Alpha should be changed. If too many of the errors are corrected as phase errors, Alpha should be increased.

Based on the phase and amplitude errors identified by the updating routine a series of correction discharges is calculated. The correction discharges are subsequently added/subtracted from the flows simulated by the hydrodynamic model.

Updating can be specified on the basis of either discharge or water level measurements. When updating on water levels, the calculation of correction discharge takes into account the conveyance values corresponding to the measured and simulated water levels.

Updating can be specified at any location in the river system where water level and/or discharge information is available in real-time.

An example of the functioning of the updating routine is shown below in Figure 5.3.

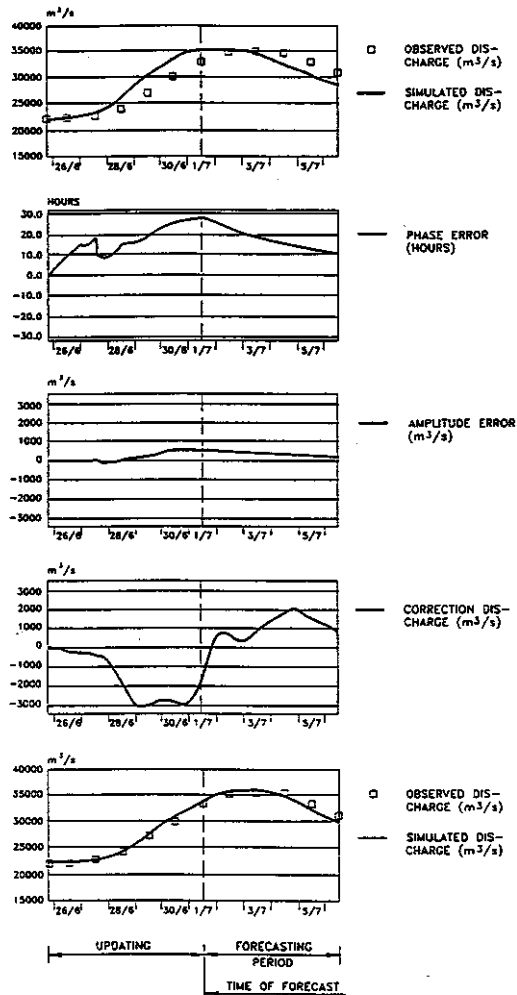


Figure 5.3 Example of updating.

### 5.2.1 Calibration Example

A simple example of an FF calibration using three days of data from a forecasting location is given below. The basis for this example is the measured and simulated hydrographs in Figure 5.4. No forecast period has been simulated i.e. the Time Constant in Forecast Period has not been calibrated. The example should only demonstrate basic principles of how to obtain a correct interpretation of phase and amplitude errors.

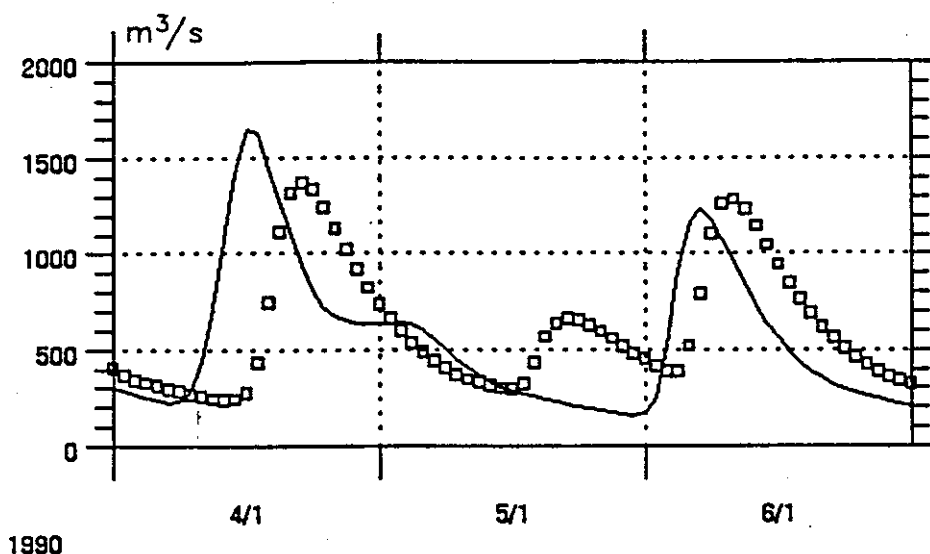


Figure 5.4 Example of measured (squares) and simulated (line) discharge at an update location.

From Figure 5.4 it appears that:

- The phase error at the peak on the 4/1 is approximately 4.8 hours.
- The phase error at the peak on the 6/1 is approximately 2.8 hours.
- The amplitude error at the two peaks are approximately  $275 \text{ m}^3/\text{s}$  and  $75 \text{ m}^3/\text{s}$  respectively.
- The amplitude error before the steep rise in the morning of 6/1 is approximately  $180 \text{ m}^3/\text{s}$ .

These findings should also be made by the updating routine and can be used as a check of the calibration results.

#### Determination of Analyse Period (AP)

Firstly selection of an appropriate Analyse Period has been investigated. Simulations with AP equal to 3, 6, 12 and 24 hours have been made and it has been assumed that  $\text{AP} = \text{Max Phase Error} = \text{Time Constant in AP}$ . Alpha has been set to 0.001 and the Typical Peak Value to  $2500 \text{ m}^3/\text{s}$ . The results are shown in Figure 5.5.

The simulation with  $\text{AP} = 3$  hours is not able to detect the 4.8 hour phase error on the 4/1. Therefore the error here is incorrectly interpreted as amplitude error. The simulation with  $\text{AP} = 24$  hours gives an incorrect negative amplitude error in the morning of the 6/1 and an amplitude error that is too large during the peak on the 4/1.



The simulations with AP = 6 and 12 hours both give approximately the same results and match our findings from the hydrograph. A final selection of AP could subsequently be made from calibration on data from other time periods from the this station.

### Determination of Alpha

For the calibration of Alpha, simulations with Alpha = 0.0001, 0.001, 0.005 and 0.05 have been made. Other parameters are AP = Time Constant in AP = Max Phase Error = 12 hours. Typical Peak Value = 2500 m<sup>3</sup>/s. The results are shown in Figure 5.6.

It is clearly seen from the results that the large value of Alpha causes the errors to be interpreted as amplitude errors. The best agreement with our findings from the hydrograph is obtained from the results with Alpha = 0.001

### Determination of other updating parameters

In a similar manner it is possible to calibrate the remaining updating parameters (see Table 5.1).

Table 5.1 Calibration of the remaining updating parameters

Parameter	Main effect	Typical value
Max phase error	Higher phase errors are automatically reduced to this value	Equal to AP
Analyse Period (AP)	Determine the period where observed and simulated data are analysed	Found by calibration
Time constant in AP	If less than AP, recent deviations may be given more weight	Equal to AP
Time constant in forecast period	Corrections at ToF are gradually decreased in the forecast period by a first order decay with this time constant.	Found by calibration
Adjust factor	Increasing/decreasing the calculated updating discharge	1.0
Alpha	An increase in Alpha will cause deviations to be interpreted more as amplitude errors	Found by calibration
Peak value	Highest expected discharge after applying the correction discharge	From observed discharge hydrographs

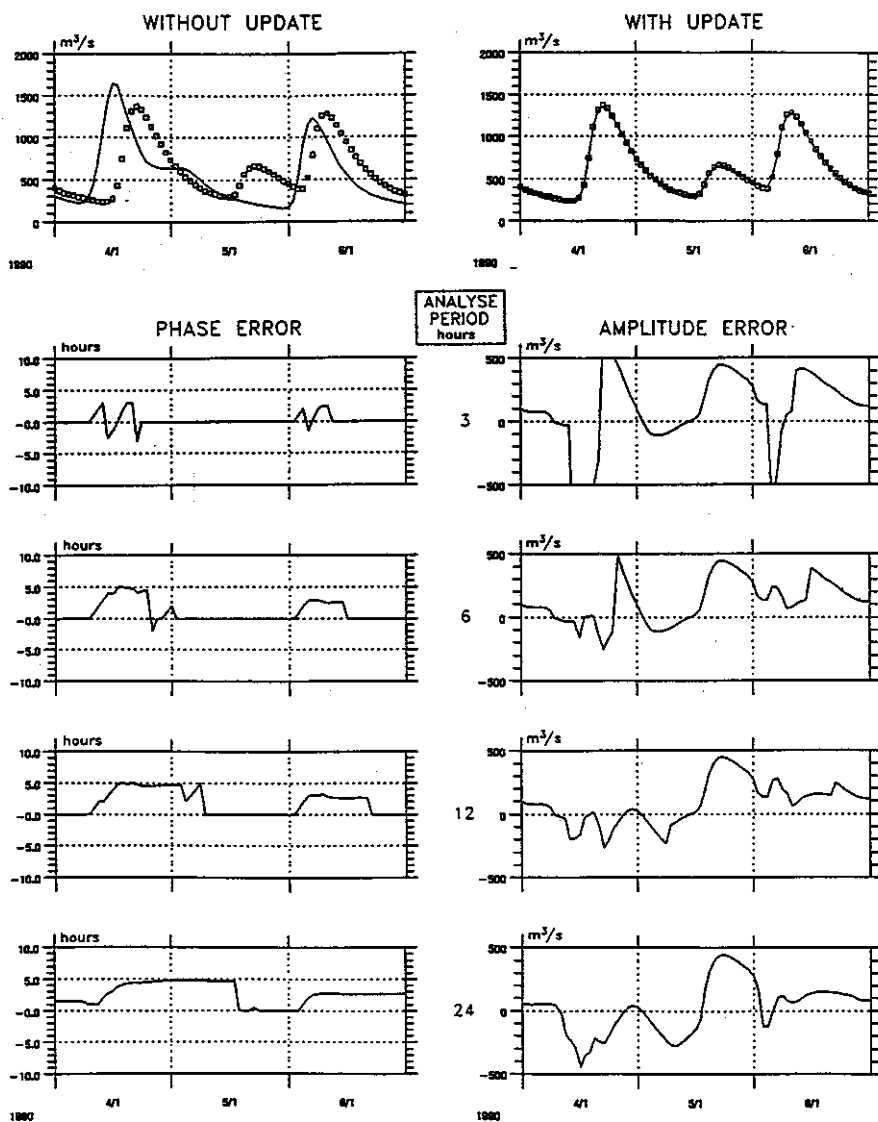


Figure 5.5 Results from calibration of the Analyse Period. Analyse Period = Time Constant in Analyse Period = Max Phase Error. Alpha = 0.001 and Typical Peak Value =  $2500 m^3/s$ .



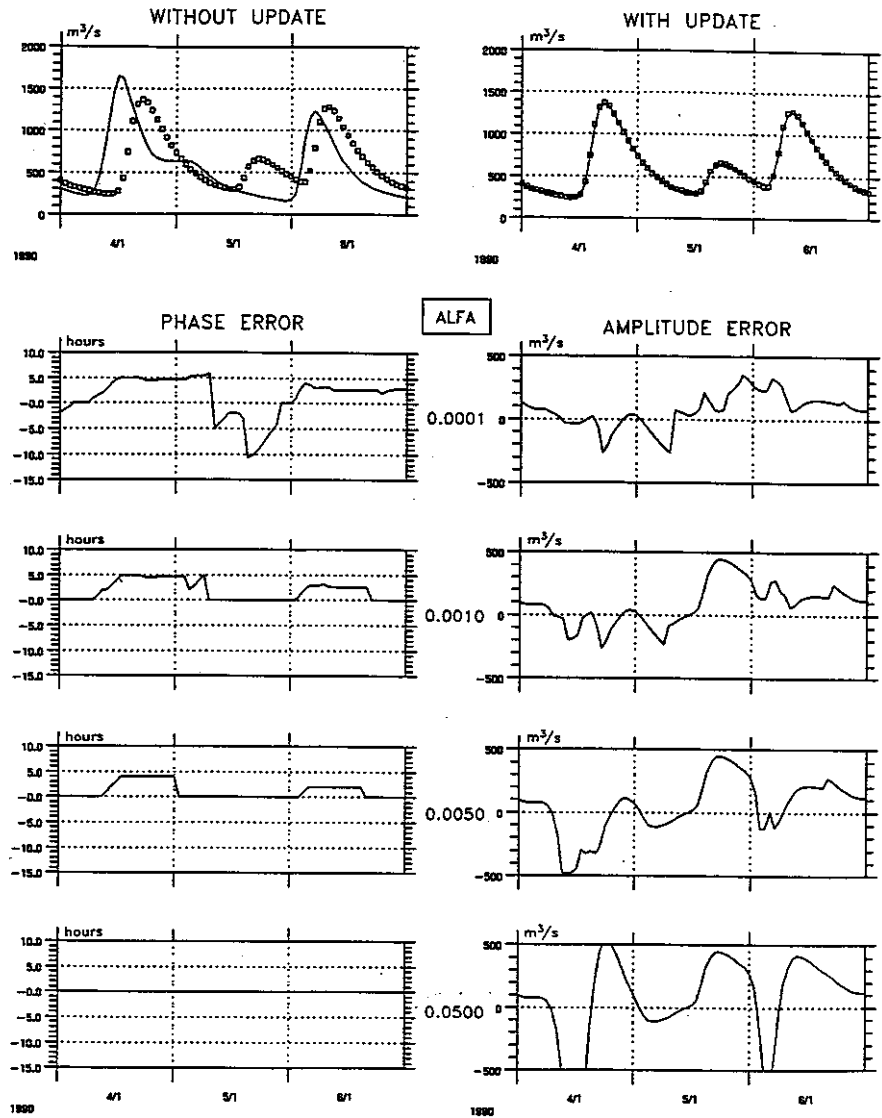


Figure 5.6 Results from calibration of Alpha. Analyse Period = Time Constant in Analyse Period = Max Phase Error = 12 hours. Typical Peak Value = 2500  $m^3/s$ .

## 5.3 References

- /61/ Refsgaard J.C. Validation and Intercomparison of Different Updating Procedures for Real-Time Forecasting, Nordic Hydrology, 28,



- pp 65-94, 1997.
- /62/ WMO Simulated Real-Time Intercomparison of Hydrological Models. Operational Hydrology Report. No. 38. 1992
- /63/ Jønch-Clausen, T and J.C. Refsgaard. A mathematical modelling system for flood forecasting, *Nordic Hydrology*, 15, pp 307-318, 1984.
- /64/ Refsgaard J.C. and V.G. Ghanekar. Flood Forecasting, Damodar. *World Water*, August 1986.
- /65/ Refsgaard, J.C., K. Havnø, H.C. Ammentorp and A. Verwey. Application of hydrological models for flood forecasting and flood control in India and Bangladesh. *Advances in Water Resources*, 11, 101-105.
- /66/ Rungø, M. J.C. Refsgaard, K. Havnø. The updating procedure in the MIKE 11 modelling system for real-time forecasting. Proceedings from the International Symposium on Hydrological Applications of Weather Radar, Salford, UK, August 1989.



# DATA ASSIMILATION

Reference





## 6 Data Assimilation in MIKE 11

Data assimilation is a technique for combining any measurements of the state of the system with the model dynamics in order to improve the knowledge of the system. The data assimilation module in MIKE 11 can be used for assimilation of water level and discharge measurements in the hydrodynamic model and for assimilation of concentration measurements in the advection-dispersion model. Furthermore, the data assimilation module can be used for uncertainty assessment and estimation of model prediction uncertainties.

The data assimilation methods implemented in the MIKE 11 DA module belongs to the class of sequential algorithms. In this case a sequential updating of the model solution is performed during a forward model integration in which the model forecast and the data are melded according to a specific melding scheme. Two different melding schemes based on the Kalman filter are available in MIKE 11:

- Ensemble Kalman filter
- Constant weighting function method

The ensemble Kalman filter is based on a stochastic model formulation in which model uncertainties are quantified and propagated through the model. This formulation also allows for general uncertainty assessment, i.e. without assimilation of measurements. The constant weighting function method is a deterministic approach that does not explicitly address model uncertainties. Both methods can be formulated in a general filtering framework.

The data assimilation module can be used either in hindcasting mode for process studies and design purposes or as part of an operational forecasting system. In either case, the module provides an improved estimate of the state of the system which is consistent with the observed data. In an operational setting the data assimilation module is used for updating the state of the system prior to the time of forecast, and hence providing improved initial conditions for the forecast. After the time of forecast the model can be corrected using forecasts of model errors.

Application examples of the MIKE 11 data assimilation module can be found in Hartnack and Madsen /69/, Madsen et al. /70/ and Madsen and Skotner /71/.

### 6.1 Data assimilation framework

The MIKE 11 model can be described in a deterministic, discrete dynamical system setting as

$$\mathbf{x}_{k+1} = \Phi(\mathbf{x}_k, \mathbf{u}_k) \quad (6.1)$$

where



$x_k$  is the state variables of the system at time step  $k$  in terms of  $h$ - and  $Q$ -points for each branch in the river system and concentration components in the advection-dispersion model (if used).

$u_k$  is the forcing terms of the system incorporating all boundary conditions, lateral inflow/outflow and possible wind fields.

$F(\cdot)$  is the model operator representing the numerical scheme of MIKE 11 (one time-step-ahead prediction operator).

It is assumed that water level, discharge and concentration measurements are available at one or more locations in the modelled river system. This is formulated in the measurement equation

$$z_k = C_k x_k \quad (6.2)$$

where

$z_k$  is the vector of measurements.

$C_k$  is a matrix that describes the relation between measurements and state variables, i.e. a mapping of state space to measurement space.

The data assimilation process is a succession of two steps. First, the model is employed to issue a forecast, and then the observed data are meld with the forecast to provide an updated state (analysis step). The analysis step is chosen to be a linear combination of the data and the model, i.e.

$$x_k^a = x_k^f + G_k (z_k - C_k x_k^f) \quad (6.3)$$

where

$x_k^f$  is the forecast state vector obtained from Eq. (6.1).

$x_k^a$  is the analysed or updated state vector.

$G_k$  is a weighting matrix (gain matrix).

The vector  $(z_k - C_k x_k^f)$ , denoted the innovation vector, includes the differences between the measurements and their model forecasted equivalents. If the measurements are independent, a sequential update procedure can be used that processes one measurement at a time

$$x_k^a(j) = x_k^a(j-1) + g_{k,j} (z_{k,j} - x_k^a(j-1)), \quad x_k^a(0) = x_k^f, \quad j = 1, 2, \dots, p \quad (6.4)$$

where



$p$  is the number of measurements.

$z_{k,j}$  is measurement No.  $j$ .

$(z_{k,j} - x_k^a(j-1))$  is the innovation in measurement point No.  $j$  after processing  $j-1$  measurements.

$g_{k,j}$  is a weighting vector (gain vector) corresponding to measurement No.  $j$  that describes how the innovation  $(z_{k,j} - x_k^a(j-1))$  is distributed on the state vector.

The shape of the gain reflects the correlation between the measurement and nearby points, taken into account measurement and model uncertainties. If the gain in the measurement position is equal to 1, measurements are assumed to be perfect. The smaller gain is chosen the larger uncertainty is assumed in the measurement compared to the model uncertainties.

The formulation of the gain matrix in Eq. (6.3) or the gain vectors in Eq. (6.4) is the most essential part of the filtering scheme, and the different schemes mainly differ from each other in the way the gains are calculated. The most comprehensive linear melding scheme is the Kalman filter where the gains are determined based on a minimisation of the expected error of the analysed state vector in terms of the errors of both model dynamics and data. In this case the gains are determined sequentially based on a dynamical evolution of the forecast covariance matrix of the state vector.

For high-dimensional systems, as considered here, the propagation of the covariance matrix is the main bottleneck, in most cases imposing an unacceptable computational burden for real-time applications. The ensemble Kalman filter (EnKF) presented by Evensen /68/ approximates the error covariance modelling by an ensemble of state vectors that are propagated according to the model equation (6.1). This approximation reduces significantly the computational burden.

Experiences with the EnKF shows that the computational requirements for obtaining a proper representation of the covariance matrix are of the order of 100 model runs, which may be too expensive in real-time applications. The constant weighting function method developed by Madsen and Skotner /71/ is based on predefined gain vectors that are assumed constant in time. In this case the filtering update is only slightly more expensive than a normal model run.

## 6.2 Ensemble Kalman filter

The Kalman filter is based on a stochastic formulation of the model equation (6.1) and measurement equation (6.2). By including possible errors on the forcing terms the system gets the following stochastic formulation:

$$\mathbf{x}_{k+1} = \Phi(\mathbf{x}_k, \mathbf{u}_k + \varepsilon_k) \quad (6.5)$$



where

$\mathbf{e}_k$  is a vector containing the model error of the forcing terms.

The stochastic representation of the measurements is given by:

$$\mathbf{z}_k = \mathbf{C}_k \mathbf{x}_k + \eta_k \quad (6.6)$$

where

$\mathbf{h}_k$  is a random measurement error vector with zero mean and covariance matrix  $\mathbf{R}_k$ .

The uncertainty of the model forecast is described by the covariance matrix  $\mathbf{P}_k^f$ . The Kalman gain to be used in the update equation (6.3) is given by

$$\mathbf{G}_k = \mathbf{P}_k^f \mathbf{C}_k^T (\mathbf{C}_k \mathbf{P}_k^f \mathbf{C}_k^T + \mathbf{R}_k)^{-1} \quad (6.7)$$

which depends on the model and measurement covariances. The model covariance expresses how the innovation vector should be distributed on the state vector, and the relation between the model and measurement covariances expresses how much weight should be put on the measurement. The smaller measurement variance as compared to the model variance, the more weight is put on the measurement.

A major shortcoming of the above formulation is the assumption that the covariance matrix  $\mathbf{P}_k$  is known a priori. For non-linear and high-dimensional systems such as MIKE 11 the evaluation of the covariance matrix requires huge computational costs and storage requirements, and hence makes the filtering infeasible for real-time applications.

In the EnKF, the covariance matrix is represented by an ensemble of possible state vectors. Each of these vectors is propagated according to the dynamical system subjected to model errors cf. Eq. (6.5), and the resulting ensemble then provides estimates of the forecast state vector and covariance matrix. In the measurement update, the Kalman gain matrix is applied for each of the forecast state vectors. To account for measurement errors, the measurements are represented by an ensemble of possible measurements. The resulting updated sample provides estimates of the updated state vector and covariance matrix.

The EnKF algorithm is summarised below. It is assumed that measurement errors are uncorrelated i.e. the covariance matrix  $\mathbf{R}_k$  is a diagonal matrix

$$\mathbf{R}_k = \text{diag}[\sigma_1^2, \dots, \sigma_p^2] \quad (6.8)$$

and hence the sequential updating algorithm in Eq. (6.4) can be applied.





Let there be given a set of  $M$  state vectors  $\mathbf{x}_{j,k}^f$ , where  $j=1,\dots,M$  and  $k$  is the time step index.

1. Each member of the ensemble is propagated forward in time according to the stochastic dynamical system given by Eq. (6.5). For each member of the ensemble the model error is drawn from a Gaussian distribution with zero mean and known covariance.
2. The forecast of the state vector is then estimated as the mean of this ensemble:

$$\bar{\mathbf{x}}_k^f = \frac{1}{M} \sum_{j=1}^M \mathbf{x}_{j,k}^f \quad (6.9)$$

3. An estimate of the covariance matrix is found according to:

$$\mathbf{P}_k^f = \frac{1}{M-1} \mathbf{S}_k^f (\mathbf{S}_k^f)^T, \quad (6.10a)$$

$$\mathbf{S}_{j,k}^f = \mathbf{x}_{j,k}^f - \bar{\mathbf{x}}_k^f, \quad (6.10b)$$

4. Each of the ensemble state vectors are updated sequentially using Eq. (6.4). The gain vector for measurement No.  $i$  is given by:

$$\mathbf{g}_k^i = \frac{1}{\mathbf{c}_k^i \mathbf{P}_{k,i-1}^a (\mathbf{c}_k^i)^T + \sigma_i^2} \mathbf{P}_{k,i-1}^a (\mathbf{c}_k^i)^T \quad (6.11)$$

In the above sub-/super-script  $i$  is a running index indicating elements corresponding to the  $i$ 'th update using the  $i$ 'th measurement  $\mathbf{z}_k^i$ . The term  $\mathbf{c}_k^i$  is the  $i$ 'th row of the information matrix  $\mathbf{C}_k$  described earlier.

5. The updated state vector and covariance matrix are estimated as:

$$\bar{\mathbf{x}}_k^a = \frac{1}{M} \sum_{j=1}^M \mathbf{x}_{j,k}^a, \quad \mathbf{P}_k^a = \frac{1}{M-1} \mathbf{S}_k^a (\mathbf{S}_k^a)^T \quad (6.12)$$

In the implementation of the EnKF the covariance matrix  $\mathbf{P}_k$  is never calculated. All calculations are based on  $\mathbf{S}_k$ .

When no data are available for updating, only steps 1-3 are carried out. This is the approach taken in MIKE 11 DA when performing uncertainty assessment and making a stochastic or ensemble forecast.

### 6.2.1 Model errors described by auto-regressive processes

The model errors are defined by auto-regressive processes of first order. Thus, for each uncertain boundary condition  $l = 1, 2, \dots, L$  the model errors are described by

$$\varepsilon_{i,k+1}^l = \phi_l \varepsilon_{i,k}^l + \delta_{i,k+1}^l, \quad i = 1, 2, \dots, M \quad (6.13)$$

where  $\delta_{i,k+1}^l$  is randomly drawn from a Gaussian distribution with zero mean and user defined standard deviation  $\sigma_{d,j}$ . Furthermore, all  $\delta_{i,k+1}^l$  are assumed to be uncorrelated. It should be emphasised that to ensure that the errors do not grow without limit the absolute value of the regression coefficients  $\phi$  must be less than unity.

By using an auto-regressive description the model error has some memory that is propagated as part of the model forecast. In this case the model state is augmented with the model errors that are updated as part of the Kalman filter update scheme. In forecast mode, the model errors at the time of forecast are phased out according to the exponential decay defined by the auto-regressive process.

### 6.3 Constant weighting function

In the constant weighting function method the gain functions in the update equation (6.4) are assumed to be constant. Three different gain functions are assumed, respectively, a constant ( $g_1$ ), a triangular ( $g_2$ ), and a mixed exponential ( $g_3$ ) distribution

$$g_1(\xi) = A, \quad \xi_{US} \leq \xi \leq \xi_{DS}$$

$$g_2(\xi) = \begin{cases} A \frac{\xi - \xi_{US}}{\xi_{MP} - \xi_{US}}, & \xi_{US} \leq \xi \leq \xi_{MP} \\ A \frac{\xi_{DS} - \xi}{\xi_{DS} - \xi_{MP}}, & \xi_{MP} \leq \xi \leq \xi_{DS} \end{cases} \quad (6.14)$$

$$g_3(\xi) = A \exp\left(-\frac{1}{2} \left(\frac{\xi'}{1/3}\right)^2\right) = \begin{cases} \xi' = \frac{\xi_{MP} - \xi}{\xi_{MP} - \xi_{US}}, & \xi_{US} \leq \xi \leq \xi_{MP} \\ \xi' = \frac{\xi - \xi_{MP}}{\xi_{DS} - \xi_{MP}}, & \xi_{MP} < \xi \leq \xi_{DS} \end{cases}$$

where

$g(\xi)$  is the gain value at the river chainage  $\xi$ .

$\xi_{US}$  is the upstream bound for the gain function.



$\xi_{DS}$  is the downstream bound for the gain function.

$\xi_{MP}$  is the measurement point.

$A$  is the gain amplitude.

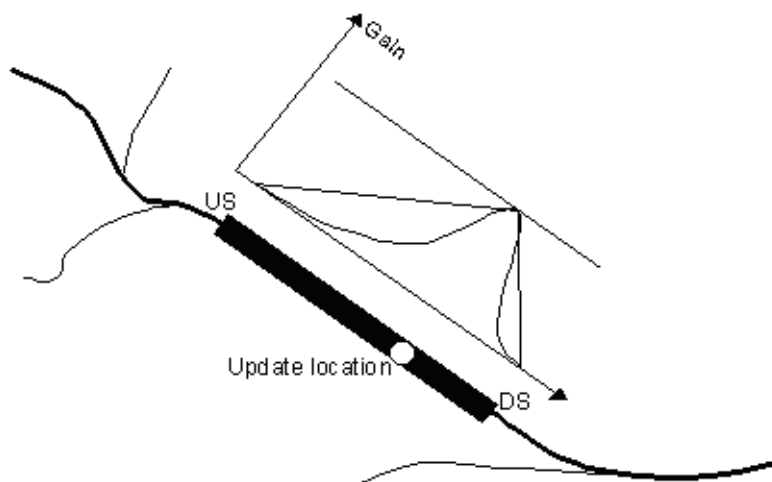


Figure 6.1 Definition of gain function for a measurement (update) location. Note that updates cannot take place across river junctions.

The definition of the gain function is illustrated in Figure 6.1. The amplitude should reflect the confidence of the observation as compared to the model forecast; that is, if  $A = 1$  the measurement is assumed to be perfect, whereas for smaller  $A$  less emphasis is put on the measurement as compared to the model forecast. The distribution and the bounds of the gain function should reflect the correlation between the model forecast error at the measurement location and the errors at nearby grid points.

The procedure updates the parts of the state vector that correspond to the measurement variable (e.g. if water levels are measured the water level grid points are updated) using the sequential algorithm in Eq. (6.4). The other parts of the state vector are implicitly updated according to the numerical scheme in the next time step.

### 6.3.1 Error forecast modelling

The filtering procedure described above can be applied to update the state of the river system up to the time of forecast (or as long as measurements are available). This updated state can then be used as initial conditions for a model forecast. In this case, however, the forecast skills of the model will be

limited to a time horizon where the initial conditions are washed out. To keep the model on the "right track" for a longer period the filtering procedure is here combined with error forecasts at the measurement points.

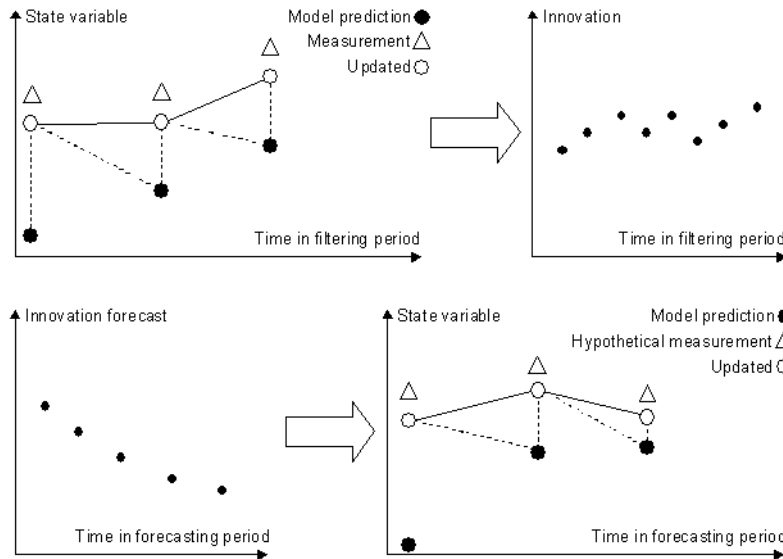


Figure 6.2 Illustration of the combined filtering and error forecast procedure.

The principle of this combined approach is illustrated in Figure 6.2. At each update time step in the filtering period (prior to the time of forecast), the model innovation is acquired at all update locations. For each update location this gives rise to a time series of innovations that covers the filtering period up to the time of forecast (or the time of the last measurement). At the end of the filtering period, an error forecast model defined at each update location is then used to propagate the innovation in the forecasting period and update the affected state variables accordingly using the filtering algorithm in Eq. (6.4).

The error forecast model can be defined as a general linear or non-linear model with a one-step ahead prediction that depends on the previous innovations ( $\varepsilon_{k-1}, \varepsilon_{k-2}, \dots$ ), the forecasted model state at the present time step ( $x_k^f$ ), the previous updated model states ( $x_{k-1}^a, x_{k-2}^a, \dots$ ), and the present and previous model forcings ( $u_k, u_{k-1}, \dots$ )

$$\varepsilon_k = f(\varepsilon_{k-1}, \varepsilon_{k-2}, \dots, x_k^f, x_{k-1}^a, x_{k-2}^a, \dots, u_k, u_{k-1}, \dots) \quad (6.15)$$

Equation (6.15) is used recursively by substituting observed innovations with forecasted values.



In the implementation, an equation parser is used that facilitates an easy and flexible definition of error forecast models such as auto-regressive, moving average models or other linear or non-linear functional forms based on common mathematical operators. Thus, it is possible to define a wide range of error forecast models tailored to the local nature of the model error at each update location.

In order to ensure a fast, accurate and objective derivation of the error forecast models, fully automatic parameter estimation techniques have been incorporated. On the basis of a user-defined time window in the filtering period prior to the time of forecast, the parameters of the error forecast model are estimated. The error forecast models are updated when a new forecast is to be issued using time series of the most recent innovations. This allows the error forecast models to adapt from one forecast to the next to the physical conditions prevailing at the time of forecast without any need for calibration or user intervention in general. In the case of a linear error forecast model, the model parameters are estimated using least squares regression techniques, whereas the shuffled complex evolution (SCE) algorithm (Duan et al. /67/) is applied for the parameter optimisation in the case of a non-linear model.

## 6.4 References

- /67/ Duan, Q., Sorooshian, S., Gupta, V., 1992, Effective and efficient global optimization for conceptual rainfall-runoff models, *Water Resour. Res.*, 28(4), 1015-1031.
- /68/ Evensen, G., 1994, Sequential data assimilation with a non-linear quasi-geostrophic model using Monte Carlo methods to forecast error statistics, *J. Geophys. Res.*, 99(C5), 10,143-10,162.
- /69/ Hartnack, J.N., and Madsen, H., 2001, Data assimilation in river flow modelling, 4th DHI Software Conference, 6-8 June, 2001, Scanti-con Conference Centre, Helsingør, Denmark
- /70/ Madsen, H., Rosbjerg, D., Damgård, J., Hansen, F.S., 2003, Data assimilation in the MIKE 11 Flood Forecasting system using Kalman filtering, *Water Resources Systems - Hydrological Risk, Management and Development (Proceedings of symposium HS02b held during IUGG2003 at Sapporo, July 2003)*. IAHS Publ. no. 281, 75-81.
- /71/ Madsen, H., and Skotner, C., 2004, Adaptive state updating in real-time river flow forecasting - A combined filtering and error forecasting procedure, *J. Hydrology*, Submitted.





# APPENDIX A

## Scientific Background







## A.1 Scientific Background

This manual forms an appendix to the MIKE 11 HD Reference Manual.

### A.1.1 Manual format

Detailed theoretical descriptions of the following headings are given in this appendix.

- Area Preserving Slot (*p. 395*)
- Culverts, Q-h Relations Calculated (*p. 397*)
- DELTA Coefficient (*p. 405*)
- The Double Sweep Algorithm (*p. 407*)
- 2-D Mapping, Interpolation Routine (*p. 417*)
- Modified Diffusive Wave Approximation (*p. 423*)
- Saint Venant Equations (*p. 425*)
- Solution Scheme (*p. 429*)
- Structures (*p. 435*)
- User Defined Structure (*p. 459*)
- Nomenclature (*p. 475*)





## A.2 Area Preserving Slot

During low flow conditions (the local water depth is less than DELH) a slot is introduced into the computations. The slot starts DELH over the bottom and extends 5 DELH below.

There are two different alternatives for the description of the slot.

The classical description is given by

$$B = \frac{\sqrt{z + 5\Delta h}}{\sqrt{6\Delta h}} B_{\Delta} \quad (\text{A.2.1})$$

where  $z$  is the level with respect to the bed level (lowest point).

As an alternative the slot may given a geometry such that the cross sectional area varies continuously across the level at which the slot is introduced (see Fig A.2.1).

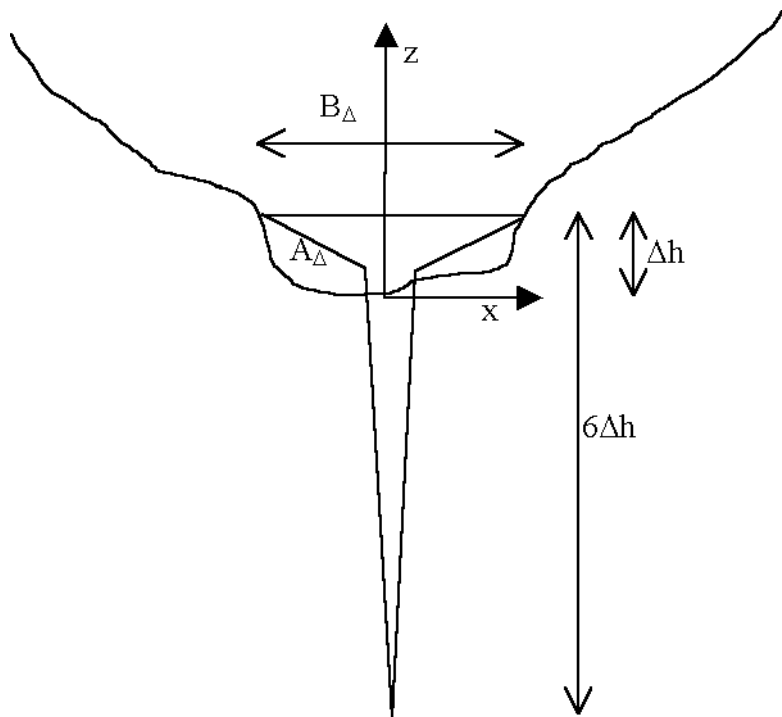


Fig A.2.1 The geometry of the area preserving slot



The slot is chosen so that the width  $B$  of the channel is given by the following expression

$$B = \begin{cases} \frac{B_{\Delta}(\Delta h - z_0)}{\Delta h(z_0 + 5\Delta h)}(z + 5\Delta h) & \text{for } -5\Delta h \leq z \leq z_0 \\ -\frac{B_{\Delta}z_0}{\Delta h(z_0 - \Delta h)}(z - \Delta h) + B_{\Delta} & \text{for } z_0 < z \leq \Delta h \end{cases} \quad (\text{A.2.2})$$

where

$A_{\Delta}$  is the cross sectional area  $\Delta h$  above the bottom

$B_{\Delta}$  is the channel width at the same level.

$\Delta h$  is the user defined DELH.

and

$$z_0 = \Delta h - \frac{2A_{\Delta}}{7B_{\Delta}} \quad (\text{A.2.3})$$

The choice of slot description is set in the MIKE11.ini file through the variable AREA\_PRESERVING\_SLOT. The default setting is the classical description e.g. (A.2.1).



## A.3 Culverts, Q-h Relations Calculated

### A.3.1 Loss coefficients

The contraction, expansion, friction and bend loss coefficients and the critical flow correction coefficient are described as follows.

#### A.3.1.1 Entrance loss

The contraction loss coefficient,  $\zeta_1$ , is a function of the inflow loss coefficient,  $\zeta_{in}$ , the culvert inflow cross-section area,  $A_{s_1}$ , and the inflow river cross-section area,  $A_1$ , see section A.10 Structures (p. 435). Typically,  $\zeta_{in}$  is set to 0.5.

$$\zeta_1 = \zeta_{in} \left( 1 - \frac{A_{s_1}}{A_1} \right) \quad (\text{A.3.1})$$

#### A.3.1.2 Expansion loss

The expansion loss coefficient,  $\zeta_2$ , is a function of the outflow loss coefficient,  $\zeta_{out}$ , specified in the Network editor → structures → culverts in the Head Loss Factor Box, the culvert outflow cross-section area,  $A_{s_2}$ , and the outflow river cross-section area,  $A_2$ , see section A.10 Structures (p. 435). Typically  $\zeta_{out}$  is set to 1.0.

$$\zeta_2 = \zeta_{out} \left( 1 - \frac{A_{s_2}}{A_2} \right)^2 \quad (\text{A.3.2})$$

#### A.3.1.3 Friction loss

The friction loss coefficient is calculated using the Manning formula, i.e.:

$$\zeta_f = \frac{2gLn^2}{R^{4/3}} \quad (\text{A.3.3})$$

where,  $L$  is the culvert length,  $n$  is Manning's coefficient and  $R$  is the mean hydraulic radius along the culvert. The Manning's  $n$  value depends on the interior surface of the culvert. Tables of values can be found in open channel or closed conduit hydraulics references such as Chow (1959), /6/ and Henderson (1966), /11/. For a concrete culvert  $n$  would typically range from 0.011 to 0.017.



### A.3.1.4 Bend and other losses

The bend loss coefficient,  $\zeta_b$ , is provided for situations where head losses other than from the above occur, for example bends, damaged culverts, trapped debris. The head loss due to  $\zeta_b$  is defined in the total head loss given below. For straight culverts in good condition a value of zero would apply.

### A.3.1.5 Total head loss through culvert

The total head loss,  $\Delta H_{loss}$ , through the culvert is given by

$$\Delta H_{loss} = \frac{Q^2}{2g} \left( \frac{\zeta_1}{A_{s_1}^2} + \frac{\zeta_f + \zeta_b}{A_{s_a}^2} + \frac{\zeta_2}{A_{s_2}^2} \right) \quad (\text{A.3.4})$$

where,  $A_{s_a}$  is the mean cross-section area along the length of the culvert, and  $Q$  is the discharge.

### A.3.1.6 Critical flow correction factor

The critical and orifice flows are multiplied by the critical flow correction factor,  $\alpha_c$ , specified in the Network editor → structures → culverts in the Head Loss Factor Box as the Free Overflow Head Loss Factor. Refer to section 1.34 Steady State Energy Equation (p. 162), for more details. Typically a value of 1.0 is used.

## A.3.2 Momentum equation coefficients

### A.3.2.1 Zero flow

The momentum equation coefficients, see section A.9 Solution Scheme (p. 429), in the case of zero flow are:

$$\alpha = 0, \beta = 1, \gamma = 0, \delta = 0 \quad (\text{A.3.5})$$

### A.3.2.2 Upstream controlled flow

For upstream controlled flow the coefficients are the same as that described for Structures (p. 435).



### A.3.2.3 Downstream controlled flow

The equations for downstream controlled flow through a culvert are an extension of those described in Structures (p. 435). The momentum equation coefficients are calculated as follows:

$$C_a = \frac{\zeta_1}{A_{s_1}^2} + \frac{\zeta_f + \zeta_b}{A_{s_a}^2} + \frac{\zeta_2}{A_{s_2}^2} - \frac{1}{A_1^2} + \frac{1}{A_2^2} \quad (\text{A.3.6a})$$

$$C_b = h_1 - h_2 \quad (\text{A.3.6b})$$

$$C_c = \text{sign}(C_a) \sqrt{\frac{2g}{|C_a|C_b}} \quad (\text{A.3.6c})$$

giving the matrix coefficients at the culvert as:

$$\alpha = -C_c, \beta = 1, \gamma = C_c, \delta = 0 \quad (\text{A.3.7})$$

### A.3.3 Critical inflow or outflow

In the case of either inflow or outflow being critical the discharge,  $Q_c$ , for a given critical depth is calculated as:

$$Q_c = \alpha_c A_c \sqrt{g \frac{A_c}{T}} \quad (\text{A.3.8})$$

where,  $A_c$  is the critical flow area and  $T$  is the flow width at the water surface.

### A.3.4 Critical inflow

Critical flow at the inflow to the culvert occurs when the culvert slope,  $S_0$ , exceeds the critical flow slope,  $S_c$ , as defined by:

$$S_0 = \frac{z_{inv_1} - z_{inv_2}}{L} \quad \text{and} \quad S_c = \left( \frac{Q_c n}{A_c R_c^{2/3}} \right)^2 \quad (\text{A.3.9})$$

where,  $z_{inv_1}$  and  $z_{inv_2}$  are the inflow and outflow invert levels of the culvert, and  $R_c$  is the hydraulic radius at critical flow.

For the calculation of  $h_1$ , the inflow water depth is taken as the critical depth. The friction losses and bend losses have no effect on the discharge for this flow condition.



### A.3.5 Critical outflow

Critical flow at the outflow to the culvert occurs when  $S_0$  is less than  $S_c$ .

Before the calculation of  $h_1$  can proceed it is necessary to determine the inflow water depth. A standard backwater analysis using a fine increment in water depth is used starting with the critical flow depth at the outflow end and working upstream. The bend losses, if any, are applied at the mid-point along the length of the culvert.

In the situation of the culvert section becoming full (i.e., submerged inflow), the friction slope becomes constant and the backwater analysis adjusts accordingly.

The upstream water level is calculated based on the inflow water depth in the culvert using the iteration procedure described in section 1.12 Culverts, Q-h Relations Calculation (p. 81).

### A.3.6 Orifice flow at inflow

Orifice flow occurs in short or steep culverts (Figure 1.23(e)). Culverts in which this flow condition occurs are sometimes referred to as "hydraulically short" (16). The flow is similar to that which occurs under a sluice gate. The discharge is calculated by:

$$Q_0 = \alpha_c C_0 A_{full} \sqrt{2g(H_1 - z_{inv_1})} \quad (\text{A.3.10})$$

where,  $C_0$  is the coefficient of discharge,  $H_1$  is the inflow energy head in the river,  $z_{inv_1}$  is the inflow invert level, and  $A_{full}$  is the full cross-section area of the culvert.

The facility to manually specify  $C_0$  as a function of  $y_1/D$  ( $y_1 = h_1 - z_{inv_1}$  and  $D =$  culvert depth) has been provided in the network editor → structures → culverts → Flow conditions under the Orifice Flow Conditions Tab. It is anticipated that this will be unnecessary in the majority of cases as a default is provided (discussed below). However, it does provide the flexibility to model a "hydraulically short" culvert, or a sluice gate (zero length) in detail if sufficient information on the discharge coefficient is available. Carter (1957), (5) provides a detailed analysis and tables of discharge coefficients for orifice flow and other flow conditions.

If no values for  $C_0$  are specified, a value of 0.65 at a  $y_1/D$  of 5.0 is adopted. When  $y_1/D$  is greater than 5.0,  $C_0$  remains constant at 0.65, while below 5.0 a linear interpolation is made with the  $C_0$  value calculated automatically as described in the following.

A value for  $C_0$  is automatically calculated at the point of inflow submergence if the flow condition is inflow critical. This allows a smooth transition to occur





between the two flow conditions. The point of inflow submergence is nominally adopted as 95% of the full culvert flow area. The  $C_0$  value calculated is shown in the first row of the  $C_0$  versus  $y/D$  tables.

### A.3.7 Full culvert flow with free outflow

The complement to orifice flow at the inflow is when the culvert is defined as "hydraulically long", i.e., the culvert is flowing full with a free outflow (Figure 1.23 (f)). In this case the discharge,  $Q_p$  is calculated using:

$$Q_p = A_{full} \sqrt{\frac{2g(H_1 - z_{obv_2})}{\zeta_1 + \zeta_f + \zeta_b + 1}} \quad (\text{A.3.11})$$

where,  $H_1$  is the inflow energy head level in the river and  $z_{obv_2}$  is the outflow obvert (soffit) level (i.e. invert plus culvert depth).

The outflow energy head level in the above equation has been set to that at the outflow obvert by assuming atmospheric pressure occurs there. This assumption is compatible with the critical outflow flow condition at the point of the outflow becoming submerged as the discharge equations are the same if  $\zeta_2$  is equal to 1.0. This is important for the transition between upstream and downstream controlled flow conditions as discussed later.

### A.3.8 Downstream controlled flow (submerged flow)

In the case of a downstream controlled flow the computation is complicated because of the influence of all three cross-sectional areas along the culvert,  $A_{s_1}$ ,  $A_{s_a}$  and  $A_{s_2}$ , and the mean hydraulic radius,  $R$ . The situation is further complicated in the case where the culvert outflow is close to critical flow conditions as the water surface profile through the culvert in these conditions is very non-linear.

### A.3.9 Partially full inflow and outflow

An iteration procedure is used to determine  $A_{s_1}$ ,  $A_{s_a}$ ,  $A_{s_2}$  and  $R$ . The iteration is made on the water levels in the culvert at the upstream and downstream ends, Equations (A.3.12a) and (A.3.12b), from which  $A_{s_1}$  and  $A_{s_2}$  are

calculated. For  $A_{s_a}$  and  $R$ , a linear interpolation of the water level at the culvert mid-point is initially used.

$$h_{s_1} = H_1 - \frac{(1 + \zeta_1)(H_1 - H_2)}{C_{a_s} A_{s_1}^2} \quad (\text{A.3.12a})$$

$$h_{s_2} = H_2 - \frac{(1 - \zeta_2)(H_1 - H_2)}{C_{a_s} A_{s_2}^2} \quad (\text{A.3.12b})$$

where

$$C_{a_s} = \frac{\zeta_1}{A_{s_1}^2} + \frac{(\zeta_f + \zeta_b)}{A_{s_a}^2} + \frac{\zeta_2}{A_{s_2}^2} \quad (\text{A.3.13})$$

$h_{s_1}$  and  $h_{s_2}$  are the water levels in the culvert at the inflow and outflow ends, while  $H_1$  and  $H_2$  are the inflow and outflow energy head levels in the river.

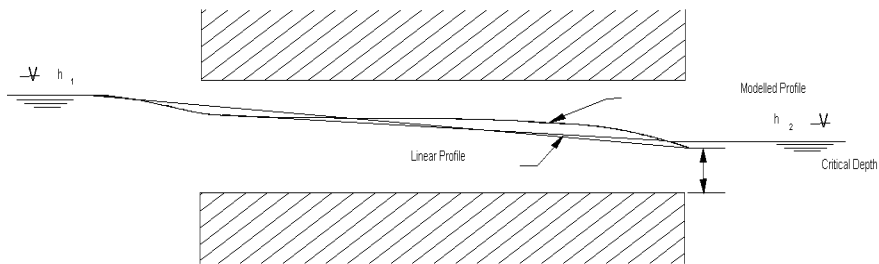


Fig A.3.2 Modelled water surface profile when profile is very non-linear

When the outflow is close to a critical flow state the water surface profile is highly non-linear, and the friction losses calculated from a linear interpolation will be too high (Fig A.3.2). To overcome this problem without using a computationally intensive backwater analysis in each iteration, a comparison is made with the friction losses calculated from the backwater analysis for critical outflow, see above. In the case of the losses from the backwater analysis being lower,  $C_{a_s}$  is calculated as:

$$C_{a_s} = \frac{2g}{Q_c^2} \left( H_1 - h_c - \frac{Q_c^2}{2gA_c^2} \right) + \frac{\zeta_2}{A_{s_2}^2} \quad (\text{A.3.14})$$



where, the subscript  $c$  refers to the critical flow conditions based on  $h_1$ . This also ensures a smooth transition between the outflow critical condition and submerged flow providing  $\zeta_2$  is less than or equal to 1.0.

The iteration procedure typically takes two to three iterations to converge. If the upstream and downstream water levels are changing rapidly more iterations are usually necessary with the number rarely exceeding ten. The maximum number of iterations is controlled by the Inter1Max variable which can be edited in the HD parameter editor →Default values.

### A.3.10 Submerged inflow and partially full outflow

This flow condition typically occurs when the culvert slope is adverse to the water surface slope as shown in Figure 1.23(h).

The iteration procedure described in “Partially full inflow and outflow (p. 401)” above is used except that the mean cross-section area is adjusted according to:

$$A_{s_a} = \frac{L_{full}}{L} A_{full} + \left(1 - \frac{L_{full}}{L}\right) \frac{A_{full} + A_{s_2}}{2} \quad (\text{A.3.15})$$

where,  $L_{full}$  is the length of the culvert which is following full and  $L$  is the total length.

A similar adjustment is made to the mean hydraulic radius.

### A.3.11 Partially full inflow and submerged outflow

This flow condition occurs in sloping culverts as illustrated in Figure 1.23(i). A similar procedure to that described in “Submerged inflow and partially full outflow” above is used.

### A.3.12 Fully submerged

Where the culvert is fully submerged (Figure 1.23(j)) the cross-sectional areas and hydraulic radius are equal to those when the culvert is full.

### A.3.13 Transition between upstream and downstream control

Whether the flow is upstream or downstream controlled is best based on a single criteria. Using a single criteria is preferable for stability reasons and for a smooth transition between flow conditions.

Analysis of the formulations described above, assuming that  $\zeta_2$  is less than or equal to 1.0, gives the following conclusions:



- in the case of either inflow or outflow being critical, then if  $H_2$  is below the critical water level,  $h_c$ , the flow will be critical. If  $H_2$  is greater than  $h_c$  then the flow can be either critical or downstream controlled. The level at which the flow becomes downstream controlled is dependent on the magnitude of  $\zeta_2$ . If  $\zeta_2$  is equal to 1.0 the change to or from submerged flow will be at  $H_2$  equal to  $h_c$ . For  $\zeta_2$  less than 1.0, which is normally the case, downstream controlled flow will occur at some point above  $h_c$ .
- similarly, the same scenario can be shown to occur for full culvert flow and orifice flow versus fully submerged flow where  $h_c$  is taken as the outflow obvert (invert plus culvert depth).

This leads to the following criteria for selecting between upstream and downstream flow controls:

- if  $H_2$  is less than either  $h_c$  at outflow (critical inflow or outflow) or the downstream obvert (orifice or full culvert flow) then the flow is upstream controlled, otherwise the flow condition which gives the lower discharge is selected

In the case of critical inflow,  $H_2$  should be taken as that immediately past the point of critical flow (i.e., at the inflow to the culvert). However, for culverts of non-zero length and/or non-zero bend loss, the energy head losses through the culvert are not known and the more conservative approach of using  $h_c$  at the outflow must be taken. A similar situation applies in the case of orifice flow.



## A.4 DELTA Coefficient

A forward centring of the  $\partial h / \partial x$  term in the numerical scheme has a dissipative influence which can be demonstrated using the Taylor-series. The forward centring is automatically introduced in MIKE 11 when the flow becomes supercritical in that particular channel section. Additionally, the centring can be specified by the user for sub-critical flows through the centring coefficient DELTA ( $0.5 < \delta < 1$ ).

Introducing the  $\delta$  value into the terms gives:

$$\frac{\partial h}{\partial x} = \delta \frac{h_{j+1}^{n+1} - h_{j-1}^{n+1}}{\Delta 2x} + (1 - \delta) \frac{h_{j+1}^n - h_{j-1}^n}{\Delta 2x} \quad (\text{A.4.1})$$

Using a Taylor series up to the third derivative, these terms become:

$$\begin{aligned} \frac{h_{j+1}^{n+1} - h_{j-1}^{n+1}}{\Delta 2x} &= \frac{\delta}{\Delta 2x} \left[ h + \frac{1}{1!} \frac{\Delta 2x}{2} \frac{\partial h}{\partial x} + \frac{1}{2!} \left( \frac{\Delta 2x}{2} \right)^2 \frac{\partial^2 h}{\partial x^2} \right. \\ &+ \frac{1}{3!} \left( \frac{\Delta 2x}{2} \right)^3 \frac{\partial^3 h}{\partial x^3} - h + \frac{1}{1!} \frac{\Delta 2x}{2} \frac{\partial h}{\partial x} + \frac{1}{2!} \left( \frac{\Delta 2x}{2} \right)^2 \frac{\partial^2 h}{\partial x^2} \\ &\left. + \frac{1}{3!} \left( \frac{\Delta 2x}{2} \right)^3 \frac{\partial^3 h}{\partial x^3} \right]_j^{n+1} = \delta \left[ \frac{\partial h}{\partial x} + \frac{(\Delta 2x)^2}{24} \frac{\partial^3 h}{\partial x^3} \right]_j \end{aligned} \quad (\text{A.4.2})$$

Similarly for the last term:

$$(1 - \delta) \frac{h_{j+1}^n - h_{j-1}^n}{\Delta 2x} = (1 - \delta) \left[ \frac{\partial h}{\partial x} + \frac{(\Delta 2x)^2}{24} \frac{\partial^3 h}{\partial x^3} \right]_j \quad (\text{A.4.3})$$

In this way the formulation of  $\partial h / \partial x$  in (A.4.1) becomes (again using a Taylor series):

$$\begin{aligned} \frac{\partial h}{\partial x} &= \delta \left[ \frac{\partial h}{\partial x} + \frac{1}{1!} \frac{\Delta t}{2} \frac{\partial^2 h}{\partial x \partial t} + \frac{1}{2!} \left( \frac{\Delta t}{2} \right)^2 \frac{\partial^3 h}{\partial x \partial t^2} \right]_j^{n+1/2} \\ &+ (1 - \delta) \left[ \frac{\partial h}{\partial x} - \frac{1}{1!} \frac{\Delta t}{2} \frac{\partial^2 h}{\partial x \partial t} + \frac{1}{2!} \left( \frac{\Delta t}{2} \right)^2 \frac{\partial^3 h}{\partial x \partial t^2} \right]_j^{n+1/2} \\ &= \frac{\partial h}{\partial x} \Big|^{n+1/2} + (2\delta - 1) \frac{\Delta t}{2} \frac{\partial^2 h}{\partial x \partial t} \Big|^{n+1/2} + \text{higher order terms} \end{aligned} \quad (\text{A.4.4})$$

which represents the dissipative effect, when  $\delta > 0.5$ , as the last term becomes positive.







If we were dealing with a one-branch system with a water level boundary at each end, then  $H_{us}$  and  $H_{ds}$  would be known. There would be only  $n$  unknowns left in the  $n$  equations, and these would be ready to solve using standard elimination technique. However as MIKE 11 handles several branches, another method has to be applied. To explain this the above  $n$  equations are shown in matrix form in equation (A.5.3).

$$\begin{bmatrix}
 \alpha_1 & \beta_1 & \gamma_1 & & & & & & & \delta_1 \\
 & \alpha_2 & \beta_2 & \gamma_2 & & & & & & \delta_2 \\
 & & \alpha_3 & \beta_3 & \gamma_3 & & & & & \delta_3 \\
 & & & \alpha_4 & \beta_4 & \gamma_4 & & & & \delta_4 \\
 & & & & \alpha_5 & \beta_5 & \gamma_5 & & & \delta_5 \\
 & & & & & \cdot & \cdot & \cdot & & \cdot \\
 & & & & & & \cdot & \cdot & \cdot & \cdot \\
 & & & & & & & \alpha_{n-2} & \beta_{n-2} & \gamma_{n-2} & \delta_{n-2} \\
 & & & & & & & & \alpha_{n-1} & \beta_{n-1} & \gamma_{n-1} & \delta_{n-1} \\
 & & & & & & & & & \alpha_n & \beta_n & \gamma_n & \delta_n
 \end{bmatrix} \tag{A.5.3}$$

Using standard elimination technique the matrix in equation (A.5.3) can be transformed to the matrix in equation (A.5.4).

$$\begin{bmatrix}
 a_1 & 1 & & & & & & & & b_1 & c_1 \\
 a_2 & & 1 & & & & & & & b_2 & c_2 \\
 a_3 & & & 1 & & & & & & b_3 & c_3 \\
 a_4 & & & & 1 & & & & & b_4 & c_4 \\
 a_5 & & & & & 1 & & & & b_5 & c_5 \\
 \cdot & & & & & & \cdot & & & \cdot & \cdot \\
 \cdot & & & & & & & \cdot & & \cdot & \cdot \\
 a_{n-2} & & & & & & & & 1 & b_{n-2} & c_{n-2} \\
 a_{n-1} & & & & & & & & & 1 & b_{n-1} & c_{n-1} \\
 a_n & & & & & & & & & & 1 & b_n & c_n
 \end{bmatrix} \tag{A.5.4}$$

From the matrix (A.5.4) it can be seen that in any grid point the variable  $Z$  (water level or discharge) is expressed as a function of the water level in the upstream and downstream node:

$$Z_j^{n+1} = c_j - a_j H_{us}^{n+1} - b_j H_{ds}^{n+1} \tag{A.5.5}$$





However, as MIKE 11 operates with branches divided by nodes at external boundary points and at internal branch connections, it is necessary to know the water levels in all nodes before the matrix in (A.5.4) can be solved according to equation (A.5.5).

## A.5.2 Node matrix

In nodes a continuity equation covering the surrounding  $h$ - and  $Q$ -points is set up:

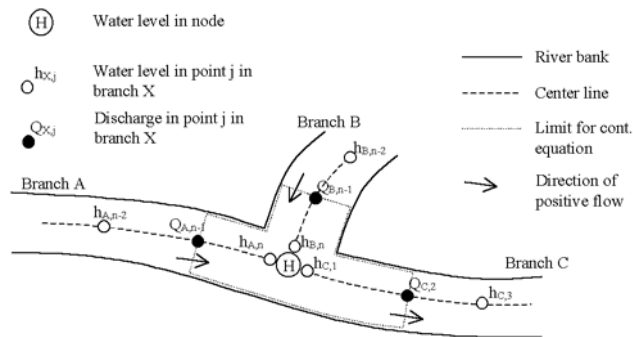


Fig A.5.3 Three-branch node with limit for continuity equation.

Fig A.5.3 gives a close look at the grid points surrounding a node. The finite difference approximation of the continuity equation around the node is given by:

$$\begin{aligned} \frac{H^{n+1} - H^n}{\Delta t} A_{fl} &= Q_I^{n+1/2} - Q_O^{n+1/2} \\ \Rightarrow \frac{H^{n+1} - H^n}{\Delta t} A_{fl} &= \frac{1}{2} (Q_{A,n-1}^n + Q_{B,n-1}^n - Q_{C,2}^n) \\ &\quad + \frac{1}{2} (Q_{A,n-1}^{n+1} + Q_{B,n-1}^{n+1} - Q_{C,2}^{n+1}) \end{aligned} \quad (\text{A.5.6})$$

where

$Q_I$  Sum of inflows

$Q_O$  Sum of outflows

$\Delta t$  Time step



In equation (A.5.6)  $Q_{A,n-1}$ ,  $Q_{B,n-1}$  and  $Q_{C,2}$  at time level  $n+1$  can be substituted according to equation (A.5.5), and the following equation is achieved:

$$\begin{aligned}
 \frac{H^{n+1} - H^n}{\Delta t} A_{fl} &= \frac{1}{2}(Q_A^n + Q_B^n - Q_C^n) \\
 + \frac{1}{2}(c_{A,n-1} - a_{A,n-1} H_{A,us}^{n+1} - b_{A,n-1} H^{n+1} & \\
 + c_{B,n-1} - a_{B,n-1} H_{B,us}^{n+1} - b_{B,n-1} H^{n+1} & \\
 + c_{C,2} - a_{C,2} H^{n+1} - b_{C,2} H_{C,ds}^{n+1}) &
 \end{aligned}
 \tag{A.5.7}$$

where

$H$  Water level in the actual node

$H_{A,us}$  Water level in the node in the upstream end of branch A

$H_{B,us}$  Water level in the node in the upstream end of branch B

$H_{C,ds}$  Water level in the node in the upstream end of branch B

An equation similar to (A.5.7) is set up in each node, giving  $N$  equations with  $N$  unknowns ( $N$  is the number of nodes). In these equations the water level in each node becomes a linear function of the water level in the nodes to which the node is directly connected. Assume a configuration of branches as in Fig A.5.4.

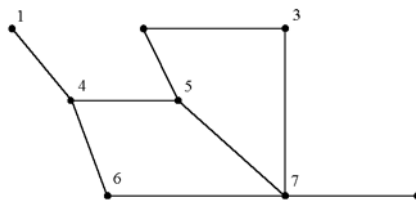


Fig A.5.4 River network with 9 branches and 8 nodes.

In the branch configuration as in Fig A.5.4 eight nodal continuity equations are set up. Fig A.5.5 shows the matrix with  $x$  indicating coefficients that are different from zero.



	1	2	3	4	5	6	7	8	RS
1	x			x					x
2		x	x		x				x
3			x	x			x		x
4	x			x	x	x			x
5		x		x	x		x		x
6				x		x	x		x
7			x		x	x	x	x	x
8							x	x	x

Fig A.5.5 Node matrix for the network in Fig A.5.4 before bandwidth minimisation (RS is the right hand side coefficients).

From the matrix in Fig A.5.5 it can for instance be seen that in node 4 (row 4 in the matrix) the continuity equation (in the form of equation (A.5.7)) becomes a function of the water level in node 1, 4, 5 and 6.

The matrix in Fig A.5.5 can be solved using the standard method of Gaussian elimination, and thus the water level in the nodes at time step  $n+1$  is known. Hereafter the water levels and discharges along the branches are calculated using equation (A.5.5).

### A.5.3 Bandwidth minimisation

The bandwidth of the matrix in Fig A.5.5 as indicated by the dashed line, is a function of the order in which the nodal points are defined. The bandwidth of the matrix in Fig A.5.5 is equal to 5. The total amount of computational time will increase with increasing bandwidth. In order to minimise the computational work and thus increase the computational speed a routine has been developed which automatically minimises the bandwidth by internal re-ordering of the nodal points. By re-ordering the above matrix the bandwidth can be reduced from 5 to 4 as shown in Fig A.5.6:



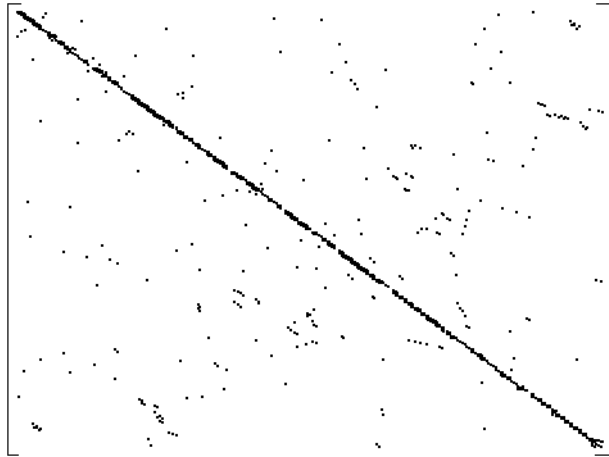
	1	4	5	6	7	2	3	8	RS
1	x	x							x
2	x	x	x	x					x
3		x	x		x	x			x
4		x		x	x				x
5			x	x	x		x	x	x
6			x			x	x		x
7					x	x	x		x
8					x			x	x

Fig A.5.6 Node matrix for the network in figure 6 after bandwidth minimisation.

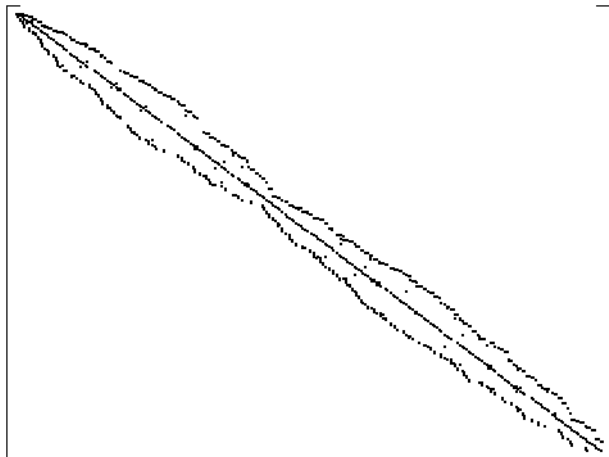


Fig A.5.7 River network with 273 nodes.

Once minimised the matrix is solved as previously explained. Using a bandwidth minimising routine becomes increasingly important as the number of nodes increases. Fig A.5.7 shows a more complex river network, and Fig A.5.8 and Fig A.5.9 shows the node matrix before and after the minimisation.



*Fig A.5.8 Branch matrix for the network in Fig A.5.7 before bandwidth minimisation.*



*Fig A.5.9 Branch matrix for the network in Fig A.5.7 after bandwidth minimisation.*

## A.5.4 Boundaries

In MIKE 11 the following three types of boundary conditions can be applied:

- Water level as a function of time

- Discharge as a function of time
- A tabulated relation between water level and discharge ( $Q/h$  boundary)

Each of the boundary types is taken into account by using a different node equation.

#### A.5.4.1 Water level as a function of time.

In this case the water level in the node at time step  $n+1$  simply becomes the value of the user-specified boundary at time step  $n+1$  ( $H_{boundary}^{n+1}$ ) i.e. in the relevant equation (or row) in the node matrix only the diagonal and the right hand side coefficient are different from zero, and equals respectively 1 and  $H_{boundary}^{n+1}$ .

#### A.5.4.2 Discharge as function of time.

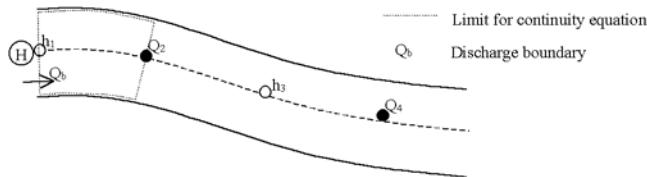


Fig A.5.10 River branch with discharge boundary.

In this case a local continuity equation covering the area indicated in Fig A.5.10 is set up. Equation (A.5.6) becomes:

$$\frac{H^{n+1} - H^n}{\Delta t} A_{fl} = \frac{1}{2}(Q_b^n - Q_2^n) + \frac{1}{2}(Q_b^{n+1} - Q_2^{n+1}) \quad (\text{A.5.8})$$

In equation (A.5.8)  $Q_2$  at time step  $n+1$  is substituted with equation (A.5.5) and equation (A.5.9) is achieved.

$$\frac{H^{n+1} - H^n}{\Delta t} A_{fl} = \frac{1}{2}(Q_b^n - Q_2^n) + \frac{1}{2}(Q_b^{n+1} - c_2 + a_2 H^{n+1} + b_2 H_{ds}^{n+1}) \quad (\text{A.5.9})$$

Equation (A.5.9) is similar to equation (A.5.7) and the coefficients in the relevant row in the node matrix can be calculated by re-arranging equation (A.5.9).



### A.5.4.3 Q/h boundary

In this case the user specifies a tabulated relation between  $h$  and  $Q$ . A continuity equation is set up at the boundary in the same way as for a discharge boundary. The discharge at the boundary  $Q_b$  is expressed as a function of the water level in the node using the tabulated relation. This is done as follows:

The index  $i$  is found such that  $H_{\text{tab},i} \leq H^n < H_{\text{tab},i+1}$ , and the ratio  $a$  is calculated according to equation (A.5.10).

$$a = \frac{Q_{\text{tab},i+1} - Q_{\text{tab},i}}{H_{\text{tab},i+1} - H_{\text{tab},i}} \quad (\text{A.5.10})$$

Using linear interpolation between the tabulated values of water levels and discharge equations (A.5.11) and (A.5.12) can be achieved:

$$Q_b^{n+1} = Q_{\text{tab},i} + a(H^{n+1} - H_{\text{tab},i}) \quad (\text{A.5.11})$$

$$Q_b^n = Q_{\text{tab},i} + a(H^n - H_{\text{tab},i}) \quad (\text{A.5.12})$$

Equations (A.5.11) and (A.5.12) are substituted into equation (A.5.8) and equation (A.5.13) is achieved:

$$\begin{aligned} \frac{H^{n+1} - H^n}{\Delta t} A_{fl} = & \frac{1}{2} (Q_{\text{tab},i} + a(H^n - H_{\text{tab},i}) - Q_2^n) \\ & + \frac{1}{2} (Q_{\text{tab},i} + a(H^{n+1} - H_{\text{tab},i}) - Q_2^{n+1}) \end{aligned} \quad (\text{A.5.13})$$

Equation (A.5.13) is similar to equation (A.5.7) and the coefficients in the relevant row in the node matrix can be calculated by re-arranging equation (A.5.13).







## A.6 2-D Mapping, Interpolation Routine

Outlined below is the interpolation routine used in MIKE 11 to generate the various two-dimensional maps.

### A.6.1 Mapping

The mapping of water levels, water depths, velocities and advection dispersion components from the one-dimensional results to two-dimensional maps are done internally in MIKE 11 through a couple of steps:

- Interpolation of cross sections at all digitised points and all interpolated water level grid points.
- Linear interpolation of results from the numerical grid to the interpolated cross sections.
- Spatial interpolation of the bed level from the cross sections to all intermediate cells in the two-dimensional grid within the river bed.
- Determination of the velocity profile at all cross sections based on conveyance distribution.
- Spatial interpolation of the required results from the cross sections to all intermediate cells in the two-dimensional grid within the river bed.

#### A.6.1.1 Interpolation of cross sections at digitised points

A number of cross sections need to be interpolated for each reach of the river. Below is illustrated a digitised river section. The circles illustrate the digitised points. The cross sections are shown as the full drawn lines.

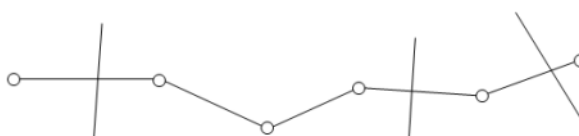


*Fig A.6.11 A close up of a digitised network with the cross sections illustrated. The digitised points are shown as circles.*

This reach is from MIKE 11's point of view seen as a straight line with cross sections perpendicular to the river centre line as illustrated in Fig A.6.12.

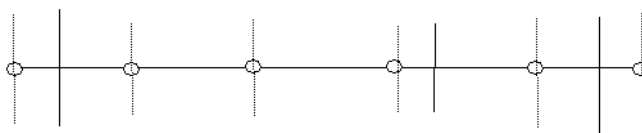


*Fig A.6.12 Digitised reach from MIKE 11's point of view only considering everything referenced according to the chainage. The dashed lines are the additionally required cross sections (interpolated).*

At every digitised point the river may have a kink. The interpolation of the water depth is greatly simplified if the river and flood way may be divided into 4 sided polygons. This may be achieved by securing that cross sections are available at every digitised point. The resulting network consists of straight line segments with a cross section at each end. The interpolation routine used for the cross sections is identical to the one found in the cross section editor. At end points without a cross section the nearest upstream or downstream cross section is reused. The latter is equivalent to the approach used internally in the numerical engine of MIKE 11.

### A.6.1.2 Linear interpolation of results from the numerical grid

Water levels, discharges and concentrations at the interpolated cross sections are simply found through linear interpolation of the values from the two nearest water level grid points. The interpolation in this step is solely based on the chainage.

### A.6.1.3 Spatial interpolation of the bed level from the cross sections

At this point the branch consists of a number of segments with a cross section at each end. Such a segment is termed a mapping box. For each of these mapping boxes a local coordinate/mapping system may be introduced as illustrated in Fig A.6.13. Note that the mapping is one to one and thus has an inverse. The linear interpolation of values may now be carried out on the rectangular mapping box and then pulled back to the mapping box in the MIKE 11 representation. From here the results may be transferred back to the original geo-referenced mapping box provided that the two cross sections defining the the flood box do not intersect as illustrated in Fig A.6.14.

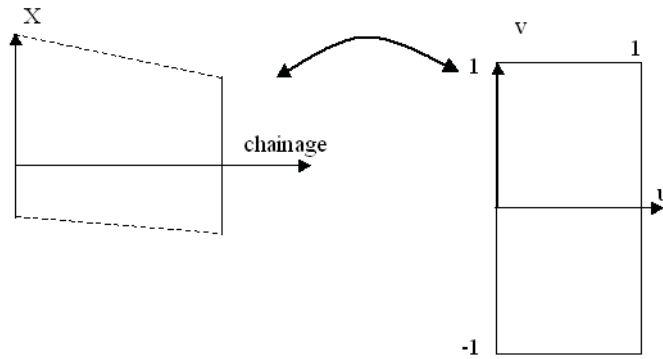


Fig A.6.13 Local mapping from MIKE 11's representation of a mapping box to a coordinate system  $(u,v)$ . The box on the right has a unit length and twice the height. The centre line from the left is mapped onto the line  $v=0$ . The extent of the cross sections of the mapping box on the left is defined by the markers 1,2 and 3.

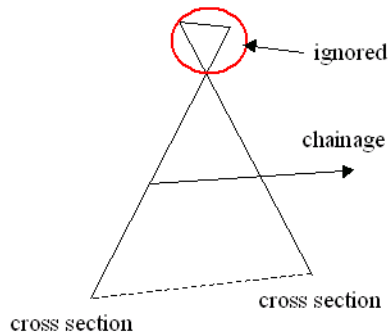


Fig A.6.14 Mapping box with intersecting cross sections. In such a case the illustrated part is ignored in the interpolation routine.

The bed level  $s$  is well defined at all the cross sections. The bed level at a set of coordinates  $(u,v)$  is defined as

$$s(u, v) = (u - 1) \cdot s(0, v) + u \cdot s(1, v) \tag{A.6.1}$$

Using the mapping back to the original system one can hereby obtain the bed level at all intermediate points.



#### A.6.1.4 Determination of the velocity profile at all cross sections

The velocity distribution in a cross section is assumed to be uniform over the depth and vary as the conveyance in the cross section in the transversal direction.

The total conveyance  $K$  is in this context defined as

$$K = \int_0^B h^{5/3} M dx \quad (\text{A.6.2})$$

Where  $h$  is the local water depth,  $B$  the water surface width and  $M$  is Manning's resistance number. Both the water depth and the resistance are functions of the transversal direction  $x$ . In the above a Manning's formulation is used for the resistance, but the approach is similar if a Chezy description is used for the resistance. The 5/3 is then substituted with 3/2 and  $M$  is replaced by the Chezy number  $C$ .

The velocity for a particular point in a cross section is defined by

$$v(x, t) = \frac{Q(t)}{K} M \cdot h^{2/3} \quad (\text{A.6.3})$$

Hereby a value for the velocity can be found at every point in the cross section and the velocity at intermediate points are found through an interpolation similar to eq. (A.6.1).

#### A.6.1.5 Spatial interpolation of the required results from the cross sections

The spatial interpolation of results depends on the type of result:

- Water levels and concentrations are simply interpolated based on the chainage and are only shown if the water level is above the local bed level.
- The water depth is determined as the water level minus the bed level and will only be displayed if the value is positive.
- The velocity is interpolated similar to the bed level and is only shown if the local water depth is positive.

### A.6.2 Generation of a Digital Elevation Model (DEM)

The generation of a digital Elevation Model (DEM) in MIKE 11 is done by determining the bed level at all the grid cells lying within a mapping box. If a cell lies in multiple mapping boxes then the average is used for the bed level.



The generation of a DEM may be augmented with one or more background DEMs. If this is the case the user supplied DEM will be applied in the grid cells where no mapping boxes are present.

If multiple DEMs are used the DEMs are ranked and the DEM with the highest rank containing data in the particular cell is used.

Finally the DEM generation allows user supplied topographical information to be used inside the mapping boxes. In this case the bed level determined through the cross sectional interpolation is overridden by the user supplied topographical values.





## A.7 Modified Diffusive Wave Approximation

The diffusive wave approximation can be written for example for the case of Chezy roughness as:

$$Q = ACR^{1/2}S^{1/2} \quad (\text{A.7.1})$$

where,  $S$  is the slope of the water surface. This equation is linearized through the following approximations:

$$Q^{n+1} \approx Q^{n+1/2} + \frac{\partial Q}{\partial h}(h^{n+1} - h^{n+1/2}) \quad (\text{A.7.2})$$

Expressions are now sought for:

$$\frac{\partial Q}{\partial h} = \frac{\partial Q}{\partial A} \frac{\partial A}{\partial h} + \frac{\partial Q}{\partial R} \frac{\partial R}{\partial h} + \frac{\partial Q}{\partial S} \frac{\partial S}{\partial h} \approx \frac{\partial Q}{\partial A} \frac{\partial A}{\partial h} + \frac{\partial Q}{\partial R} \frac{\partial R}{\partial h} \quad (\text{A.7.3})$$

From the basic equation we have:

$$\frac{\partial Q}{\partial A} = CR^{1/2}S^{1/2} \quad \text{and} \quad \frac{\partial A}{\partial h} = b_s \quad (\text{A.7.4})$$

$$\frac{\partial Q}{\partial S} = \frac{1}{2}AC\sqrt{\frac{R}{S}} \quad \text{and} \quad \frac{\partial S}{\partial h} \approx \frac{1}{\Delta x} \quad (\text{A.7.5})$$

Inserting this in the above linearized expression gives:

$$Q^{n+1} = Q^{n+1/2} + \left( C\sqrt{RS}b_s + \frac{1}{2\Delta x}AC\sqrt{\frac{R}{S}} \right) (h^{n+1} - h^{n+1/2}) \quad (\text{A.7.6})$$

giving:

$$Q^{n+1} = Q^{n+1/2} + \left( \frac{b_s\Delta x S}{A} + \frac{1}{2} \right) \frac{AC}{\Delta x} \sqrt{\frac{R}{S}} (h^{n+1} - h^{n+1/2}) \quad (\text{A.7.7})$$







## A.8 Saint Venant Equations

MIKE 11 applied with the fully dynamic descriptions solves the vertically integrated equations of conservation of volume and momentum (the 'Saint Venant' equations), which are derived on the basis of the following assumptions:

- the water is incompressible and homogeneous, i.e. without significant variations in density
- the bottom slope is small
- the wave lengths are large compared to the water-depth. This ensures that the flow everywhere can be regarded as having a direction parallel to the bottom, i.e. vertical acceleration can be neglected and a hydrostatic pressure variation along the vertical can be assumed
- the flow is sub-critical

For a rectangular cross-section with a horizontal bottom and a constant width, the conservation of mass and momentum can be expressed as follows (in the first instance neglecting friction and lateral inflows):

Conservation of mass:

$$\frac{\partial(\rho Hb)}{\partial t} = -\frac{\partial(\rho Hb\bar{u})}{\partial x} \quad (\text{A.8.1})$$

Conservation of momentum:

$$\frac{\partial(\rho Hb\bar{u})}{\partial t} = -\frac{\partial\left(\alpha'\rho Hb\bar{u}^2 + \frac{1}{2}\rho gbH^2\right)}{\partial x} \quad (\text{A.8.2})$$

where,  $\rho$  is the density,  $H$  the depth,  $b$  the width,  $\bar{u}$  the average velocity along the vertical and  $\alpha'$  the vertical velocity distribution coefficient.

Introducing the bottom slope,  $l_b$ , and allowing for the channel width to vary will give rise to two more terms in the momentum equation. These terms describe the projections in the flow direction of the reactions of the bottom and side-walls to the hydrostatic pressure.



The momentum equation now becomes:

$$\begin{aligned} \frac{\partial(\rho H b \bar{u})}{\partial t} &= - \frac{\partial\left(\alpha' \rho H b \bar{u}^2 + \frac{1}{2} \rho g b H^2\right)}{\partial x} + \frac{\partial b \rho g H^2}{\partial x} - \rho g H b l_b \\ &= - \frac{\partial(\alpha' \rho H b \bar{u}^2)}{\partial x} - b \frac{\partial\left(\frac{1}{2} \rho g H^2\right)}{\partial x} - \rho g H b l_b \end{aligned} \quad (\text{A.8.3})$$

When the water level,  $h$ , is introduced into the relationship instead of water depth:

$$\frac{\partial h}{\partial x} = l_b + \frac{\partial H}{\partial x} \quad (\text{A.8.4})$$

and the equations are divided by  $\rho$ , the conservation laws of mass and momentum become:

$$\frac{\partial(Hb)}{\partial t} = - \frac{\partial(Hb\bar{u})}{\partial x} \quad (\text{A.8.5})$$

$$\frac{\partial(Hb\bar{u})}{\partial t} = - \frac{\partial(\alpha' H b \bar{u}^2)}{\partial x} - H b g \frac{\partial h}{\partial x} \quad (\text{A.8.6})$$

These equations can be integrated to describe the flow through cross-sections of any shape when divided up into a series of rectangular cross sections as shown in Fig A.8.15:

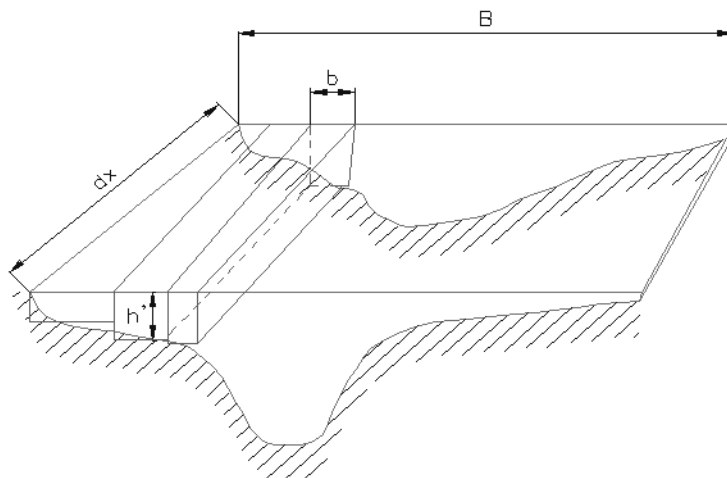


Fig A.8.15 Cross-section divided into a series of rectangular channels

According to the previous assumptions,  $\partial h / \partial x$  is constant across the channel and no exchange of momentum occurs between the subchannels. If the integrated cross sectional area is called  $A$  and the integrated discharge  $Q$ , and  $B$  is the full width of the channel, then:

$$A = \int_0^B H db \quad (\text{A.8.7})$$

$$Q = \int_0^B H \bar{u} db = \bar{u} A \quad (\text{A.8.8})$$

Integrating the mass and momentum conservation equations and introducing Equations (A.8.7) and (A.8.8) yields:

$$\frac{\partial Q}{\partial x} + \frac{\partial A}{\partial t} = 0 \quad (\text{A.8.9})$$

$$\frac{\partial Q}{\partial t} + \frac{\partial \left( \alpha \frac{Q^2}{A} \right)}{\partial x} + gA \frac{\partial h}{\partial x} = 0 \quad (\text{A.8.10})$$



Including the hydraulic resistance, e.g. using the Chezy description and the lateral inflow;  $q$  into these equations leads to the basic equations used in MIKE 11:

$$\frac{\partial Q}{\partial x} + \frac{\partial A}{\partial t} = q \quad (\text{A.8.11})$$

$$\frac{\partial Q}{\partial t} + \frac{\partial \left( \alpha \frac{Q^2}{A} \right)}{\partial x} + gA \frac{\partial h}{\partial x} + \frac{gQ|Q|}{C^2 AR} = 0 \quad (\text{A.8.12})$$



## A.9 Solution Scheme

The solution to the combined system of equations at each time step is performed according to the procedure outlined below. The solution method is the same for each model level (kinematic, diffusive, dynamic).

The transformation of Equations (A.8.11) and (A.8.12) in section A.8 Saint Venant Equations (*p. 425*), to a set of implicit finite difference equations is performed in a computational grid consisting of alternating  $Q$ - and  $h$ -points, i.e. points where the discharge,  $Q$  and water level  $h$ , respectively, are computed at each time step, see Fig A.9.16. The computational grid is generated automatically by the model on the basis of the user requirements.  $Q$ -points are always placed midway between neighbouring  $h$ -points, while the distance between  $h$ -points may differ. The discharge will, as a rule, be defined as positive in the positive  $x$ -direction (increasing chainage).

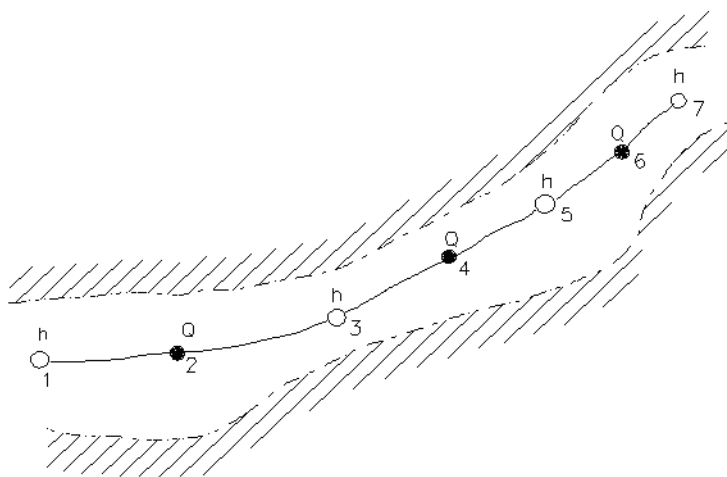


Fig A.9.16 Channel section with computational grid

The adopted numerical scheme is a 6-point Abbott-scheme as shown in Fig A.9.17.

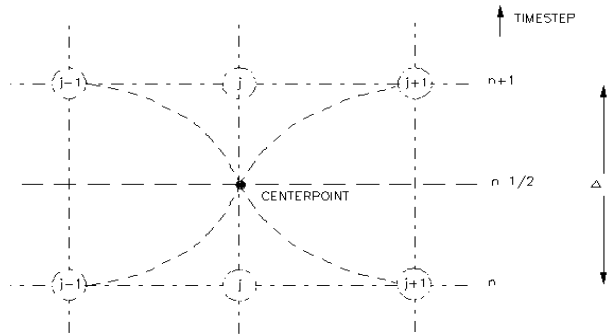


Fig A.9.17 Centred 6-point Abbott scheme

## A.9.1 Continuity equation

In the continuity equation the storage width,  $b_s$ , is introduced as:

$$\frac{\partial A}{\partial t} = b_s \frac{\partial h}{\partial t} \quad (\text{A.9.1})$$

giving:

$$\frac{\partial Q}{\partial x} + b_s \frac{\partial h}{\partial t} = q \quad (\text{A.9.2})$$

As only  $Q$  has a derivative with respect to  $x$ , the equation can easily be centred at an  $h$ -point, see Fig A.9.18.

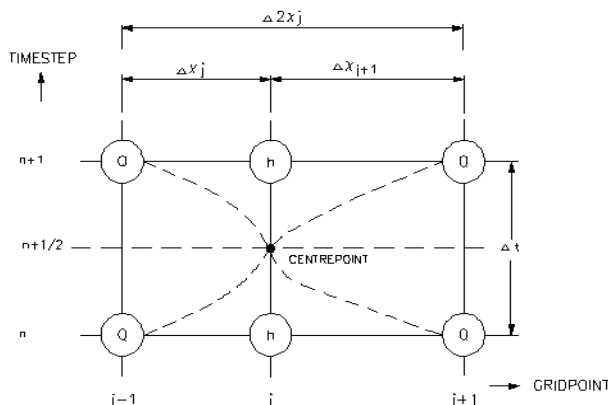


Fig A.9.18 Centring of continuity equation in 6-point Abbott scheme

The derivatives in Equation (A.9.2) are expressed at the time level,  $n+1/2$ , as follows:

$$\frac{\partial Q}{\partial x} \approx \frac{\frac{(Q_{j+1}^{n+1} + Q_{j+1}^n)}{2} - \frac{(Q_{j-1}^{n+1} + Q_{j-1}^n)}{2}}{\Delta 2x_j} \quad (\text{A.9.3})$$

$$\frac{\partial h}{\partial t} \approx \frac{(h_j^{n+1} - h_j^n)}{\Delta t} \quad (\text{A.9.4})$$

$b_s$  in Equation (A.9.2) is approximated by:

$$b_s = \frac{A_{o,j} + A_{o,j+1}}{\Delta 2x_j} \quad (\text{A.9.5})$$

where:

$A_{o,j}$  is the surface area between grid point  $j-1$  and  $j$

$A_{o,j+1}$  is the surface area between grid point  $j$  and  $j+1$

$\Delta 2x_j$  is the distance between point  $j-1$  and  $j+1$

Substituting for the derivatives in Equation (A.9.2) gives a formulation of the following form:

$$\alpha_j Q_{j-1}^{n+1} + \beta_j h_j^{n+1} + \gamma_j Q_{j+1}^{n+1} = \delta_j \quad (\text{A.9.6})$$



where,  $\alpha$ ,  $\beta$  and  $\gamma$  are functions of  $b$  and  $\delta$  and, moreover, depend on  $Q$  and  $h$  at time level  $n$  and  $Q$  on time level  $n+1/2$ .

## A.9.2 Momentum equation

The momentum equation is centred at  $Q$ -points as illustrated in Fig A.9.19.

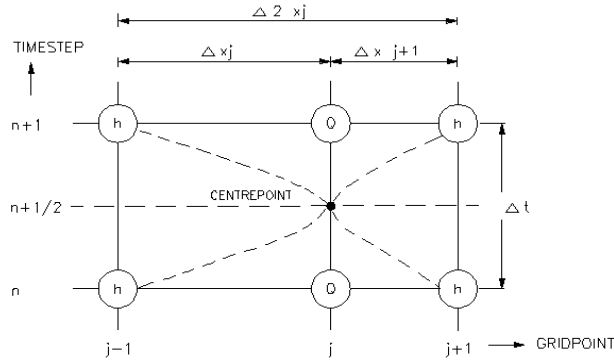


Fig A.9.19 Centring of momentum equation in 6-point Abbott scheme

The derivatives of Equation (A.8.12) in section A.8 Saint Venant Equations (p. 425), are expressed in the following way:

$$\frac{\partial Q}{\partial t} \approx \frac{Q_j^{n+1} - Q_j^n}{\Delta t} \quad (\text{A.9.7})$$

$$\frac{\partial \left( \alpha \frac{Q^2}{A} \right)}{\partial x} \approx \frac{\left[ \alpha \frac{Q^2}{A} \right]_{j+1}^{n+1/2} - \left[ \alpha \frac{Q^2}{A} \right]_{j-1}^{n+1/2}}{\Delta 2x_j} \quad (\text{A.9.8})$$

$$\frac{\partial h}{\partial x} \approx \frac{\frac{(h_{j+1}^{n+1} + h_{j+1}^n)}{2} - \frac{(h_{j-1}^{n+1} + h_{j-1}^n)}{2}}{\Delta 2x_j} \quad (\text{A.9.9})$$

For the quadratic term in (A.9.8), a special formulation is used to ensure the correct sign for this term when the flow direction is changing during a time step:

$$Q^2 \approx \theta Q_j^{n+1} Q_j^n - (\theta - 1) Q_j^n Q_j^n \quad (\text{A.9.10})$$





where,  $\theta$  can be specified by the user (THETA coefficient under the Default values in the HD parameter editor) and by default is set to 1.0.

With all the derivatives substituted, the momentum equation can be written in the following form:

$$\alpha_j h_{j-1}^{n+1} + \beta_j Q_j^{n+1} + \gamma_j h_{j+1}^{n+1} = \delta_j \quad (\text{A.9.11})$$

where,

$$\alpha_j = f(A)$$

$$\beta_j = f(Q_j^n, \Delta t, \Delta x, C, A, R)$$

$$\gamma_j = f(A)$$

$$\delta_j = f(A, \Delta x, \Delta t, \alpha, q, v, \theta, h_{j-1}^n, Q_{j-1}^{n+1/2}, Q_j^n, h_{j+1}^n, Q_{j+1}^{n+1/2})$$

To obtain a fully centred description of  $A_{j+1}$ , these terms should be valid at time level  $n+1/2$  which can only be fulfilled by using an iteration. For this reason, the equations are solved by default two times at every time step, the first iteration starting from the results of the previous time step, and the second iteration using the centred values from this calculation. The number of iterations can be changed using the NOITER coefficient.





## A.10 Structures

Some of the structure types described in section 1.34 Steady State Energy Equation (p. 162) share the same mathematical treatment. These are:

- broadcrested weir, control structures (overflow and non surcharged underflow structures), dambreak (crest flow and breach flow)
- special weir,  $Q = f(h)$

Their Mathematical treatment is described below.

### A.10.1 Mathematical treatment

The structure description combines a wide range of elements including weirs, narrow cross sections, flood plains, etc. It is obtained by replacing the momentum equation with an  $h$ - $Q$ - $h$  relationship, an  $h$ - $Q$  relationship, or a  $Q$  assignment.

The grid used to describe a structure consists of  $h$ -points at either side, and a  $Q$ -point at the structure, see Fig A.10.20.

$Q_s$  and  $h_s$  will be used in the following to describe the discharge and the water level at the structure, respectively, i.e. at point  $j$ .

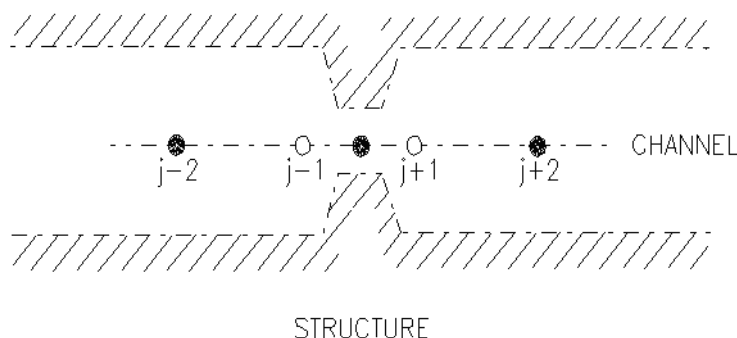


Fig A.10.20 Channel with structure and grid

Through numerical experiments, it has been found that the weir discharge relation is best described at time level  $n+1$ . If the relation is centred at time level  $n+1/2$ , the product  $Q_n Q_{n+1}$ , used for the description of the head loss at the weir, may have the same magnitude for a large number of possible combinations of  $Q_n$  and  $Q_{n+1}$  values. In the centred mass equation, the average value of  $Q_n$  and  $Q_{n+1}$  is used and oscillations introduced in the numerical process are slightly, or not at all, damped.



Numerically, the description of a compatibility condition forward in time is very convenient. Unlike the numerical description of partial differential equations, no numerical damping of the physical processes is introduced in this way, as the compatibility condition should hold at any point in time. The only error introduced comes from the linearization of the quadratic relation at the new time level.

The solution technique is to replace the coefficients in the general momentum equation:

$$\alpha_j h_{j-1}^{n+1} + \beta_j Q_j^{n+1} + \gamma_j h_{j+1}^{n+1} = \delta_j \quad (\text{A.10.1})$$

with modified coefficients.

The evaluation of these coefficients is outlined in the following discussion.

The description generally used for flow through a structure is given by:

$$\Delta H = \zeta \frac{V_s^2}{2g} \quad (\text{A.10.2})$$

where,  $\Delta H$  is the energy head loss over the structure,  $\zeta$  is a head loss coefficient and  $V_s$  is the mean cross-sectional velocity at the structure.

In MIKE 11 HD the head loss is divided into inflow (contraction) and outflow (expansion) components.

In the case of a sudden expansion the energy loss can be described as (A.10.2) and as:

$$\Delta H = f \frac{(V_s - V_2)^2}{2g} \quad (\text{A.10.3})$$

Setting (A.10.2) equal to (A.10.3) gives:

$$\zeta_2 \frac{V_s^2}{2g} = f \frac{(V_s - V_2)^2}{2g} \quad (\text{A.10.4})$$

which can be reduced to:

$$\zeta_2 = f \left(1 - \frac{V_2}{V_s}\right)^2 \quad (\text{A.10.5})$$



$f$ , is equal to the user defined outflow head loss coefficient ( $\zeta_{out}$ ) and (A.10.5) becomes equal to:

$$\zeta_2 = \zeta_{out} \left(1 - \frac{V_2}{V_s}\right)^2 \quad (\text{A.10.6})$$

Equation (A.10.6) can also be written in the form:

$$\zeta_2 = \zeta_{out} \left(1 - \frac{Q_2 A_s}{A_2 Q_s}\right)^2 \quad (\text{A.10.7})$$

Which in case of a single structure ( $Q_s = Q_2$ , see Fig A.10.21) is equal to:

$$\zeta_2 = \zeta_{out} \left(1 - \frac{A_s}{A_2}\right)^2 \quad (\text{A.10.8})$$

For a parallel structure (A.10.7) cannot be reduced to (A.10.8) as ( $Q_s \neq Q_2$ ) consequently equation (A.10.6) can be applied instead.

A similar approach can be used for adjustment of inflow head loss:

$$\zeta_1 = \zeta_{in} \left(1 - \frac{V_1}{V_s}\right) \quad (\text{A.10.9})$$

where,  $\zeta_1$  and  $\zeta_2$  are the adjusted inflow and outflow head loss coefficients calculated using the inflow and outflow loss coefficients ( $\zeta_{in}$  and  $\zeta_{out}$ ) specified in the network editor → Structures → Head Loss Factor. A minimum value for  $\zeta_1$  and  $\zeta_2$  can be specified in the HD parameter editor under the Default values tab as ZetaMin. In the case  $A_s \rightarrow A_1$  the solution can become unstable (no friction) and specification of a minimum value of  $\zeta_{1,2}$ , ensures a stable solution.

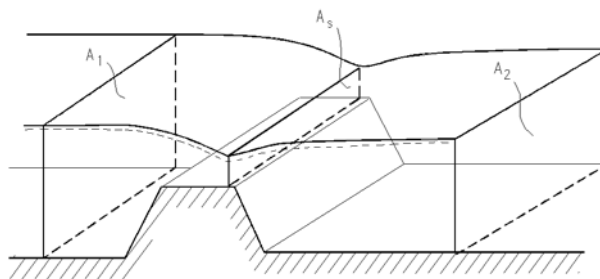


Fig A.10.21 Cross-sectional flow areas at a structure



## A.10.2 Expansion and Contraction Coefficients

As described in the previous section, flow through a structure is described according to:

$$\Delta h = \zeta_t \frac{Q^2}{2gA^2} \quad (\text{A.10.10})$$

This equation  $\zeta_t$  describes the total head loss coefficient, which is composed of entrance ( $\zeta_1$ ) and exit ( $\zeta_2$ ) coefficients. For subcritical flow the coefficients are related to the input parameters  $\zeta_{in}$  and  $\zeta_{out}$  and the changes in velocity ( $v$ ) and area ( $A$ ):

$$\zeta_t = \zeta_1 + \zeta_2 = \zeta_{in} \left(1 - \frac{v_1}{v_s}\right) + \zeta_{out} \left(1 - \frac{A_s}{A_2}\right)^2 \quad (\text{A.10.11})$$

For subcritical flow through a structure there is an upstream contraction and a downstream expansion, so equation (A.10.11) works fine. When there is supercritical flow there is an upstream expansion and a downstream contraction. Thus if supercritical flow occurs then the loss coefficients in MIKE 11 are no longer valid. To accommodate supercritical flow, calculation of the of entrance ( $\zeta_1$ ) and exit ( $\zeta_2$ ) coefficients are expanded:

$$\zeta_1 \begin{cases} = \zeta_{in} \left(1 - \frac{v_1}{v_s}\right); v_1 < v_s \\ = \zeta_{in} \left(1 - \frac{A_1}{A_s}\right)^2; v_1 > v_s \end{cases} \quad (\text{A.10.12a})$$

$$\zeta_2 \begin{cases} = \zeta_{out} \left(1 - \frac{A_s}{A_2}\right)^2; v_s > v_2 \\ = \zeta_{out} \left(1 - \frac{v_s}{v_2}\right); v_s < v_2 \end{cases} \quad (\text{A.10.12b})$$

Care must be taken when selecting loss coefficients, particularly in situations where both subcritical and supercritical flow conditions occur. When flow conditions change from subcritical to supercritical (or the Froude number  $F_R$  becomes greater than 1), the loss coefficients  $\zeta_{in}$  and  $\zeta_{out}$  (specified in the Head Loss Factors box) are modified:



- If  $F_R > 1$  in upstream h-point then  $\zeta_{in} = \zeta_{in} / 2$
- If  $F_R > 1$  in downstream h-point then  $\zeta_{out} = \zeta_{out} / 2$

Note that this adjustment is not made for bridge structures.

### A.10.3 Determination of structure geometry

For structure types broad crested weir and special weir and the structure geometry is given while the geometry of control structures (crest level) and dambreak structures (crest level and breach width) changes during the computation.

### A.10.4 Determination of flow regime

Given the upstream and downstream water levels and the discharge, and assuming that these three values are compatible with each other, the type of flow can be determined as follows.

For zero flow the upstream and downstream water levels are both below the structure invert (crest level) and the flow regime is subcritical, or the flow direction is opposite valve regulation.

For differentiating between critical and drowned flow it is assumed, in the first instance, that the flow at the weir crest is critical.

The critical discharge is determined for broad crested weirs and special weirs via the tabulated  $Q/H$ -relation while it in case of structures with time dependent geometry is computed by critical flow iteration during the simulation. The pre-processed  $Q/H$ -relation for broad crested weirs are based on the assumption of a single structure, hence when the broad crested weir is a part of a composite structure the  $Q/H$  relation is no longer valid. In this case the critical discharge is computed by iteration during the simulation. When special weirs are included in a composite structure it is assumed that the user defined  $Q/H$  relations for critical flow takes the changed hydraulic conditions into account. When the upstream flow regime is supercritical, the  $Q/H$  relations are also recalculated.

When a long culvert is a part of a composite structure there is no critical discharge iteration i.e. the computed  $Q/H$  relation is used to estimate the critical discharge. This approach is assumed valid as the structure area usually is much smaller than the upstream area i.e.  $A_s \ll A_1$  hence no need for iteration.

Critical flow occurs (for  $\zeta_2 > 1$ ) when the energy head at the crest is larger than the downstream energy head, viz:

$$h_s + (1 - \zeta_2) \frac{Q_s^2}{2gA_s^2} \geq h_2 + \frac{Q_s^2}{2gA_2^2} \quad (\text{A.10.13})$$



Critical flow occurs (for  $\zeta_2 \leq 1$ ) (for outflow head loss  $\leq 1$ ) when the water level at the crest is larger than the downstream energy head, viz:

$$h_s \geq h_2 + \frac{Q_s^2}{2gA_2^2} \quad (\text{A.10.14})$$

If the flow is not critical a submerged discharge iteration is performed and the submerged discharge is compared with the critical and the smallest is taken, viz:

critical flow:

$$Q_{\text{critical}} < Q_{\text{submerged}}$$

submerged flow:

$$Q_{\text{critical}} > Q_{\text{submerged}}$$

## A.10.5 Determination of flow regime (with Supercritical Flow)

Subcritical flow types can be determined given the upstream and downstream water levels and the discharge, and assuming that these three values are compatible with each other. However, energy levels in MIKE 11 are influenced by the convective suppression factor  $\beta$  (see Suppression of convective acceleration term (*p. 171*)). This means that energy head, particularly at high velocities, can become distorted.

The type of flow therefore considers upstream and downstream water levels, discharge and upstream and downstream Froude numbers ( $F_R$ ). If  $F_R < 1$  then subcritical flow, if  $F_R = 1$  then critical flow and if  $F_R > 1$  then supercritical flow. Using the Froude number upstream ( $F_{R1}$ ) and downstream ( $F_{R2}$ ) of the structure, the following tests are made to decide the flow condition inside the structure:

- If  $F_{R1} < 1$  and  $F_{R2} > 1$  and  $F_{R1+} < 1$  then flow through structure = critical
- If  $F_{R1} > 1$  and  $F_{R2} < 1$  then flow through structure = critical
- If  $F_{R1} < 1$  and  $F_{R2} < 1$  and  $E_2 < h_1$  then flow through structure = critical
- If  $F_{R1} > 1$  and  $F_{R2} > 1$  then flow through structure = supercritical
- If  $F_{R1} < 1$  and  $F_{R2} > 1$  and  $F_{R1+} > 1$  then flow through structure = supercritical
- If  $F_{R1} < 1$  and  $F_{R2} < 1$  and  $E_2 > h_1$  then flow through structure = subcritical

Note the conditions:





- $F_{R1+}$  is the Froude number at the q point immediately upstream of the structure. This is included to enable a transition from critical to supercritical flow, depending upon conditions further upstream. If the q point upstream of the structure does not lie on the same branch or does not exist at all, this test is removed.
- $E_2$  is downstream energy level,  $h_1$  is upstream water level – this indicates a free overfall condition with upstream subcritical flow.  $E_2$  includes the  $\beta$  factor and (for the flow condition test only) is calculated as:

$$E_2 = \left( h + \beta \frac{Q^2}{2gA^2} \right)_2 \quad (\text{A.10.15})$$

- For zero flow the upstream and downstream water levels are both below the structure invert (crest level) and the flow regime is subcritical, or the flow direction is opposite valve regulation. If flow is supercritical then zero flow is impossible.

## A.10.6 Zero flow

For the zero flow case the coefficients are set as follows:

$$\alpha_j = 0, \beta_j = 1, \gamma_j = 0, \delta_j = 0 \quad (\text{A.10.16})$$

## A.10.7 Drowned flow

For drowned flow the head loss over the structure is represented as:

$$\left( h + \frac{Q_s^2}{2gA^2} \right)_{j-1} - \left( h + \frac{Q^2}{2gA^2} \right)_{j+1} = \zeta \frac{Q_s |Q_s|}{2gA_s^2} \quad (\text{A.10.17})$$

The velocity heads in the upstream and downstream sections need to be described implicitly, as they can be large in magnitude.

Collecting the velocity heads, the equation becomes:

$$h_{j-1} - h_{j+1} = \frac{Q_s |Q_s|}{2g} \left( \frac{\zeta}{A_s^2} - \frac{1}{A_{j-1}^2} + \frac{1}{A_{j+1}^2} \right) \quad (\text{A.10.18})$$



Expressing  $Q$  at time level  $n+1$  can be done as follows:

$$Q_s^{n+1} = \frac{\sqrt{2g(h_{j-1} - h_{j+1})}}{\sqrt{A_s^2 - \frac{1}{A_{j-1}^2} + \frac{1}{A_{j+1}^2}}} \quad (\text{A.10.19})$$

which by re-arranging gives:

$$Q_s^{n+1} = (h_{j-1}^{n+1} - h_{j+1}^{n+1}) \sqrt{\frac{2g}{(h_{j-1}^{n+1} - h_{j+1}^{n+1}) \left( \frac{\zeta}{A_s^2} - \frac{1}{A_{j-1}^2} + \frac{1}{A_{j+1}^2} \right)}} \quad (\text{A.10.20})$$

Collecting terms in relationship (A.10.20) for flow in both the positive and negative  $x$ -directions over this weir, the coefficients become:

$$\alpha_j = -\sqrt{\frac{2g}{a_a b_a}} \quad (\text{A.10.21a})$$

$$\beta_j = 1 \quad (\text{A.10.21b})$$

$$\gamma_j = \sqrt{\frac{2g}{a_a b_a}} \quad (\text{A.10.21c})$$

$$\delta_j = 0 \quad (\text{A.10.21d})$$

where,

$$a_a = \frac{\zeta}{A_s^2} - \frac{1}{A_{j-1}^2} + \frac{1}{A_{j+1}^2} \quad (\text{A.10.22a})$$

$$b_a = h_{j-1}^{n+1} - h_{j+1}^{n+1} \quad (\text{A.10.22b})$$

For the computation of these coefficients, values for  $\zeta$  and  $A_s$  are required. Especially, close to the critical flow state, the solution becomes quite sensitive to  $A_s$  values which can be described by the energy head at the structure and the discharge as follows:

$$H_s = h_s + \frac{Q_s^2}{2gA_s^2} \quad (\text{A.10.23})$$

where,  $A_s = f(h_s)$



The solution is found by iterative use of the following equations:

$$A_s, \zeta_1, \zeta_2 = f(h_1, h_2, h_s) \quad (\text{A.10.24a})$$

$$\zeta = \zeta_1 + \zeta_2 \quad (\text{A.10.24b})$$

$$H_s = H_1 - \frac{\zeta_1}{\zeta}(H_1 - H_2) \quad (\text{A.10.24c})$$

$$h_s = H_s - \frac{H_1 - H_2}{\zeta} \quad (\text{A.10.24d})$$

Convergence is normally obtained within a few iterations. A maximum number of iterations is specified in the HD parameter editor under the Default Values tab as the Inter1Max coefficient.

When the water surface gradient across the structure changes sign, so do the denominators in the square roots of Equation (A.10.8). Close to the zero point, the solution is badly defined, and the slightest change in water level difference will cause a large change in discharge. This is a result of the local vertical slope of the response function, see Fig A.10.22, and can produce an instability.

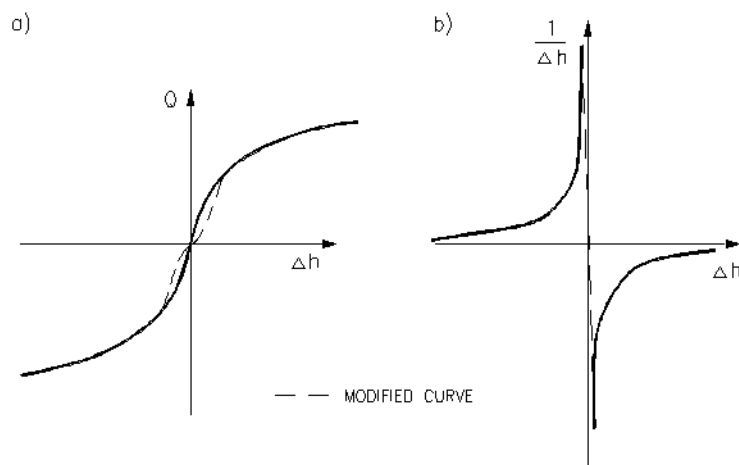


Fig A.10.22  $Q = f(\Delta h)$  response function and effect of local modification of  $1/\Delta h$

The problem can be overcome by a local modification of the  $1/\Delta h$  function in the discontinuous region, see b) in Fig A.10.22. The corresponding effect on the  $Q = f(\Delta h)$  curve is shown in a) in Fig A.10.22. The range of  $\Delta h$  over which the modification is applied can be selected according to the current case to



be simulated, in order to introduce minimum falsification. This is done in the HD parameter editor → Default Values using the Delhs Coefficient.

### A.10.7.1 Drowned Flow, Supercritical

When drowned flow occurs during subcritical flow conditions, the energy equation is applied to calculate the head loss (A.10.17 (p. 441)). This equation should also be applicable during supercritical flow. However, during supercritical flow this equation becomes very sensitive to small changes in head drop and structure area, to such an extent that it cannot be applied to the MIKE 11 structure routines (even if the convective terms are suppressed using the  $\beta$  factor).

So when a structure is in supercritical flow conditions, the momentum equation is solved across the structure rather than the energy equation. This is applied in the same way as for a normal q point in MIKE 11, except that structure geometry is used (the estimate for structure depth and area) and that friction losses are substituted by the structure losses.

The general momentum equation is:

$$\alpha h_{j-1}^{n+1} + \beta Q_j^{n+1} + \gamma h_{j+1}^{n+1} = \delta \quad (\text{A.10.25a})$$

The structure is located at a Q point (j), with an upstream h point (j-1) and a downstream h point (j+1). If the  $\beta$  factor is set to 1 the coefficients in the general momentum equation are updated to the following values:

$$\text{CO1} = \alpha = -gA_s \quad (\text{A.10.25b})$$

$$\text{CO2} = \beta = 2\Delta x \Delta t + \frac{\zeta_t Q}{2gA_s^2} \quad (\text{A.10.25c})$$

$$\text{CO3} = \gamma = gA_s \quad (\text{A.10.25d})$$

$$\text{CO4} = \delta = gA_s \Delta \left( h_{j-1}^n - h_{j+1}^n \right) + (\theta - 1) \frac{\zeta_t Q^2}{2gA_s^2} + 2\Delta x \Delta t Q \quad (\text{A.10.25e})$$

The parameters used in the calculations are  $\Delta$  (DELTA Coefficient (p. 405)),  $\theta$  (THETA in Coefficients, HD default parameters (p. 63)),  $\zeta_t$  (NEED REF TO GO HERE!),  $\Delta t$  (time step) and  $\Delta x$  (grid step).



To estimate the depth in a supercritical structure an iterative solution is used. From an initial estimate of structure area the structure water depth is calculated using the energy equation. Structure area is then updated using the existing  $Q/H$  relations. Iterations continue until successive structure area estimates are within a specified tolerance (CONV\_F) or exceed a given maximum (MAX\_ITER or INTER1MAX, Default Values (p. 323)).

## A.10.8 Free overflow

For free overflow a tabulated relationship is used to define  $Q$  as a function of the upstream water level,  $h_1$ . The table is calculated automatically in the case of a broadcrested weir or defined by the user for special weirs. The number of points in the table is defined by the user.

### A.10.8.1 Critical discharge

The critical discharge over a broadcrested weir is found by integrating the local critical velocity  $\sqrt{gh_s}$  over the structure width. Thus the critical discharge is given by

$$Q_c = \int_0^W \sqrt{gh_s(x)} h_s(x) dx \quad (\text{A.10.26})$$

where  $W$  is the structure width,  $h_s(x)$  the local structure depth and  $x$  a coordinate along the cross sectional profile. The velocity head at the structure is determined as

$$H_{\text{velocity}} = \frac{\int_0^W \frac{1}{2} \sqrt{gh_s(x)} h_s^2(x) dx}{\int_0^W \sqrt{gh_s(x)} h_s(x) dx} \quad (\text{A.10.27})$$

For a rectangular weir the structure depth is independent of  $x$  and eqs. (A.10.26)-(A.10.27) become

$$Q_c = \sqrt{gh_s} h_s W \quad (\text{A.10.28})$$

$$H_{\text{velocity}} = \frac{1}{2} h_s \quad (\text{A.10.29})$$

The actual discharge has a correction factor,  $\alpha_c$ , applied which can be determined in practice by comparing the tabulated function generated by the model with the measured, or otherwise expected, relationship.



The locally linear relationship, see Fig A.10.23, with coefficients defined at time level  $(n+\frac{1}{2})\Delta t$  then becomes:

$$Q_j^{n+1} = a_1 h_{j-\text{sign}(Q)}^{n+1} + b_1 \tag{A.10.30}$$

giving coefficients in the relationship (A.10.1), for flow in both the positive and negative x-direction, as:

$$\alpha_j = -a_1 \frac{(1 + \text{sign}(Q))}{2} \tag{A.10.31a}$$

$$\beta_j = \frac{1}{\text{FOF}} \tag{A.10.31b}$$

$$\gamma_j = -a_1 \frac{(1 - \text{sign}(Q))}{2} \tag{A.10.31c}$$

$$\delta_j = b_1 \tag{A.10.31d}$$

where,

$$\text{FOF} = \text{free overflow factor} \tag{A.10.32a}$$

$$a_1 = \text{sign}(Q) \frac{Q_k - Q_{k-1}}{h_k - h_{k-1}} \tag{A.10.32b}$$

$$b_1 = \text{sign}(Q) Q_{k-1} - a_1 h_{k-1} \tag{A.10.32c}$$

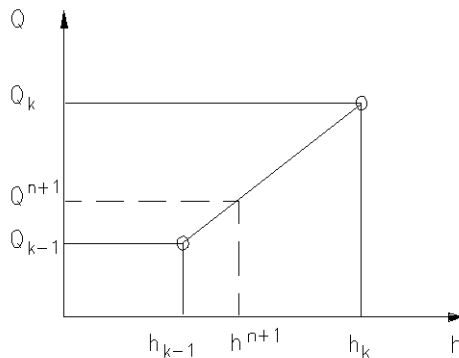


Fig A.10.23 Linearized relationship used for the implicit description of a Q-h relation



For structures with time dependent geometry the free over flow discharge is computed as follows.

The head loss over the structure is represented by:

$$\left( h + \frac{Q^2}{2gA^2} \right)_{j-1} - \left( h_2 + \frac{Q_s^2}{2gA_s^2} \right) = \zeta_1 \frac{Q_s |Q_s|}{2gA_s^2} \quad (\text{A.10.33})$$

Collecting the velocity heads and expressing  $Q_s$  at time level  $n+1$ , the equation becomes:

$$Q_s = \sqrt{\frac{2g(h_{j-1} - h_s)}{\frac{1 + \zeta_1}{A_s^2} - \frac{1}{A_{j-1}^2}}} \quad (\text{A.10.34})$$

which by rearranging gives:

$$Q_s^{n+1} = (h_{j-1}^{n+1} - h_s) \sqrt{\frac{2g}{(h_{j-1} - h_s) \left( \frac{1 + \zeta_1}{A_s^2} - \frac{1}{A_{j-1}^2} \right)}} \quad (\text{A.10.35})$$

Collecting terms in relationship(A.10.35) for flow over this weir, the coefficients become:

$$\alpha_j = - \sqrt{\frac{2g}{a_a b_b}} \text{FOF} \quad (\text{A.10.36a})$$

$$\beta_j = 1 \quad (\text{A.10.36b})$$

$$\gamma_j = 0 \quad (\text{A.10.36c})$$

$$\delta_j = -h_s \sqrt{\frac{2g}{a_a b_b}} \text{FOF} \quad (\text{A.10.36d})$$

where,

$$a_a = \frac{1 + \zeta_1}{A_s^2} - \frac{1}{A_{j-1}^2} \quad (\text{A.10.37a})$$

$$b_b = h_{j-1} - h_s \quad (\text{A.10.37b})$$







## A.11 Heat Balance Module

### A.11.1 General Description

The heat balance module is used for simulation of heat transfer between the water body and its surroundings. The heat balance equation can be expressed as:

$$q = q_{trib} + q_r + q_p - q_e - q_c + q_s - q_{sr} - q_{su} + q_l - q_{lr} - q_{lu} - q_a + q_g + q_{sed} \quad (\text{A.11.1})$$

where

$\Delta q$	change in the heat capacity of the water body.
$q_{trib}$	is heat transfer from tributary inflow.
$q_r$	is the heat transfer from diffuse sources.
$q_p$	is the heat transfer from precipitation.
$q_e$	is loss of energy due evaporation.
$q_c$	is the convective heat transfer.
$q_s$	is the shortwave radiation.
$q_{sr}$	is the reflected shortwave radiation.
$q_{su}$	is the shortwave radiation emitted from the water body.
$q_l$	is the longwave radiation above the sea surface.
$q_{lr}$	is the reflected longwave radiation.
$q_{lu}$	is the emittance of longwave energy from the water body.
$q_a$	is the loss of energy from outflow.
$q_g$	is the heat exchange between ground and water body.
$q_{sed}$	is the heat exchange between sediment and water body.



Some of the terms have been excluded from the heat balance module, since they have no, or only minor influence on the total heat budget. Furthermore, some of the terms are lumped into a single term, e.g. as for the longwave radiation. The following terms are set to zero in the heat balance module:

$$qr = 0, \quad qp = 0, \quad qg = 0, \quad qsed = 0, \quad qlr = 0 \quad \text{and} \quad qsu = 0,$$

After which equation (A.11.1) can be reduced to:

$$\Delta q = q_{trib} - q_c + q_s - q_{sr} + q_l - q_{lu} - q_a \quad (\text{A.11.2})$$

## A.11.2 Convection

The heat exchange due to convection depends on the type of boundary layer between the sea surface and the atmosphere. Generally, this boundary layer is known to be turbulent and the following relationships between heat exchange and wind speed, air and sea temperature can be established /4/:

If  $T_{air} > T_w$  :

$$q_c = \rho_{air} C_{air} C_c |W_{10} - U| (T_w - T_{air}) \quad (\text{A.11.3})$$

otherwise:

$$q_c = \rho_{air} C_w C_c |W_{10} - U| (T_w - T_{air}) \quad (\text{A.11.4})$$

where

$\rho_{air}$  is the air density (kg/m<sup>3</sup>)

$C_{air}$  is the specific heat of air, 1007 J/(kg · K°)

$C_w$  is the specific heat of water, 4186 J/(kg · K°)

$W_{10}$  is the wind speed 10 m above the sea surface

$U$  is the surface flow velocity

$T_w$  is the absolute temperature of the sea

$T_{air}$  is the absolute temperature of the air

$C_c$  is the sensible transfer coefficient, given as  $1,41 \cdot 10^{-3}$



The convective heat flux varies between 0-100 W/m<sup>2</sup>.

### A.11.3 Vaporisation

By combining Dalton's law /3/ with the formulation proposed by Friehe & Smith (1976) /4/ the following relationship for the vaporative heat loss can be derived :

$$q_e = LC_e(a + bW_2)(Q_w - Q_a) \quad (\text{A.11.5})$$

where

$L$  is the latent heat of vaporization,  $2,5 \cdot 10^6$  j/kg

$C_e$  is the moisture coefficient,  $1,32 \cdot 10^{-3}$

$W^2$  is the wind speed 2 m above sea surface

$Q_w$  is the water vapour density close to the surface

$Q_a$  is the water vapour density in the atmosphere

$a$  and  $b$  is user specified coefficients

Measurements of  $Q_w$  and  $Q_a$  are not directly available, but  $Q_w$  and  $Q_a$  can be related to the vapour pressure as /4/ :

$$Q_w = \frac{0,2167}{T_w} e_w \quad (\text{A.11.6})$$

and

$$Q_a = \frac{0,2167}{T_{air}} e_a \quad (\text{A.11.7})$$



The vapour pressure close to the sea surface  $e_w$  can be expressed by the water temperature, under the condition that the air close to the sea surface is saturated and have the same temperature as the water:

$$e_w = 6,11 e^{K\left(\frac{1}{T_k} - \frac{1}{T_w}\right)} \quad (\text{A.11.8})$$

where

$K$  is a constant being 5418 K

$T_k$  is the temperature at 0° C being 273.15 K

The vapour pressure in the air above the sea surface  $e_a$  depends on the air temperature and the relative humidity  $R$ :

$$e_a = R6,11 e^{K\left(\frac{1}{T_k} - \frac{1}{T_{air}}\right)} \quad (\text{A.11.9})$$

By combining equation (A.11.5) with equations (A.11.8) and (A.11.9) the final expression for the evaporative heat loss yields:

$$I_e = P(a + bW_2) \left[ \frac{e^{K\left(\frac{1}{T_k} - \frac{1}{T_w}\right)}}{T_s} - \frac{Re^{K\left(\frac{1}{T_k} - \frac{1}{T_{air}}\right)}}{T_{iar}} \right] \quad (\text{A.11.10})$$

where  $P$  is a latent constant being 4370 J · K/m<sup>3</sup>.

During cooling of a water mass the heat loss due to vaporization has a major effect and typical varies between 0-100 W/m<sup>2</sup>.

## A.11.4 Shortwave Radiation

Radiation from the sun consist of electromagnetic waves with wave lengths varying from 1000 to 30000 Å. Most of the radiation will be absorbed in ozone layer, leaving only a fraction of the energy to reach the surface of the Earth. Furthermore the spectrum changes, when sunrays pass through the atmosphere. Most of the infrared and ultraviolet compound is absorbed, so the solar radiation on the earth mostly consist of light with wave lengths between 4000-9000 Å. This radiation is termed the shortwave radiation.

The intensity of the shortwave radiation depends on:



1. The distance between the earth and the sun.
2. The declination angle and latitude.
3. Extraterrestrial radiation.
4. Cloudiness and amount of water vapor in the atmosphere.

The calculation of the shortwave radiation is based on the following formulations.

#### A.11.4.1 Distance between the Earth and the Sun

The mean distance between the Earth and the Sun  $r_0$  is 149597890 km.

Spencer /1/ has developed the following expression to determine the eccentricity correction factor  $E_0$ .

$$E_0 = \left(\frac{r_0}{r}\right)^2 = 1,000110 + 0,034221 \cos \Gamma + 0,001280 \sin \Gamma + 0,000719 \cos 2\Gamma + 0,000077 \sin 2\Gamma \quad (\text{A.11.11})$$

where  $\Gamma$  is the day angle given as :

$$\Gamma = 2\pi \frac{(d_n - 1)}{365} \quad (\text{A.11.12})$$

where

$r$  is the actual distance between the Earth and the Sun expressed in km.

$d_n$  is the day number given as 1 the 1<sup>st</sup> day of January and 365 the 31<sup>st</sup> day of December. It is assumed that February always have 28 days.

#### A.11.4.2 Solar Declination and Day Length

The daily rotation of the Earth around the polar axes contributes to changes of the solar radiation. The seasonal radiation is governed by the declination



angle. Spencer /1/ presented the following expression to determine the declination angle  $\delta$ .

$$\begin{aligned} \delta = & (0,006918 - 0,399912 \cos \Gamma + 0,070257 \sin \Gamma - \\ & 0,006758 \cos 2\Gamma + 0,000907 \sin 2\Gamma - \\ & 0,002697 \cos 3\Gamma + 0,00148 \sin 3\Gamma) \end{aligned} \quad (\text{A.11.13})$$

where  $\delta$  is measured in radians.

The day length  $N_d$  varies with  $\delta$ . For a given latitude  $\phi$  (North positive, South negative) the day length is expressed as:

$$N_d = \frac{24}{\pi} (-\tan \phi \tan \delta) \quad (\text{A.11.14})$$

and the sunrise angle  $\omega_{sr}$  is:

$$\omega_{sr} = \cos^{-1}(-\tan \phi \tan \delta) \quad (\text{A.11.15})$$

### A.11.4.3 Extraterrestrial Radiation

The intensity of shortwave radiation on a surface parallel with the surface of the Earth changes with the angle of incident. The highest intensity is measured at noon where the sun is in zenith and the lowest during sunrise and sunset. The extraterrestrial intensity of shortwave radiation on a surface parallel to the Earth surface  $q_0$  can be expressed as /1/:

$$q_0 = q_{sc} E_0 \left( \sin \delta \sin \phi + \left( \frac{24}{\pi} \right) \sin \left( \frac{\pi}{24} \right) \cos \delta \cos \phi \cos \omega_j \right) \quad (\text{A.11.16})$$

where

$\omega_j$  is defined in equation (A.11.25) and is called the hour angle

$q_{sc}$  is the solar constant measured to 1376 W/m<sup>2</sup>

By integrating equation (A.11.16) over one day, the daily extraterrestrial radiation  $H_0$  is derived as:

$$H_0 = \frac{24}{\pi} q_{sc} E_0 \cos \phi \cos \delta (\sin \omega_{sr} - \omega_{sr} \cos \omega_{sr}) \quad (\text{A.11.17})$$



#### A.11.4.4 Radiation under Cloudy Skies

For determination of daily radiation under cloudy skies  $H$ , Ångström /1/ has proposed the following relationship between the daily insolation and the number of bright sunshine hours  $n$ :

$$\frac{H}{H_0} = a + b \frac{n}{N_d} \quad (\text{A.11.18})$$

Rietvald found the values of  $a$  and  $b$ , could be determined based on the mean annual value of bright sunshine hours  $\bar{n}$  and the average length of a day  $\bar{N}_d$  19 given as:

$$a = 0,1 + 0,24 \left( \frac{\bar{n}}{\bar{N}_d} \right) \quad (\text{A.11.19})$$

and

$$b = 0,38 + 0,08 \left( \frac{\bar{N}_d}{\bar{n}} \right) \quad (\text{A.11.20})$$

The coefficients  $a$  and  $b$  are subject to changes according to topographical shading.

The average hourly shortwave radiation  $q_s$  can the be found as:

$$q_s = \left( \frac{H}{H_0} \right) q_0 (a_3 + b_3 \cos \omega_i) \quad (\text{A.11.21})$$

where

$$a_3 = 0,409 + 0,5016 \sin \left( \omega_{sr} - \frac{\pi}{3} \right) \quad (\text{A.11.22})$$

and

$$b_3 = 0,6609 - 0,4767 \sin \left( \omega_{sr} - \frac{\pi}{3} \right) \quad (\text{A.11.23})$$

$\omega_i$  is the hour angle.



If the time is measured in local time, the hour angle is given as:

$$\omega_i = \frac{\pi}{12} \left( 12 + \text{correction for summertime} - \frac{E_t}{60} - \frac{4}{60} (L_s - L_E) - \text{local time in hours} \right) \quad (\text{A.11.24})$$

$E_t$  is varying during the year and is called the equation of time given as:

$$E_t = (0,000075 + 0,001868 \cos \Gamma - 0,032077 \sin \Gamma - 0,014615 \cos 2\Gamma - 0,04089 \sin 2\Gamma)(229,18) \quad (\text{A.11.25})$$

where  $E_t$  is measured in minutes.

The time meridian  $L_s$  is the standard longitude for the time zone and  $L_E$  is the local longitude (west positive, east negative). The longitude correction is 4 minutes for every degree.

The summer time correction is + 1 hour, if the clock is 1 hour ahead.

#### A.11.4.5 Albedo

Solar radiation that impinges on the sea surface does not all penetrate the water surface. Parts of the radiation are reflected back to its surroundings, and are lost from the system unless it is backscattered from the atmosphere or the surrounding topography. This reflection of the solar energy is termed the albedo. The amount of energy which is lost due to albedo, depends on the angle of incidence and angle of refraction. The reflection  $\alpha$  can be expressed in Fresnel's law /7/, which is valid for a smooth sea:

$$\alpha = \frac{1}{2} \left( \frac{\sin^2(i-r)}{\sin^2(i+r)} + \frac{\tan^2(i-r)}{\tan^2(i+r)} \right) \quad (\text{A.11.26})$$

where

$i$  is the angle of incidence

$r$  is the refraction angle

The reflected shortwave radiation can now be expressed as:

$$q_{sr} = \alpha q_s \quad (\text{A.11.27})$$

The reflection coefficient  $\alpha$  varies from 5 - 40 %.





## A.11.5 Longwave Radiation

A body or a surface emits electromagnetic energy at all wave lengths of the spectrum. The longwave radiation consists of waves with wave length between 9000-25000 Å. The radiation in this interval is termed the infrared radiation and is emitted from the atmosphere and the sea surface. The longwave emittance from the sea surface to the atmosphere minus the longwave radiation from the atmosphere to the sea surface is called the net longwave radiation. Brunt has related the net longwave radiation with the following parameters:

1. Cloudiness defined by number of sunshine hours.
2. Air temperature measured in Kelvin degrees.
3. Vapour pressure in the air, at the actual level of relative humidity and air temperature.

The formulation used in MIKE is based on Brunt's general equation for net out-going longwave radiation /2/ given as:

$$q_{nl} = q_{lu} - q_l = \sigma T_n^4 (a - b \sqrt{e_d})(c + d) \quad (\text{A.11.28})$$

where  $a$ ,  $b$ ,  $c$  and  $d$  are coefficients given as:

$$a = 0,56, \quad b = 0,77 \text{ mb}^{-1/2}, \quad c = 0,10, \quad d = 0,90 \quad (\text{A.11.29})$$

$e_d$  is the vapour pressure at dew-point temperature measured in mb

$n$  is the number of sunshine hours

$N_d$  is the number of possible sunshine hours

$\sigma$  is Stefan Boltzman's given as  $5,6697 \cdot 10^{-8} \frac{\text{W}}{(\text{m}^2 \cdot \text{K})}$



## A.11.6 References

- /1/ Muhammed Iqbal, An introduction to solar radiation, Academic Press, 1983.  
ISBN 0-12-373752-4
- /2/ M.E.Jensen, R.D. Burman, and R.G. Allen, Evapo-transpiration and Irrigation Requirements, ASCE 1990.  
ISBN 0-87262-763-2
- /3/ Peter S. Eagleson, Dynamic Hydrology, McGraw-Hill, 1970.
- /4/ Swedish Council for Building Research, Jörgen Sahlberg, A hydrodynamic model for heat contents calculation on lakes at the ice formation date.  
Document D4:1984, 1984
- /5/ Gunnar Lindh and Martin Falkenmark, En inledning til vatten-resurslären, Norway 1972.
- /6/ Poul Harremoës and Anders Malmgren-Hansen, Lærebog i vand-forening, Polyteknisk forlag, Denmark 1990.  
SBN 87-502-0671-0
- /7/ Robert G. Wetzel, Limnology, Saunders College Publishing, 1983.  
ISBN 0-03-057913-9



## A.12 User Defined Structure

### A.12.1 General

#### A.12.1.1 Introduction

The user defined structure is available to create customised structures in MIKE 11. However, the potential application goes beyond this, allowing for the customisation of almost any specialist application or modification to MIKE 11.

When activated, the user defined structure will access a DLL (Dynamic Link Library) written by the user. The Network Editor interface contains a number of variables that can be used in the DLL. In addition, the DLL can access any variable in MIKE 11 through several records.

The following gives a description of the user defined structure, including coding issues and a description of parameters. Two examples of possible applications are given. The first example also provides an insight into the computational requirements for developing a structure within the MIKE 11 solution scheme.

#### A.12.1.2 Requirements

Obviously, knowledge of computer programming is necessary. MIKE 11 is written in PASCAL using Borland DELPHI. Any code written must be compatible with the compiled unit files (DCU) provided. The easiest way to ensure this is to have Delphi and write your programs in PASCAL.



The user defined structure option has an extremely broad area of possible application. It is possible to modify or interrogate most components of MIKE 11. However, there is a difference between knowledge of hydraulics and knowledge of computational hydraulics. An understanding of computational



hydraulics is essential if you wish to modify or insert anything into the MIKE 11 computational scheme. On the other hand, coding to produce customised output formats shouldn't be as difficult to achieve.

### A.12.1.3 General Coding Issues

When a user defined structure is specified, MIKE 11 will search for a procedure in a dynamic link library (DLL). The name of the DLL and the name of the procedure can be either default names or can be specified in the network editor interface.

The specifications of the DLL must match the specifications that MIKE 11 is expecting. This includes specific compiler details and variable access. The DLL must use the MIKE 11 unit **rivdecl**, which contains record declarations. There are several DCU files that are linked into the project to do this.

The basic structure of the DLL is shown below:

```
Library struc1;
uses sysutils, Classes, rivdecl;
procedure user_written_code ( user_ptr : weir_struct; {information on structures}
                             grid_ptr : grid_struct; {information on grid structure}
                             mm_act   : mm_ptr;      {information on simulation}
                             iter_nr  : integer;     {iteration when procedure called}
                             nt       : integer );   {timestep when procedure called}
cdecl; export;
var
// insert local variables here
begin
// user defined code goes here
end;
exports user_written_code;
begin
end.
```

### A.12.1.4 MIKE 11 Interface

A structure must be defined in the network editor to access the user defined code. Note that a structure will always alter the network. If you wish to use the user defined code in a non-intrusive way (say to produce customised output formats), create a dummy branch (with dummy boundaries) and place it in the network file isolated from the actual model network.

The Network Editor interface provides application specific information to the user written code (Fig A.12.24):

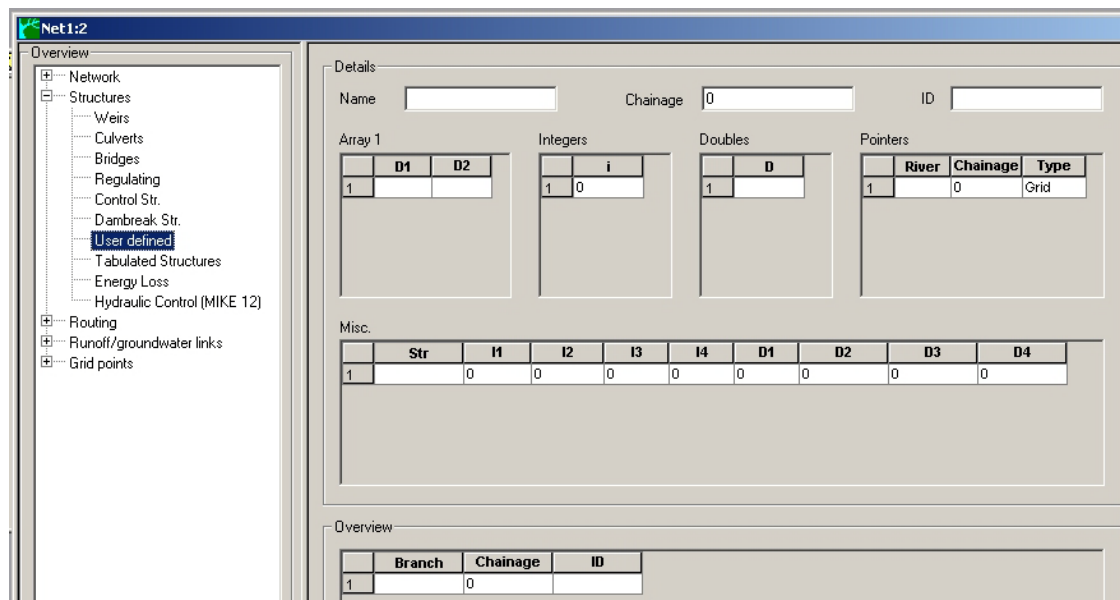


Fig A.12.24 Network Editor Interface

### A.12.1.5 Description of Parameters

The user defined code calls five parameters. The last two are variables, while the first three are records. Details are as follows:

#### user\_ptr

**user\_ptr** is a pointer of type **weir\_struct**, declared in the unit **rivdecl**. It contains information relating to the structures in the model and their specifications. Some useful variables within the record are as follows:

- **location** - where is the structure
- **location.id\_name** - name of branch
- **location.id\_mil** - chainage of structure
- **weir\_grid** - see next description of **grid\_ptr**
- **struc\_type** - user defined in this case

Further, the following are the entries inserted in the User Defined Structure dialog box in the network editor. These are also located in the **user\_ptr** record. The descriptions in brackets reference the title and column title of each entry in the dialog:

- **NoOfUserDefinedArrays** (Array 1)



- **UserDefArray1Col1[]** (Array 1, D1) - Array of 2 column arrays
- **UserDefArray1Col2[]** (Array 1, D2)
- **NoOfUserDefinedIntegers** (Integers)
- **UserDefInteger[]** (Integers, I) - Array of integers
- **NoOfUserDefinedDoubles** (Doubles)
- **UserDefDouble[]** (Doubles, D) - Array of Doubles (double precision reals)
- **NoOfUserDefinedPointers** (Pointers)
- **UserDefPointer[].P1String** (Pointers, River) - Array of pointers to a grid, branch or node, where each pointer contains a string (river name), double (chainage) and integer (grid=1, branch=2, node=3)
- **UserDefPointer[].P2Double** (Pointers, Chainage)
- **UserDefPointer[].P3Integer** (Pointers, Type)
- **UserDefPointer[].UserDefGridP** (not shown in dialog) - If type is Grid, pointer to grid variables at location
- **UserDefPointer[].UserDefBranchP** (not shown in dialog) - If type is Branch, pointer to branch variables at location
- **UserDefinedPointer[].UserDefNodeP** (not shown in dialog) - If type is Node, pointer to node variables at location
- **NoOfUserDefinedMiscData** (Misc)
- **UserDefMiscData[].P1String** (Misc, Str) - Array of record containing string, integer and doubles. The first string entry (if not NIL) is the name of the DLL. The second string entry (if not NIL) is the name of the procedure. Otherwise, default values are 'USER\_WRITTEN\_DLL.DLL' and 'user\_written\_code'.
- **UserDefMiscData[].P2Integer** (Misc, I1)
- **UserDefMiscData[].P3Integer** (Misc, I2)
- **UserDefMiscData[].P4Integer** (Misc, I3)
- **UserDefMiscData[].P5Integer** (Misc, I4)
- **UserDefMiscData[].P6Double** (Misc, D1)
- **UserDefMiscData[].P7Double** (Misc, D2)
- **UserDefMiscData[].P8Double** (Misc, D3)
- **UserDefMiscData[].P9Double** (Misc, D4)
- **UserDefTextfile** - Type textfile, use to assign a globally declared unit number to a file name.



## grid\_ptr

**grid\_ptr** is a pointer of type **grid\_struct**, declared in the unit **rivdecl**. It contains information relating to all the grid points in the model. Some useful variables within the record (among many others) are as follows:

- **grid\_loc** - as for location in **user\_ptr**.
- **area** - cross-sectional area
- **flarea** - storage area at water level **h**
- **radius** - hydraulic or resistance radius
- **resnum** - resistance number
- **width** - width of cross-section
- **dx** - distance between structure and grid point downstream
- **d2x** - distance between upstream and downstream grid points.
- **xcoor** - x-coordinate of point
- **ycoor** - y-coordinate of point
- **h** - water level at time  $n+1/2$
- **q** - discharge at time  $n+1/2$
- **hq0** - water level (h point) or discharge (q point) at time **n**
- **hq1** - water level (h point) or discharge (q point) at time **n+1**
- **co1, co2, co3, co4** - coefficients applied to solution scheme
- **prev\_grid** - pointer to previous grid (same information listed here except at previous grid)
- **next\_grid** - pointer to previous grid (same information listed here except at next grid)
- **actlev** - pointer to cross-section information - also useful to determine if grid point is h point or Q point (for Q point, **actlev** = NIL)

## mm\_act

- **mm\_act** is a pointer of type **mm**, declared in the unit **rivdecl**. It contains information relating to the MIKE 11 simulation, which is essentially all the information. Some useful variables within the record (among many others) are as follows:
- **nnt** - number of time steps
- **dt** - time step in seconds
- **time\_on\_monitor** - pointer to time on monitor, containing year, month, day, hour, min, sec, datestring, timestring
- **time\_act** - pointer to current simulation time, containing year, month, day, hour, min, sec, datestring, timestring



- **time\_start\_simul** - pointer to simulation start time, containing year, month, day, hour, min, sec, datestring (not used), timestring (not used)
- **time\_end\_simul** - pointer to simulation end time, containing year, month, day, hour, min, sec, datestring (not used), timestring (not used)
- **nr\_iter** - iteration number (same as variable called explicitly)
- **progDir** - directory location of executable
- **dataDir** - directory location of simulation files

iter\_nr

- The structure routines are called at each iteration in a given time step (see the User Reference A.8 for details on this). **iter\_nr** is the number of the particular iteration.

nt

- The time step of the particular structure call.

## A.12.2 Example: Structure with Form Loss Coefficient

### Description

This is an example of a structure defined by a simple loss coefficient applied to the velocity head. The equation is:

$$\Delta h = F \frac{v^2}{2g} \quad (\text{A.12.1})$$

where:

- $\Delta h$  is head drop across the structure;
- $F$  is an input form loss coefficient;
- $v$  is velocity through the structure; and
- $g$  is gravity.

MIKE 11 uses flows, so the equation can be rewritten in terms of flow  $Q$  and area  $A$ . Flow direction is dependent upon the sign of  $\Delta h$ . To include this direction dependency, the equation can be rewritten:

$$Q = \Delta h \sqrt{\frac{2gA^2}{F|\Delta h|}} \quad (\text{A.12.2})$$





## Scheme Formulation

To incorporate this structure into MIKE 11, the equation must be re-arranged into a finite difference form, with a staggered grid centred on a q point:

$$\alpha h_{j-1}^{n+1} + \beta Q_j^{n+1} + \gamma h_{j+1}^{n+1} = \delta \quad (\text{A.12.3})$$

where;

- $\alpha$ ,  $\beta$ ,  $\gamma$  and  $\delta$  are coefficients (co1, co2, co3 and co4 in the MIKE 11 code);
- $n$  is the time step; and
- $j$  is space step.

Consider the structure equation at a time mid-way between time steps at  $n+1/2$  and across a staggered grid centred on a Q point:

$$Q_j^{n+1/2} = (h_{j-1} - h_{j+1})^{n+1/2} \sqrt{\frac{2gA^2}{F|(h_{j-1} - h_{j+1})^{n+1/2}|}} \quad (\text{A.12.4})$$

Placing the terms on one side:

$$-\sqrt{\frac{2gA^2}{F(h_{j-1} - h_{j+1})^{n+1/2}}} h_{j-1}^{n+1/2} + Q_j^{n+1/2} + \sqrt{\frac{2gA^2}{F(h_{j-1} - h_{j+1})^{n+1/2}}} h_{j+1}^{n+1/2} = 0 \quad (\text{A.12.5})$$

The values of  $h$  and  $Q$  are only solved at times  $n$  and  $n+1$ . Therefore, a time-centring factor ( $\theta$ ) is used to describe the terms (say  $h$ ):

$$h^{n+1/2} = \theta h^{n+1} + (1 - \theta) h^n \quad (\text{A.12.6})$$

Assuming that  $(h_{j-1} - h_{j+1})^{n+1/2} = (h_{j-1} - h_{j+1})^n = \Delta h$  within the square root term, the equation now becomes:

$$\theta \left[ -\sqrt{\frac{2gA^2}{F|\Delta h|}} h_{j-1}^{n+1} + Q_j^{n+1} + \sqrt{\frac{2gA^2}{F|\Delta h|}} h_{j+1}^{n+1} \right] + (1 - \theta) \left[ -\sqrt{\frac{2gA^2}{F|\Delta h|}} h_{j-1}^n + Q_j^n + \sqrt{\frac{2gA^2}{F|\Delta h|}} h_{j+1}^n \right] = 0 \quad (\text{A.12.7})$$



Rearranging this into the finite difference form:

$$-\theta \sqrt{\frac{2gA^2}{F|\Delta h|}} h|_{j-1}^{n+1} + \theta Q|_j^{n+1} + \theta \sqrt{\frac{2gA^2}{F|\Delta h|}} h|_{j+1}^{n+1} = \quad (\text{A.12.8})$$

$$1 - \theta) \left[ \sqrt{\frac{2gA^2}{F|\Delta h|}} h|_{j-1}^n - Q|_j^n - \sqrt{\frac{2gA^2}{F|\Delta h|}} h|_{j+1}^n \right]$$

Thus, the coefficients in the equation become:

$$\text{co1} = \alpha = -\theta \sqrt{\frac{2gA^2}{F|\Delta h|}} \quad (\text{A.12.9})$$

$$\text{co2} = \beta = \theta \quad (\text{A.12.10})$$

$$\text{co3} = \gamma = \theta \sqrt{\frac{2gA^2}{F|\Delta h|}} \quad (\text{A.12.11})$$

$$\text{co4} = \delta = (1 - \theta) \left[ \sqrt{\frac{2gA^2}{F|\Delta h|}} h|_{j-1}^n - Q|_j^n - \sqrt{\frac{2gA^2}{F|\Delta h|}} h|_{j+1}^n \right] \quad (\text{A.12.12})$$

Note that if  $\Delta h = 0$ , the square root term has no solution. In this case,  $\text{co1} = 1$ ,  $\text{co2} = 0$ ,  $\text{co3} = -1$  and  $\text{co4} = 0$ .

## MIKE 11 Variables Required

To code this, the following parameters are required. `grid_ptr` is at the Q point, which is a user defined structure:

- $\alpha = \text{grid\_ptr}^{\wedge}.\text{co1}$
- $\beta = \text{grid\_ptr}^{\wedge}.\text{co2}$
- $\gamma = \text{grid\_ptr}^{\wedge}.\text{co3}$
- $\delta = \text{grid\_ptr}^{\wedge}.\text{co4}$
- $\Delta = \text{grid\_ptr}^{\wedge}.\text{area}$
- $Q_j^n = \text{grid\_ptr}^{\wedge}.\text{hq0}$
- $h_{j-1}^n = \text{grid\_ptr}^{\wedge}.\text{prev\_grid}^{\wedge}.\text{hq0}$
- $h_{j+1}^n = \text{grid\_ptr}^{\wedge}.\text{next\_grid}^{\wedge}.\text{hq0}$



## MIKE 11 Application

A simple model has been created for this structure. It consists of a rectangular channel (length 1000 m, width 100 m and slope of 1 in 1000) with the structure in the centre (chainage 500 m). Water level boundaries at each end are specified. The upstream water level is fixed at 1 m (which is also the initial water level). The downstream water level is lowered at a linear rate from 1 m to 0.5 m over a period of 1½ hours. It is then maintained at 0.5 m for an additional 1½ hours. Bed friction is Manning  $M = 30$ , and the time step is 1 minute.

The user defined structure has been defined. The first string in the Miscellaneous entry contains the name of the DLL that will be accessed by MIKE 11. The second string contains the name of the procedure that will be accessed. Note that if no entries are specified, the default DLL is 'USER\_WRITTEN\_DLL.DLL' and the procedure name is 'user\_written\_code'. For this example:

- `user_ptr^.UserDefMiscData[1].P1String = 'form_loss_struc1.DLL'`
- `user_ptr^.UserDefMiscData[2].P1String = 'user_written_code'`

For flexibility for this particular problem, the time centring factor and form loss coefficient are specified in the interface. The first double in the Double entry is the time centring factor ( $\theta$ ). The second entry is the form loss coefficient ( $F$ ). Thus, the variables `theta` and `formC` are local variables defined by:

- `user_ptr^.UserDefinedDouble[1] = theta`
- `user_ptr^.UserDefinedDouble[2] = formC`

## User Defined Code

The code for this example is as follows:

```

library form_loss_struc1;

uses
  dialogs,           // message dialogs
  math,              // power function
  sysutils, classes,
  rivdecl;           // access to MIKE11

procedure user_written_code ( user_ptr : weir_struct; {information on structures}
                             grid_ptr  : grid_struct; {information on grid points}
                             mm_act    : mm_ptr;      {information on simulation}
                             iter_nr   : integer;     {iteration when procedure called}
                             nt        : integer );   {timestep when procedure called}

cdecl; export;

const
  grav = 9.81;

var
  theta,
  formC,
  h_ups,
  h_dws,

```



```
sqterm      : double;
stemp       : string;

begin {user_written_code}

// if first timestep and first iteration, print a message to screen with
// the values of THETA and FORMC
if (nt = 1) and (iter_nr = 1) then
begin
  stemp := 'USER DEFINED STRUCTURE WITH FORM LOSS COEFFICIENT' + chr(13) +
    chr(13) +
    'User Defined DLL: form_loss_struct1' + chr(13) +
    'Written by CFN' + chr(13) +
    'THETA = ' +
    FloatToStrF(user_ptr^.UserDefDouble[1],ffixed,5,2) + chr(13) +
    'FORMLOSS = ' +
    FloatToStrF(user_ptr^.UserDefDouble[2],ffixed,5,2);
  messagedlg(stemp,mtinformation,[MBOK],0);
end;

// assign local variables theta and formc
theta := user_ptr^.UserDefDouble[1];
formc := user_ptr^.UserDefDouble[2];

// assign local variables h_ups and h_dws
// defined from prev_grid (upstream) and next_grid (downstream)
h_ups := grid_ptr^.prev_grid^.hq0;
h_dws := grid_ptr^.next_grid^.hq0;

// set terms of momentum coefficient for case of h_ups = h_dws
grid_ptr^.co1 := 1;
grid_ptr^.co2 := 0;
grid_ptr^.co3 := -1;
grid_ptr^.co4 := 0;

// if there is a water level gradient change the terms
if h_ups <> h_dws then
begin
// calculate the square root term, used in the momentum terms
sqterm := sqrt( 2*grav * power(grid_ptr^.area,2) / formc / abs(h_ups - h_dws) );

// terms of momentum coefficient
grid_ptr^.co1 := -theta * sqterm;
grid_ptr^.co2 := theta;
grid_ptr^.co3 := theta * sqterm;
grid_ptr^.co4 := (1-theta) * (sqterm * h_ups - grid_ptr^.hq0 - sqterm * h_dws);

end;

end; {of user_written_code}

exports user_written_code;
begin
end.
```

## Testing

Run this simulation using a range of different form loss coefficients and time centring coefficients. THETA can vary between 0 and 1. THETA = 0.5 is a fully centred scheme. When  $0 < \text{THETA} < 0.5$  the solution scheme is unstable. For THETA = 0.5 the solution is stable and non-dissipative. For  $0.5 < \text{THETA} < 1.0$  the solution is stable and dissipative.

This structure is identical to an energy loss structure, applying a user defined energy loss coefficient (specified in the Network Editor). Repeat this test



using an energy loss structure rather than a user defined structure. The results should be identical.

## A.12.3 Example: User Defined Output

MIKE 11 simulations can be performed over very long periods of time. To minimise output file size there is a **Storing Frequency** option in the simulation editor, where results are saved at a specified frequency of the simulated time step. However situations arise where output is required at every time step at specific locations, while in the same simulation still having global output at a longer time step.

Consider for example long term tidal variation in an estuary, where analysis of tidal range (difference in maximum and minimum water levels during a tidal cycle) and mean sea level change (moving average of tide levels) is required. Calculation of these parameters requires model output at small time increments (of the order of 15 to 30 minutes for semi-diurnal tidal cycles). Depending on the size of the model, extraction of this information at all grid points for a long term simulation would produce a large output file. To reduce output file size there is an option in the network editor to select which grid points will store results. However, this may not always be the most convenient solution.

This example will describe the programming required to create a time series output of water levels or flows at specified locations in a model. The output will be at each simulation time step. Details are as follows:

- The DLL name is 'TIME\_SERIES\_OUTPUT.DLL'.
- The procedure name is user\_written\_code.
- The user defined structure will be inserted into a dummy branch of an existing model. The structure will not be used or considered as part of the existing model.
- It is intended that this code will be generic. This means it should be applicable to many different applications.
- The output file format will be CSV (comma separated ASCII format), which can be easily read using EXCEL. The output file is 'time\_series\_output.csv' which has a column separator ';'.

The coding must consider that the user defined code is called prior to the final sweep in the solution scheme. This means that water levels and flows for the current time step have not yet been calculated and that the results from the previous time step must be presented. The code writes the result from the previous time step on one line, then writes the current time on the next line. This staggered approach will produce a file where the output time is consistent with the standard MIKE 11 result files.

The variable saved to output is hq0. As well as being the results of the previous time step, hq0 is water levels at h points and flows at Q points. Therefore



output using this program can be either water level or flow, depending upon selection of h or Q output point.

## Application

The following shows an example where time series output has been specified in an existing model. The model network initially consisted of three branches. An additional dummy branch (called DUMMY) has been created which is not connected to the other branches. This branch contains the user defined structure. Dummy boundary conditions (say uniform water levels at each end of the branch) are applied. The tabular view of the user defined structure is as follows:

The screenshot displays the 'User defined' structure configuration in the Network Editor. The 'Details' panel shows the following information:

- Name: dummy
- Chainage: 10
- ID: d

The 'Pointers' section contains the following table:

	River	Chainage	Type
1	senegal_main2	30316.87	Grid
2	senegal_est4	53850	Grid

The 'Misc' section contains the following table:

	Str	I1	I2	I3	I4	D1	D2	D3	D4
1	h:\user_defined_struct\struc1\time_series_output.dll	0	0	0	0	0	0	0	0
2	user_written_code	0	0	0	0	0	0	0	0
3	h:\user_defined_struct\example2\test.csv	0	0	0	0	0	0	0	0
4	;	0	0	0	0	0	0	0	0

The 'Overview' section at the bottom shows the following table:

Branch	Chainage	ID	
1	dummy	10	d

Fig A.12.25 Network Editor Tabular View of Example 2

The structure is location at chainage 10 in the dummy branch. There are two **Pointers** to grid points, defined by the **River** name and **Chainage**. The Type of both is **Grid**. These pointers will be the locations at which model results will be presented.

In the **Misc** field, the first string (**Str**) entry contains the name of the DLL. The second string entry contains the name of the procedure. The third string entry contains the name of the output file, which is read by the user defined code. The fourth string contains the column separator to be used in the output file. If no entries are specified in the Misc field, the default DLL is 'USER\_WRIT-TEN\_DLL.DLL', the procedure name is 'user\_written\_code', the output file is 'time\_series\_output.csv', and the column separator is ','.



## User Defined Code

The code for this example is as follows:

```

Library time_series_output;

uses
  Sysutils, Classes,
  rivdecl;      // access to MIKE11

procedure user_written_code ( user_ptr : weir_struct; {information on structures}
                              grid_ptr : grid_struct; {information on grid points}
                              mm_ptr   : mm_ptr;      {information on simulation}
                              iter_nr  : integer;     {iteration when procedure called}
                              nt       : integer );    {timestep when procedure called}

cdecl; export;

var
  outfile      : string;
  i            : integer;
  delim       : string;
  grid_act    : grid_struct;
  branch_act  : branch_struct;
  hout       : array [1..50] of double; // up to 50 output locations

begin {user_written_code}

// only perform saving of output if at the last iteration of each timestep!!
if (iter_nr = mm_act^.nr_iter) then
  begin

// use default column separator unless specified in UDS input
  delim := ',';
  if user_ptr^.NoOfUserDefinedMiscData > 3 then
    delim := user_ptr^.UserDefMiscData[4].P1String;

// loop through branches and grid points in branches to find locations that
// match user defined pointer list
  branch_act := mm_act^.first_branch;
  while branch_act <> NIL do // loop branches, starting at first branch
  begin
    grid_act := branch_act^.fgrid_ptr;
    while grid_act <> NIL do // loop all grid points in branch
    begin
      for i := 1 to user_ptr^.NoOfUserDefinedPointers do // loop pointer list
      begin
        if user_ptr^.UserDefPointer[i].UserDefGridP = grid_act then
          begin
            // assign values to hq0
            // hp0 is result at previous timestep -
            // the latest (h) has not been calculated yet.
            hout[i] := grid_act^.hq0;
          end;
        end;
        grid_act := grid_act^.next_grid;
      end;
      branch_act := branch_act^.next_bran;
    end;
  end;

// first timestep, so find filename, assign file to unit, rewrite and write headers
// the name of the output file is 'time_series_output.csv'
// unless specified otherwise in MiscData[3]
if (nt = 1) then
  begin
    outfile := mm_act^.dataDir + 'time_series_output.csv';
    if user_ptr^.NoOfUserDefMiscData > 2 then
      outfile := user_ptr^.UserDefMiscData[3].P1String;

    assignfile(user_ptr^.UserDefTextfile,outfile);
    rewrite(user_ptr^.UserDefTextfile);
  end;

```



```
write(user_ptr^.userdefTextfile,'Timestep' + delim + 'DATE' + delim + 'TIME');
for i := 1 to user_ptr^.NoOfUserDefinedPointers do // loop through pointer list
  write(user_ptr^.UserDefTextfile,
    delim +
    user_ptr^.UserDefPointer[i].P1String + ' ' +
    FloatToStrF(user_ptr^.UserDefPointer[i].P2Double,ffixed,6,3));
  writeln(user_ptr^.UserDefTextfile);
end

// if not first timestep, write out results in hout to output file
// keep on the same line, but put a new line at the end
else
begin
  for i := 1 to user_ptr^.NoOfUserDefinedPointers do
    write(user_ptr^.UserDefTextfile, delim + FloatToStrF(hout[i],ffixed,10,5));
    writeln(user_ptr^.UserDefTextfile);
  end;

// if the last timestep then close the file
// if not, as time is offset write the current timestep on a new line
if (nt >= mm_act^.nnt) then
  close(user_ptr^.UserDefTextfile)
else
  write(user_ptr^.UserDefTextfile, InttoStr(nt) + delim +
    mm_act^.time_act.datestring + delim +
    mm_act^.time_act.timestring);

end; {of last iteration}
end; {of user_written_code}

exports user_written_code;
begin
end.
```

## Output

Output is in a CSV format, which can be opened using Excel:





	A	B	C	D	E	F
1	Timestep	DATE	TIME	SENEGAL_MAIN2 30316.900	SENEGAL_EST4 53850.000	
2	1	1-JUN-2000	00:17:30	-0.06685	-0.06685	
3	2	1-JUN-2000	00:20:00	-0.06685	-0.06685	
4	3	1-JUN-2000	00:22:30	-0.06685	-0.06686	
5	4	1-JUN-2000	00:25:00	-0.06685	-0.06687	
<b>6</b>	5	1-JUN-2000	00:27:30	-0.06685	<b>-0.06694</b>	
7	6	1-JUN-2000	00:30:00	-0.06685	-0.06722	
8	7	1-JUN-2000	00:32:30	-0.06685	-0.06805	
9	8	1-JUN-2000	00:35:00	-0.06685	-0.07	
10	9	1-JUN-2000	00:37:30	-0.06685	-0.07373	
11	10	1-JUN-2000	00:40:00	-0.06685	-0.07952	
12	11	1-JUN-2000	00:42:30	-0.06685	-0.08695	
13	12	1-JUN-2000	00:45:00	-0.06685	-0.09492	
14	13	1-JUN-2000	00:47:30	-0.06685	-0.10235	
15	14	1-JUN-2000	00:50:00	-0.06685	-0.10883	
16	15	1-JUN-2000	00:52:30	-0.06685	-0.11465	
17	16	1-JUN-2000	00:55:00	-0.06685	-0.12033	
18	17	1-JUN-2000	00:57:30	-0.06685	-0.12609	
19	18	1-JUN-2000	01:00:00	-0.06685	-0.13187	
20	19	1-JUN-2000	01:02:30	-0.06685	-0.13773	





## A.13 Nomenclature

$A$  flow area

$A_1$  inflow river cross-section area

$A_2$  outflow river cross-section area

$A_{bc}$  critical flow area in breach

$A_c$  critical flow area

$A_e$  effective flow area

$A_{full}$  full cross-section area of culvert

$A_{s_1}$  culvert inflow cross-section area

$A_{s_2}$  culvert outflow cross-section area

$A_{s_a}$  average of  $A_{s_1}$  and  $A_{s_2}$

$B$  full width of channel

$b$  width of rectangular channel

$b$  gate width

$b_s$  structure width

$b_s$  storage width

$C$  Chezy coefficient

$C_c$  contraction coefficient

$C_{cal}$  calibration coefficient

$C_d$  discharge coefficient

$C_o$  discharge coefficient

$C_r$  Courant number

$C_w$  wind friction coefficient

$D$  pipe diameter, culvert depth

$dHb$  change in breach level

$dWb$  change in breach width



$Fr$  Froude number

$f$  Darcy friction factor

$H_1$  inflow energy head

$H_2$  outflow energy head

$H_B$  level of breach bottom

$h_{s_1}$  inflow water level in culvert

$h_{s_2}$  outflow water level in culvert

$h$  water elevation

$h_1, h_{us}$  upstream water elevation

$h_2, h_{ds}$  downstream water elevation

$h_b$  water level at breach

$h_{bc}$  water level at breach at critical flow

$h_c$  water level at critical flow

$I_b$  bottom slope

$IN$  infiltration capacity of flood plains

$K$  channel conveyance

$K$  time constant for linear reservoir

$k_s$  pipe roughness

$L$  length of pipe or culvert

$L$  wave length

$L_b$  length of breach in flow direction

$L_{full}$  length of culvert flowing full

$M$  Manning number

$n$  Manning's  $n$

$P$  wetted perimeter

$Q$  discharge

$Q_b$  breach flow



- $Q_{bc}$ critical flow in breach
- $Q_c$ critical flow
- $Q_o$ orifice flow
- $Q_P$ primed flow
- $Q_P$ discharge through a pipe
- $Q_R$ return flow
- $q$ lateral inflow per unit width
- $q_{loss}$ total water loss rate
- $q_{lossINF}$ infiltration loss rate
- $q_{lossRS}$ loss rate from river to retention storage
- $q_t$ sediment transport rate per unit width
- $r_f$ resistance factor
- $r_r$ relative resistance
- $R$ resistance or hydraulic radius
- $R_h$ hydraulic radius
- $R_t$ resistance radius
- $S$ water surface slope
- $S_c$ critical flow slope
- $S$ storage content of linear infiltration storage
- $S_{max}$ maximum retention storage
- $S_o$ culvert slope
- $S_s$ side slope of breach
- $T$ duration of event (wave period)
- $t_{fac}$ topographic factor
- $u$ average velocity along vertical
- $V_1$ velocity at  $h_1$
- $V_{10}$ velocity 10 m above water surface



$V_b$  velocity in breach  
 $V_{bc}$  critical velocity in breach  
 $WB$  width of breach bottom  
 $W_{FL}$  filled retention storage (flood width)  
 $W_{min}$  minimum river width for which losses occur  
 $W_R$  average (flooded) river width  
 $W$  water width corresponding to water elevation  $h$   
 $w$  gate opening  
 $x$  side erosion index  
 $y$  local water depth  
 $y_p$  depth of water in pipe  
 $y_s$  depth at vena contracta  
 $y_1$  upstream water depth  
 $y_2$  downstream water depth  
 $Z_c$  weir crest elevation  
 $z_{inv_1}$  inflow culvert invert level  
 $z_{inv_2}$  outflow culvert invert level  
 $z_{obv}$  obvert level of pipe  
 $z_{obv_2}$  outflow obvert level  
 $\alpha$  momentum distribution coefficient  
 $\alpha'$  vertical velocity distribution coefficient  
 $\alpha_c$  free overflow factor  
 $\varepsilon$  porosity of sediment  
 $\rho$  density  
 $\rho_a$  density of air  
 $\tau_r$  bed resistance term  
 $\tau_w$  wind shear stress



$\mu$ submerged flow coefficient or weir discharge coefficient

$\zeta$ headloss coefficient

$\zeta_{in}$ inflow loss coefficient

$\zeta_{out}$ outflow loss coefficient

$\zeta_1$ contraction loss coefficient

$\zeta_2$ expansion loss coefficient

$\zeta_b$ bend loss coefficient

$\zeta_f$ friction loss coefficient

$\Delta H$ inflow head loss

$\Delta H_{loss}$ total head loss

$\Delta R_p$ change in pipe radius







# APPENDIX B

## The MIKE11.ini file





## B.1 MIKE11.ini file Settings

### B.1.1 Introduction

The MIKE11.ini-file offers a possibility of changing settings within the calculation part of MIKE 11 by adjusting values of below listed environment variables.

### B.1.2 MIKE 11 GIS Linkage

Linkage of MIKE 11 Results with the ArcView based MIKE 11 GIS Interface.

Usage of MIKE 11 GIS Interface may require activation of variables to produce and export simulation information to text-files.

The default settings should only be changed if 3D-analyst is not installed. If required the ON/OFF switch can be used to ensure that ASCII results are ported to the msd directory. The switch should be set to ON if 3D Analyst is not installed.

#### Variables available:

##### M11GIS\_OUTPUT

Values: ON/OFF

##### M11GIS\_FILE\_FORMAT

Values: ASCII/BINARY (Must be ASCII on PC-version)

##### M11GIS\_DATABASE

Values: DATABASE NAME (Not Used in PC-Version)

### B.1.3 MIKE 11 HD Settings

#### HD-Variables no 1:

Flow-directions used when applying Wind stress in a HD-simulation is calculated automatically during reading of input data. The calculated flow directions is saved in a ASCII file named 'FLOWDIR.TXT' by activating the variable:

##### CREATE\_FLOWDIR\_FILE

Values: ON/OFF

In case the calculated flow-directions needs to be modified the user can manually edit the text-file 'FLOWDIR.TXT' and activate the variable:



### FLOWDIR\_FROM\_FILE

Values: ON/OFF

By activating this variable, MIKE 11 HD will read and utilise flow-directions from the ASCII text-file.

### HD-Variables no 2:

Previous versions of MIKE 11 (before version 4.01) only included the Divide section feature (Cross section database) in Sediment Transport morphological simulations.

Version 4.01 or newer can utilise this feature also in pure HD-simulation.

Activate / deactivate by setting the variable:

### DIVIDE\_FLP\_AND\_RIVER\_IN\_HDSIMUL

Values: ON/OFF

### HD-Variables no 3:

Maximum depth exceedance. The exceedance of water level above any cross section bank-levels during a simulation can be controlled by adjusting the variable:

### WL\_EXCEEDANCE\_FACTOR

Values: Any positive integer.

Default = 4

### HD-Variables no 4:

Coefficient for centering iterative calculation of sub-merged discharge. Default value is 1.0, corresponding to full centering towards to most recently calculated value. Only values between 0.5 and 1.0 allowed.

### STRUCTURE\_ITERATION\_CENTERING

Values: 0.5-1.0

### HD-Variables no 5:

After reading of input files, non-critical errors may occur in some of the input data. These warnings are informed to the user by a message box, and a user action is required to continue the simulation.

To avoid this user action, it is possible to switch off the appearance of the warnings message box with the below variable.

### SHOW\_WARNING\_MESSAGEBOX

Values: ON/OFF



### HD-Variables no 6:

Variable defining the maximum allowable number of iterations during one time step in situations where one or several control structures are solved using the iterative calculation mode.

#### MAX\_GATE\_ITERATIONS

Values: Any positive integer.

Default value is 50.

### HD-Variables no 7:

A new and improved structure solution has been implemented.

In some situations results close to the structure can be different from results obtained using the previous structure solution. To keep using the old solution this variable should equal ON.

#### OLD\_STRUCTURE\_SOLUTION

Values: ON/OFF.

Default is OFF meaning that the new solution is used.

### HD-Variables no 8:

Transition from critical to subcritical flow through submerged underflow structures is discontinuous in nature. To avoid numerical problems the 'SUB-MERGED\_UNDERFLOW\_COEFFICIENT' is introduced to make a smooth transition. This coefficient only works when OLD\_STRUCTURE\_SOLUTION is equal to OFF.

#### SUBMERGED\_UNDERFLOW\_COEFFICIENT

Values: 0.0-1.0

Default value is 0.0. If the value is increased the transition is made less abrupt.

### HD-Variables no 9:

Variables defining up- and downstream grid size for precalculated tables.

Default value 0.1 meter.

**BRIDGE\_TABLE\_GRID\_UPSTREAM=0.1**

**BRIDGE\_TABLE\_GRID\_DOWNSTREAM=0.1**

Variable defining maximum number of iterations for precalculating tables.

**BRIDGE\_TABLE\_MAX\_ITERATIONS=50**

## HD-Variables no 10:

Bridges using the FHWA method for submergence uses per default two orifice equations for submergence. The user may choose to use different to restrict the calculation method for orifice type flow:

0 : No orifice equation is used

1 : Only submerged orifice equation used

2 : Both submerged orifice (downstream) and non-submerged orifice equation.

Default value

**BRIDGE\_ORIFICE\_FLOW=2**

The reach length for the FHWA method is determined based on an equal conveyance tube analysis. If the reach length should only be based on the physical distance from the adjacent cross section to the bridge the variable 'USE\_FHWA\_REACH\_LENGTH' may be used.

Default value

**USE\_FHWA\_REACH\_LENGTH = ON**

## HD-Variables no 11:

The velocity distribution coefficient for bridge calculations is set to unity per default. The coefficient may be calculated based on conveyance distribution. To do the latter the variable 'USE\_ALPHA' may be used.

Default value

**USE\_ALPHA = OFF**

## HD-Variables no 12:

When the h-Q-h relations calculated for bridges a filter may be applied. There are three different filters available. Whether or not a filter is applied is controlled by the variables '**SMOOTH\_BRIDGE\_SURFACE**' and '**SMOOTH\_BRIDGE\_SURFACE\_LOOPS**'. The first variable takes values in the range -1-3 where

-1 : The H-Q-H surface is forced to be increasing for increasing water level difference.



0 : No filter

1 : Filter with weights on adjacent terms in the grid given by

1	1	1
1	1	1
1	1	1

2 : Filter with weights as below

1	1	1
1	4	1
1	1	1

3 : Filter given by

1	2	1
2	4	2
1	2	1

The second variable controls the number of times the filter is applied. The greater the value the smoother the h-Q-h relation.

Default values

**SMOOTH\_BRIDGE\_SURFACE = 0**

**SMOOTH\_BRIDGE\_SURFACE\_LOOPS = 0**

### HD-Variables no 13:

The generation of H-Q-H relations for bridges may be time consuming. The H-Q-H relation may be read from a previous run. To achieve this the preprocessed file(s) need to be present in the working directory (the location of the sim11 file). To enable this feature the variable '**BRIDGE\_PREPROCESSED**' should be set to ON.

Further the format of the preprocessed files should also be specified. The two formats available are 'ASCII' and 'DFS2'. The format is set using the variable '**BRIDGE\_FILE\_FORMAT**'.



Default values

**BRIDGE\_PREPROCESSED = OFF**

**BRIDGE\_FILE\_FORMAT = DFS2**

#### HD-Variables no 14:

At low flow conditions a slot is introduced. The amount of water in this slot may be included in the calculation of the mass error by setting this variable to ON. This setting has no effect on the rest of the simulation only on the mass error calculation for water levels in the slot.

##### SLOT\_VOLUME\_CORRECTION

Values: ON/OFF.

Default is OFF.

#### HD-Variables no 15:

The critical discharge calculation over a broad crested weir is part of the necessary preprocessing of data. The critical discharge is found as an integration of the local critical velocity over the whole weir cross sectional area. This integration may either be carried out numerically using the trapezoidal rule or analytically using linear interpolation between data points. The latter is achieved by setting WEIR\_QH\_CALC\_NUM\_INTEGRATE to OFF. Earlier versions of MIKE 11 used the former integration i.e. numerical integration. Thus to ensure backward compatibility this switch should be set to ON. Default is ON. Also note that to make this setting work the MIKE11.ini file MUST be located in the WINDOWS or WINNT directory.

##### WEIR\_QH\_CALC\_NUM\_INTEGRATE

Values: ON/OFF.

Default is OFF.

#### HD-Variables no 16:

Variable used to fade out the effect of the momentum equation for low flow conditions. Only used for dynamic simulations.

##### QZERO\_METHOD

Values: ON/OFF.

Default is ON.

#### HD-Variables no 17:

Variable used to implement an area preserving slot for low flow conditions.





### AREA\_PRESERVING\_SLOT

Values: ON/OFF.

Default is OFF.

### HD-Variables no 18:

Variable used in connection with the 'Triple Zone Approach' for bed resistance specification in the HD Parameter file. Variable BEDRES\_TRANSFER\_INTERVAL defines the depth below the zone divider where a cosine transfer function is activated to go from one zone's bed resistance value to another zones value.

### BEDRES\_TRANSFER\_INTERVAL

Values: positive real numbers

Default is 0.1

### HD-Variables no 19:

Variable used to activate lateral outflow corrections. For low flow conditions this initiates a check on the amount of water available before extraction through a lateral outflow. If a possible lateral outflow demand cannot be met a warning is issued at the end of the simulation along with the total unsatisfied demand (volume of water for the whole period).

### Q\_LAT\_CORRECTION

Values: ON/OFF.

Default is ON.

### HD-Variables no 20:

Variable used to revert back to the 1999b version. Due to improvements and error corrections in version 2000 the results obtained using this version may differ from results obtained in version 1999b. In order to avoid recalibration of a 1999b setup the variable 1999B\_REVERSABILITY has been introduced.

### 1999B\_REVERSABILITY

Values: ON/OFF.

Default is OFF.

### HD-Variables no 28:

Variable used to enable the reading of lateral sources from a result file. Only effective for hydrodynamic simulations using lateral inflows from SHE.

### LATERAL\_INFLOW\_FROM\_RESULT\_FILE

Values: ON/OFF.



Default is OFF.

### HD-Variables no 30:

Temporary switch for defining language in Engine. Final implementation will make simulation editor able to send information about current language version.

Present Language-types available:

0: Standard/Default - working as all previous releases of English versions

1: Japanese/MultiByteCharacterSet version - Case sensitivity on strings file-names etc. activated!

#### LANGUAGE\_VERSION

Values: 0/1.

Default is 0.

### HD-Variables no 31:

Froude value at which the effect of fully submerged bridges and bridge piers are ignored.

#### BRIDGE\_FROUDE\_CRITERIA

Values: positive real numbers

Default is 0.6

### HD-Variables no 32:

Switch between radius formulations in QSSVEG:

1. As requested by CTI (based on integrated  $y^{5/3}$ )
2. Resistance radius as default in M11 (based on integrated  $y^{3/2}$ )
3. Hydraulic radius ( $R=A/P$ )

#### QSSVEG\_RADIUS

Values: 1,2,3.

Default is 1.

### HD-Variables no 33:

Switch between suppression strategies of convective terms in QSSVEG:



1. The Froude number is calculated for each of the panels upstream and downstream and the maximum of these Froude numbers is used for determining the suppression factor.
2. A suppression factor is calculated and used for each panel upstream and downstream. Thus the suppression factor is specific to each panel in the cross sections.
3. No suppression is applied to the convective terms. Caution is recommended when using this possibility since it may cause severe numerical instability.

#### QSSVEG\_SUPPRESSION\_STRATEGY

Values: 1,2,3

Default: 1

#### HD-Variables no 34:

To increase the numerical stability of the algorithm an upstream centering of the friction terms may be applied.

#### QSSVEG\_CENTERING\_FRICTION

Values: ON/OFF

Default: OFF

#### HD-Variables no 35:

Please note that when utilizing the quasi two dimensional steady state with vegetation module, additional data can be obtained by setting the following switch: CREATE\_QSSVEG\_VELOCITY\_FILE=ON

With this setting 8 .txt-files are generated and saved in the working directory i.e. where the simulation file is stored.

The files are titled:

**QSSVEG\_velocities:** Velocity and area of the individual panels.

**QSSVEG\_velocities\_add1:** Energy slope, low water channel width, high water channel width, Radius, wetted perimeter and Manning's n of the individual panels.

**QSSVEG\_velocities\_add2:** Height of water/water interface, water/vegetation interface of the individual panels.

**QSSVEG\_velocities\_add3:** Mixing coefficients of the individual panels.

**QSSVEG\_velocities\_add4:** Shear forces of the individual panels normalised with density.



**QSSVEG\_junctions:** The appropriate parameters used for obtaining the water level increment due to the junction and the water level increment in the channels meeting at the junction.

**QSSVEG\_sandbars\_curves:** Water level increments due to sandbars and river curvature.

**QSSVEG\_bridges:** The water level increments due to bridges.

#### CREATE\_QSSVEG\_VELOCITY\_FILE

Values: ON/OFF

Default: OFF

#### HD-Variables no 36:

For use with the quasi two dimensional steady state with vegetation module when utilizing the water level increment due to curvature feature. The limit on the ratio of the curvature radius to the width for which the increment is to be added.

#### LIMIT\_ON\_QSSVEG\_CURVATURE\_CALC

Values: Any positive value.

Default: 10

### B.1.4 MIKE 11 AD/WQ Settings

#### AD-Variables no 1:

Automatic creation of Error log-file from AD-Simulations containing e.g. Courant number warnings can be disabled by changing the variable:

#### ADLOG

Values: ON/OFF

#### AD-Variables no 2:

When water is abstracted in the AD-model (from negative lateral sources or evaporation) the concentration of the abstracted water is the same as that in the abstraction point/reach.

The 'ZERO\_CONC\_IN\_AD\_LAT\_OUTFLOW' variable introduces a switch to the AD-model so that abstracted water is removed with a concentration of zero, typically resulting in an increasing concentration in the water body during the abstraction.

#### ZERO\_CONC\_IN\_AD\_LAT\_OUTFLOW

Values: ON/OFF.



Default is OFF





# INDEX



<b>A</b>	
Ackers and White model . . . . .	243
Advection-dispersion . . . . .	187
Advection-dispersion equation . . . . .	192
Discretization . . . . .	202
<b>B</b>	
Bandwidth minimisation . . . . .	411
Bed forms . . . . .	211
Anti-dunes . . . . .	212
Dunes . . . . .	211
Plane bed . . . . .	212
Ripples . . . . .	211
Bed load . . . . .	252
Bed resistance . . . . .	18
Bottom level	
Updating . . . . .	216
Boundaries . . . . .	413
Discharge as function of time . . . . .	414
Q/h boundary . . . . .	415
Water level as a function of time . . . . .	414
Boundary conditions . . . . .	30, 193
Non-cohesive sediment transport . . . . .	227
Resolution . . . . .	31
Branch matrix . . . . .	407
Bridges . . . . .	31, 149
Piers . . . . .	36, 37, 150
Submerged . . . . .	60, 151
<b>C</b>	
Closed boundary	
AD . . . . .	194
Cohesive sediment transport . . . . .	187, 188
Advanced . . . . .	188
Deposition . . . . .	194
Erosion . . . . .	197
Computational grid . . . . .	65
Area selection . . . . .	65
Branch selection . . . . .	66
Concentration boundary . . . . .	194
Continuity equation	
Advection-dispersion . . . . .	201
Hydrodynamic . . . . .	430
Control structures . . . . .	67
Drowned flow . . . . .	75
Free flow . . . . .	74
Overflow . . . . .	72
Underflow . . . . .	72
Cross sections . . . . .	75
Culverts . . . . .	397
Critical inflow . . . . .	399
Critical inflow or outflow . . . . .	399
Critical outflow . . . . .	400
Full flow . . . . .	401
Fully submerged . . . . .	403
Loss coefficients . . . . .	397
Momentum equation . . . . .	398
Orifice flow . . . . .	400
Partially full . . . . .	401, 403
Submerged flow . . . . .	401
Transition up-/downstream controlled flow . . . . .	403
Culverts, Q-h Relations Calculated . . . . .	81
Closed/Open section switch . . . . .	86
Construction of Q-h relationships . . . . .	85
Flooded areas . . . . .	87
Flow descriptions . . . . .	82
Flow direction . . . . .	87
Specification . . . . .	82
Velocities . . . . .	87
<b>D</b>	
Dambreak Structure . . . . .	87
Breach geometry . . . . .	88
Erosion based breach development . . . . .	89
Flow calculations . . . . .	94
Known breach development geometry . . . . .	89
Limiting cross-section . . . . .	93
Piping failure . . . . .	89, 90
Darcy-Weisbach . . . . .	19, 26
Diffusive wave approximation . . . . .	423
Digital Elevation Model (DEM) . . . . .	420
Dispersion coefficient . . . . .	196
Double sweep algorithm . . . . .	407
Dune	
Dimension . . . . .	235
Equilibrium height . . . . .	228
Equilibrium length . . . . .	230
Non-equilibrium height . . . . .	234
Non-equilibrium length . . . . .	234





<b>E</b>		
Energy Loss	98	
Engelund & Fredsøe model	252	
Engelund & Hansen model	256	
Erosion	191	
Gradual	192	
Instantaneous	192	
External	129	
<b>F</b>		
Flood forecasting	365	
Adjust factor	372	
Alpha	372	
Analysis period	371	
Phase error	371	
Time constant	371	
Updating procedure	366	
Flood plains	115	
Flooded areas	99	
Flow description	118	
Diffusive wave	119	
Dynamic wave	118	
Kinematic wave	119	
Which description should I use?	119	
Flow resistance	235, 237	
Dune dimension	235	
White et al.	239	
<b>G</b>		
General description		
Advection-dispersion module	187	
Hydrodynamic module	18	
Non-cohesive sediment transport module	210	
Graded sediment	222	
<b>H</b>		
Hydraulic radius	21	
Hydrodynamic default parameters	63	
ALPHA	63	
DELH	63	
DELHS	63	
DELTA	64, 405	
EPS	64	
FroudeExp	64	
FroudeMax	64	
Inter1Max	64	
MaxIterSteady	64	
NODE Compatibility	64	
Nolter	65	
Theta	65	
Zeta Min	65	
<b>I</b>		
Initial conditions	120	
Auto start	120	
Combined auto start and user specified	120	
Hot start	120	
User-specified	120	
Internal	128	
<b>J</b>		
Junctions	152	
<b>K</b>		
Kinematic Routing	120	
<b>L</b>		
Lateral inflows	125	
Low flow conditions	126	
Non-cohesive sediment transport	222	
Slot	126	
Zero flow	126	
<b>M</b>		
mapping	417	
Mass balance	197	
Mass transport	197	
Mixing coefficients		
Adjacent vegetation zones	143	
Vegetation zones	142	
Momentum equation		
Discretization	432	
Morphological model	213	
<b>N</b>		
NAM	277	
Accumulation and melting of snow	286	
Adjustment of temperature and precipitation to altitude zones	289	
Altitude-distributed snowmelt model		



- 287
- Base temperature (snow/rain) T0 300
- Baseflow . . . . . 284
- Baseflow time constant CKBF . . . 298
- Basic modelling components . . . 282
- Capillary flux . . . . . 285
- Crop coefficients and irrigation losses . . . . . 301
- Degree-day coefficient C<sub>snow</sub> . . . 300
- Evapotranspiration . . . . . 282
- Extended groundwater components
- 284
- Extended snow melt components 290
- Groundwater depth for unit capillary flux GWLFL1 . . . . . 299
- Groundwater recharge . . . . . 284
- Infiltration factor K<sub>0inf</sub> . . . . . 301
- Initial conditions . . . . . 302
- Interflow . . . . . 283
- Interflow and overland flow routing . 283
- Irrigation module . . . . . 291
- Lower groundwater storage . . . 285
- Lower zone or root zone storage 282
- Maximum groundwater depth causing baseflow GWLBF0 . . . . . 298
- Maximum water content in root zone storage L<sub>max</sub> . . . . . 295
- Maximum water content in surface storage U<sub>max</sub> . . . . . 295
- Model parameters . . . . . 294
- Model Structure . . . . . 280
- Overland flow . . . . . 282
- Overland flow runoff coefficient CQOF . . . . . 296
- Radiation coefficient Crad . . . . 300
- Rainfall degree-day coefficient Crain 300
- Ratio of groundwater catchment to topographical catchment area Carea 298
- Recharge to lower groundwater storage CQLow . . . . . 298
- Root zone threshold value for groundwater recharge TG . . . . . 298
- Root zone threshold value for interflow TIF . . . . . 297
- Root zone threshold value for overland flow TOF . . . . . 297
- Shallow groundwater reservoir description . . . . . 285
- Snow module . . . . . 286
- Soil moisture content . . . . . 284
- Specific yield SY . . . . . 299
- Structure of the altitude-distributed snowmelt module . . . . . 287
- Structure of the irrigation module 292
- Surface storage . . . . . 282
- Time constant for interflow CKIF 296
- Time constant for routing interflow and overland flow CK12 . . . . . 296
- Time constant for routing lower baseflow CKlow . . . . . 298
- Node matrix . . . . . 409
- Non-cohesive sediment transport . . . 209
- Non-cohesive transport module . . . . 188
- O**
- Open Boundary Inflow
- AD . . . . . 193
- P**
- Pumps . . . . . 127
- Q**
- Quasi-steady solution . . . . . 129
- Horizontal branches . . . . . 131
- Relaxation . . . . . 130
- Undefined solution . . . . . 132
- Underflow . . . . . 131
- Quasi-two dimensional steady flow with vegetation . . . . . 133
- Energy equation . . . . . 147
- Governing equations . . . . . 133, 134
- Suppression of convective terms 148
- Upstream centering of friction term . 148
- Zone classification . . . . . 133
- R**
- Relative resistance . . . . . 20



Resistance radius . . . . .	21	Wind . . . . .	182
-----------------------------	----	----------------	-----

**S**

Saint Venant Equations . . . . .	159
Saint Venant equations . . . . .	425
<b>Conservation of mass</b> . . . . .	425
<b>Conservation of momentum</b> . . . . .	425
Sandbars effect on the water level . . . . .	155
Scientific background	
<b>Hydrodynamic</b> . . . . .	393
Sediment	
<b>Consolidation</b> . . . . .	192
<b>Deposition</b> . . . . .	191
<b>Settling</b> . . . . .	190
<b>Sliding</b> . . . . .	191
Sediment transport models . . . . .	210
Shear stress distribution . . . . .	189
Smart and Jaeggi model . . . . .	260
Solution scheme	
<b>Advection-dispersion</b> . . . . .	201
<b>Dynamic</b> . . . . .	160
<b>Hydrodynamic</b> . . . . .	429
<b>Quasi-steady</b> . . . . .	129
Stability conditions	
<b>Dynamic solver</b> . . . . .	161
Structures . . . . .	435
<b>Determination of flow regime</b> 439, 440	
<b>Drowned flow</b> . . . . .	441
<b>Free overflow</b> . . . . .	445
<b>Geometry</b> . . . . .	439
<b>Mathematical treatment</b> . . . . .	435
<b>Regulating</b> . . . . .	156
<b>Zero flow</b> . . . . .	441
Suspended load . . . . .	230, 232

**T**

Transport boundary . . . . .	194
------------------------------	-----

**V**

van Rijn model . . . . .	262
--------------------------	-----

**W**

Water level variations due to curves . . . . .	154
Weir	
<b>Broadcrested</b> . . . . .	63
<b>Formula</b> . . . . .	180
<b>Special</b> . . . . .	160

